Departamento de Física Moderna

UNIVERSIDAD DE CANTABRIA

ESTADISTICA DE TRANSITORIOS EN SISTEMAS OPTICOS NO LINEALES

Angel Valle Gutiérrez

Memoria presentada para optar al título de Doctor en Ciencias Físicas

Agradecimientos

Quiero expresar desde estas líneas mi más sincero agradecimiento a los Doctores Luis Pesquera y Miguel Angel Rodríguez por la dirección de esta tesis. Las ayudas, explicaciones, críticas y sugerencias recibidas de ellos en todo momento han sido las razones fundamentales de que este trabajo haya podido salir adelante.

También quiero agradecer a:

Drs. Claudio Mirasso, Pere Colet, Salvador Balle y Maxi San Miguel (Universitat de les Illes Balears), Fernando Moreno y Francisco González (Universidad de Cantabria), Antonio Mecozzi y Paolo Spano (Fondazione Ugo Bordoni, Roma) y a Jorge Tredicce (Instituto Nonlineaire de Niza) por sus importantes aportaciones a este trabajo.

Dr. Francisco Carrera, Laura Cayón, Juan Manuel López y José Revuelta por haber hecho del despacho compartido un lugar agradable para el trabajo y a los demás miembros del Departamento de Física Moderna, que de una u otra forma me han ayudado a lo largo de estos últimos años

Mis padres, mi familia y a Gemma. A ellos dedico este trabajo.

1993

INDICE

0.- Introducción

0.1- Panorámica general

Este trabajo aborda el estudio de la estadística de transitorios en sistemas ópticos no lineales. Tres de estos sistemas serán objeto de nuestra atención: dispositivos ópticos biestables, laseres de gas y laseres de semiconductor.

Este estudio se engloba dentro del marco más general del conocimiento de las propiedades estadísticas de la radiación electromagnética. De la comprensión de estas propiedades en la radiación procedente de fuentes en equilibrio térmico surgen algunas de las ideas básicas de la física moderna. Posteriormente, la aparición del laser provoca un nuevo impulso en el estudio de la naturaleza estadística de la luz. El laser es un ejemplo de la mecánica estadística fuera del equilibrio cuya descripción puede hacerse con un conjunto reducido de variables macroscópicas[1]. La evolución dinámica de estas variables sufre grandes cambios dependiendo de los valores de los parámetros de control externos del laser, por ejemplo: el encendido, oscilaciones, formación de patterns, caos temporal, caos espaciotemporal, etc [2–9]. Estos cambios están asociados al hecho de que el laser cruza inestabilidades asociadas con bifurcaciones. Se han realizado muchos estudios de la estabilidad dinámica y estructural del laser y otros sistemas ópticos no lineales dentro del marco general de la teoría de

sistemas dinámicos [2–9]. Una posible clasificación de los estudios anteriores referidos al laser puede hacerse atendiendo al número efectivo de grados de libertad del sistema [10]. Si consideramos los laseres en que se selecciona un modo, éstos vienen descritos por ecuaciones para el campo eléctrico E, polarización, P, e inversión de población, D. En los laseres de clase A (Ar^+, He–Ne, colorante...) pueden eliminarse dos de estas variables (P y D). En laseres de clase B (rubi, YAG, CO_2, semiconductor...) se precisan dos variables (E,D) y en los de clase C (infrarrojo lejano...) las tres variables. Una parte considerable del estudio de transitorios se ha dedicado al estudio del comportamiento dinámico de los sistemas ópticos no lineales cuando el parámetro de control cruza el punto de bifurcación con una cierta dependencia temporal. Esta dependencia puede modificar profundamente el comportamiento dinámico del sistema (ver parte 0.1.1).

Cuando un sistema en un estado estable se aproxima a una inestabilidad las fluctuaciones dominan la dinámica del sistema[11, 12]. De hecho, la relajación de una inestabilidad solo se puede iniciar si hay fluctuaciones presentes en el sistema. El ruido aparece por tanto como un factor crucial para una descripción correcta del comportamiento del laser al cruzar una bifurcación. El origen del ruido puede ser interno (generado por el sistema independientemente de su entorno) o externo (asociado a parametros de control externos fluctuantes). Una de las causas fundamentales de la aleatoriedad en el campo de radiación es la emisión espontánea, proceso de naturaleza puramente cuántica. Diversos tratamientos cuánticos de la luz laser consiguen deducir ecuaciones de evolución de los operadores que describen este tipo de radiación[13, 14]. El posterior desarrollo de estas ecuaciones permite la obtención de

una ecuación clásica de tipo Fokker–Planck que describe la evolución temporal de las propiedades estadísticas de la radiación laser. Esta descripción también puede llevarse a cabo mediante ecuaciones diferenciales estocásticas con un ruido blanco. Tanto la ecuación de Fokker–Planck como las ecuaciones diferenciales estocásticas son herramientas adecuadas para el estudio de bifurcaciones en presencia de ruido. En la parte 0.1.2 se da un resumen de los estudios acerca de la influencia del ruido en las bifurcaciones, haciendo un especial hincapié en las bifurcaciones dinámicas.

La confirmación experimental de las teorías que dan cuenta de las propiedades estadísticas de la luz laser es llevada a cabo mediante medidas de contaje fotoeléctrico[15, 16]. En estos experimentos se pone claramente de manifiesto el cambio de estadística que sufre la luz laser durante su encendido, etapa en la cual los efectos del ruido de emisión espontánea son especialmente importantes. Dentro del estudio de la estadística del encendido de los sistemas ópticos no lineales y en especial de los laseres, dos tipos de problemas han sido los más extensamente tratados. El primero se refiere a la descripción estadística del tiempo en el que se observa la emisión laser y es estudiado mediante el método de los tiempos de paso en el régimen lineal de la amplificación laser [17–20]. El segundo problema es la descripción de las fluctuaciones que experimenta la intensidad del laser antes de su llegada al estado estacionario [15, 16]. Estas fluctuaciones son de orden uno (a este hecho se debe su nombre de fluctuaciones anómalas), mientras que las fluctuaciones antes y después del transitorio son del orden de la intensidad del ruido de emisión espontánea.

El conocimiento de la estadística del encendido del laser es importante tanto desde

un punto de vista fundamental (es un ejemplo de relajación de un estado inestable) como desde un punto de vista aplicado (por ejemplo el caracter aleatorio del encendido limita la máxima velocidad de funcionamiento de los sistemas de comunicación por fibra óptica).

En el resto de este apartado un resumen de los trabajos existentes, tanto teóricos como experimentales, de bifurcaciones dinámicas e influencia del ruido en las bifurcaciones es llevado a cabo en el contexto de los sistemas ópticos no lineales. Dentro de estos sistemas dedicaremos una atención especial al laser de semiconductor por su relevancia para este trabajo.

0.1.1- Bifurcaciones dinámicas

El estudio de sistemas cerca de una bifurcación es interesante pues ligeros cambios del parámetro de control externo llevan a grandes cambios en su comportamiento global. Entre estas bifurcaciones destacamos, por su especial relevancia en este trabajo, la que tiene lugar en el encendido del laser, similar a una transicion de fase de segundo orden[21, 22]. Una transición análoga a las de primer orden se da en el laser de colorante[23, 24]. Esta ha sido atribuida bien al tiempo de correlación no nulo del ruido externo en las pérdidas [23, 25, 26] o bien a un parámetro de ganancia aleatorio de carácter blanco[27]. El estudio de las bifurcaciones en sistemas ópticos no lineales se hizo en un principio considerando un cambio instantáneo del parámetro de control de un lado a otro de la bifurcación. Posteriormente, el efecto de la dependencia temporal del parámetro de control al cruzar la bifurcación fue considerado tanto en

trabajos teóricos [28–37] como experimentales [38–44].

Ya en los primeros trabajos teóricos se predijo que cuando el laser es encendido mediante un barrido del parámetro de control a través del punto de inestabilidad aparece un retraso entre el tiempo en que se observa la bifurcación dinámica y el tiempo en que se cruza la inestabilidad[28, 30–32]. En todos estos trabajos el tiempo en que se produce la bifurcación dinámica, t^*, es definido como el tiempo en que la intensidad del laser recupera su valor inicial. Este tiempo se puede calcular teóricamente mediante una linealización de las ecuaciones pero en cambio es difícil de ser medido debido al nivel de ruido en la salida laser [32, 40]. Cuando se considera un laser en el límite de buena cavidad se demuestra que el retraso depende del valor inicial del parámetro de control y de la velocidad de barrido, v[28]. Posteriores estudios experimentales introducen una nueva definición de bifurcación dinámica como el tiempo en que la intensidad alcanza su pendiente máxima, T [40]. Este tiempo se puede medir fácilmente pero su evaluación teórica requiere la solución de un problema no lineal[32]. En las medidas llevadas a cabo se observa una dependencia diferente de t^* y T con la velocidad de barrido. Esta diferencia solo se da en el límite de velocidades grandes siendo ambas definiciones equivalentes en el límite de velocidades reducidas[33]. La transición entre ambos comportamientos ha sido analizada en función de los valores del parámetro de control inicial y la velocidad de barrido[35].

Posteriores mejoras en las teorías anteriores fueron desarrolladas teniendo en cuenta imperfecciones en la bifurcación [36]. Estas imperfecciones consisten en sumar un término a las ecuaciones de evolución de la intensidad del laser. Este término

tiene en cuenta el hecho de que la intensidad del laser por debajo del umbral no es exactamente nula sino que tiene un valor finito debido por ejemplo a la emisión espontánea. Estas imperfecciones afectan al retraso en la bifurcación de forma que éste es de orden uno cuando la imperfección es mucho menor que v y nulo cuando la imperfección es de orden uno. La transición entre ambos comportamientos aparece cuando el valor de la imperfección es de orden v[31]. El retraso en la bifurcación ha sido también analizado con imperfecciones periódicas en el tiempo[32].

El estudio del retraso en la bifurcación ha sido también realizado en otros sistemas ópticos no lineales como laseres de clase B [34, 41, 43], laseres con absorbente saturable [29, 38, 39] y dispositivos ópticos biestables modulados periodicamente[44]. El sistema más estudiado de los anteriores es el laser con absorbente saturable. El retraso predicho teoricamente [29] es observado en experimentos efectuados en laseres de CO_2 con un absorbente intracavitario. Este retraso se traduce además en un aumento con la velocidad de barrido del ancho del ciclo de histéresis producido al aumentar y disminuir el parámetro de control más alla de los puntos extremos del ciclo [38,39]. Un ciclo de histéresis aparece también cuando un dispositivo óptico biestable es modulado periódicamente mediante un parámetro de control dinámico sinusoidal. Estudios teóricos y experimentales indican la existencia de leyes de escala sencillas entre el aumento del area del ciclo de histéresis y la frecuencia de encendido[44]

0.1.2 Influencia del ruido en bifurcaciones

El efecto de las fluctuaciones en un sistema dinámico no lineal es mayor a me-

dida que éste se aproxima a un punto de bifurcación. Cuando ésto ocurre las características de un sistema pueden sufrir grandes cambios respecto a las que tiene cuando su evolución es determinista. El estudio de la influencia del ruido en bifurcaciones ha sido llevado usando diversos métodos. Se han usado entre otros, diagramas de bifurcación estocásticos [45], exponentes de Lyapunov estocásticos[46], estudio de soluciones estacionarias con un parámetro de control estocástico [12]... Pasamos ahora a estudiar la influencia del ruido en una bifurcación dependiendo del régimen de tiempos considerado. En la parte (i) tratamos el caso de tiempos lo suficientemente grandes para que el sistema llegue al estado estacionario correspondiente a un parámetro de control aleatorio. En la parte (ii) consideramos el régimen de tiempos transitorio, previo a la llegada al régimen estacionario, en el cual las propiedades estadísticas del sistema cambian con el tiempo.

(i) Influencia del ruido en el estado estacionario

Se ha realizado un gran esfuerzo en el estudio de estos cambios cuando el sistema alcanza su estado estacionario bajo la influencia de un parámetro de control aleatorio. En este caso, fluctuaciones de un parámetro de control multiplicativo pueden dar lugar a transiciones inducidas por ruido [12]. Estas aparecen al cambiar la intensidad del ruido externo más allá de un cierto valor crítico. Ejemplos de estas transiciones son la creación de nuevos estados [47, 48] o el corrimiento de la bifurcación respecto de su valor determinista [49]. Corrimientos de la bifurcación inducidos por ruido externo multiplicativo han sido observados experimentalmente en osciladores electrónicos [50], cristales líquidos nemáticos [51] y en simulaciones analógicas [52, 53]. Los corrimientos

pueden ser hacia valores más pequeños del parámetro de control (avances) o más grandes (retrasos) dependiendo del tipo de ruido multiplicativo.

En una de las bifurcaciones más estudiadas, la bifurcación de Hopf, se han predicho teóricamente tanto avances [54] como retrasos [50, 54–56]. La localización de la bifurcación de Hopf en presencia de ruido multiplicativo coloreado puede avanzarse o retrasarse dependiendo del período de rotación de la variable de fase y del tiempo de correlación del ruido [54] Este avance, sin embargo, no ha sido observado en las simulaciones analógicas [53]. De todas formas, la definición de bifurcación de Hopf en presencia de ruido aparece como un asunto no trivial [53, 57]. Esta definición puede hacerse por ejemplo atendiendo a características topológicas de la distribución de probabilidad estacionaria [53] o bien recurriendo a parámetros de orden basados en la circulación de las variables del ciclo límite [57]. Otro indicador de la importancia del ruido cerca del punto de bifurcación es el espectro de potencia. Estudios teóricos y experimentales de la bifurcación de Hopf en presencia de ruido externo aditivo indican la aparición de nuevas líneas en el espectro de potencia a medida que el sistema se aproxima a la bifurcación determinista desde valores inferiores a ésta [58].

La influencia del ruido cerca de una bifurcación no solo ha sido descrita usando ecuaciones diferenciales estocásticas o ecuaciones de Fokker–Planck. De hecho también se ha estudiado en sistemas descritos por mapas en transición al caos mediante desdoblamiento de período [59, 60] o por ecuaciones diferenciales con retraso [61].

(ii) Influencia del ruido durante el transitorio.

El estudio de la influencia del ruido durante el transitorio en sistemas que cruzan una bifurcación ha estado ligado históricamente al estudio de las propiedades estadísticas de la luz en sistemas ópticos no lineales y en especial en el laser. Una posible clasificación de estos estudios, relevante para este trabajo, puede hacerse atendiendo a la dependencia temporal del parámetro de control al cruzar esa bifurcación.

Cambio instantáneo del parámetro de control

El problema que ha sido más estudiado es el del cambio instantáneo del parámetro de control a través de la bifurcación. En el caso del encendido del laser esta bifurcación es del tipo pitchfork supercrítico. Cuando el bombeo (diferencia entre el parámetro de ganancia y el de pérdidas) pasa de un valor negativo a otro positivo de forma instantánea se inicia debido a la presencia del ruido de emisión espontánea un proceso de relajación que es estudiado dentro del marco general de la relajación de estados inestables [62–64]. En la relajación de estados inestables se pueden distinguir tres etapas. La primera está dominada por las fluctuaciones inducidas por la emisión espontánea alrededor del estado inestable. Esta etapa admite una descripción lineal. La segunda etapa está dominada por el régimen no lineal en el cual el ruido de emisión espontánea ya no tiene efecto apreciable. En esta etapa las fluctuaciones iniciales se amplifican, dando lugar a las fluctuaciones anómalas. La etapa final consiste en la relajación de fluctuaciones alrededor del estado estacionario final. De entre los anteriores estudios de relajación de estados inestables destacamos por su especial

relevancia en este trabajo la teoría Cuasideterminista[64]. La idea básica de esta teoría es que la descripción de fluctuaciones en el régimen no lineal puede llevarse a cabo tomando un simple promedio sobre la distribución de valores iniciales aleatorios del campo laser[64].

Se han llevado a cabo estudios experimentales y teóricos de la estadística en transitorios en una gran variedad de laseres[65]. Para laseres de clase A (He-Ne, Ar^+, colorante), cuya evolución se puede estudiar con una sola variable (campo eléctrico), el acuerdo teoría experimento es muy bueno tanto para la descripción de la evolución temporal de los momentos de la intensidad [15, 16, 64] como para la descripción de los tiempos de encendido en los cuales la emisión laser se observa [17, 18, 20, 66]. Para laseres de clase B , que son sistemas descritos mediante dos variables relevantes (campo eléctrico e inversión de población), existen resultados teóricos y experimentales en estadística de tiempos de paso tanto para laseres de CO_2[41, 67] como de semiconductor [42, 68] . La evolución temporal de los momentos de la intensidad ha sido también estudiada de forma teórica y experimental para laseres de semiconductor [42, 68, 69] y de CO_2[67]. Por último también existen estudios experimentales en laseres de clase C (FIR)[70], en cuya descripción interviene, además de las variables anteriores, la polarización del medio.

En la óptica no lineal se pueden encontrar otros sistemas que presentan inestabilidades en el encendido distintas a las del laser. Ejemplos de éstos son los dispositivos ópticos biestables y láseres con absorbente saturable cuyos encendidos requieren que el parámetro de control atraviese bifurcaciones de tipo saddle node y pitchfork su-

percrítica, respectivamente. Estudios de la influencia del ruido en el transitorio han sido llevados a cabo tanto para biestabilidad óptica, [71–76] como para laseres con absorbente saturable [39, 77, 78]. En estos sistemas se observa la aparición de un ciclo de histéresis cuyos extremos son puntos de estabilidad marginal. La descripción de la relajación de estos estados tiene una dificultad adicional con respecto a la de la relajación de estados inestables. Esta consiste en la no existencia de un régimen inicial de tipo lineal. Otro hecho común a ambos sistemas es la existencia de un fenómeno de biestabilidad transitoria debido a las fluctuaciones[71, 72]. El estudio de la estadística de transitorios en dispositivos ópticos biestables pasivos presenta además una dificultad adicional que es la falta de simetría de inversión. Este tipo de fenómenos también aparecen en otros sistemas que exhiben una bifurcación de tipo saddle node como por ejemplo reacciones químicas exotérmicas de comportamiento explosivo [79]. La descripción de las fluctuaciones anómalas y la biestabilidad transitoria que aparecen en el transitorio de dispositivos ópticos biestables ocupará el capítulo 1 de este trabajo.

Barrido del parámetro de control

Un primer estudio teórico acerca de la influencia del ruido en una bifurcación dinámica se hizo mediante la integración numérica de las ecuaciones de Fokker Plank que describen la intensidad de un laser en el límite de buena cavidad con un barrido lineal del parámetro de bombeo[80]. Se demostró que que el retraso que aparece en la solución del problema determinista persiste cuando la velocidad de barrido es mayor que la intensidad del ruido de emisión espontánea, desapareciendo en el caso contrario [80]. Una forma adecuada de caracterizar una bifurcación dinámica en presencia de

ruido es mediante la estadística del tiempo de primer paso de la intensidad del sistema óptico no lineal por un cierto umbral[80, 81]. En esta descripción la condición inicial de evolución es determinada consistentemente a partir de las fluctuaciones presentes por debajo del umbral[81]. De esta forma no es necesario introducir una condición inicial distinta de cero, como se hizo en la descripción determinista, para que el sistema pueda relajar[81]. Se ha estudiado otra forma de caracterizar una bifurcación dinámica que también utiliza el concepto de umbral[82]. Esta consiste en conocer el tiempo en que el promedio de la intensidad atraviesa un cierto umbral. Debido a que este tiempo puede ser muy distinto al tiempo medio de primer paso por ese mismo umbral, ambas caracterizaciones no son equivalentes[83]. De ellas, la basada en la estadística de tiempos de paso es la usada usualmente en los experimentos [38–42]. Se han realizado estudios de simulación analógica en los que se verifican las predicciones de las anteriores teorías analíticas[83, 84]. Asímismo el papel del ruido de emisión espontánea ha sido considerado analítica y numericamente [85] en oscilaciones de ciclo límite de un laser con absorbente saturable. Cuando la solución de ciclo límite evoluciona lentamente el problema se reduce al del cruce del punto de bifurcación con una velocidad finita. Se ha demostrado que las oscilaciones dependen drásticamente del ruido siempre que la intensidad de éste supere un cierto valor crítico [85]. La dependencia de la velocidad de barrido ha sido también discutida en conexión con inestabilidades de fluídos [86] y teorías generales para el decaimiento de estados inestables[87].

La mayor parte de estudios experimentales en sistemas ópticos no lineales con un barrido del parámetro de control se concentran en la medida de tiempos de paso

por un umbral que está en la zona lineal [39, 41, 42]. Este barrido en el parámetro de control se ha realizado de diversas formas, por ejemplo: disminuyendo lentamente las pérdidas en el tiempo en el caso de laseres de CO_2[41] o provocando un aumento lineal en el tiempo de la ganancia de un laser de semiconductor mediante un cambio instantáneo de su corriente de inyección[42]. También se han realizado medidas de la estadística del tiempo de máxima pendiente de la intensidad y de la dependencia temporal de los momentos de la intensidad de un laser de Ar^+[40]. La interpretación de este experimento necesita una teoría que describa la evolución de la intensidad también en la zona no lineal. El desarrollo de esta teoría [88] ocupa el capítulo 2 de este trabajo.

Modulación del parámetro de control

Un problema relacionado al del barrido surge cuando el parámetro de control atraviesa periódicamente el punto de inestabilidad. Se ha demostrado en sistemas descritos por la ecuación homogénea de Ginzburg Landau dependiente del tiempo que el efecto combinado de modulación periódica y fluctuaciones induce un corrimiento bien definido en el punto de inestabilidad [89]. En el contexto de los sistemas ópticos no lineales se han estudiado experimentalmente sistemas como laseres con absorbente saturable modulados, [38, 39], laseres de colorante modulados en los que se pone de manifiesto el fenómeno de resonancia estocástica [90], y de semiconductor modulados[91–93] mediante cambios periódicos en la corriente de inyección. Este último problema ha sido estudiado también mediante métodos numéricos [94, 95] y analíticos [93, 96].

Distintos métodos han sido desarrollados para el estudio de sistemas estocásticos modulados: solución analítica en el límite esférico ($n \to \infty$) de un modelo simétrico de n componentes [89], una generalización de los procedimientos de empalme de Suzuki [97], aproximación de integral de camino[98], etc... El desarrollo de un nuevo método para el análisis de la estadística de pulsos en un sistema modulado [99] y su aplicación a laseres de gas [99] y semiconductor [96] ocuparán los capítulos 3 y 4 de este trabajo.

Dependencia aleatoria del parámetro de control

El ejemplo más estudiado en el contexto de los sistemas ópticos no lineales de sistema con una variación aleatoria de su parámetro de control es el laser de colorante. Este presenta fluctuaciones anómalas de su intensidad en el estado estacionario atribuidas a ruido externo en el parámetro de bombeo[100]. La descripción de las propiedades estadísticas de la intensidad durante el transitorio y de los tiempos de paso ha sido llevada a cabo siendo el acuerdo entre teoría y experimento muy bueno[18, 66]. Otro ejemplo de sistema con ruido en el parámetro de control es el del laser de Ar^+, estudiado en el capítulo 5 de este trabajo, pues la amplitud de la señal de radiofrecuencia que actúa sobre el modulador Acusto–Optico enciendiendo y apagando el laser, fluctúa dando lugar a un factor de pérdidas aleatorio. En este capítulo se presentan resultados de medidas de los tiempos de encendido de un laser de Ar^+ modulado. También se desarrolla una aproximación teórica para el cálculo de la estadística de los tiempos de encendido cuando el tiempo de aplicación del modulador es corto.

0.1.3 Estadística de transitorios en laseres de semiconductores

En los últimos años el estudio de las fluctuaciones en laseres de semiconductor ha suscitado un gran interés debido a varias razones [65, 101–103]. La más importante se refiere al uso de estos dispositivos en aplicaciones prácticas como los sistemas de comunicaciones ópticas. En sistemas de comunicaciones basados en la detección directa de la intensidad óptica es importante reducir las fluctuaciones en el tiempo de encendido, minimizar el efecto del encendido de un modo secundario del laser y del cambio dinámico de la frecuencia ('chirping') y obtener una relación máxima en potencia encendido–apagado (on/off), mientras en sistemas coherentes se requiere una gran pureza espectral. Otra razón, de tipo fundamental, se refiere a las diferencias de estos laseres respecto de otros no basados en una estructura de bandas de los niveles electrónicos. Estas diferencias están relacionadas con la presencia de dos términos en las ecuaciones de balance que describen el comportamiento del laser. El primero es el término de saturación en la ganancia que da cuenta de la reducción de la ganancia cuando la potencia óptica dentro de la cavidad aumenta[104]. Este término es responsable del amortiguamiento de las oscilaciones de relajación típicas de laseres de clase B. El segundo término es el factor de ensanchamiento de línea, α[105]. Este término tiene en cuenta que la parte real de la susceptibilidad a la frecuencia laser no se anula en un sistema compuesto por dos bandas de energía electrónicas. Los principales efectos de este factor son el aumento del ruido en la fase [105, 106] y el chirping debido a la modulación de la intensidad[107]. En los sistemas de comunicación de detección directa el chirping produce una distorsión del pulso debido a la dispersión en la fibra óptica.

Uno de los problemas antes mencionados, las fluctuaciones en el tiempo de encendido originadas por el ruido de emisión espontánea limitan el diseño de sistemas de comunicaciones ópticas basados en la intensidad trabajando a velocidades de GHz. En estos sistemas es deseable minimizar el tiempo de encendido y sus fluctuaciones y a la vez maximizar la relación encendido–apagado y evitar efectos de 'pattern'. El compromiso entre estos requerimientos tiene que establecerse para determinar las condiciones óptimas de operación del laser. Las propiedades estadísticas del tiempo de encendido han sido estudiadas experimentalmente[91–93], numéricamente [94, 95] y analíticamente [68, 93, 96]. Se ha demostrado además que se pueden relacionar propiedades estadísticas de los pulsos del laser como altura o rango de chirp en frecuencia con la estadística de tiempos de encendido [68, 108].

Otro de los problemas mencionados es el del ruido de partición modal. Este puede limitar el diseño de sistemas de comunicaciones ópticas, incluso cuando laseres de tipo DFB son usados, dando lugar a un gran 'Bit Error Rate' (BER)[101]. Este hecho es debido a que el laser puede encenderse inicialmente debido al ruido de emisión espontánea en un modo secundario con una longitud de onda distinta de la del modo principal. Después de la transmisión en una fibra óptica dispersiva, el modo secundario llega al receptor en un tiempo distinto del tiempo de llegada del modo principal, pudiendo provocar un error en la comunicación. El conocimiento de la probabilidad de encendido del modo secundario es por tanto un problema de gran interés que se ha estudiado de forma experimental [109] , teórica [109–112] y de simulación numérica [113].

El estudio de estos problemas de competencia entre modos ocupará el resto de este trabajo. Como primer paso para el análisis del problema de la competencia entre modos durante el encendido hemos estudiado en el capítulo 6 la estadística durante el transitorio de laseres de gas de anillo bimodales [114]. Por último, en los capítulos 7 y 8 estudiaremos la estadística durante el transitorio de un laser de semiconductor cuasimonomodo [112] haciendo un especial hincapié en el cálculo del BER debido al ruido de partición de modos en laseres modulados tanto con una secuencia periódica de la corriente de inyección como con una pseudoaleatoria.

0.2 Resumen del trabajo

En este trabajo se aborda el estudio de la dinámica de transitorios en sistemas ópticos no lineales mediante el estudio tanto analítico como de simulación numérica de las ecuaciones que describen la evolución temporal de su intensidad. La metodología matemática utilizada es la de los procesos estocásticos [11, 12, 115–118]. El estudio de la estadística de transitorios ha sido llevada a cabo básicamente usando las ideas contenidas en la Teoría Cuasideterminista [64]. En esta teoría la evolución de la intensidad del laser se separa en dos regímenes: uno en que la intensidad es pequeña y el ruido de emisión espontánea tiene gran importancia y otro en que la intensidad es grande evolucionando de forma determinista. El primer régimen determina las propiedades estadísticas del laser, pudiéndose calcular éstas de forma analítica. En el segundo régimen la evolución dinámica puede conocerse mediante la resolución de una ecuación diferencial ordinaria. De esta forma la estadística durante el transitorio puede conocerse de forma numérica y en algunos casos analítica sin necesidad de

recurrir a la simulación de las ecuaciones diferenciales estocásticas que describen la evolución durante todo el transitorio. Además una parte de esta tesis incluye trabajo experimental realizado sobre un laser de Ar^+. Damos ahora un pequeño resumen del trabajo realizado, desglosándolo por capítulos.

En el capítulo 1 estudiamos la relajación de un estado marginal en dispositivos biestables ópticos. Demostramos que es posible caracterizar las fluctuaciones anómalas que aparecen en transitorios de estados marginales mediante el uso de la estadística de tiempos de paso por un cierto umbral. El máximo de las fluctuaciones se expresa en términos de los estados inicial y final. Esta caracterización de las fluctuaciones anómalas está relacionada con el fenómeno de bimodalidad transitoria. Analizamos la existencia de tal bimodalidad en términos de un parámetro adimensional. Nuestros resultados son verificados mediante el uso de simulación numérica. Presentamos también aplicaciones al modelo de biestabilidad absorbente de Bonifacio–Lugiato.

El capítulo 2 trata de la estadística en el transitorio de un laser en el límite de buena cavidad encendido mediante una disminución lineal en el tiempo de las pérdidas. El estudio es llevado a cabo mediante el uso de la Teoría Cuasideterminista (QDT) para dos casos: en el primero, caso I, el parámetro de control , $a(t)$, cambia sin límite mientras que en el segundo, caso II, $a(t)$ alcanza un valor fijo. La validez de la QDT es analizada para ambos casos. Caracterizamos las fluctuaciones anómalas por el tiempo en el cual aparece el máximo, t_m, y por el valor de este máximo, σ_m. Nuestros resultados demuestran que t_m coincide con el promedio del tiempo de máxima velocidad de crecimiento de la intensidad, T. Demostramos que en el caso I

t_m^{-1} y σ_m escalan con $\sqrt{v}$ y que las fluctuaciones relativas están dadas por una función de scaling universal. El scaling de t_m concuerda con estudios experimentales. En el caso II calculamos analíticamente T,t_m y σ_m y demostramos que los momentos de la intensidad están dados a través de una variable de escala. Todos los resultados son verificados mediante simulaciones numéricas.

En el Capítulo 3 desarrollamos un nuevo método para el análisis de la estadística de pulsos en sistemas modulados basado en una generalización de la Teoría Cuasideterminista. Con este método se pueden obtener fácilmente las propiedades estacionarias de los pulsos mediante la solución de una ecuación integral para la densidad de probabilidad de tiempos de paso por un cierto umbral. En general esta ecuación debe resolverse mediante métodos numéricos. Sin embargo, se pueden obtener expresiones analíticas en casos límite. Hemos comparado este método con simulaciones en un laser de gas con modulación de dos valores (encendido-apagado) obteniendo un acuerdo excelente en todas las situaciones.

La aplicación del método del capítulo anterior a un laser de semiconductor monomodo ocupa el capítulo 4. Calculamos el valor medio y la varianza del tiempo de encendido de un laser de semiconductor de un modo modulado a frecuencias de Ghz. Los resultados obtenidos con este método concuerdan con simulaciones numéricas de las ecuaciones de balance del laser.

En el capítulo 5 presentamos medidas de propiedades estadísticas de tiempos de encendido en un laser de Ar^+ monomodo modulado mediante el uso de un modulador acusto óptico (AOM). El valor medio del tiempo de encendido $< \tau >$ aumenta

linealmente con el tiempo de aplicación de AOM, t_{off}, antes de alcanzar un valor constante para valores grandes de t_{off}. La varianza del tiempo de encendido, σ_τ, desarrolla un máximo en función de t_{off}. Estos resultados se explican con el uso de un modelo que incluye el ruido de emisión espontánea y fluctuaciones en el factor de pérdidas debido al carácter aleatorio de la señal de radiofrecuencia que actúa sobre el modulador. Obtenemos expresiones analíticas para la pendiente de $< \tau >$ en función de t_{off}, para el tiempo en que σ_τ desarrolla un máximo y para el valor de ese máximo.

El estudio de la estadística de transitorios en laseres de gas de anillo de dos modos ocupa el capítulo 6. Este estudio es desarrollado incluyendo el régimen no lineal de evolución. Cuando ambos modos están bien por encima del umbral, obtenemos expresiones explícitas para las densidades de probabilidad de la intensidad durante el transitorio usando la teoría Cuasideterminista. Cuando los parámetros de bombeo son similares, la densidad de probabilidad de la intensidad del modo secundario decae de forma algebraica debido a la competición entre ambos modos. El modo principal decae de forma simétrica y la densidad de probabilidad de la intensidad total está centrada alrededor de su valor medio con muy poca dispersión (ruido de partición de modos). Las fluctuaciones anómalas de ambos modos son caracterizadas por su valor máximo y por el tiempo en que aparece ese valor. También consideramos el caso de un modo secundario muy deprimido. Desarrollamos una aproximación nueva para describir el régimen transitorio del modo secundario. Además calculamos la densidad de probabilidad de ambos modos durante el transitorio y la probabilidad de excitación del modo secundario.

El capítulo 7 trata del estudio de la estadística de transitorios de un laser de semiconductor cuasi monomodo con una corriente de bias por debajo del umbral. Caracterizamos la estadística de los sucesos raros en los cuales el modo secundario tiene una potencia considerable en términos de los valores de la potencia de salida en el instante de encendido y de las potencias promediadas del modo principal y secundario sobre la duración del pulso óptico. El tiempo de encendido se define como el tiempo en el cual la potencia total de salida alcanza un valor prefijado. La estadística de partición de potencia en el tiempo de encendido se obtiene analítica y numéricamente para distintas corrientes de excitación y diversas diferencias de ganancia entre los dos modos. Resultados numéricos para la estadística de partición de potencias promediadas durante la emisión del pulso son presentados. También desarrollamos una aproximación analítica para calcular la cantidad anterior. Encontramos además una relación simple entre ambas caracterizaciones.

Por último en el capítulo 8 estudiamos la estadística de transitorios en un laser de semiconductor cuasimonomodo modulado mediante una secuencia pseudoaleatoria de bits "1" y "0". Calculamos mediante una aproximación analítica cotas superiores e inferiores a la supresión del modo lateral (SMSR) necesaria para obtener un BER de 10^{-9}. Encontramos que la diferencia de pérdidas entre el modo lateral y el modo principal ($\Delta\alpha$) para una corriente de bias del 10 por ciento por encima de la umbral debe estar entre 25 y 28 cm^{-1} a frecuencias de 5 GHz. Observamos efectos de pattern en la salida del laser para una corriente de bias por encima del umbral debido a la secuencia pseudoaleatoria de bits en la entrada. Para un valor especial de la corriente de bias ligeramente por debajo de la umbral estos efectos de pattern desaparecen y

el SMSR $(\Delta\alpha) = 25.7cm^{-1}$ es independiente de la frecuencia de modulación.

[1] H. Haken, *Synergetics. An Introduction*, Springer–Verlag, Berlin (1977).

[2] N. B. Abraham, P. Mandel, and L. M. Narducci in *Progress in Optics*, Vol. XXV, edited by Emil Wolf, North Holland, Amsterdam (1988)

[3] *Instabilities and Chaos in Quantum Optics II* edited by N. B. Abraham, F. T. Arecchi, and L. A. Lugiato, Plenum Press, New York (1988).

[4] *Coherence and Quantum Optics VI*, edited by J. H. Eberly, L. Mandel, and E. Wolf, Plenum Press, (1989)

[5] *Dynamics of Nonlinear Optical Systems* edited by L. Pesquera and F. J. Bermejo, World Scientific, Singapore (1989).

[6] *Nonlinear Dynamics in Optical Systems* edited by N. B. Abraham, F. T. Arecchi, and L. A. Lugiato, Opt. Soc. Am., Washington, (1991).

[7] *Nonlinear Dynamics and Quantum Phenomena in Optical Systems* edited by R. Vilaseca and R. Corbalán, Springer Verlag, Berlin (1991).

[8] *Lectures in the sciencies of Complexity*, edited by D. L. Stein, Addison Wesley, Reading, Massachutssets (1988).

[9] *J. Opt. Soc. Am. B* **7** *(nos. 6 and 7)*, special issues on transverse effects in nonlinear optical systems, edited by N. B. Abraham and W. J. Firth (1990).

[10] F. T. Arecchi, G. L. Lippi, G. P. Puccioni, and J. R. Tredicce, Opt. Comm. **51**,

3081 (1985).

[11] N. G. Van Kampen, *Stochastic Processes in Physics and Chemistry*, North Holland, Amsterdam (1981).

[12] W. Horsthemke and R. Lefever, *Noise Induced Transitions*, Springer Verlag, Berlin (1983).

[13] H. Haken, *Light* Vol. II, North Holland, Amsterdam (1985).

[14] M. Sargent III, M. O. Scully, and W. E. Lamb Jr., *Laser Physics*, Addison Wesley, Reading, Massachutssets (1974).

[15] F. T. Arecchi, V. de Giorgio, and B. Querzola, Phys. Rev. Lett. **19**, 1168 (1967).

[16] D. Meltzer and L. Mandel, Phys. Rev. Lett. **25**, 1151 (1970).

[17] F. T. Arecchi and A. Politi, Phys. Rev. Lett **45**, 1219 (1980); F. T. Arecchi, A. Politi, and L. Ulivi, Nuovo Cimento B **71**, 119 (1982).

[18] R. Roy, A. W. Yu and S. Zhu, Phys. Rev. Lett, **55**, 2794 (1985); Phys. Rev. **A34** 4333 (1986).

[19] R. Roy, A. W. Yu and S. Zhu in *Noise in Nonlinear Dynamical Systems*, eds. F. Moss and P. McClintock, Cambridge University Press (1988).

[20] M. R. Young, and S. Singh, Phys. Rev. **A35**, 1453 (1987); J. Opt. Soc. Am. **B5**, 1011 (1988).

[21] V. De Giorgio, M. O. Scully, Phys. Rev. **A2**,1170.

[22] R. Graham and H. Haken, Z. Phys. 213, 240 (1968); R. Graham and H. Haken,

235, 166 (1970);R. Graham and H. Haken, 237, 31 (1970).

[23] P. Lett, E. C. Cage and T. Chyba, Phys. Rev. **A35**, 746 (1987).

[24] M. San Miguel in *Instabilities and Chaos in Quantum Optics II* edited by N. B. Abraham, F. T. Arecchi, and L. A. Lugiato, Plenum Press, New York (1988).

[25] M. Aguado and M. San Miguel, Phys. Rev. **A37**, 450 (1988).

[26] E. Peacock-López, F. J. de la Rubia, B. J. West and K. Lindenberg, Phys. Rev **A39**, 4026 (1989).

[27] M. Aguado, E. Hernández García and M. San Miguel, Phys. Rev **A38**, 5670 (1988).

[28] P. Mandel and T. Erneux, Phys. Rev. Lett. **53**, 1818 (1984).

[29] T. Erneux and P. Mandel, Phys. Rev. **A30**, 1902 (1984).

[30] P. Mandel and T. Erneux, IEEE J. Quantum. Electron. **QE–21**, 1352 (1985).

[31] T. Erneux and P. Mandel, SIAM J. Appl. Math. **46**, 1 (1986).

[32] P. Mandel and T. Erneux, J. Stat. Phys. **48**, 1059 (1987).

[33] P. Mandel, Opt. Comm. **64**, 549 (1987).

[34] T. Erneux and P. Mandel, Phys. Rev. **A39**, 5179 (1989).

[35] T. Erneux and P. Mandel, Opt. Comm. **85**, 43 (1991).

[36] P. Mandel in *Far from equilibrium Phase Transitions*, ed. L. Garrido, Springer Verlag, Berlin, (1988).

[37] P. Mandel in *Instabilities and Chaos in Quantum Optics II* edited by N. B. Abraham, F. T. Arecchi, and L. A. Lugiato, Plenum Press, New York (1988).

[38] P. Glorieux and D. Dangoisse, IEEE. J. Quantum Electron. **QE–21**, 1486 (1985).

[39] E. Arimondo, D. Dangoisse, C. Gabbanini, E. Menchi, and P. Papoff, J. Opt. Soc. Am. B 4, 892 (1987); E. Arimondo, D. Dangoisse and L. Fronzoni, Europhys. Lett. 4 287 (1987).

[40] W. Scharpf, M. Squicciarini, D. Bromley, C. Green, J.R. Tredicce, and L. M. Narducci, Opt. Comm. **63**, 344 (1987); W. Scharpf, *Delayed bifurcation at threshold in argon–ion lasers.* Ph. D. Thesis, Drexel University (1988).

[41] F. T. Arecchi, W. Gadomski, R. Meucci, and J. A. Roversi, Opt. Comm. **65**, 47 (1988); F. T. Arecchi, R. Meucci, and J. A. Roversi, Europhys. Lett. **8**, 225 (1989); F. T. Arecchi, W. Gadomski, R. Meucci, and J. A. Roversi, Phys. Rev. **A39**, 4004 (1989); F. T. Arecchi, W. Gadomsky, R. Meucci, and J. A. Roversi, Opt. Comm **70**, 155 (1989); M. Ciofini, R. Meucci, and F. T. Arecchi, Phys. Rev. **A42**, 482 (1990).

[42] P. Spano, A. D'Ottavi, A. Mecozzi, and B. Daino, Appl. Phys. Lett. **52**, 2203 (1988); A. Macozzi, S. Piazzolla, A. D'Ottavi, and P. Spano, Phys. Rev. **A38**, 3136 (1988); P. Spano, A. D'Ottavi, A. Mecozzi, B. Daino, and S. Piazzolla, IEEE J. Quantum Electron **QE–25**, 1440 (1989).

[43] D. Bromley, E. J. D'Angelo, J. R. Tredicce and S. Balle, Opt. Comm. (in press).

[44] P. Jung, G. Gray, and R. Roy, Phys. Rev. Lett. **65**, 1873 (1990).

[45] F. J. de la Rubia and W. Kliemann in *Noise and Nonlinear Phenomena in Nuclear Systems*, ed. by J. L. Muñoz Cobo and F. C. Filippo, Plenum Press, New York (1988).

[46] L. Arnold, W. Kliemann, in *Probabilistic Analysis and related Topics*, vol. 3, A. T. Barucha–Reid, Academic Press, New York (1983).

[47] W. Horsthemke and R. Lefever, Phys. Lett. A **64** 19 (1977).

[48] L. Arnold, W. Horsthemke and R. Lefever, Z. Phys. B **22** 867 (1978).

[49] W. Horsthemke and M. Malek Mansour, Z. Phys B **24** 307 (1976).

[50] S. Kabashima and T. Kawakubo, Phys. Lett. A **70** 375 (1979).

[51] S. Kai, T. Kai, M. Takata, and K. Hisakawa, J. Phys. Soc. Jpn. **47** , 1379 (1979); T. Kawakubo, A. Yanagita, and S. Kabashima, J. Phys. Soc. Jpn. **50**, 1451 (1981).

[52] S. D. Robinson, F. Moss, and P. V. E. McClintock, J. Phys. A **18** L89 (1985).

[53] L. Fronzoni, R. Manella, P. V. E. Mc Clintock, and F. Moss, Phys. Rev. **A36** 834 (1987).

[54] R. Lefever and J. Wm Turner, Phys. Rev. Lett. **56** 1631 (1986).

[55] R. Graham, Phys. Rev. **A25**, 3234 (1982).

[56] M. C. Mackey, A. Longtin, and A. Lasota, J. Stat. Phys. **60**, 735 (1990).

[57] M. San Miguel and S. Chaturvedi, Z. Phys. B **40**, 167 (1980).

[58] C. Jeffries and K. Wiesenfield, Phys. Rev. **A31** 1077 (1985); K. Wiesenfield, J.

Stat. Phys. **38**, 1971 (1985).

[59] J. Crutchfield, M. Nauenberg, and J. Rudnick, Phys. Rev. Lett. **46** 933 (1981).

[60] B. Shraiman, C. E. Wayne and P. C. Martin, Phys. Rev. Lett. **46** 935 (1981).

[61] A. Longtin, Phys. Rev **A** 44 4801 (1991).

[62] M. Suzuki, Adv. Chem. Phys. **46**, 195 (1981).

[63] F. Haake, Phys. Rev. Lett. **41**, 1685 (1978); F. Haake, J. W. Haus and R. Glauber, Phys. Rev. **A23**, 3255 (1981).

[64] F. de Pasquale, and P. Tombesi, Phys Lett. **A72**, 7 (1979); F. de Pasquale, P. Tartaglia and P. Tombesi, Physica **99A**, 581 (1979); Phys. Rev. **A25**, 466 (1982).

[65] M. San Miguel, in *Laser Noise*, ed. R. Roy, SPIE, Boston, 272 (1990).

[66] F. De Pasquale, J. M. Sancho, M. San Miguel and P. Tartaglia, Phys. Rev. Lett. **56**, 2473 (1986);Phys. Rev. **A334360** (1986).

[67] S. Balle, M. San Miguel, N. B. Abraham, J. R. Tredicce (preprint).

[68] S. Balle, P. Colet and M. San Miguel, Phys. Rev. **A43** 498 (1991).

[69] P. Spano, A. Mecozzi, and A. Sapia, Phys. Rev. Lett. **64**, 3003 (1990); A. Mecozzi, P. Spano and A. Sapia, Opt. Lett. **15**, 1067 (1990).

[70] P. Glorieux and D. Dangoisse, in *Handbook of Molecular Lasers*, edited by P. K. Cheo, Marcel Dekker, New York (1989).

[71] L. Lugiato in *Progress in Optics XXI*, ed. E. Wolf, North Holland (1984).

[72] L. Lugiato en *Frontiers in Quantum Optics*, eds. E. R. Pike and S. Sarkar, Adam Hilger (1986).

[73] R. Deserno, R. Kume, F. Mitschke and J. Mlyneck, SPIE Proc 700, 83 (1986); W. Lange, F. Mitschke, R. Deserno and J. Mlyneck, Phys. Rev. **A32**, 1271 (1985);W. Lange en *Dynamics of nonlinear optical systems* eds. L. Pesquera and F. J. Bermejo, World Sci. (1989).

[74] G. Broggi and L. Lugiato, Phys. Rev. **A29**, 2949 (1984); G. Broggi, L. Lugiato and A. Colombo, Phys. Rev. **A32**, 2803 (1985).

[75] P. Colet, M. San Miguel, J. Casademunt and J. M. Sancho, Phys. Rev. **A39**, 149 (1989).

[76] A. Valle, L. Pesquera and M. A. Rodríguez, Opt. Comm. **79**, 1561 (1990).

[77] P. Colet, F. de Pasquale, M. O. Cáceres and M. San Miguel, Phys. Rev. **A41**, 1901 (1990); F. Papoff, D. Dangoisse, A. Fioretti, E. Arimondo, P. Colet and M. San Miguel in *Nonlinear Dynamics in Optical Systems* ed. N. B. Abraham, F. T. Arecchi and P. Mandel, Opt. Soc. Am. Washington (1991); P. Colet, F. de Pasquale and M. San Miguel, Phys. Rev. A (1991).

[78] M. Mortazavi and S. Singh, Phys. Rev. Lett. **64**, 741 (1990).

[79] F. Baras, G. Nicolis, M. Malek Mansour and J. W. Turner, J. Stat Phys **32**, 1 (1983); M Frankowicz, M. Malek Mansour and G. Nicolis, Physica **125 A** 237 (1984).

[80] G. Broggi, A. Colombo, L. Lugiato and P. Mandel, Phys. Rev. **A33**, 3635 (1986).

[81] M. C. Torrent and M. San Miguel, Phys. Rev. **A38** 245 (1988).

[82] H. Zeghlache, P. Mandel, and C. Van den Broeck, Phys. Rev. **A40**, 286 (1989).

[83] N. G. Stocks, R. Manella and P. V. E. McClintock, Phys. Rev **A40** 5361 (1989).

[84] R. Manella, F. Moss and P. V. E. McClintock, Phys. Rev. **A35**, 2560 (1987); R. Manella, P. V. E. McClintock and F. Moss , Phys. Lett. **A120**, 11 (1987).

[85] M. Giorgiou and T. Erneux, Phys. Rev. **A45**, 6636 (1992).

[86] G. Ahlers, M. C. Cross, P. C. Hohenberg and S. Safran, J. Fluid. Mech. **110**, 297 (1981).

[87] B. Caroli, C. Caroli and D. Saint James, Physica **108A**, 233 (1981).

[88] A. Valle, L. Pesquera and M. A. Rodríguez, Phys. Rev **A45**, 5243 (1992).

[89] F. de Pasquale, Z. Racz, M. San Miguel and P. Tartaglia, Phys. Rev. **A30**, 5228 (1984);M. San Miguel in *Instabilities and Nonequilibrium Structures II* 285, Kluwer Acad. Pub. (1989).

[90] B. McNamara, K. Wiesenfeld, Phys. Rev. **A39**, 4854 (1989).

[91] A. Sapia, A. D'Ottavi, P. Spano, P. Colet, C. Mirasso and M. San Miguel Appl. Phys. Lett. **61**, 1748 (1992).

[92] P. Spano, A. D'Ottavi, A. Mecozzi, and S. Piazzolla, IEEE J. Quantum. Electron, **25**, 1440 (1989)

[93] S. Balle, C. Mirasso, A. Sapia and P. Spano, enviado a publicar.

[94] C. Mirasso, P. Colet and M. San Miguel, Opt. Lett. **16**, 1753 (1991); IEEE J.

Quantum Electron. **29**, 23 (1993)

[95] C. Mirasso, P. Colet and M. San Miguel, IEE Proc. J, (1993); P. Colet, C. Mirasso and M. San Miguel, IEEE J. Quantum. Electron, en imprenta

[96] A. Valle, M. A. Rodríguez and C. R. Mirasso, Opt. Lett. **17**, 1523 (1992).

[97] J. B. Swift, P. C. Hohenberg, and G. Ahlers, Phys. Rev. **A43**, 6572 (1991).

[98] M. O. Caceres, A. Becker and L. Kramer, Phys. Rev. **A43**, 6581 (1991).

[99] A. Valle, M. A. Rodríguez and L. Pesquera, Phys. Rev. **A**, en imprenta.

[100] K. Kaminishi, R. Roy and L. Mandel, Phys. Rev **A24**, 370 (1981); A. Abate, H. J. Kimble, L. Mandel, Phys. Rev. **A14**, 788 (1976); P. Lett, R. Short, and L. Mandel, Phys. Rev. Lett. **52** 341 (1984).

[101] G. P. Agrawal in *Laser Noise*, ed. by R. Roy, SPIE, Boston (1990).

[102] G. P. Agrawal and N. K. Dutta, *Long wavelength semiconductor lasers* , Van Nostrand Reinhold company, New York (1986).

[103] P. Spano, A. Mecozzi, A. Sapia and A. D'Ottavi in *Nonlinear Dynamics and quantum phenomena in optical systems*, eds. R. Vilaseca and R. Corbalán, Spinger Verlag, Berlin (1991).

[104] M. Yamada and Y. Suematsu, IEEE J. Quantum. Electron. **QE15**, 743 (1979).

[105] C. H. Henry, IEEE J. Quantum Electron. **QE18**, 259 (1982).

[106] P. Spano, S. Piazzolla, and M. Tambourini, IEEE J. Quantum Electron, **QE19**, 1195 (1983).

[107] K. Kishino, S. Aoki, and Y. Suematsu, IEEE J. Quantum Electron., **QE18**, 343 (1982).

[108] S. Balle, P. Colet, and M. San Miguel, Phys. Rev. **A43**, 498 (1991); S. Balle, N. B. Abraham, P. Colet and M. San Miguel, IEEE J. Quantum Electron **29** 33 (1993).

[109] A. Mecozzi, A. Sapia, P. Spano, and G. P. Agrawal, IEEE J. Quantum. Electron. **QE27** 332, (1991).

[110] J. C. Cartledge, IEEE J. Quantum Electron, **QE26**, 2046 (1990).

[111] T. B. Anderson and B. Clarke, IEEE J. Quantum Electron, **QE29**, 3 (1993).

[112] A. Valle, P. Colet, L. Pesquera and M. San Miguel, aceptado en IEE Proc. **J**.

[113] S. E. Miller, IEEE J. Quantum Electron. **QE25** 1771 (1989); IEEE J. Quantum Electron **QE26** 242 (1990).

[114] A. Valle, A. Mecozzi, L. Pesquera, M. A. Rodríguez and P. Spano, aceptado en Phys. Rev. **A**.

[115] P.Hanggi and H.Thomas, Phys.Rep. 88, 209 (1982).

[116] C.W. Gardiner, "Handbook of Stochastic Methods", Springer Verlag 1983

[117] H.Risken, "The Fokker–Planck Equation. Methods of Solution and applications", Springer Verlag, 1984.

[118] Noise in Nonlinear Dynamical Systems, edited by F.Moss and P.McClintock (Cambridge University Press, 1989).

Chapter 1

Relaxation from a marginal state in optical bistability. Anomalous fluctuations and first–passage time statistics

1.1 Introduction

In optical bistability the output intensity presents a hysteresis cycle when plotted versus the intensity of the driving laser. For the value of the incident intensity associated with the end points of the hysteresis cycle the dynamics is determined by a potencial with a marginal state. The normal form of this type of potencial is given by

$$V_m(x) = -a(x-x_0)^3 + b(x-x_0)^4 - \beta(x-x_0) \qquad (a,b>0). \tag{1}$$

In optical bistability β is the difference between the incident intensity and its value at the end point of the hysteresis cycle. The marginal state occurs for $\beta = 0$ at $x = x_0$.

We analyze here the decay of marginally stable states including the effects of fluctuations. A typical experiment concerning relaxation close to marginality in an optical bistable device is as follows [1–7]. The incident intensity is suddenly switched from a small value close to the one associated with the end point of the lower branch of the hysteresis cycle. Then, the system will eventually relax to a state in the upper branch.

The transient behavior of optical bistable systems is experimentally well known [1–6] (see refs. [4, 6] for recent reviews). Experimental results show intense fluctuations both in the first passage time (FPT) of a given level and in the output light intensity when the control parameter is suddenly placed near the end point of the

hysteresis cycle. This gives evidence for a transient from either a marginal or a near–to–marginal point. Moreover, the so–called transient bimodality is another sign of marginality [7]. Fluctuations in the FPT, in the output light intensity and transient bimodality are also seen in analogue simulations [2] and numerical calculations [7]. Most of the results found in experimental systems have been reproduced with these simulations. However, there are few theoretical studies of this problem [8–14].

Most of the theoretical analysis of relaxation from marginal states are devoted to the calculation of FPT statistics. Using asymptotic FPT statistics (small noise intensity D) it has been shown [11] that the relaxation time is given by a universal scaling function of the parameter

$$k = (\beta/a)(a/D)^{2/3}, \tag{2}$$

which measures deviation from marginality. This prediction has been recently tested on an electronic circuit [15].

The other alternative point of view to describe a relaxation process is the transient evolution of statistical moments. In the marginal case this approach is directly connected with the phenomenon of transient bimodality [7]. Here we analyze the existence of such a bimodality in terms of an adimensional parameter $\eta = t_d/\sigma_T$, where σ_T is the variance of the time T that the process take to leave the marginal state, and t_d is the deterministic time required to reach a point close to the steady state in the upper branch. Transient bimodality is shown to appear when η is small. This analysis of transient bimodality suggests that a good description of the statistical properties during the relaxation process can be achieved with a step function approximation of the stochastic paths centered at the escape time T. Anomalous fluctuations in transients from states close to marginality can then be characterized using FPT statistics [12]. We show that the maximum of the fluctuations happens in the median of the

FPT distribution. The value of this maximum is given in terms of the initial and final states. This characterization of anomalous fluctuations is directly related to the existence of transient bimodality. Our predictions are then valid whenever η is small, even when k is not very small ($k \approx 1$).

These results are universal in the sense that they are independent of the details of the model provided the noise is white and additive. The central assumption is the existence of a potencial with a cubic saddle point. Since we are mainly interested in optical bistable systems, we check the validity of our predictions with simulations of the Bonifacio–Lugiato model of absorptive bistability in the good cavity case.

1.2 Formulation of the problem

We consider a one dimensional system which can be described by the following Langevin equation,

$$\dot{x} = -V'(x) + \xi(t), \tag{3}$$

where $\xi(t)$ is a white noise with an intensity D, x is the relevant variable of our system (amplitude of the transmitted field in optical bistability) and the explicit expression for the potential $V(x)$ is not needed. In terms of the probability density $P(x,t)$, eq. (3) is equivalent to a Fokker–Planck equation

$$\partial P(x,t)/\partial t = \partial[V'(x)P]/\partial x + D\partial^2 P(x,t)/\partial x^2. \tag{4}$$

Although our analysis can be applied to any case, we focus our attention to marginal initial states which are relevant to optical bistable systems. For the sake of comparison with standard theories we also consider the well studied case of decay from unstable points [16] associated with the potential

$$V_u = -c(x - x_0)^2 + d(x - x_0)^4. \tag{5}$$

In both cases we can distinguish three regions in the decay from a state x_0 (either an unstable or near–to–marginal point). In the first region the system is close to x_0 and the evolution is then dominated by the noise. In the second the system leaves the state x_0 and the noise effects have a relatively small influence on the evolution which is essentially deterministic. In the third region a final state x_s is approached and the evolution around x_s is again dominated by the fluctuations. When the noise is weak ($D << 1$) the noise dominated regions are small. Then we can approximate the potential by $V(x) \approx -c(x-x_0)^2$ (unstable case) and by $V(x) \approx -a(x-x_0)^3-\beta(x-x_0)$ (marginal case) in the first region, and by $V(x) \approx \gamma(x-x_s)^2 + V(x_s)$ in the third region.

We first analyze the marginal case. When $\beta = 0$ the state x_0 is a marginal point. In this case a simple analysis shows that the first (noise dominated) region corresponds to $\mid x - x_0 \mid << x_1 = (D/a)^{1/3}$ (we have checked this with numerical simulations). When $\beta \neq 0$ the deterministic evolution due to the term $-\beta(x-x_0)$ is dominated by the noise in the region $\mid x - x_0 \mid << x_2 = (D/\beta)$. Finally, the cubic term $-a(x-x_0)^3$ is negligible with respect to the linear term $-\beta(x-x_0)$ when $\mid x - x_0 \mid << x_3 = (\beta/a)^{1/2}$. Since $x_1/x_2 = k$, $x_3/x_2 = k^{3/2}$ and $x_3/x_1 = k^{1/2}$, the parameter k appears in the analysis in a natural way. When $k << 1$, $x_3 << x_1 << x_2$, and we can distinguish the following regions: a first region, $\mid x-x_0 \mid << x_1$, dominated by the noise; the deterministic region, $x_1 << (x-x_0) << (x_s-x_0) - (D/2\gamma)^{1/2}$, where the β term is negligible; and a third region around x_s again dominated by the noise. Since the β term is always negligible, it is clear than in this case ($k << 1$) we are close to marginality [11]. On the contrary when $k >> 1$, $x_2 << x_1 << x_3$, and there is a region defined by $x_2 << \mid x - x_0 \mid << x_3$, where the evolution is mainly due to the β term of the potential. When $\beta < 0$ relaxation occurs via an activation mechanism of escape through a barrier due to fluctuations. For $\beta > 0$ the relaxation

is essentially deterministic. Therefore for $k >> 1$ we are far from marginality [11]. Finally, when $k \approx 1$ we can distinguish the same regions as in the case $k << 1$, but now when $\mid x - x_0 \mid \approx x_1 \approx x_2 \approx x_3$ the β term must be considered. However, this case is similar to the marginal one in the sense that there is no region of interest in which a linear approximation is meaningful.

The relaxation process from a state of marginal stability requires then a nonlinear description right from the beginning. This is the essential difficulty in the description of the decay of a marginal state. On the contrary in the unstable case there is a noise dominated region $\mid x - x_0 \mid << (D/2c)^{1/2}$ and a linear deterministic region $(d/2c)^{1/2} << \mid x - x_0 \mid << (c/d)^{1/2}$, where the cuadratic term in the potential (5) is negligible. Therefore the initial stage of the relaxation process is associated with linear stochastic dynamics, so that an initial description in terms of gaussian statistics is possible [16].

We note that an approximation for the stochastic path occuring in the decay process has been recently obtained in the subcritical pitchfork bifurcation [14]. In this case, and close to the instability, the equation of motion is $\dot{x} \approx (x - x_0)^3$. However, this approximation is not suitable for the kind of marginality analyzed here. The saddle–node case lacks an inversion symmetry $(x - x_0) \rightarrow -(x - x_0)$ in the relaxation from x_0. The difficulty is then that a different approximation is required for the stochastic paths in wich initially $x(t)$ becomes positive or negative.

Our strategy in the following is to extract some information about the transient time–dependent variance of x from the FPT distribution. The most relevant information can be qualitatively obtained form the analysis of transient bimodality.

1.3 Transient bimodality

As it is known from experimental and numerical results [1–7], transient bimodality

is a signature of decay from marginal states. This phenomenon means that the probability distribution, which is initially one–peaked develops a second peak during a sizeable interval of time evolution [7]. In the last stages of the time evolution the first peak gradually disappears and the system approaches the stationary one–peaked distribution. The physical meaninig is that during a sizable interval of time the system can be found in two states, initial and final, with similar probability.

The reason for the existence of transient bimodality becomes clear if we consider the form of the potencial V_m in a situation close to marginality (see eq. (1)). The probability distribution is initially a delta function, $P(x,0) = \delta(x - x_0)$ which sits for a long time in the noise dominated region (flat part of the potential). As a consequence of diffusion and of the asymmetry of the potential, it broadens and develops a tail in the direction of the potential well. As soon as the leading edge of the tail reaches the boundary of the deterministic region, it is quickly transferred to the bottom of the potential, thereby giving rise to the second peak. Only later the first peak disappears, thus restoring a one–peaked distribution around the steady state x_s. Therefore transient bimodality appears when the evolution exhibits a long induction stage near x_0 followed by a rapid transition to the stable state x_s [7]. This phenomenon has been discussed [17, 7] in chemical and optical systems and observed [1–6] in optical and electronic systems.

According to the above discussion, transient bimodality can be characterized in the following way. The time that the process take to leave the state x_0 or escape time, T, is of the order FPT needed to reach the threshold of the deterministic region. The transition time, t_d, is the time required to cross this region. Transient bimodality is possible when t_d is shorter than σ_T (the variance of T). Therefore the parameter $\eta = t_d/\sigma_T$ can be used to characterized this phenomenon. The physical meaninig of η can be better understood with the help of fig. 1, where the range of scape time is

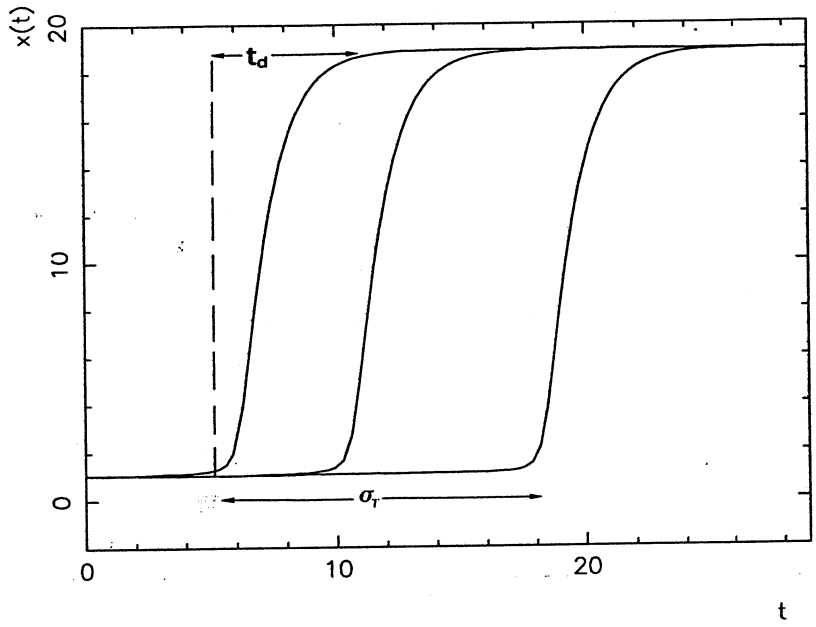

Fig. 1. Schematic plot of temporal dependence of state variable in three sucessive switching events

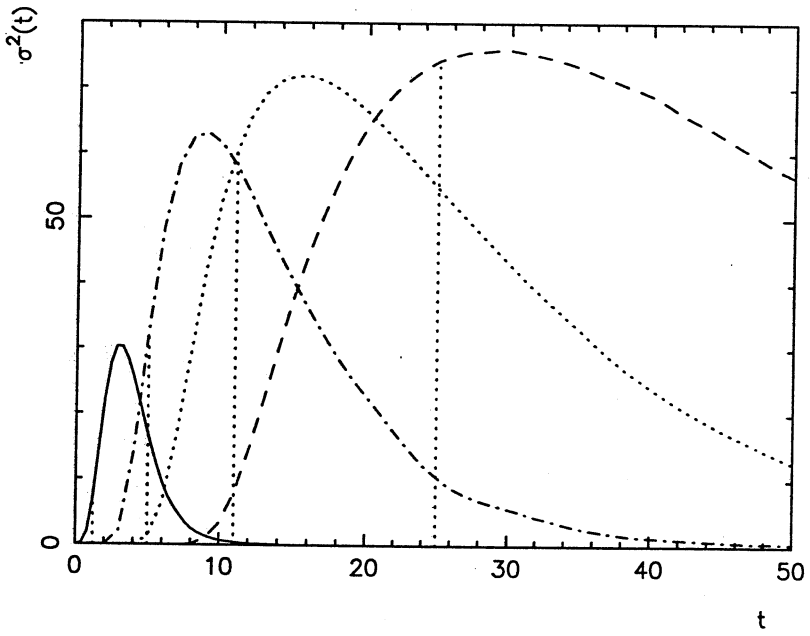

Fig. 2. Variance $\sigma^2(t)$ versus time for different values of D. Solid line: $D = 10^{-1}, \eta = 1.8$; dot–dashed line: $D = 10^{-3}, \eta = 0.6$; dotted line: $D = 10^{-4}, \eta = 0.37$; dashed line: $D = 10^{-5}, \eta = 0.2$. Vertical dotted lines correspond to t_m. The parameters in (21) are taken to be $C = 20$, $y = 21.0264$.

roughly given by σ_T. It is clear that the parameter η is proportional to the probability that the system is in the deterministic region between the peaks. The probability that the system lies at the peaks in x_0 and x_s tends to one when η decreases. Therefore, the smaller the parameter η is, the more perfect is the bimodality. The calculation of η is straightforward in most cases. For example, in the unstable case, using the asymptotic values of σ_T ($D << 1$), we have , $\eta \sim O(-lnD)$. As expected, transient bimodality as defined above is not possible in this case when $D \to 0$.

In the marginal case and taking the same approximation for σ_T [11] we have $\eta \sim O(D^{1/6})$ which shows that bimodality will appear when D is small. Hence, as the noise intensity decreases, η decreases. Bimodality is then favoured. In such a situation it is easy to see from simple statistical arguments that the maximum of the fluctuations is reached when the two peaks have the same area. This correspond to a time given by the median of the escape time distribution. The value of the maximum of the variance is $(x_0-x_s)^2/4$, where x_0 and x_s are the position of the peaks. Moreover when η is small, it is clear that a stochastic path, $x(t)$, is very close to x_0 until a time T at which it jumps nearly instantaneously to a point close to the steady state x_s. It makes sense an approximation given by

$$x(t) = x_s\theta(t-T) + x_0\theta(T-t), \tag{6}$$

where θ is the Heaviside step function. The statistical properties of $x(t)$ can then be obtained from the distribution for the passage time T. In the following section we use this analysis to characterize transient fluctuations.

1.4 Characterization of anomalous fluctuations

Our keypoint in this section is to extract some information about $P(x,t/x_0)$ and associated moments from the FPT statistics and more specifically from $W_{x0}(a_0,T)$

which is the FPT probability density. Here x_0 and a_0 are the starting and final position. This can be done with the use of the approximation

$$P(x,t/x_0) \approx P_d(x,t/x_0) = \int_0^\infty W_{x0}(a_0,T)\delta[x - x(a_0,t-T)]dT, \qquad (7)$$

where a_0 is required to belong to the deterministic region and $x(a_0,t)$ is the deterministic trajectory starting at a_0, i.e., $x(a_0,0) = a_0$. This approximation means that the exact trajectory which crosses a_0 in time T is replaced by the deterministic trajectory which crosses a_0 in a time T and evolving towards either the future ($t > T$) or the past ($t < T$). Note that the greatest error in this approximation will happen when x belongs to the noise regions. However, when the noise is weak these regions are small, and consequently the errors in the moments are also small. This approximation gives then a good description of anomalous fluctuations during the transient, since they are not of order D.

With the use of eq. (7) the transient fluctuations are given by

$$\sigma^2(t) = \langle x^2\rangle - \langle x\rangle^2 = \int_0^\infty W_{x0}(a_0,T)x(a_0,t-T)^2dT - \left(\int_0^\infty W_{x0}(a_0,T)x(a_0,t-T)dT\right)^2. \qquad (8)$$

This approximation is accurate for a large variety of relaxation process . If we consider a situation such that there is transient bimodality we can go one step further in the approximation. According to the discussion of section 1.3, the trajectory $x(a_0,t-T)$ can be approximated by a step function $x_s\theta(t-T)+x_0\theta(T-t)$ with an error of order η. Then we get

$$\sigma^2(t) = (x_s - x_0)^2\left[\int_0^t W_{x0}(T)dT - \left(\int_0^t W_{x0}(T)dT\right)^2\right], \qquad (9)$$

where we have dropped a_0, since in this case the FPT distribution is rather independent of the explicit value of the level for any a_0 clearly away from the marginal state.

Eq. (9) establish a connection between the transient fluctuations and the passage distribution. A similar idea has been used in the analysis of relaxation from a marginal state in a subcritical pitchfork bifurcation [14].

With the use of eq. (9) it is easy to show that the maximum of the variance happens in the median of $W_{x0}(T)$,

$$\frac{1}{2} = \int_0^{t_{max}} W_{x0}(T)dT, \tag{10}$$

and that it has a value given by

$$\sigma_m^2 = \sigma^2(t_{max}) = (x_s - x_0)^2/4, \tag{11}$$

in agreement of the qualitative discussion of section 3. These two quantities, t_{max} and σ_m^2, are useful to characterize fluctuations. Therefore we have shown how to describe anomalous fluctuations with the use of FPT statistics.

The accuracy and validity of our approach is substantiated in the next section by numerical simulations for the Bonifacio– Lugiato potential [18].

1.5 Transient fluctuations for the Bonifacio– Lugiato potential

To check the validity of eqs. (9)–(11) we compare these predictions with simulations results for the Bonifacio–Lugiato model of absorptive bistability [18]. In this model the potential is

$$V_y(x) = -yx + x^2/2 + Cln(1 + x^2), \tag{12}$$

where y is the incident field, x is the amplitude of the transmitted field and C is the bistability parameter. A hysteresis cicle exists for $C > 4$. We take $C = 20$ in all our numerical simulations. For this value of the bistability parameter the potential V_y has a marginal point $x = x_0 = 1.0543$ when $y = y_M = 21.026373$

(upswitching threshold). An expansion of (12) for x close to the marginal state yields $V_y(x) \approx V_y(x_0) - a(x-x_0)^3 - \beta(x-x_0)$ with $\beta = y - y_M$ and $a = 2.8021$.

Simulations are performed approximating the white Gaussian noise $\xi(t)$ by a Poisson one [19]. White Poisson noise is given by a sequence of delta peaks at random times determined by a Poisson counting process. In all simulations we take $\lambda = 100$, where λ is the mean time difference between pulses. The amplitude of the pulses is exponentially distributed with a mean value $\omega_0 = (D/\lambda)^{1/2}$. In figs. 2, 3 results correspond to averages over 5000 trajectories. We have checked that the same results are obtained with 2000 trajectories. Results in table 1 are then derived using 2000 trajectories. We have also checked that the same results are obtained with the simulation method indicated in ref. [20]. To get the FPT distribution corresponding to the escape time T, we take $a_0 = 5(D/3a)^{1/3} + x_0$. We have checked that a_0 belongs to the deterministic region .

We show in fig. 2 the transient evolution of the variance $\sigma^2(t)$ for relaxation very close to marginality ($y = 21.0264$) with the initial condition at x_0 and for different values of the noise intensity. In this case the parameter k, which measures deviation from marginality, takes its greatest value $k = 0.04$ for $D = 10^{-5}$. We observe that the median t_m of the FPT distribution of T approaches the time associated to the maximum of the variance when the noise intensity D and the parameter η decrease. As concerns the maximum of the variance, the value predicted by (13) is $\sigma_m^2 = 79.78$. The simulation results show that this value is approached when η and D decrease. Therefore, our predictions (10) and (11) are valid close to marginality ($k << 1$) when the parameter η is small. We have also checked that eq. (9) is valid in this case.

As concerns transient bimodality, fig. 3 shows that for $D = 10^{-4}$ the two peaks have almost the same area when the maximum of the variance is reached ($t_{max} \approx 15$). This result is in agreement with the discussion in section 1.3.

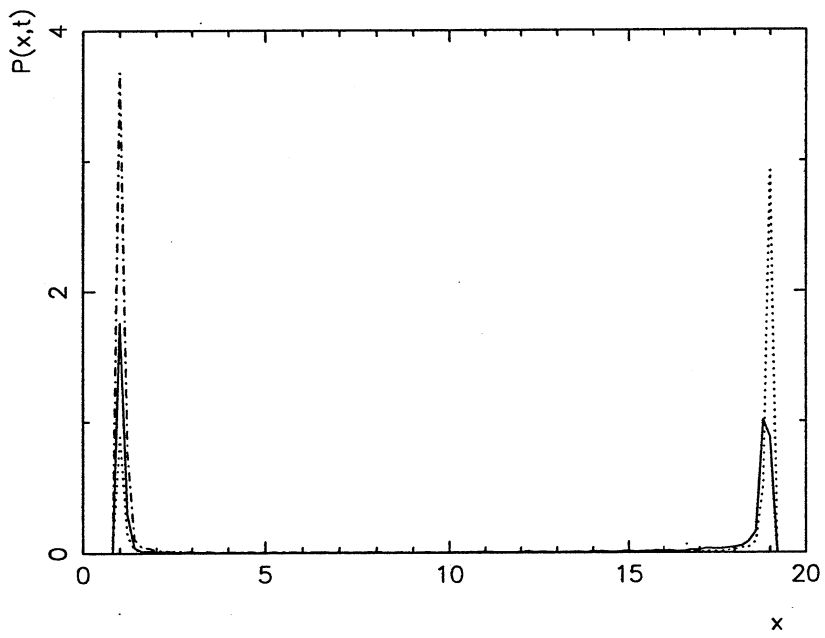

Fig. 3. Time evolution of the probability distribution for $t = 5(- . - .), t = 15(- - - -), t = 25(....)$. Parameters values are the same as in the dotted line in Fig. 2.

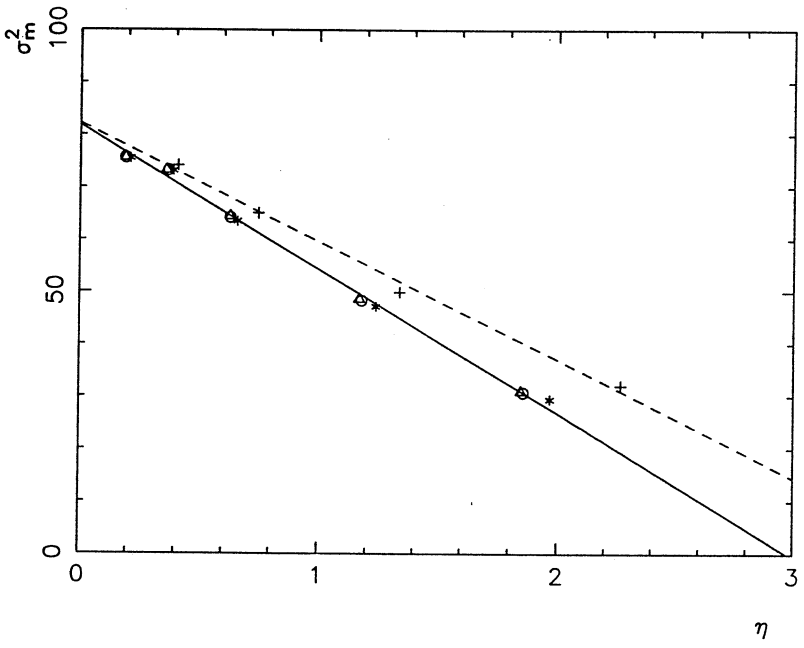

Fig. 4. Maximum of the variance versus η for different values of k.+ : $k = 1$; $*$: $k = 10^{-1}$; O : $k = 10^{-2}$ and triangles: $k = 10^{-3}$

We remark that the validity of eqs. (9)–(11) is directly related to η and not to k. The result in fig. 2 show that our predictions are valid only when η is small, even if k is always very small ($k \leq 0.04$). In fact these parameters have an opposite behavior with the noise intensity. When D increases, k decreases (see eq. (2)) and, since σ_T also decreases, η increases (see fig. 2).

We now analyze the validity of (10)–(11) when the system begins to deviate from marginality by increasing k and for different values of the noise intensity D. In all simulations we take $\beta > 0$, which corresponds to most of the experimental results. As concerns t_{max}, we observe (see table 1) that t_m approaches t_{max} when the parameter η is small, even for $k = 1$. In fact our results do not substantially change with k when the system is close to marginality ($k = 10^{-1}, 10^{-2}, 10^{-3}$). From table 1 we see that t_{max} is always greater than t_m. This result can be explained with a simple model introduced below.

In fig.4 we plot σ_m^2 versus the parameter η for different values of k. The corresponding values of D can be obtained from table 1. We see that, as for t_{max} and t_m, the maximum of the variance does not change with k when this parameter is small. In this case our results can be fitted with the straight line

$$\sigma_m^2 = -27.46\eta + 81.83 \qquad (13)$$

Another straight line with a slope -22.28 can be used to fit the values of σ_m^2 for $k = 1$. It is clear from fig. 4 that our numerical results get close to the theoretical value $\sigma_m^2 = 79.778$ when η is small.

We now explain our results $\eta > 0$ with the following simple model. We consider that for times close to t_{max} the probability distribution in the deterministic regions between the peaks can be taken as nearly uniform. In this region the trajectories can be approximated by straight lines (see fig. 1). The model is then valid when

the escape time distribution is nearly constant in an interval around t_{max} of width t_d (note that only trajectories leaving x_0 at these times contribute to the probability mass in the region between the peaks). We have checked this assumption when η is small. Since the variation in the total probability of the deterministic region, q_d, is the difference between changes in the probabilities of the peaks at x_0 and x_s, we can take q_d as a constant for time close to t_{max}. Using this model, it is easy to show that the maximum of the variance happens when the probability associated to the peak at x_0 is $p_0 = (1 - q_d)/2$. Again the maximum is reached when both peaks have the same probability. This result shows that $t_{max} > t_m$ is in agreement with the numerical simulations. The magnitude of the maximum is given by

$$\sigma_m^2 = (x_s - x_0)^2/4 - (x_s - x_0)^2 q_d/6 = 79.778 - 53.185 q_d. \qquad (14)$$

According to the discussion in section 1.3 q_d is proportional to η. Therefore close to marginality we get (13) with $q_d = 0.5\eta$. This gives a rough estimate for the probability corresponding to the region between peaks at times close to t_{max} as a function of the parameter η. Our results substantiate then the theoretical analysis of section 1.3.

D	k			
	1	10^{-1}	10^{-2}	10^{-3}
10^{-1}	0.9	1.3	1.3	1.3
	2.2	3	3	3
	0.59	0.56	0.56	0.56
	3.66	1.97	1.86	1.85
10^{-2}	1.7	2.5	2.7	2.7
	3.6	4.8	5	5
	0.52	0.48	0.46	0.46
	2.27	1.24	1.18	1.17
10^{-3}	3.7	5.1	5.5	5.5
	6.3	8.2	8.5	8.5
	0.41	0.38	0.35	0.35
	1.34	0.66	0.63	0.63
10^{-4}	7	11	11	12
	10.5	15	15	16
	0.33	0.26	0.26	0.25
	0.75	0.39	0.37	0.36
10^{-5}	16	23	25	25
	21.5	28.5	29	29
	0.25	0.19	0.13	0.13
	0.41	0.21	0.19	0.19

Table 1. First row: t_m; second row:t_{max}; third row: $\epsilon = \mid t_m - t_{max} \mid / t_{max}$; fourth row: η.

REFERENCES

[1] W. Lange, F. Mitschke, R. Deserno and J. Mlyneck, Phys. Rev. A **32**, 1271 (1985).

[2] F. Mitschke, R. Deserno, J. Mlyneck and W. Lange, IEEE J. Quantum Electron. **QE–21**, 1435 (1985).

[3] W. Lange, R. Deserno, F. Mitschke and J. Mlyneck in *From optical bistability towards optical computing*, edited by P. Mandel, S. D. Smith and B. S. Wherrett, (North–Holland, Amsterdam, 1987) p. 230.

[4] W. Lange in *Instabilities and chaos in quantum optics II*, edited by N. B. Abraham, R. T. Arecchi and L. A. Lugiato, (Plennum, New York, 1988) p. 265; W. Lange in *Noise in nonlinear dynamical systems, Vol. 3*, edited by F. Moss and P. McClintock, (Cambridge University Press, 1989) p. 159; W. Lange in *Dynamics of nonlinear optical systems*, edited by L. Pesquera and J. Bermejo, (World Scientific, Singapore, 1989) p. 118.

[5] E. Arimondo, D. Dangoisse and L. Fronzoni, Europhys. Lett. 4, 287 (1987); E. Arimondo, D. Dangoisse C. Gabbanini, E. Menchi and F. Papoff, J. Opt. Soc. Am. B 4 892 (1987);

[6] E. Arimondo in *Noise in nonlinear dynamical systems, Vol. 3*, edited by F. Moss and P. McClintock, (Cambridge University Press, 1989) p. 119.

[7] G. Broggi and L. A. Lugiato, Phys. Rev. A **29** 2949 (1984); G. Broggi L. A. Lugiato and A. Colombo, Phys. Rev. A **32** 2803 (1985).

[8] B. Caroli, C. Caroli and C. Roulet, Physica **101A**, 581 (1980).

[9] F. T. Arecchi, A. Politi and L. Ulivi, Nuovo Cimento **71 B**, 119 (1982).

[10] W. Horsthemke and D. E. Sigetti, Phys. Rev. A, to be published.

[11] P. Colet, M. San Miguel, J. Casademunt and J. M. Sancho, Phys. Rev. **A 39**, 149 (1989).

[12] M. A. Rodríguez and L. Pesquera in *Dynamics of nonlinear optical systems*, edited by L. Pesquera and J. Bermejo, (World Scientific, Singapore, 1989) p. 273.

[13] J. M. Sancho in *Synergetics, order and chaos* edited by M. G. Velarde, (World Scientific, Singapore, 1989) p. 580.

[14] P. Colet, F. de Pasquale, M. O. Caceres and M. San Miguel, Phys. Rev. **A 41**, 1901 (1990).

[15] F. Mitschke, C. Boden and W. Lange, Phys. Rev. **A 39**, 3690, (1989).

[16] M. Suzuki, Adv. Chem. Phys. **46**, 195 (1981); F. de Pasquale, P. Tartaglia and P. Tombesi, Phys. Lett. **78 A** 129 (1980).

[17] F. Baras, G. Nicolis, M. Malek–Mansour and J. W. Turner, J. Stat. Phys. **32** 1 (1983).

[18] L. A. Lugiato in *Progress in optics XXI*, edited by E. Wolf, (North Holland, Amsterdam, 1984) p. 71.

[19] E. Hernández–García, L. Pesquera and M. A. Rodríguez, Phys. Rev **A 36** 5774 (1987).

[20] J. M. Sancho, M. San Miguel, S. L. Katz and J. D. Gunton, Phys. Rev. **A 26**,

1589 (1982).

Chapter 2

Transient statistics for a good cavity laser with swept losses

2.1 Introduction

The laser switch–on can be considered as a dynamical bifurcation with a control parameter that is continuously swept in time through the instability point. It has been shown that because of the critical slowing down displayed by the laser first threshold, the dynamical bifurcation is delayed with respect to the time at which the instability point is crossed [1]. Deterministic analysis of this problem in the context of laser physics include the laser with saturable absorber [2] , the laser Lorenz equations [3], as well as their good–cavity limit [4, 5], class–B lasers [6] and intrinsic optical bistability[7]. Fluctuations have been considered for the laser in the good cavity limit by numerical integration [8], analogic simulations [9] and analytic methods in the linear regime [10–12]. Experimental results for CO_2 lasers with saturable absorber [13], Ar^+ lasers [14], CO_2 lasers [15] and semiconductor lasers [16] are now available. Sweeping–rate dependence has also been discussed in connection with fluid instabilities [17] and general theories for the decay of unstable states [18].

Numerical integration of the Fokker–Planck equation, which describes the action of spontaneous emission noise in a good cavity laser, has shown that the delay persists when the sweeping rate is larger than the intensity of the noise [8]. The dynamical bifurcation has been characterized in terms of first–passage times distribution [10] and using the averaged intensity [11]. However, experiments in an Ar^+ laser driven across the threshold region by a variation of the cavity losses analyze another magnitude, T, that is the time at which the intensity has its maximum slope. This study indicates that the sweeping rate, v, and T, satisfy the relation $\sqrt{v}T \sim$ constant [14]. A

theoretical determination of T requires the solution of a non–linear problem because at this time the system has already started to be attracted by the stationary solution. An analysis of the non–linear deterministic equation has been carried out and shows the same $v^{1/2}$ dependence for T if the sweeping rate is large enough [4]. When the effect of spontaneous emission noise is considered, the time T becomes a random variable and anomalous large transient fluctuations in the non–linear regime appear [19, 20]. A non–linear stochastic description is then desirable to study this problem.

In this paper the study of the anomalous fluctuations for a good cavity laser with swept losses is made by generalizing the Quasideterministic theory [21] (QDT) to this problem [22]. This generalization is performed for two cases: in the first one (I), the control parameter increases linearly for any time with a sweeping rate, v, and in the second case (II), it increases in the same way until it reaches a fixed value a. The first case is of interest in the study of slow variations of the control parameter. The second one allows us to calculate corrections to the instantaneous–change case. In both cases, we study the validity conditions of the QDT. The QDT is shown to be valid in case I when the sweeping rate is large with respect to the intensity of spontaneous emission noise, D, and in case II when D is much smaller than the final control parameter, a. We characterize the anomalous fluctuations by the time , t_m, at which the maximum of the variance of the intensity happens and by the value of this maximum, σ_m. Numerical simulations show that if the sweeping rate is of the order of D the maximum of the fluctuations disappears and the delay in the bifurcation becomes negligible. When the sweeping rate is larger than D, t_m is found to coincide with the average of T, $\langle T \rangle$, for both cases I and II. This magnitude, T is shown to have small fluctuations. These results are explained using the QDT.

In case I we find using the QDT and numerical simulations that t_m^{-1} and σ_m scale with $\sqrt{v}$. This is in agreement with the experimental results for $\langle T \rangle$ in an Ar^+ laser

[14]. With the use of the QDT relative fluctuations of the intensity are shown to be given by an universal scaling function. In case II we find , by using the QDT, that the time dependence of the moments of the intensity is given through a scaling variable. This result generalizes the dynamical scaling obtained in the instantaneous–change case[19, 21]. We also obtain analytical expressions for t_m and σ_m including corrections to the instantaneous–change case as well as for the mean value and the variance of T. We check these predictions with numerical simulations.

The outline of the paper is as follows: in section 2.2 the model and QDT are presented. In sections 2.3 and 2.4 the validity conditions of QDT are obtained and the analysis of anomalous fluctuations is performed for cases I and II respectively. Finally, in section V we summarize the most important results and draw conclusions.

2.2 Model and Quasideterministic theory (QDT)

The single mode on–resonance laser can be described near threshold and in the good cavity limit by the following equation

$$\dot{E} = aE - B \mid E \mid^2 E + \xi(t), \tag{1}$$

where $E = E_1 + iE_2$, is the electric field complex amplitude, $a = \Gamma - \kappa$ (Γ and κ are the gain and loss parameters, respectively) and $B = \beta\Gamma$ (β is a positive parameter which involves the coupling constant and the polarization and population-inversion decay rates). The complex random term, $\xi = \xi_1 + i\xi_2$, models the spontaneous emission noise. It is taken as a Gaussian white noise of zero mean and correlation

$$\langle \xi^*(t)\xi(t') \rangle = 2D\delta(t - t'). \tag{2}$$

We will study a laser which is continuously driven from below to above threshold at a sweeping rate, v, by changing the loss parameter in this way: $\kappa(t) = \kappa_0 - vt$,

with a fixed gain parameter. This corresponds to the experimental set up of Ref. 14. Therefore the control parameter is $a(t) = a_0 + vt$ $(a_0 < 0, v > 0)$ where $a_0 = \Gamma - \kappa_0$. The time at which $a(t)$ changes sign is denoted by $\bar{t}$, $(\bar{t} = -a_0/v)$. The static bifurcation is then reached at $\bar{t}$. We will distinguish two cases. In the first one (I) the control parameter is changed without bound

$$a(t) = \begin{cases} a_0 & \text{if } t < 0 \\ a_0 + vt & \text{if } t > 0 \end{cases} . \tag{3}$$

In the second case (II) $a(t)$ reaches a fixed value, a, at $t_1 > \bar{t}$

$$a(t) = \begin{cases} a_0 & \text{if } t < 0 \\ a_0 + vt & \text{if } 0 < t < t_1 \\ a = a_0 + vt_1 & \text{if } t > t_1 \end{cases} . \tag{4}$$

The first case is of interest when the stationary state value is obtained as a function of the control parameter. The second case is of interest in the study of fast variations of the control parameter when switching on the laser.

From a deterministic analysis a time t^*, at which the system becomes dynamically unstable, can be defined as the time at which the solution of the linearized deterministic equation starts to grow exponentially [1]

$$\int_0^{t^*} a(s)ds = 0. \tag{5}$$

It can be shown that in cases I and II, if $t_1 > 2\bar{t}$, $t^* = 2\bar{t}$ and in case II, if $t_1 < 2\bar{t}$, $t^* = (a - a_0)^2/2av$. In this deterministic framework $t^* - \bar{t}$ is the delay in the bifurcation. In a stochastic description the dynamical bifurcation point has been characterized in terms of first–passage times [10] and using the time dependence of the mean intensity [11]. Numerical integration of the Fokker–Planck equation has shown that for a linear variation in time of the gain parameter, the presence of the spontaneous emission

white noise decreases the delay with respect to the deterministic value [8]. In fact, this delay disappears when $v \sim D$. We have checked with numerical simulations [23] of equation (2.1) that this result also holds in the case of swept losses [22].

The stochastic analysis of the dynamical bifurcation point only involves the linear regime. In order to analyze the anomalous fluctuations non-linear terms must be taken into account. To perform this analysis we generalize the QDT [21] to the case of a linear variation of the cavity losses [22].

Let us assume that the initial electric field $E_i(0)$ is distributed according to the Gaussian distribution below threshold. Therefore the initial intensity has an exponential distribution with mean value, $\langle I(0) \rangle = D/ \mid a_0 \mid$. This is valid when non-linear terms are negligeable, i.e. $\langle I(0) \rangle << \mid a_0 \mid /B$. The linearized version of (2.1) can be solved with this initial condition. The solution for the intensity is

$$I(t) = \mid h(t) \mid^2 e^{2\int_0^t a(s)\,ds}, \tag{6}$$

where $h(t)$ is a complex Gaussian process with variance [10]:

$$\langle \mid h(t) \mid^2 \rangle = \frac{D}{\mid a_0 \mid} + 2D \int_0^t e^{-2\int_0^s a(s')\,ds'} ds. \tag{7}$$

In the linear solution $\mid h(t) \mid^2$ plays the role of an effective random initial condition for the deterministic evolution. The QDT consists in replacing the actual process (2.1) by a process obtained from the nonlinear deterministic solution of (2.1) changing the initial condition by $\mid h(t) \mid^2$

$$I(t) = \frac{\mid h(t) \mid^2 e^{2\int_0^t a(s)\,ds}}{1 + 2B \mid h(t) \mid^2 \int_0^t e^{2\int_0^s a(s')\,ds'} ds}. \tag{8}$$

This approximation is valid whenever two different stages of evolution can be distinguished: an initial linear fluctuating regime and a nonlinear regime where the evolution is esentially deterministic. This corresponds to the existence of a time, t_0, in the linear regime such that for times larger than t_0 the process $\mid h(t) \mid^2$ becomes a

random independent variable $\mid h(\infty) \mid^2$. For these times the evolution will be deterministic. In the following sections we use this criteria to obtain the regions of validity of the QDT.

2.3 Anomalous Fluctuations. Case I

In this section we consider the case I (see (2.3)). We begin our analysis of the validity conditions of QDT for this case by calculating the average of the process $\mid h(t) \mid^2$. If we substitute (2.3) in (2.7) we obtain:

$$\langle \mid h(t) \mid^2 \rangle = \frac{D}{\mid a_0 \mid}\Big[1 + \frac{2 \mid a_0 \mid}{\sqrt{v}} e^{a_0^2/v} \int_{-|a_0|/\sqrt{v}}^{\sqrt{v}(t-\bar{t})} e^{-s^2}\, ds\Big]. \tag{9}$$

This stochastic process becomes a time–independent random variable, $\mid h(\infty) \mid^2$ when $\sqrt{v}(t-\bar{t}) > 2$. In this time regime the QDT expression for the intensity (2.8) can be written as

$$I(t) = \frac{\mid h(\infty) \mid^2 e^{v(t-\bar{t})^2 - v\bar{t}^2}}{1 + 2B \mid h(\infty) \mid^2 \int_0^t e^{v(s-\bar{t})^2 - v\bar{t}^2}\, ds}. \tag{10}$$

We can also deduce (3.2) if there is a matching time t_0 , $(t_0 > \bar{t})$, such that the nonlinear terms are negligible for times smaller than t_0 and $\sqrt{v}(t_0 - \bar{t}) > 2$. If this last relation holds, $\mid h(t_0) \mid^2 = \mid h(\infty) \mid^2$, and the evolution for $t > t_0$ is then deterministic. The evolution before t_0 is well approximated by the linearized equation (2.6) if the following condition is satisfied

$$\langle I(t_0) \rangle \; << \; (a_0 + vt_0)/B, \tag{11}$$

where $I(t_0)$ is given by

$$I(t_0) = \mid h(t_0) \mid^2 e^{v(t_0-\bar{t})^2 - v\bar{t}^2}, \tag{12}$$

and the second term is the stationary intensity at t_0. The intensity for times greater than t_0 is the solution of the nonlinear deterministic equation with the random initial condition, $I(t_0)$:

$$I(t) = \frac{I(t_0) e^{2\int_{t_0}^{t}(a_0+vs)ds}}{1 + 2BI(t_0)\int_{t_0}^{t} e^{2\int_{t_0}^{s}(a_0+vs')ds'} ds}. \tag{13}$$

If we substitute $I(t_0)$ given by (3.4) in (3.5) we obtain the following expression for the intensity:

$$I(t) = \frac{|\, h(t_0)\,|^2\, e^{v(t-\bar{t})^2 - v\bar{t}^2}}{1 + 2B\,|\, h(t_0)\,|^2 \left[\int_0^t e^{v(s-\bar{t})^2 - v\bar{t}^2} ds - \int_0^{t_0} e^{v(s-\bar{t})^2 - v\bar{t}^2} ds\right]}. \tag{14}$$

We can consider two cases $\sqrt{v} >> |\, a_0\,|$ (fast sweeping) and $\sqrt{v} << |\, a_0\,|$ (slow sweeping). If $\sqrt{v} >> |\, a_0\,|$ the condition (3.3) is equivalent to

$$\frac{BD}{|\, a_0\,|\sqrt{v}} << x_0\, e^{-x_0^2}, \tag{15}$$

where $x_0 = \sqrt{v}(t_0 - \bar{t})$. If this last condition holds, it can be shown that

$$2B\langle |\, h(t_0)\,|^2\rangle \int_0^{t_0} \exp[v(s-\bar{t})^2 - v\bar{t}^2] ds << 1. \tag{16}$$

Therefore if (3.7) holds with $x_0 > 2$, we obtain the QDT expression (3.2) from (3.6). The validity condition of QDT in the case of fast sweeping is then given by

$$\frac{BD}{|\, a_0\,|\sqrt{v}} << 10^{-2} \quad \text{if } \sqrt{v} >> |\, a_0\,|\,. \tag{17}$$

We now consider the case of slow sweeping ($\sqrt{v} << |\, a_0\,|$). For the linear description to be valid up to a time $t_0 > \bar{t}$, the average of the second term in the denominator of (2.8) has to be very small,

$$2B\langle |\, h(\bar{t})\,|^2\rangle \int_0^{\bar{t}} e^{2\int_0^s (a_0+vs')\, ds'} ds << 1. \tag{18}$$

After some calculations we then obtain a necessary condition for the validity of the QDT in the case of slow sweeping:

$$\frac{BD}{|\, a_0\,|\sqrt{v}} << e^{\frac{-a_0^2}{v}} \quad \text{if } \sqrt{v} << |\, a_0\,|\,. \tag{19}$$

These conditions agree when $\sqrt{v} > |\, a_0 \,|$ with the ones [18] found for the validity of the Suzuki matching procedure [19]. However, when $\sqrt{v} << |\, a_0 \,|$ we get a more stringent condition. The difference between both cases is that in the first case $\langle I(t) \rangle$ is for times $t \approx \bar{t}$ of the same order than $\langle I(0) \rangle$, whereas in the second case $\langle I(\bar{t}) \rangle >> \langle I(0) \rangle$. Therefore, for a linear description to be valid up to the matching time $t_0 > \bar{t}$, the sweeping across the bifurcation must be faster in the second case.

We have checked with numerical simulations that if the condition (3.9) is satisfied in the case $\sqrt{v} > |\, a_0 \,|$, the QDT describes correctly the anomalous fluctuations as it can be seen in the Fig. 1. We also give an example in Fig. 2 in which the condition (3.9) is not verified. In this last figure we see how the QDT description of the average and variance fails to describe the results of the numerical simulations of Eq. (2.1).

We now study the transient anomalous fluctuations of the intensity using the QDT. It is well known that in the decay of an unstable state (instantaneous change of the pump parameter) fluctuations, $\sigma^2 = \langle I^2 \rangle - \langle I \rangle^2$, have an anomalously large maximum [18–20]. However, when $v \approx D$ the maximum disappears as it can be seen in Fig. 3. In this situation the intensity follows adiabatically the steady–state value associated with the instantaneous control parameter [8]. We will characterize anomalous fluctuations by the time at which the maximum takes place, t_m, and by the value of this maximum σ_m. We also consider the time T, at which the intensity reaches its maximum rate of growth. This time has been measured for a Ar^+ laser with swept losses [14].

We have performed simulations of (2.1) for B=1/2, D=0.001, a_0=–0.5 and a_0=–0.05 and for several values of the sweeping rate. In Fig. 4, $\log\langle T \rangle$ and $\log t_m$ are represented vs. the logarithm of the sweeping rate for $a_0 = -0.5$. In the figure we see that t_m coincides with the average of T for a large range of values of v. This last fact can be explained in the framework of the QDT by considering that the largest

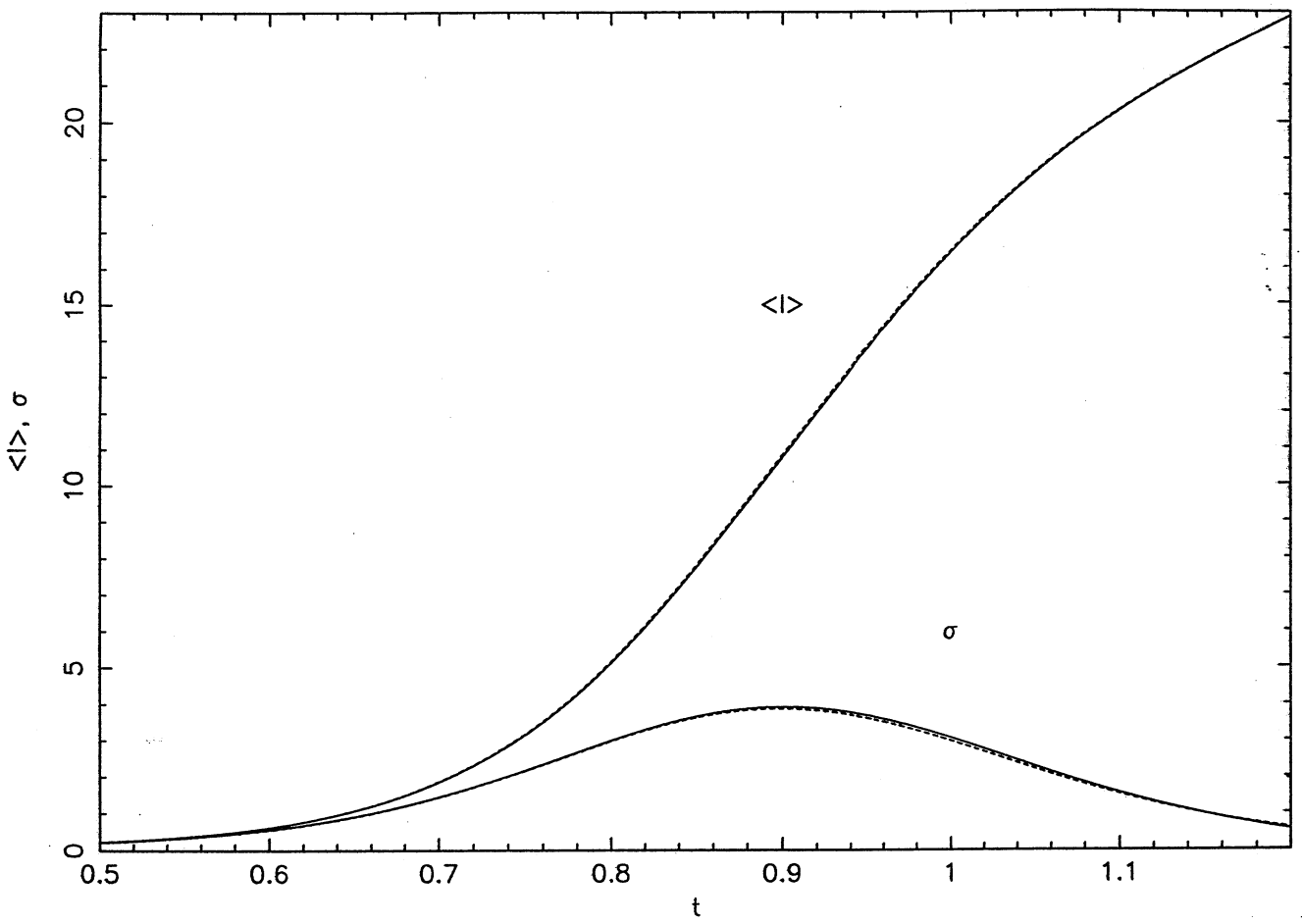

Fig. 1. Average intensity and fluctuations vs. time for $B = 1/2, D = 10^{-3}, a_0 = -0.05$ and v=10 calculated from simulation (solid line) and from QDT (dotted line).

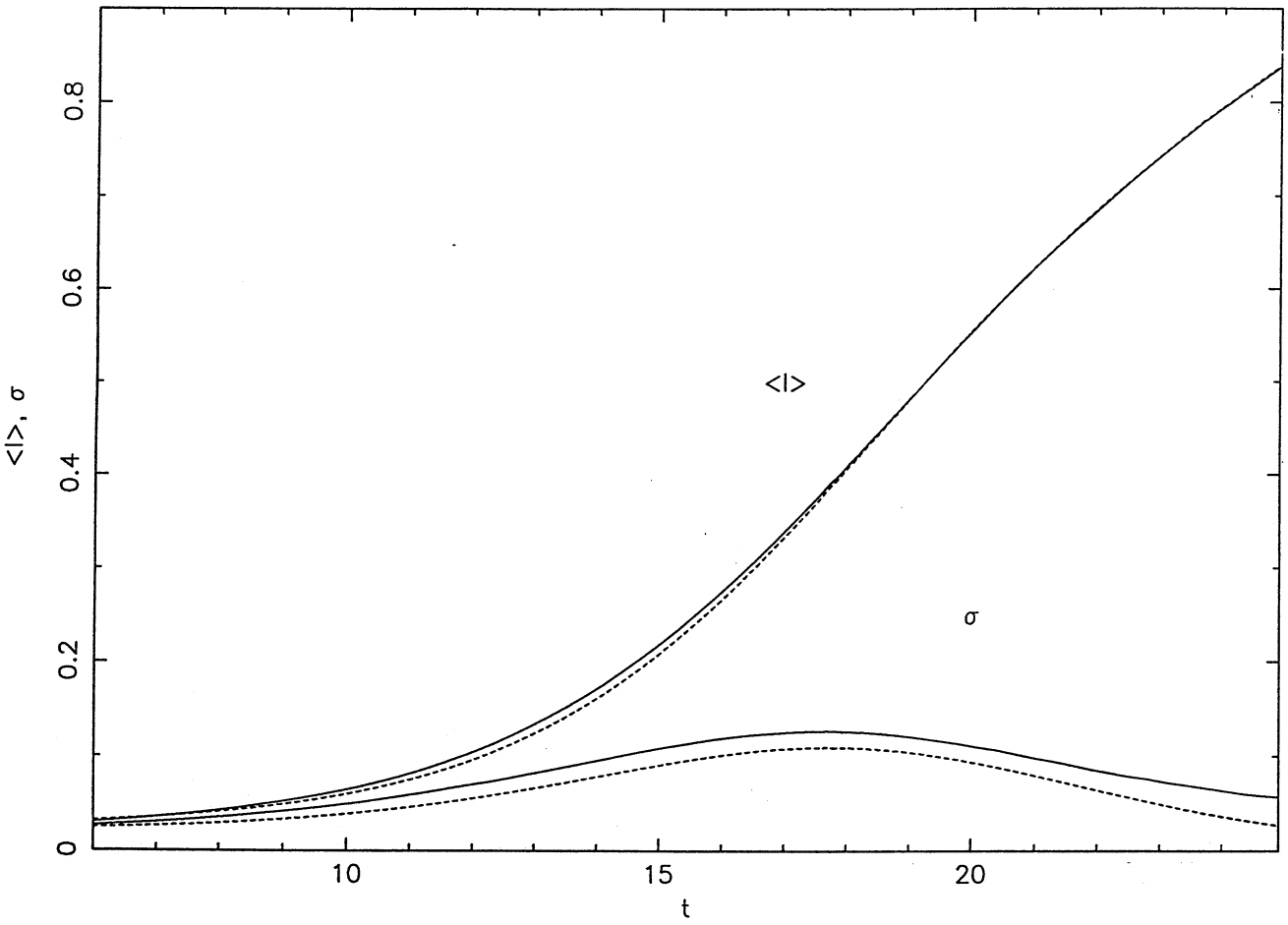

Fig. 2. Average intensity and fluctuations vs. time for $B = 1/2, D = 10^{-3}, a_0 = -0.05$ and v=0.02 calculated from simulation (solid line) and from QDT (dotted line).

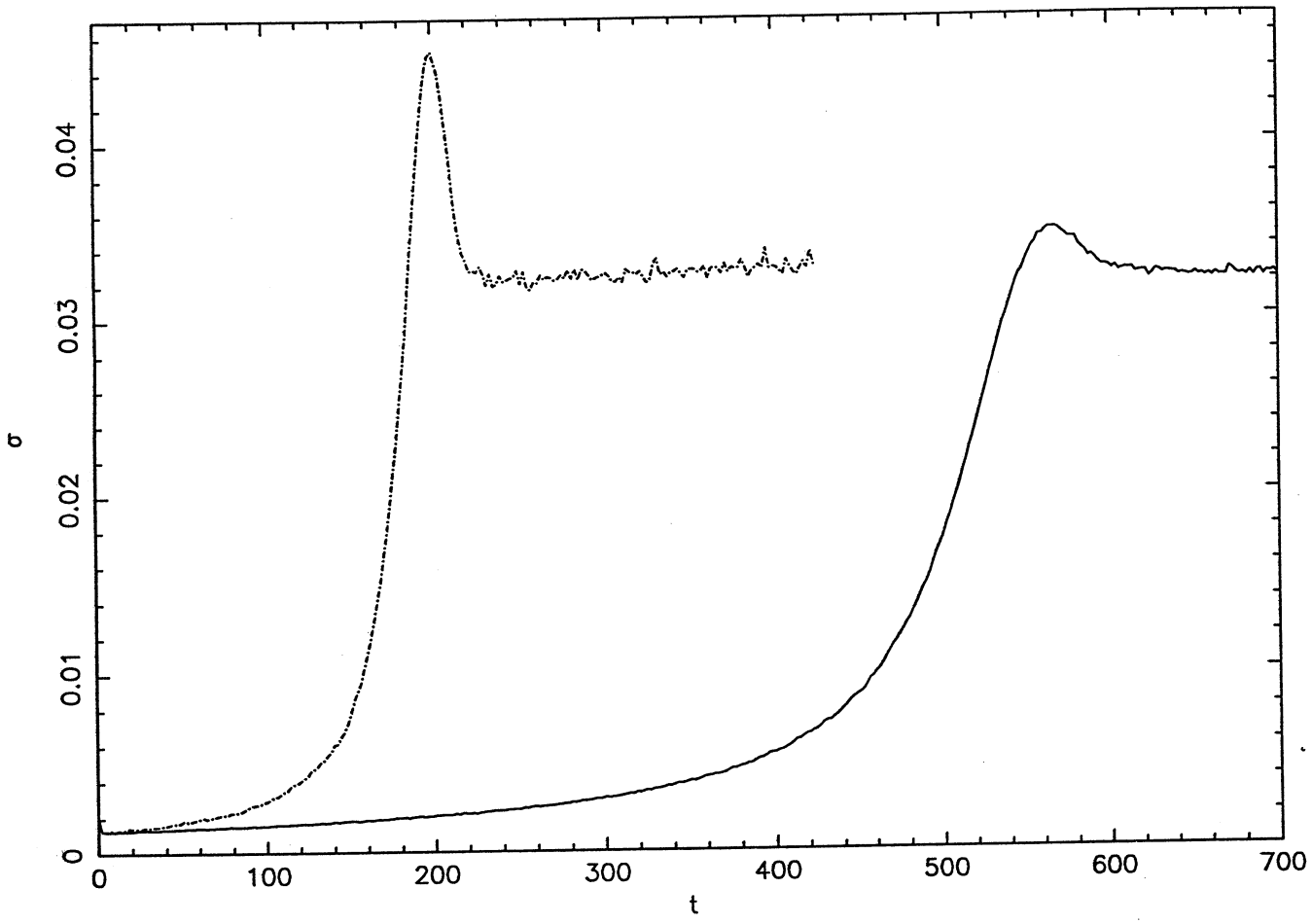

Fig. 3. Fluctuations vs. time for $B = 1/2, D = 10^{-3}, a_0 = -0.5$ and $v = 0.003$ (dash–dotted line), 0.001 (solid line). The anomalous fluctuations peak disappears if $v \to D$.

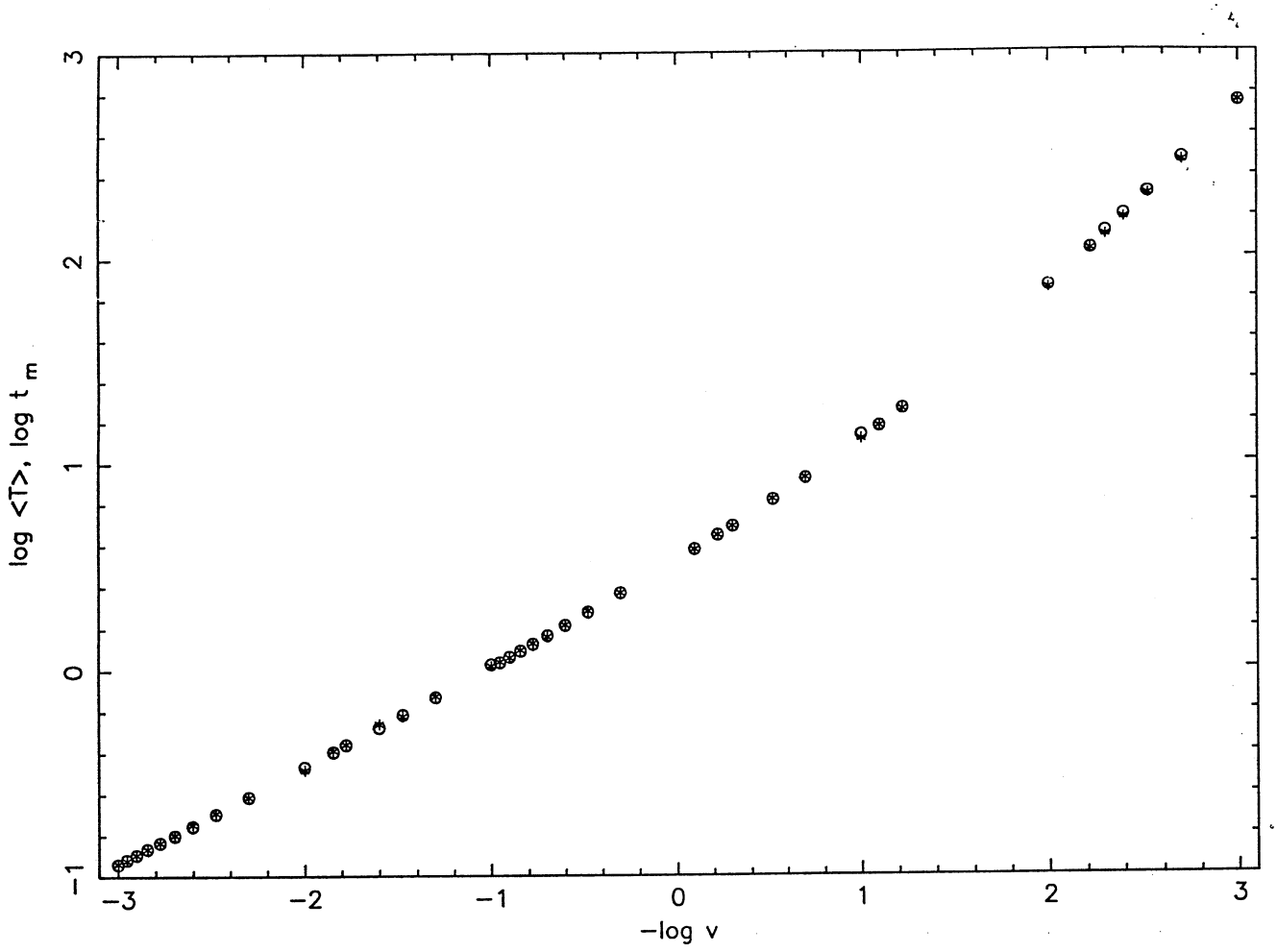

Fig. 4. $\mathrm{Log}_{10}\,\langle T\rangle$, (circles), and $\log_{10} t_m$, (stars), vs. -$\log_{10} v$. If $\sqrt{v} > \mid a_0 \mid$ the points describe a straight line with a slope 0.499.

amplification of the initial fluctuations occurs at the time of maximum rate of growth of the intensity, T. This time T is well defined (relative fluctuations smaller than 0.06) when $v > 1$ for $a_0 = -0.5$. This corresponds to the region of validity of QDT. We also observe in Fig. 4 that for these values of v, ($\mid a_0 \mid < \sqrt{v}$), the scaling $\sqrt{v}\langle T\rangle \approx$ constant is verified. This scaling is in agreement with experimental data [14] and with deterministic analysis for large enough v [4, 5]. An explanation in the framework of QDT for both the scaling $\sqrt{v}\,\langle T\rangle \approx$ constant and for the small relative fluctuations $\sigma_T/\langle T\rangle$ (where $\sigma_T^2 = \langle T^2\rangle - \langle T\rangle^2$) can be given in the following way. An equation for T can be obtained from (3.2) by setting $\left[\frac{d^2 I}{dt^2}\right]_{t=T} = 0$:

$$\frac{e^{X^2}}{A + \int_0^X e^{u^2} du} = \frac{X}{2}\left[3 - \sqrt{1 - 4/X^2}\right], \tag{20}$$

where

$$A = \frac{\sqrt{v} e^{a_0^2/v}}{2B \mid h(\infty) \mid^2} + \int_0^{|a_0|/\sqrt{v}} e^{u^2} du, \tag{21}$$

and $X = \sqrt{v}(T - \bar{t})$. This condition is similar to the one found in the deterministic analysis of the Ref. 4. The difference lies in the random character of the initial condition $\mid h(\infty) \mid^2$. The condition (3.12) is an implicit equation whose solution only depends on the random variable A. It can be shown by deriving (3.12) with respect to A that the variation of the root X is $\Delta X \approx e^{-X^2}\Delta A$. When $\sqrt{v} > \mid a_0 \mid$, it is easy to see from (3.1) that large variations of v change slightly the distribution of $\mid h(\infty) \mid^2$. Then the changes in A are essentially due to the $\sqrt{v}$ factor. Due to the e^{-X^2} factor there is a large range of sweeping rates such that $\Delta X << 1$ and then $X \approx$ constant, (note that in the nonlinear regime $X > 2$). Then in this case ($\sqrt{v} > \mid a_0 \mid$) we get $\sqrt{v}\langle T\rangle \approx$ constant with small fluctuations for T.

Therefore, we have shown that the $T = O(v^{-1/2})$ law is correct provided that $\sqrt{v} > \mid a_0 \mid$. This result agrees with the deterministic analysis [5]. If $\sqrt{v} << \mid a_0 \mid$

the deterministic result [4, 5] is different: $T = O(v^{-1})$. The same conclusion can be obtained including fluctuations, when the QDT is valid, that is for small enough values of the intensity of the noise with respect to the sweeping rate (see (3.11)). In the limit $v \to 0$ we get from (3.12) and (3.13) the following expression for T:

$$T \approx 2\frac{\mid a_0 \mid}{v}\Big[1 + \frac{1}{4}\frac{v}{a_0^2} ln(1 + \frac{\mid a_0 \mid}{B \mid h(\infty) \mid^2})\Big]. \tag{22}$$

This result is in agreement with the deterministic analysis [4]: the domain where $T \approx t^* = 2 \mid a_0 \mid /v$ increases when $\mid a_0 \mid$ increases or when the initial condition increases.

The expression for σ_m can be found from (3.2) by averaging over the initial condition $\mid h(\infty) \mid^2$

$$\frac{\sigma_m}{\sqrt{v}} = \frac{\beta_m\Big[\frac{1}{\beta_m} - e^{\beta_m} E_1(\beta_m) - e^{2\beta_m} E_1(\beta_m)^2\Big]^{1/2}}{2Be^{-x_m^2}\int_{-\frac{|a_0|}{\sqrt{v}}}^{x_m} e^{u^2} du}, \tag{23}$$

where β_m is the value of the following function

$$\beta = \frac{\sqrt{v} e^{a_0^2/v}}{2B\langle \mid h(\infty) \mid^2 \rangle \int_{-|a_0|/\sqrt{v}}^{x} e^{u^2} du}, \tag{24}$$

at t_m, $x_m = \sqrt{v}(t_m - \bar{t})$ and $E_1(\beta)$ is the Exponential–Integral function [25]. As it can be seen from Fig. 5, where log σ_m is plotted vs. log v, $\sigma_m/\sqrt{v} \approx$ constant when $\sqrt{v} >\mid a_0 \mid$. We can understand qualitatively this scaling in the following way. First, the denominator in (3.15) does not change with v, due to the scaling $x_m \approx \langle X \rangle \approx$ constant. Second, the numerator is a function which changes slowly for the values of β_m found in the simulations. For instance, β_m varies between 0.17 and 0.22 when v varies between v=6 and 600, for the values of the parameters a_0=–0.5,$D = 10^{-3}$ and B=0.5. This variation of β_m produces a change in the numerator of (3.15) smaller than 3%. Note that if we take into account that X has small fluctuations and $\langle X \rangle \approx x_m$ we can write (3.12) in the form

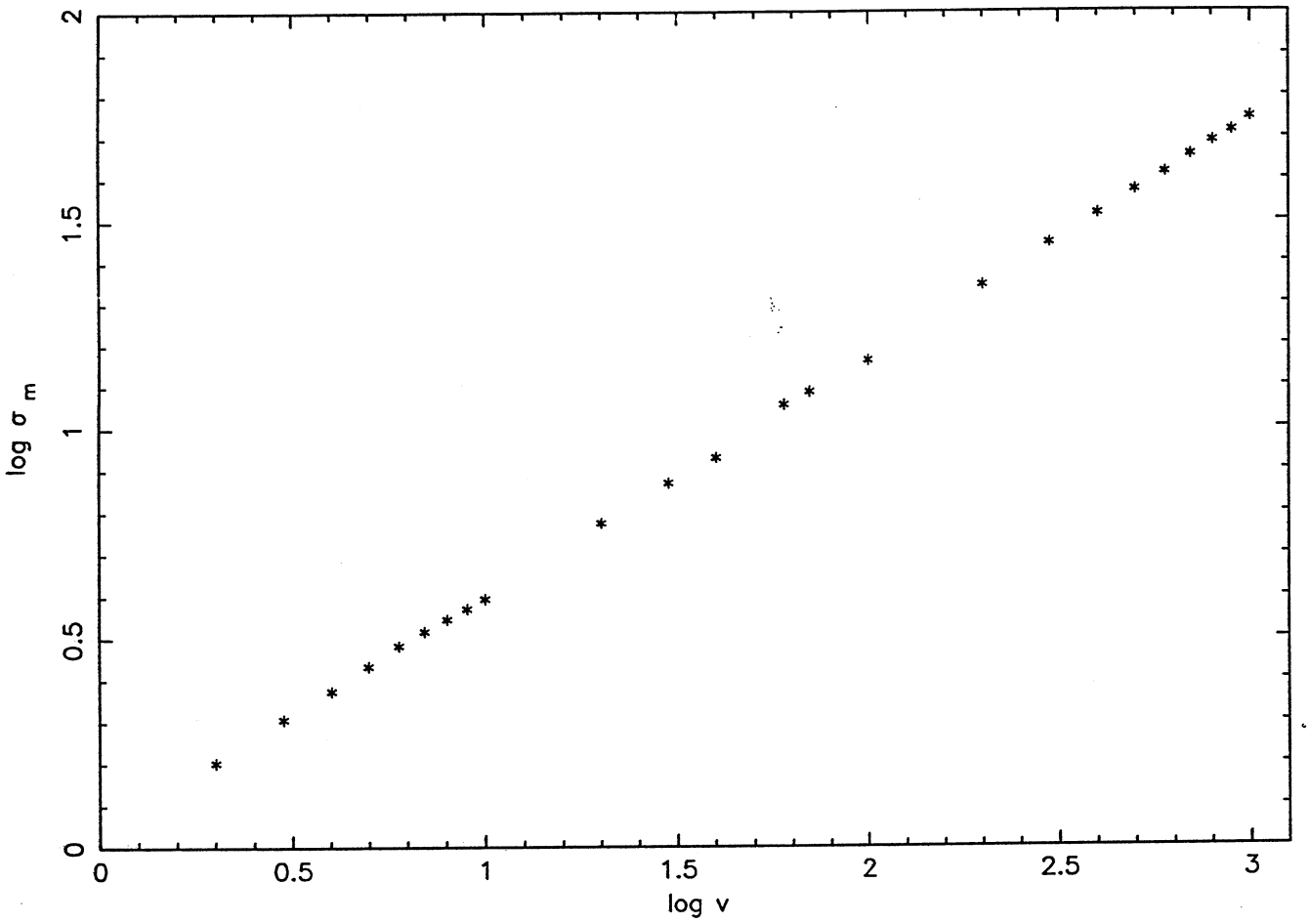

Fig. 5. Maximum fluctuations vs. $\log_{10} v$ for $B = 1/2, D = 10^{-3}, a_0 = -0.5$.When $\sqrt{v} > \mid a_0 \mid$ the points describe a straight line with a slope 0.567.

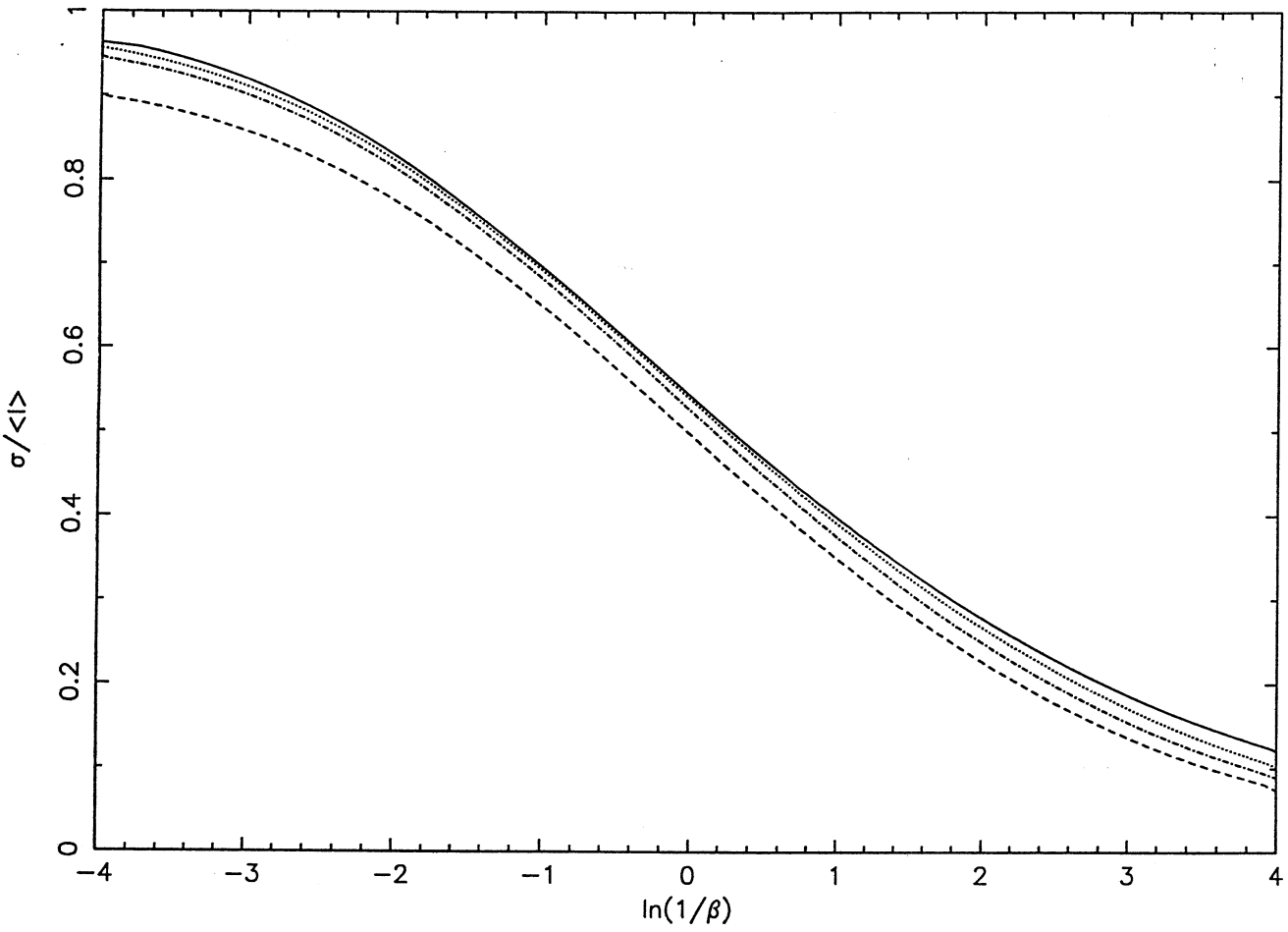

Fig. 6. Relative fluctuations vs. $\ln \beta^{-1}$ for the scaling function (solid line) and $B = 1/2, D = 10^{-3}, a_0 = -0.5$ and $v = 5$ (dashed line), 50 (dash–dotted line), 500 (dotted line).

$$\frac{1}{(1+\beta_m)e^{-X^2}\int_{-|a_0|/\sqrt{v}}^{X} e^{u^2}du} = \frac{X}{2}\left[3-\sqrt{1-4/X^2}\right]. \qquad (25)$$

Therefore for the scaling $X \approx$ constant to be correct $(1+\beta_m)$ should vary slowly with v.

The relative fluctuations for all times are given from (3.2) by the following universal scaling function

$$\frac{\sigma}{\langle I\rangle} = \frac{\beta\left[\frac{1}{\beta} - e^{\beta}E_1(\beta) - e^{2\beta}E_1^2(\beta)\right]^{1/2}}{1-\beta e^{\beta}E_1(\beta)}. \qquad (26)$$

In Fig. 6 we show that increasing v this scaling function is approached. This corresponds to the fact that the accuracy of the QDT approximation increases with v (see (3.9)). This scaling has a different nature than the one found in the instantaneous–change case [18, 19] for the time dependence of $\langle I^n(t)\rangle$. Note that due to the fact that $a(t)$ is always changing with time, (2.3), the moments of the intensity (see for instance (3.15)) do not scale directly with $\beta(t)$. In case II we find a generalization of the dynamical scaling for $\langle I^n(t)\rangle$.

2.4 Anomalous fluctuations. Case II

In this case the control parameter reaches a fixed value a in t_1 $(t_1 > t)$(see (2.4)). This is an interesting case because it permits us to calculate corrections, owing to the finite sweeping rate, to the instantaneous change assumption made in classical studies of transient statistics [18, 19].

We can distingish two cases: In the first one, $a >> \sqrt{v}$, the anomalous fluctuations peak occurs before t_1. This corresponds to the case I (slow sweeping). In the second case, $a < \sqrt{v}$, the times of interest are larger than t_1. This is an interesting case because the instantaneous change–case is included here. As in the previous section we begin our analysis of the validity conditions of QDT in this case by calculating the average of the process $\mid h(t) \mid^2$ from (2.4) and (2.7)

$$\langle \mid h(t) \mid^2 \rangle = \Big[\frac{D}{\mid a_0 \mid} + \frac{2D}{\sqrt{v}} e^{v\bar{t}^2} \int_{-\sqrt{v}\,\bar{t}}^{\sqrt{v}(t_1-\bar{t})} e^{-u^2} du\Big] + \frac{D}{a} e^{vt_1^2} \Big[e^{-2at_1} - e^{-2at}\Big], \quad (27)$$

valid for times $t > t_1$. This stochastic process becomes a time–independent random variable, $\mid h(\infty) \mid^2$ when $2at >> 1$. In this time regime the QDT expression for the intensity (2.4) can be written as

$$I(t) = \frac{\mid h(\infty) \mid^2 exp[-vt_1^2 + 2at]}{1 + 2B \mid h(\infty) \mid^2 \Big[\frac{e^{-v\bar{t}^2}}{\sqrt{v}} \int_{-\sqrt{v}\bar{t}}^{\sqrt{v}(t_1-\bar{t})} e^{u^2} du + \frac{e^{-vt_1^2}}{2a}(e^{2at} - e^{2at_1})\Big]}. \quad (28)$$

In a similar way than for case I, the QDT will be valid when there exists a time t_0 in the linear regime such that $at_0 >> 1$ and $\langle I(t_0) \rangle << a/B$. When $a >> \mid a_0 \mid$ this is equivalent to the following condition:

$$\frac{BD}{\mid a_0 \mid a} << 10^{-2} \quad (29)$$

Numerical simulations show that when (4.3) is fulfilled the approximation given by (4.2) is accurate. Recently another approximation based on a step function for $I(t)$ has been considered [12]. This kind of approximation gives very good results in the relaxation from a marginal state [24]. However, Eq. (4.2) shows that the step function approximation can not be correct in the relaxation from an unstable state.

If we consider a range of parameters such that (4.3) is fulfilled, an analysis of the anomalous fluctuations can be performed by using the QDT. The advantage of this case respect to the case I is that we are able to get analytical expressions of t_m and $\langle T \rangle$ in which the corrections to the instantaneous change case due to the finite sweeping rate are included. The moments of the intensity can be calculated by averaging (4.2) over the distribution of $\mid h(\infty) \mid^2$. They show a temporal dependence given by a dynamical scaling parameter θ:

$$\theta = \frac{1}{2B\langle \mid h(\infty) \mid^2 \rangle \Big[\alpha + \frac{\gamma}{2}(e^{2a(t-t_1)} - 1)\Big]}, \quad (30)$$

where:

$$\gamma = \frac{e^{(a^2-a_0^2)/v}}{a}, \tag{31}$$

$$\alpha = \frac{e^{-a_0^2/v}}{\sqrt{v}} \int_{-|a_0|/\sqrt{v}}^{a/\sqrt{v}} e^{u^2} du, \tag{32}$$

This generalize the dynamical scaling found in the instantaneous–change case [18,19]. Unlike the case I, this scaling holds directly for $\langle I^n(t)\rangle$. This is due to the fact that for the times of interest ($t > t_1$) the pump parameter is constant. We can now write the averaged intensity and the variance as functions of θ:

$$\langle I(\theta)\rangle = \frac{a}{B}(1 + C\theta)(1 - \theta e^{\theta} E_1(\theta)), \tag{33}$$

$$\sigma(\theta) = \frac{a}{B}(1 + C\theta)\theta(1/\theta - e^{\theta}E_1(\theta) - e^{2\theta}E_1^2(\theta))^{1/2}, \tag{34}$$

where:

$$C = B\langle |\, h(\infty)\,|^2\rangle(\gamma - 2\alpha). \tag{35}$$

The moments depend on θ and C in the same way that in the instantaneous–change case, but changing C and the scaling parameter θ. The corresponding parameters, θ_∞ and C_∞ of the instantaneous–change case are:

$$\theta_\infty = \frac{a}{BD(\frac{1}{a} + \frac{1}{|a_0|})(e^{2at} - 1)}, \tag{36}$$

$$C_\infty = \frac{BD}{a}\Big(\frac{1}{a} + \frac{1}{|\,a_0\,|}\Big). \tag{37}$$

When $v >> a^2$ we obtain that θ and C coincide with the corresponding ones of the Q–switching.

Now we will characterize the anomalous fluctuations by t_m and σ_m like in the previous case. The value of θ at t_m can be calculated from the condition $\frac{d\sigma}{d\theta}\Big]_{\theta=\theta(t_m)} = 0$ This condition is an implicit equation whose root depends very slightly on C when (4.3) holds, because $C \approx \frac{BD}{a|a_0|}$ is very small. The root of the equation is $\theta(t_m)$=0.4188. Now, t_m can be found from (4.4)

$$t_m = \frac{1}{2a}\ln\Big[\frac{1}{B\theta(t_m)\gamma\langle \mid h(\infty)\mid^2\rangle} - \frac{2\alpha}{\gamma} + 1\Big] + t_1 \tag{38}$$

We now calculate T by setting $\frac{d^2I}{dt^2}\Big]_{t=T} = 0$, where $I(t)$ is given by (4.2):

$$T = \frac{1}{2a}\Big[\ln\frac{1}{B\gamma\langle \mid h(\infty)\mid^2\rangle} + \ln\Big(\frac{\langle \mid h(\infty)\mid^2\rangle}{\mid h(\infty)\mid^2} - C\Big)\Big] + t_1 \tag{39}$$

The average and variance of T are easily calculated by averaging over the exponential distribution of $\mid h(\infty)\mid^2$ and they read

$$\langle T\rangle = \frac{1}{2a}\Big[\ln\frac{1}{B\gamma\langle \mid h(\infty)\mid^2\rangle} + \gamma_{Euler}\Big] + t_1 \tag{40}$$

$$\sigma_T = \frac{0.6413}{a} \tag{41}$$

where γ_{Euler}=0.5772. In the case $a >> \mid a_0 \mid$, simple expressions of t_m and $\langle T\rangle$ with corrections of the order (a/v) to the instantaneous change case can be calculated:

$$t_m \approx \frac{1}{2a}\Big[\ln\frac{a\mid a_0\mid}{BD} + 0.8704\Big] + \frac{a}{2v} \tag{42}$$

$$\langle T\rangle \approx \frac{1}{2a}\Big[\ln\frac{a\mid a_0\mid}{BD} + 0.5772\Big] + \frac{a}{2v} \tag{43}$$

The main contribution to t_m and $\langle T\rangle$ comes from the logarithmic term because if QDT is valid then this term dominates as it can be seen from (4.3). Due to the same main dependence of t_m and $\langle T\rangle$ we obtain, as in case I, that the time at which the maximum appears is nearly the average of T. In fact, t_m is always slightly greater than $\langle T\rangle$. The fact that t_m and $\langle T\rangle$ are nearly equal can be infered from the analysis made in the instantaneous–change case [19–21]. In this paper we show this equivalence in an analytic way. In Fig. 7 the theoretical expressions shows a good agreement with the results of the simulations, when the condition $a < \sqrt{v}$ is fulfilled. We also see in this figure that the relation $t_m > \langle T\rangle$ is verified according to the equations (4.16) and (4.17). Another interesting fact is that the variance of T only depends

on the final value of the control parameter. The comparison between the results of the simulations for σ_T and those ones from equation (4.15) can be made showing a relative error always lower than 2% for the parameters of Fig. 5.

Finally, the value of σ_m can be easily calculated from (4.8) for $\beta = 0.4188$, therefore σ_m is proportional to the stationary value of the intensity:

$$\sigma_m = 0.2381\frac{a}{B} \tag{44}$$

This expression has been also checked with numerical simulations.

2.5 Conclusions

In this paper the Quasideterministic Theory, (QDT), is generalised to explain the statistical properties of the intensity of a good cavity laser when the losses are varied linearly in time. This generalization has been performed in two cases, I and II. In the first case the control parameter changes without bound and in the second one it reaches a fixed value. We have shown that QDT is valid when the spontaneous emission noise is much smaller than the sweeping rate, in case I, and than the final control parameter, in case II. We have checked the validity conditions of QDT using numerical simulations.

The QDT has been also used [26, 27] to study the statistical properties of the transient response of a gain–switched semiconductor laser. When saturation effects are negligible, this problem is equivalent to a type A laser with swept losses. The intensity fluctuations, σ, also show for semiconductor lasers large transient anomalous fluctuations associated with the decay of an unstable state as in lasers of type A. However, due to the relaxation oscillations that characterize the non–linear regime of lasers of type B, these fluctuations follow the relaxation oscillations. Another

difference is the existence of a local minimum in σ at the time that the mean intensity reaches a maximum in the oscillation.

The QDT is used to analyze the anomalous fluctuations of the intensity appearing in the non–linear regime of type A lasers with swept losses. To characterize these anomalous fluctuations, we have studied the time, t_m, at which the maximum fluctuations appear and the value of this maximum σ_m. t_m is found to coincide with the average of the time, T, at which the intensity has its maximum slope.

In case I, when the sweeping rate is large enough with respect to the initial value of the parameter, we have found that t_m and σ_m scale with the sweeping rate in this way: $t_m^{-1} \approx \sqrt{v}$ and $\sigma_m \approx \sqrt{v}$. We have also shown that the dependence on time of the relative fluctuations is given through a scaling variable. In case II, when the sweeping rate is large enough with respect to the final value of the pump parameter, we have seen that the moments of the intensity depend on time through a scaling variable, that generalizes the dynamical scaling found in the instantaneous–change case. Due to the fact that the control parameter is constant at the times of interest we have been able to calculate t_m and $\langle T \rangle$ showing in an analytic way that $t_m \approx \langle T \rangle$. To finish the characterization of the anomalous fluctuations we have also calculated σ_m that is proportional to the stationary intensity. All these facts, predicted by the Quasideterministic Theory, have been checked with numerical simulations.

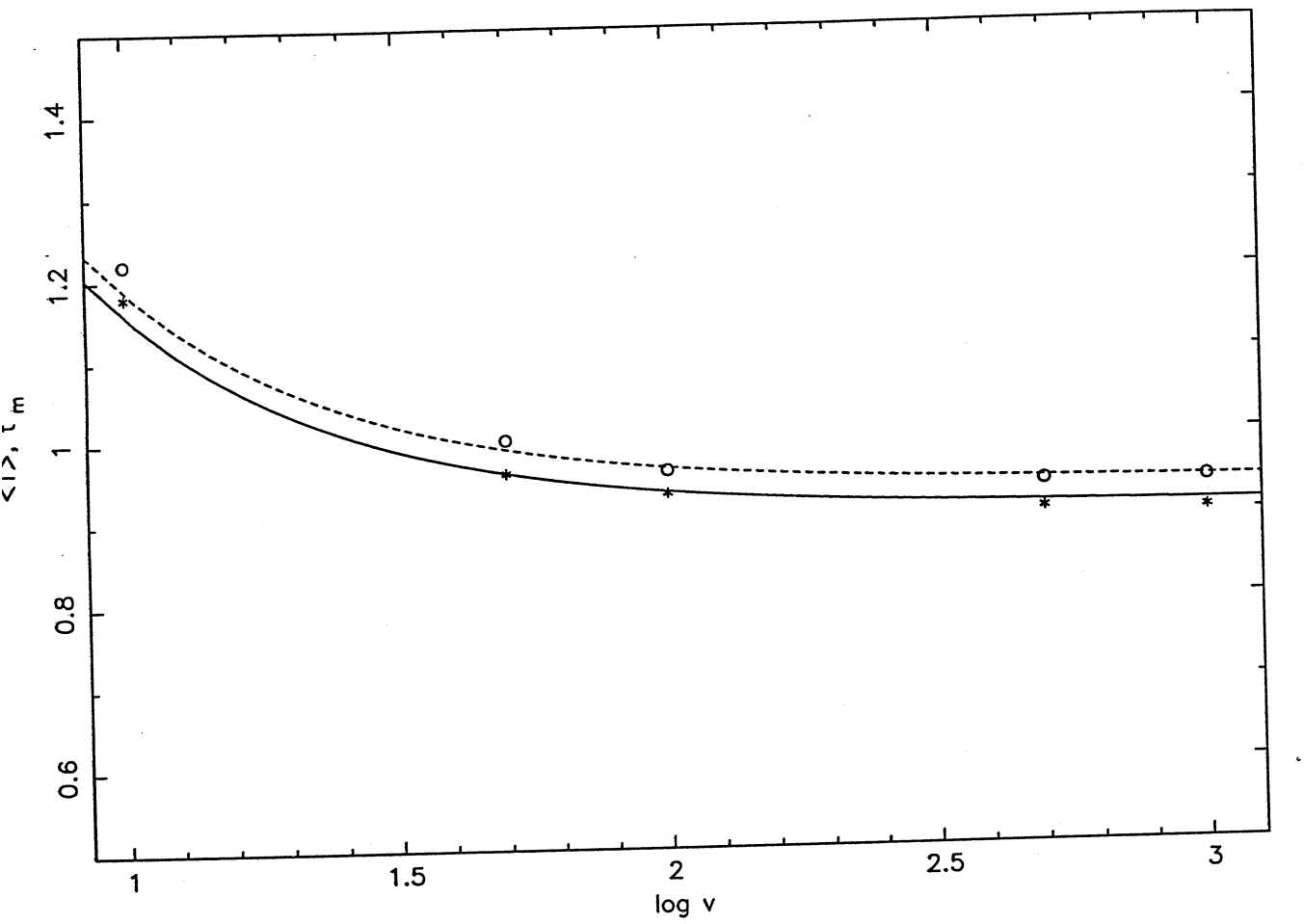

Fig. 7.$\langle T\rangle$ and t_m vs. $\log_{10} v$. for $B = 1/2, D = 10^{-3}, a = 5, a_0 = -0.5$ Circles($\langle T\rangle$) and stars(t_m) are the results of the simulations and the lines are calculated from (4.16) and (4.17).

REFERENCES

[1] P. Mandel, in *Far from Equilibrium Phase Transitions*, Vol. 319 of *Lecture Notes in Physics*, edited by L. Garrido (Springer, Berlin, 1988), p.218; P. Mandel in *Instabilities and Chaos in Quantum Optics II*, edited by N.B. Abraham, F.T. Arecchi and L.A. Lugiato (Plenum, New York, 1988), p.321.

[2] P. Mandel and T. Erneux, Phys. Rev. **A 30**, 1893 (1984); **30**, 1902 (1984).

[3] P. Mandel and T. Erneux, Phys. Rev. Lett. **53**, 1818 (1984).

[4] P. Mandel, Opt. Comm. **64**, 549 (1987).

[5] T. Erneux and P. Mandel, Opt. Comm (in press).

[6] T. Erneux and P. Mandel, Phys. Rev. **A 39**, 5179 (1989).

[7] P. Mandel and T. Erneux, IEEE J. Quantum Electron. **QE–21**, 1352 (1985).

[8] G. Broggi, A. Colombo, L. Lugiato, and P. Mandel, Phys. Rev **A 33**, 3635 (1986).

[9] R. Manella, F. Moss and P. V. E. McClintock, Phys. Rev. **A 35**, 2560 (1987); N. G. Stocks, R. Manella and P. V. E. McClintock, Phys. Rev. **A 40** 5361 (1989); N. G. Stocks, R. Manella and P. V. E. McClintock, Phys. Rev. **A 42**, 3356 (1990).

[10] M. C. Torrent and M. San Miguel, Phys. Rev. **A 38**, 245 (1988); M. C. Torrent, F. Sagués and M. San Miguel, Phys. Rev. **A 40** 6662 (1989).

[11] H. Zeghlache, P. Mandel and C. Van den Broeck, Phys. Rev. **A 40**, 286 (1989); C. Van den Broeck and P. Mandel, Phys. Lett. **122A**, 36 (1987).

[12] M. O. Caceres and A. Becker, Phys. Rev. **A**, 696 (1990).

[13] P. Glorieux, IEEE J. Quantum Electron. **QE–21**, 1486 (1985); E. Arimondo, D. Dangoisse, C. Gabbanini, E. Menchi and F. Papoff, J. Opt. Soc. Am. **B4**, 892 (1987).

[14] W. Scharpf, M. Squicciarini, D. Bromley, C. Green, J.R. Tredicce and L.M. Narducci, Opt. Comm. **63**, 344 (1987).

[15] F. T. Arecchi, W. Gadomski, R. Meucci and J. A. Roversi, Opt. Comm. **65**, 47 (1988); F. T. Arecchi, R. Meucci and J. A. Roversi, Europhys. Lett. **8**, 225 (1989); F. T. Arecchi, W. Gadomski, R. Meucci and J. A. Roversi, Phys. Rev. **A 39**, 4004, (1989); F. T. Arecchi, W. Gadomsky, R. Meucci and J.A. Roversi, Opt. Comm. **70**, 155 (1989); M. Ciofini, R. Meucci and F. T. Arecchi, Phys. Rev. **A 42**, 482 (1990).

[16] P. Spano, A. D'Ottavi, A. Mecozzi and B. Daino, Appl. Phys. Lett. **52**, 2203 (1988); A. Mecozzi, S. Piazzolla, A. D'Ottavi, and P. Spano, Phys. Rev. **A 38**, 3136 (1988); P. Spano, A. D'Ottavi, A. Mecozzi, B. Daino, and S. Piazzolla, IEEE, J. Quantum Electron., **25**, 1440 (1989).

[17] G. Ahlers, M. C. Cross, P. C. Hohenberg, and S. Safran, J. Fluid Mech. **110**, 297 (1981).

[18] B. Caroli, C. Caroli and D. Saint James, Physica **108A**, 233 (1981).

[19] M. Suzuki, Adv. Chem. Phys. **46**, 195 (1981).

[20] F. T. Arecchi, V. De Giorgio, and B. Querzola, Phys. Rev. Lett. **19**, 1168 (1967); D. Meltzer and L. Mandel, ibid. **25**, 1151 (1970).

[21] F. de Pasquale, P. Tartaglia and P. Tombesi, Phys. Rev. **A 25**, 466 (1982).

[22] A. Valle, L. Pesquera and M. A. Rodríguez in *Nonlinear Dynamics and Quantum*

Phenomena in Optical Systems, edited by R. Vilaseca and R. Corbalán, (Springer, Berlin,1991)

[23] Simulations have been performed following the algorithm described in J.M. Sancho, M. San Miguel, S.L. Katz and J.D. Gunton, Phys. Rev. **A 26**, 1589 (1982). Averages were taken over 5,000 realizations using a step of integration Δ=0.001 for the case I, and Δ=0.0001 for the case II.

[24] A. Valle, L. Pesquera and M. A. Rodríguez, Opt. Comm. **79**, 156 (1990); P. Colet, F. de Pasquale, M. O. Caceres and M. San Miguel, Phys. Rev. **A 41**, 1901 (1990).

[25] *Handbook of Mathematical Functions*, edited by M. Abramowitz and I. Stegun (Dover, New York, 1970).

[26] S. Balle, P. Colet and M. San Miguel, Phys. Rev. **A 43**, 498 (1991).

[27] A. Mecozzi, P. Spano and A. Sapia, Opt. Lett. **15**,1067 (1990).

Chapter 3

Statistical properties of pulses.Application to modulated gas lasers

3.1 Introduction

The decay of unstable states is one of the fundamental problems of nonequilibrium statistical mechanics in which nonlinearities and fluctuations are crucial to have a correct description of the decay processes [1]. The usual analysis of this process is based on stochastic models of the Langevin type in which fluctuations are modeled by a white noise. In most theoretical analysis it is assumed that the control parameter is instantaneously changed bringing the system from a stable to an unstable state[1,2]. The effect of the finite velocity in the change of the control parameter has been also studied in some cases[3–6]. A related situation is the one in which the control parameter is periodically changed through the instability point. This problem is relevant for several physical systems: modulated convection[7], stochastic resonance[8], Q–switched lasers[9], and gain switched modulated semiconductor lasers[10]. Periodically modulated stochastic systems have been studied with the use of different methods: analytical solutions for the spherical limit $n \to \infty$ of a symmetric n–component model[11], a generalization of Suzuki's matching procedures[3b], continuous–matrix–fraction method[12], path–integral approach[14]... .

In this paper we develop a new method for the analysis of modulated stochastic systems. Following the main idea of the quasideterministic theory [2] (QDT) we consider two kinds of evolutions. When the variable of interest is greater than a certain threshold value fluctuations can be neglected and the evolution is deterministic. In the opposite case, non–linearities are non important and the evolution is described by a linear stochastic equation

that can be solved. All the statistical properties can be obtained from the distribution of the passage time, τ, by the threshold. After an initial transient a periodic distribution, independent of the initial conditions, is obtained for the passage time distribution $P(\tau)$. In this steady–state case the condition that the statistical properties of the passage time are the same for two consecutive periods leads to an integral equation for $P(\tau)$. This equation is the main result of the method. The passage time distribution $P(\tau)$ is obtained by solving the integral equation with the use of numerical methods. However, analytical expressions can be obtained in some cases.

Here we are mainly interested in the steady state statistical properties of pulses for the "intensity" (modulus of the variable of interest). Then for symmetric potentials we do not consider the switching problem from the positive to negative attractor[11]. The pulses can be characterized in terms of their height and width. The probability density of these magnitudes can be obtained from the distribution of the passage times, $P(\tau)$, using the deterministic evolution. Then the statistical properties can be derived from the solution of the integral equation for $P(\tau)$. We apply this method to a Q–switched gas laser. In this system the quality factor of the cavity is changed periodically, and the laser is then switched on and off in the same way. This leads to the formation of pulses for the laser intensity.

The chapter is organized as follows. In sec. 3.2 we describe the method in a one-dimensional general system, defining the relevant variables and obtaining the basic equations. In sec. 3.3 we introduce the modulated gas laser model in terms of stochastic equations for the field and translate the formulation of section 3.2 extending it to complex variables. As result of these generalizations we get an integral equation for $P(\tau)$ with an analytical kernel. In sec. 3.4 we consider a kind of modulation in which the laser is

switched on and off during a certain time. We compare our method with simulations for the passage time and pulse height statistics. We also obtain analytical expressions for the probability density and the mean passage time in two limits: when below threshold the laser reaches the steady state and in the deterministic limit when fluctuations are negligible. These expressions are directly obtained from the integral equation and their range of validity is derived.

3.2 The method

The method is basically an extension to general stages of evolution of the quasideterministic approach, originally used for the decay from unstable states[2]. Here we only analyse the statistics of unimodal pulses when the system is in a steady–state regime but more general cases could be treated. Then, we consider that after an initial transient, the relevant quantities, such as the passage time distribution, are independent of the initial conditions.

In the spirit of the quasideterministic theory we distinguish two kinds of evolutions, one when the variable of interest is small and variations are mainly governed by noise and other when the noise can be neglected and the evolution is esentially deterministic. The quasideterministic theory can be applied when the first kind of evolution is linear or can be linearized. Therefore, this restriction gives the condition of validity of the theory. In our analysis of unimodal pulse formation one finds two regions of the first kind in the first and last part of the period (see fig. 1). The intermediate time of growth and decay are governed by deterministic processes. Fluctuations are originated in the first kind of evolution, when the noise is important, and they are propagated in the deterministic region with an amplification process during the growth and reduction of fluctuations in the decay.

In order to outline the method let us consider an equation modelling pulse formation:

$$\dot{x}(t) = F(a(t), x) + \eta(t) \tag{1}$$

where $a(t)$ is a periodic input with period T, $a(t+T) = a(t)$, F is a nonlinear function with the following conditions:

$$F(a(t), 0) = 0,$$

$$F(a(t), x) \simeq a(t)x, \quad \text{when} \quad \mid x \mid \leq x_0 \tag{2}$$

and $\eta(t)$ is the source of fluctuations, here modelled by a Gaussian white noise with intensity D and correlation:

$$\langle \eta(t)\eta(s) \rangle = D\delta(t-s). \tag{3}$$

D must be small enough to guarantee the validity of the quasideterministic aproach, i.e noise can be neglected when $\mid x \mid > x_0$. We restrict our study to the case of unimodal pulses, assuming that $a(t)$ has an increasing followed by a decreasing evolution with minimum $a_{min} < 0$ and maximum $a_{max} > 0$. We also assume that there are two atractors, $x_{min} = 0$ and $x_{max} >> x_0$, in the equation (1) for $\mid x \mid$ corresponding to values a_{min} and a_{max} of $a(t)$ respectively. We consider two different situations: the atractors for x are positive or the evolution is symmetric, $F(a(t), x) = -F(a(t), -x)$. With these conditions a possible evolution of $a(t)$ and $\mid x(t) \mid$ is depicted in figure 1. We show in this figure the different regions of evolution. The first region is defined from the beginning of the period with $a(0) = a_{max}$ until a time τ such that $\mid x(\tau) \mid = x_0$. It is a region dominated by fluctuations where the linearized equation

$$\dot{x}(t) = a(t)x(t) + \eta(t) \tag{4}$$

holds. As we will see the passage time to threshold x_0 , τ , plays an important role in this method.

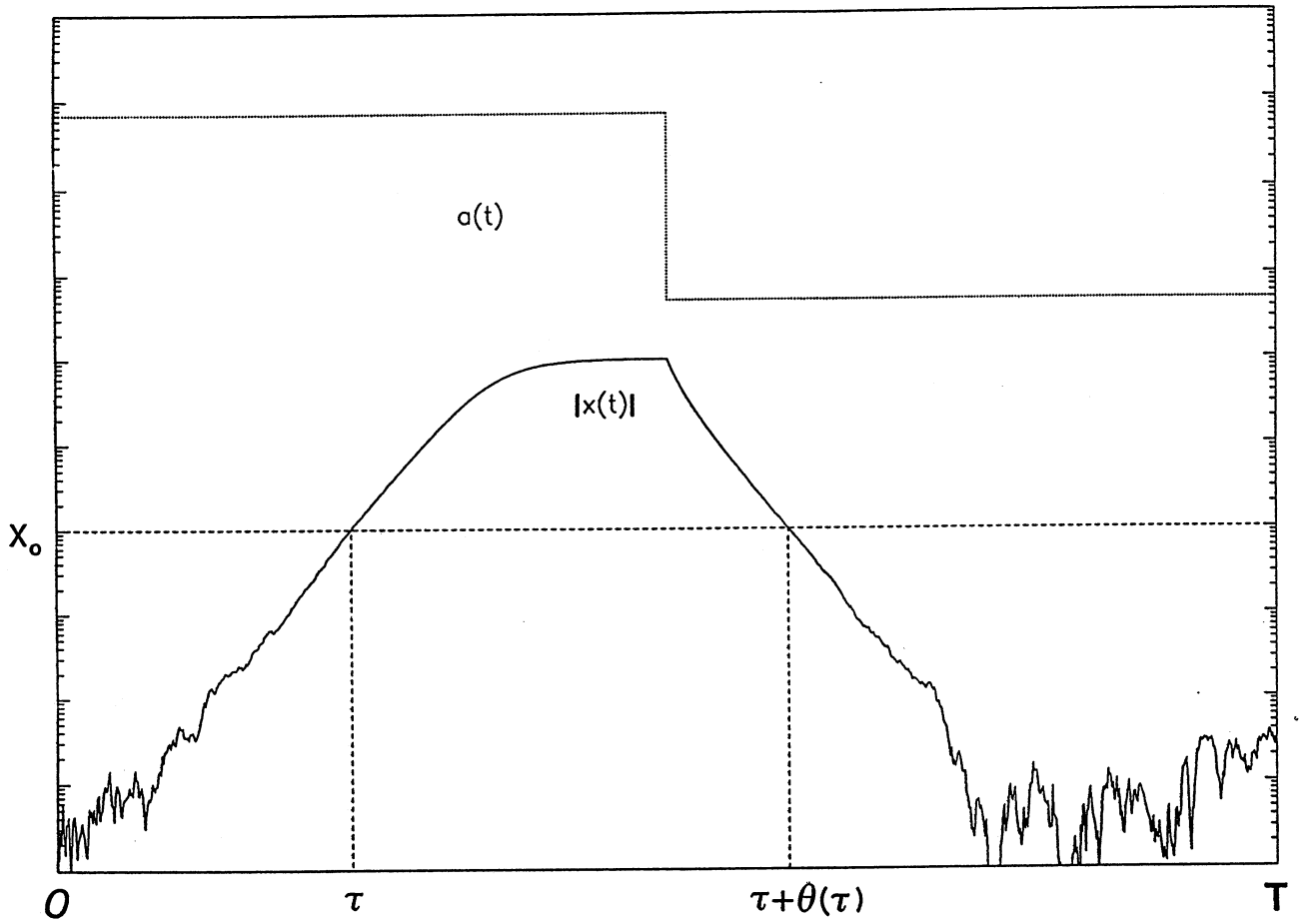

Fig. 1.- Time evolution of one pulse. We plot $x^2(t)$ (solid line) in logarithmic scale and the control parameter, $a(t)$ (dotted line) in arbitrary units.

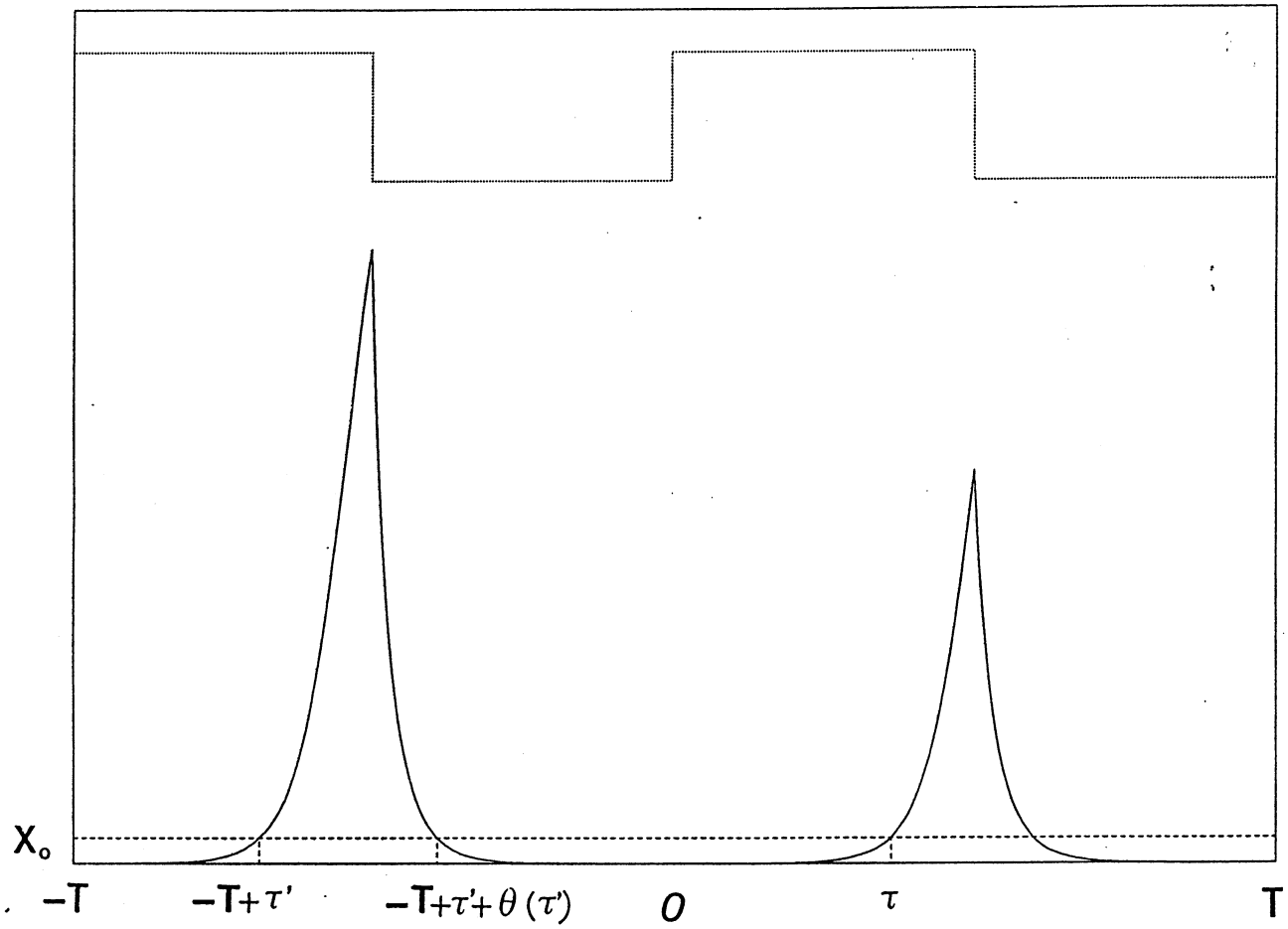

Fig. 2.- Time evolution of two consecutive pulses (solid line) and $a(t)$ (dotted line). Definition of time regions.

In the second region, from τ to $\tau + \theta(\tau)$, the evolution is considered deterministic. $\theta(\tau)$ is the time spent in the deterministic region. Since x_0 is a fixed value $\theta(\tau)$ can be calculated from the deterministic equation

$$\dot{x}(t) = F(a(t), x(t)) \tag{5}$$

as a function of τ. The last region from $\tau + \theta(\tau)$ to the end of period T is again a noise dominated region where the evolution is correctly described by eq. (4).

Once the regions of evolution have been defined, we can proceed with the calculation of statistical quantities through the function $W(\tau/\tau\prime)$ defined as the conditional probability to have a passage time τ when the passage time of the previous period was $\tau\prime$. The passage time is defined as a delay time between the beginning of the period with $a = a_{max}$ and the emission of the pulse defined by $\mid x(\tau) \mid = x_0$ A graphical picture of the evolution in two periods of time is given in figure 2. The time origin has been taken at the end of the first period and beginning of the second one. When the control parameter a takes large negative values during a large enough fraction of the period, all the pulses decay from its maximum value to reach the threshold given by x_0. In this case the possible formation of double modal pulses can be neglected and all trajectories with value x_0 in $-T + \tau\prime + \theta(\tau\prime) \in (-T, 0)$ reach again x_0 in the following period $\tau \in (0, T)$. Then $W(\tau/\tau\prime)$ is the first passage time probability with the initial condition x_0 in time $-T + \tau\prime + \theta(\tau\prime)$. Since in this region the evolution is linear this probability can be calculated from the corresponding Fokker-Planck equation with zero boundary conditions in x_0. However, since the evolution when $\mid x \mid > x_0$ is deterministic, the probability of return to x_0 when $a(t)$ is increasing can be neglected. Then, it is possible to obtain an approximated solution in an easy way by using the passage time, instead of the first passage time. Solving (4) we

write $x^2(t)$ as

$$x^2(t) = h^2(t)\exp[2\int_{-(T-\tau\prime-\theta(\tau\prime))}^{t} a(s)ds] \tag{6}$$

where

$$h(t) = h_0 + \int_{-(T-\tau\prime-\theta(\tau\prime))}^{t} \exp[-\int_{-(T-\tau\prime-\theta(\tau\prime))}^{t\prime} a(s)ds]\eta(t\prime)dt\prime. \tag{7}$$

with $h_0^2 = x_0^2$, $h(t)$ is a Gaussian variable with mean and variance given by:

$$\langle h(t)\rangle = h_0 \tag{8a}$$

$$\sigma_h^2(t) = D\int_{-(T-\tau\prime-\theta(\tau\prime))}^{t} exp\Big(-2\int_{-(T-\tau\prime-\theta(\tau\prime))}^{t\prime} a(s)ds\Big)dt\prime \tag{8b}$$

Substituting now $\mid x(t) \mid$ by x_0 and t by τ in eq.(6) we find a relation between h^2 and τ given by :

$$h^2(\tau) = \frac{x_0^2}{exp(2\int_{-(T-\tau\prime-\theta(\tau\prime))}^{\tau} a(s)ds)} \tag{9}$$

that allows us to calculate statistical properties of τ from those of $h^2(\tau)$.For instance, the conditional probability $W(\tau/\tau\prime)$ is

$$W(\tau/\tau\prime) = P_{h^2(\tau)}(h^2(\tau))|\frac{dh^2}{d\tau}| = P_{h^2(\tau)}(h^2(\tau)) \mid 2a(\tau) \mid\mid h^2(\tau) \mid \tag{10}$$

where, since $h(\tau)$ is Gaussian:

$$P_{h^2(t)}(x) = \frac{1}{2\sqrt{2\pi x}\sigma_h(t)}(e^{-\frac{(\sqrt{x}-x_0)^2}{2\sigma_h^2(t)}} + e^{-\frac{(\sqrt{x}+x_0)^2}{2\sigma_h^2(t)}}). \tag{11}$$

When fluctuations are not negligible the evolution at the end of the period is dominated by the noise, i.e. $\langle\mid x(0) \mid\rangle << x_0$. Then a large time such that $e^{-2a_{max}\tau} << 1$ is needed to cross the threshold x_0 and consequently $\sigma_h^2(\tau)$ can be taken as constant, σ_h^2.

As we will show the knowledge of $W(\tau/\tau\prime)$ allows the calculation of any relevant statistical quantity using only the deterministic eq. (5). The passage time probability

density in the n period, $P_n(\tau)$, follows the chain equation:

$$P_n(\tau) = \int_0^T W(\tau/\tau\prime)P_{n-1}(\tau\prime)d\tau\prime \tag{12}$$

This equation is valid or any pair of consecutive pulses, including the first two pulses, but in this case the system must start at $\mid x(0) \mid < x_0$ with $a(0) = a_{min}$. Now we focus the attention on the calculation of stationary quantities. If we assume that after an initial transient a periodic passage time distribution, independent of the initial condition, is obtained, this stationary probability $P(\tau)$ must be solution of the integral equation:

$$P(\tau) = \int_0^T W(\tau/\tau\prime)P(\tau\prime)d\tau\prime \tag{13}.$$

This equation represents the consistency condition used more indirectly in other methods [3b,14]. The passage time probability by itself is a relevant quantity used in experimental measurements. Moreover it allows the calculation of other statistical quantities . For instance, the probability density of the modulus of the pulse heigths $P_H(y)$ can be inmediatly calculated as:

$$P_H(y) = P(\tau(y))|\frac{d\tau}{dy}| \tag{14}$$

being $\tau(y)$ a function obtained from the deterministic equation (5) that gives the initial time τ needed to have a heigth y for $\mid x \mid$ starting from x_0. The same applies to the probability density of pulse width P_θ.

We conclude this section recalling that with this method the calculation of all relevant quantities pass through the solution of the consistency equation (13).

3.3 Modulated Gas Lasers

Pulses of gas lasers can be obtained by modulation of the pump parameter varying the quality factor of the cavity (Q–switching). The single mode on–resonance laser can be described near threshold and in the good cavity limit by the following equation:

$$\dot{E} = a(t)E - A|E|^2E + \phi(t) \tag{15}$$

where $E = E_1 + iE_2$ is the complex electric field, a is the pump parameter and $\phi = \phi_1 + i\phi_2$ is the spontaneous emision noise modelled by a complex Gaussian white noise of zero mean, intensity D and correlations

$$\langle \phi_i(t)\phi_j(t\prime)\rangle = D\delta_{i,j}\delta(t - t\prime). \tag{16}$$

For D small this equation fulfils the requirements of the previous section but some modifications are necessary in order to take into account the complexity of the field E. First we define the noise dominated region by means of a condition over the light intensity:

$$I = E_1(t)^2 + E_2(t)^2 < I_0. \tag{17}$$

In this region the evolution is linear in such a way that the equations for field components $E_i(t), (i = 1, 2)$ are decoupled:

$$\dot{E}_i(t) = a(t)E_i(t) + \phi_i(t) \tag{18}$$

and as in the previous section they can be solved giving:

$$E_i(t) = h_i(t)\exp(\int_{-(T-\theta(\tau\prime)-\tau\prime)}^{t} a(s)ds) \tag{19}$$

where:

$$h_i(t) = h_{i0} + \int_{-(T-\theta(\tau\prime)-\tau\prime)}^{t} exp(-\int_{-(T-\theta(\tau\prime)-\tau\prime)}^{t\prime} a(s)ds)\phi_i(t\prime)dt\prime, \tag{20}$$

$$h_{10}^2 + h_{20}^2 = I_0.$$

$h_i(t)$ are uncorrelated Gaussian processes with mean h_{i0} and variance, $\sigma_{hi}^2 = \sigma_h^2$, given by (8b). The evolution of the intensity can be written in this linear region as:

$$I(t) = (h_1^2(t) + h_2^2(t))exp(2\int_{-(T-\theta(\tau\prime)-\tau\prime)}^{t} a(s)ds) \tag{21}$$

and operating like in section 2 we can obtain an expression of $W(\tau/\tau\prime)$ in terms of the probability of $\Gamma(t) = h_1^2 + h_2^2$ as:

$$W(\tau/\tau\prime) = P_\Gamma(\Gamma(\tau))|\frac{d\Gamma(\tau)}{d\tau}| \tag{22}$$

where from the definition of τ and (21):

$$\Gamma(\tau) = I_0 exp(-2\int_{-(T-\theta(\tau\prime)-\tau\prime)}^{\tau} a(s)ds). \tag{23}$$

The probability density of Γ can be straighforwardly obtained from its definition and the statistics of h_1 and h_2 giving:

$$P_\Gamma(x) = \frac{1}{2\sigma_h^2}\exp(-\frac{(I_0+x)}{2\sigma_h^2})\mathbf{I_0}(\frac{\sqrt{xI_0}}{\sigma_h^2}). \tag{24}$$

being $\mathbf{I_0}$ the Bessel function of the first order[15]. Finally, the calculation of $\theta(\tau)$ involves only the deterministic equation for the intensity:

$$\dot{I} = 2a(t)I - 2AI^2 \tag{25}$$

that fortunately has analytical solution. Giving the initial, $I(\tau\prime) = I_0$, and final, $I(\tau\prime+\theta) = I_0$, conditions we obtain for θ the implicit equation:

$$1 + 2AI_0\int_{\tau\prime}^{\theta+\tau\prime} exp(\int_{\tau\prime}^{s} 2a(s\prime)ds\prime)ds = exp(\int_{\tau\prime}^{\theta+\tau\prime} 2a(s)ds). \tag{26}$$

Summarizing, for the calculation of stationary quantities in a modulated gas laser we must first calculate the function $\theta(\tau\prime)$ through the equation (26), then obtain the kernel $W(\tau/\tau\prime)$ by means of expresions (22) (24) and finally solve the consistency equation (13). In general some of these problems would require the use of standard numerical methods of low computing time, moreover, with this method it is possible to find an analytic solution for some limiting cases.

3.4 On–Off Modulation. Analytical results and simulations

In this section we are going to consider a very used kind of modulation that involves only two values, on-off, of the parameter $a(t)$. In a laser this modulation is obtained when the pump parameter is suddenly switched between a value $-a_b$ below to a value a above threshold with a modulation period T. The laser is above threshold during a fraction α of the modulation period, $T_{on} = \alpha T$, and below threshold during $T_{off} = (1-\alpha)T$. In this case (26) can be exactly solved giving for $\theta(\tau\prime)$:

$$\theta(\tau\prime) = -\frac{1}{2a_b} ln\Big[\frac{e^{-2(a+a_b)(\alpha T-\tau\prime)}}{1+\frac{AI_0}{a_b}}\big(1+\frac{AI_0}{a}(e^{2a(\alpha T-\tau\prime)}-1)+\frac{AI_0}{a_b}e^{2a(\alpha T-\tau\prime)}\big)\Big], \qquad (27)$$

where we have neglected pathological situation of very low probability in which the laser is on in T_{off} or off in T_{on}. In what follows we also take this assumption making τ and $\tau\prime$ smaller that T_{on} and $\tau+\theta(\tau)$ greater than T_{on}. From (8b) we obtain for the variance σ_h^2:

$$\sigma_h^2 = \frac{De^{2a_b(T-\theta(\tau\prime)-\tau\prime)}}{2}\Big[\frac{1}{a_b}(1-e^{-2a_b(T-\theta(\tau\prime)-\tau\prime)})+\frac{1}{a}(1-e^{-2a\tau})\Big] \;;\tau,\tau\prime < T_{on} \qquad (28)$$

Using (22) and (24) we obtain for the conditional probability $W(\tau/\tau\prime)$:

$$W(\tau/\tau\prime) = \frac{aI_0}{\sigma_h^2}e^{2a_b(T-\theta(\tau\prime)-\tau\prime)}\exp\frac{-I_0(1+e^{2a_b(T-\theta(\tau\prime)-\tau\prime)-2a\tau})}{2\sigma_h^2}$$

$$e^{-2a\tau}\mathbf{I_0}(\frac{I_0 e^{a_b(T-\theta(\tau\prime)-\tau\prime)-a\tau}}{\sigma_h^2}). \tag{29}$$

Conditions of validity of the method can be explicitely obtained analysing the conditions of existence of regions separated by the threshold I_0. I_0 must be in a deterministic region so it is far away the region of domain of the noise:

$$I_0 >> \frac{D}{min\{a, a_b\}} \tag{30}$$

On the other hand I_0 must be in a linear region where saturation is negligible:

$$\frac{AI_0}{a_b} << 1 \ , \frac{AI_0}{a} << 1. \tag{31}$$

The existence of I_0 and as a consequence the general condition of validity of this method comes from the simultaneous validity of the above conditions, yielding:

$$D << [\frac{min\{a, a_b\}^2}{A}]. \tag{32}$$

From now on we shall consider values of parameters in agreement with these conditions.

In order to calculate the stationary passage time probability density $P(\tau)$ we must deal with the consistency equation (13) with integral kernel given by (29). In general it is not possible to solve analytically this integral equation and therefore we use a standard numerical algorithm. The results obtained with this method are shown in figure 3 (solid line). These results are compared with simulations (histograms) obtaining a very good agreement as can be seen in the above figure. In order to be sure that the system is in steady state conditions we have considered an initial transient of the order of 100 pulses. In figure 4 and 5 we plot mean and variances of τ versus the adimensional parameter a_bT. Theory and simulation are again very close for any value of a_bT.

The mean value and variance of the passage time increase with $a_b T$ and $(1-\alpha)$, fraction of the time spent below threshold, in such a way that they are nearly constant for the same value of α and the product of $a_b T$. In the figures 4 and 5 two different behaviours are observed. For $a_b T$ large the mean passage times and variances saturate going to the limit of the repetitive Q-switching (no modulation effects). In this case the laser intensity below threshold is mainly due to the spontaneous emission noise and the steady state of the intensity with parameter a_b is reached in the decay of the pulse. The second situation happens when $a_b T$ is small and the passage time is a linear function of $a_b T$ with a slope that increases with $(1-\alpha)$. In this case the intensity at the end of the pulse has an apreciable value and the switching is deterministic.

From the analysis of the kernel (29) it is possible to obtain analytic results for these limiting situations. In the first situation fluctuations in the decay of the pulse must attain the stationary state, i.e. $\langle I(0)\rangle \sim \langle I\rangle_{stationary} = D/a_b$. From eqs. (20), (21) and (30) we have

$$\langle I(0)\rangle \sim \frac{D}{a_b} + I_0 e^{-2a_b(T-\theta(\tau\prime)-\tau\prime)} \tag{33}$$

and therefore we obtain the condition

$$e^{-2a_b(T-\theta(\tau\prime)-\tau\prime)} << \frac{D}{a_b I_0} \tag{34}$$

Using eqs. (27) and (31), we conclude that (34) holds when a_b and T_{off} are large:

$$e^{-2a_b T(1-\alpha)} << A\frac{D}{a_b}(\frac{1}{a}+\frac{1}{a_b}) \tag{35}$$

Now taking into account (34) and the estimation

$$e^{-2a\tau} \sim \frac{\langle I(0)\rangle}{I_0} = \frac{D}{a_b I_0} \tag{36}$$

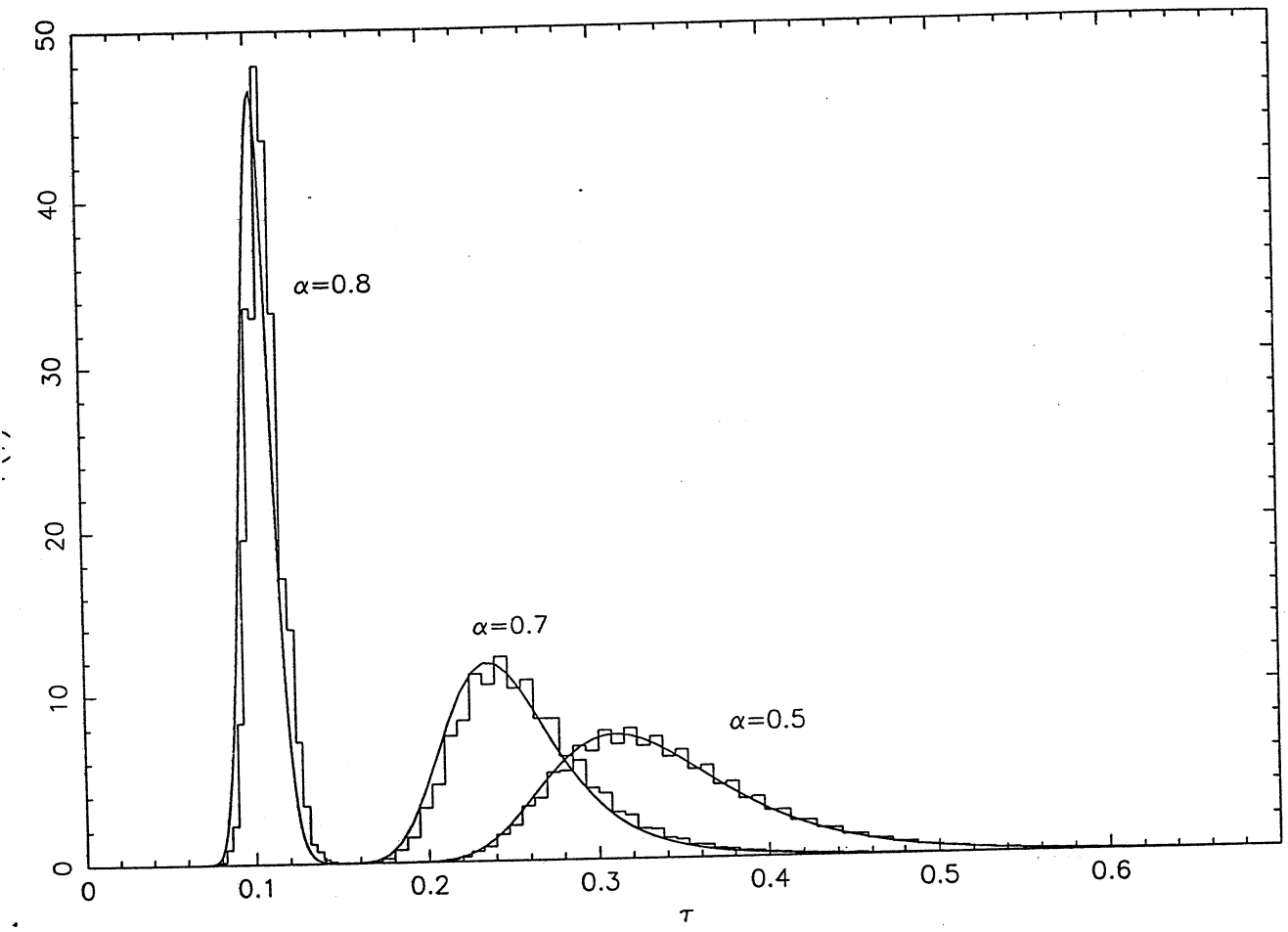

Fig. 3.- Probability density function $P(\tau)$ given by simulations (histograms) and by our method (solid line). The parameters are $a = 10, a_b = 10, T = 1.5, D = 10^{-3}, A = 1$ and $I_0 = 0.1$

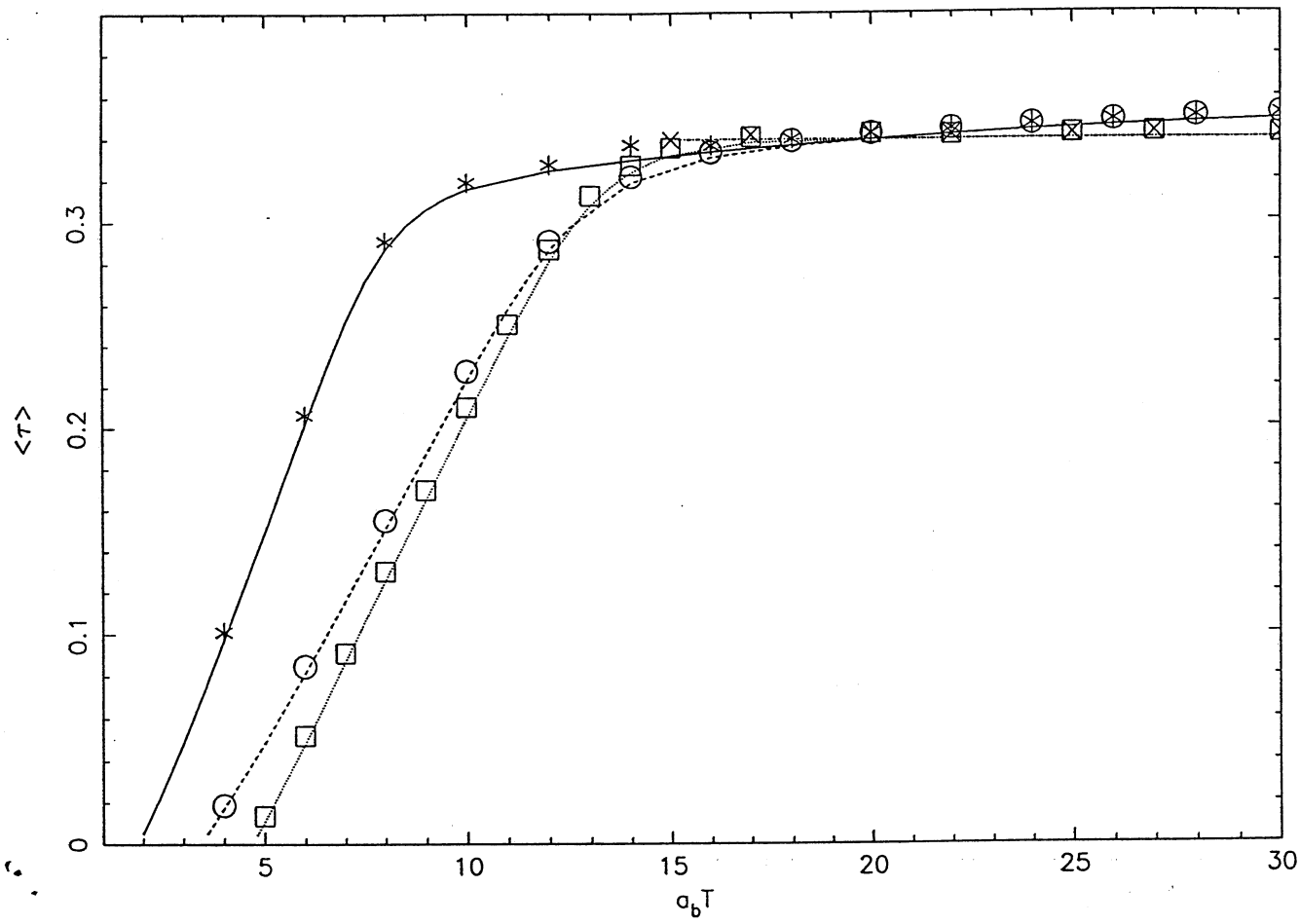

Fig. 4.- Mean switch–on time $\langle\tau\rangle$ as a function of $a_b T$. Symbols correspond to simulations and curves are the results of the method. The parameters are $T = 2, \alpha = 0.4$ (solid line and stars), $T = 2, \alpha = 0.6$ (dashed line and circles), $a_b = 10, \alpha = 0.4$ (dot–dashed line and crosses) and $a_b = 10, \alpha = 0.6$ (dotted line and squares). The other parameters are $a = 10, D = 10^{-3}, A = 1$ and $I_0 = 0.1$

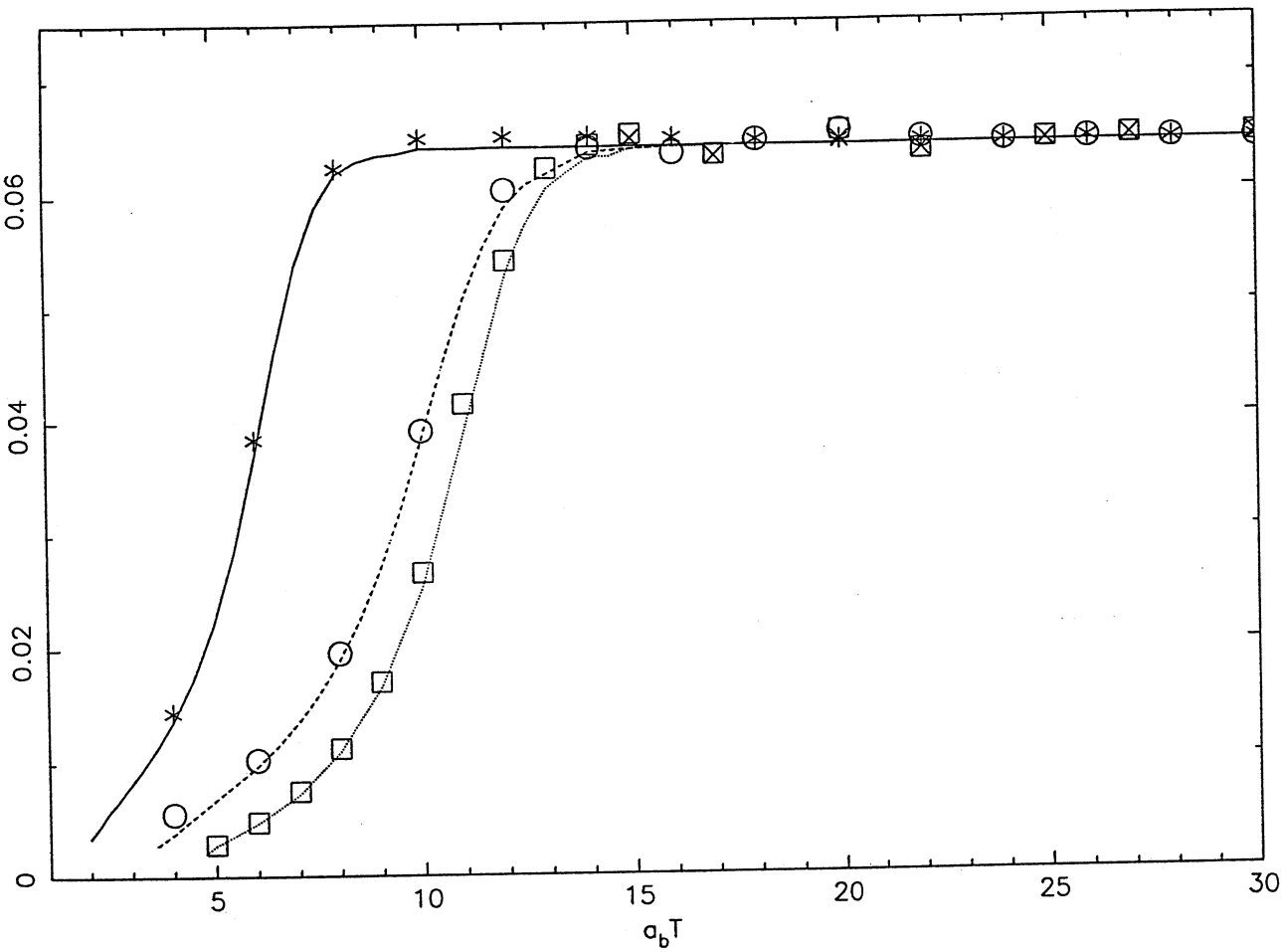

Fig. 5.- Variance of the passage time as a function of $a_b T$. Parameters are the same that in Fig. 4.

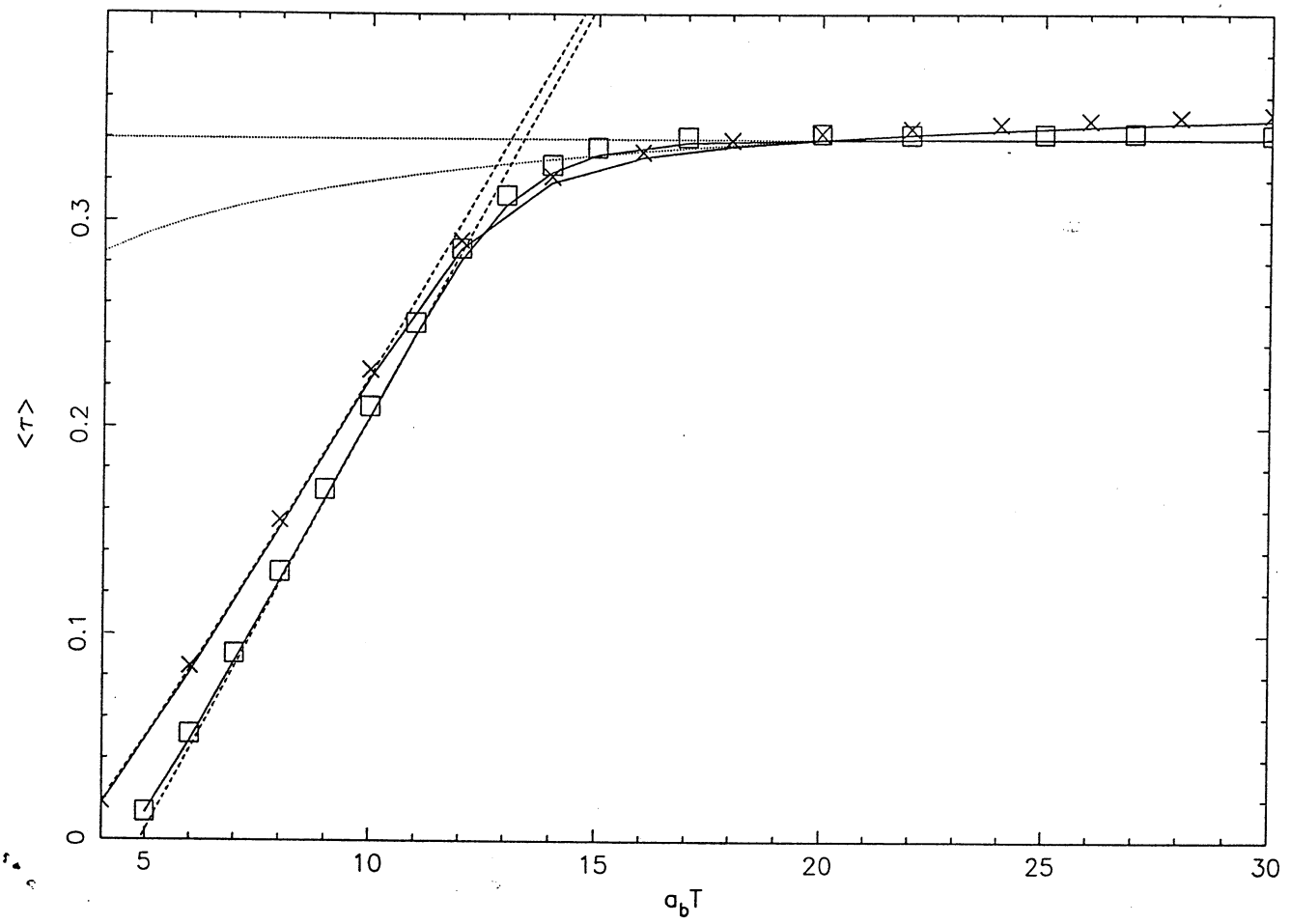

Fig. 6.- Mean switch–on time as a function of $a_b T$. We also plot the analytical approximations given by eqs. (39), (dotted line), and (46) ,(dashed line). Parameters are the same that in Fig. 4 with $\alpha = 0.6$.

it is easy to see that the argument of the Bessel function in eq. (29) is very small. Then, using[15] $\mathbf{I_0}(x) \sim 1$, the conditional probability becomes separable:

$$W(\tau/\tau\prime) = \frac{2aI_0}{(\frac{D}{a_b}+\frac{D}{a})} e^{-2a\tau} \exp\Big(-\frac{I_0}{(\frac{D}{a_b}+\frac{D}{a})} e^{-2a\tau}\Big)$$

$$\exp\Big(-\frac{I_0}{(\frac{D}{a_b}+\frac{D}{a})} \exp(-2a_b(T-\theta(\tau\prime)-\tau\prime))\Big) \tag{37}$$

and a trivial solution of the consistency equation writes:

$$P(\tau) = N \exp\Big(-2a\tau - \frac{I_0}{(\frac{D}{a_b}+\frac{D}{a})} e^{-2a\tau}\Big) \tag{38}$$

with N being a normalization constant. This is the clasical result of the case without modulation (repetitive switch-on). The mean passage time and variance are readily obtained as[5]:

$$\langle\tau\rangle \sim \frac{1}{2a}\Big(ln\frac{I_0}{D(\frac{1}{a}+\frac{1}{a_b})} - \psi(1)\Big),\ \ \sigma_\tau^2 \sim \frac{\psi\prime(1)}{4a^2} \tag{39}$$

where ψ and $\psi\prime$ are the Digamma function and its derivative respectively[15], recovering the known result without modulation (see figure 6). We have checked with numerical simulations that this approximation is valid when (35) holds.

On the other hand, we can now see that the second physical situation just corresponds to a very large value of the argument in $\mathbf{I_0}$. In this case $I(0)$ must be large enough for the fluctuations to be negligible. Taking into account that the argument of $\mathbf{I_0}$ can be written in the following form

$$x \sim \frac{2I_0}{D\big[\frac{1}{a_b}(1-e^{-2a_b(T-\theta(\tau\prime)-\tau\prime)})+\frac{1}{a}(1-e^{-2a\tau})\big]} > 2\frac{I(0)}{D(\frac{1}{a_b}+\frac{1}{a})} \tag{40}$$

we conclude that in this case, $x >> 1$. Now we consider the assymptotic expansion[15]:

$$\mathbf{I_0}(x) \sim \frac{e^x}{\sqrt{2\pi x}} \tag{41}$$

in (29):

$$W(\tau/\tau\prime) \sim a\sqrt{\frac{I_0}{2\pi\sigma_h^2\prime}}$$

$$\exp\Big(-\frac{3}{2}a\tau + \frac{1}{2}a_b(T-\theta(\tau\prime)-\tau\prime)\Big)\exp\Big[-\frac{I_0\big(e^{-a_b(T-\theta(\tau\prime)-\tau\prime)}-e^{-a\tau}\big)^2}{2\sigma_h^2\prime}\Big], \qquad (42)$$

where $\sigma_h^2\prime = \sigma_h^2\exp(-2a_b(T-\theta(\tau\prime)-\tau\prime))$. From equations (28) and (30) we have $\frac{\sigma_{h\prime}^2}{I_0} << 1$, and the conditional probability leads to:

$$W(\tau/\tau\prime) \sim \delta(\tau-\gamma(\tau\prime)) \qquad (43)$$

with:

$$\gamma(\tau\prime) = \frac{1}{2a}\Big[ln\big(AI_0(\frac{1}{a}+\frac{1}{a_b}) + \exp(2a(\tau\prime-\alpha T)) + 2a_bT(1-\alpha)\Big]. \qquad (44)$$

With this kernel the consistency equation (13) has the solution

$$P(\tau) = \delta(\tau-\tau_D) \qquad (45)$$

where τ_D satisfies $\tau_D = \gamma(\tau_D)$. This equation has a solution only when $a_b(1-\alpha) < a\alpha$, i.e. when the laser is in average during a period above treshold. In this case the solution is

$$\tau_D = \frac{1}{2a}\big[ln(AI_0(\frac{1}{a}+\frac{1}{a_b})) + 2a_bT(1-\alpha) - ln(1-e^{-2a\alpha T+2a_b(1-\alpha)T})\big] \qquad (46)$$

This solution corresponds to a limit in which, after transients, the intensity attains a deterministic stationary state (see fig. 6). Since $a_bT_{off} < aT_{on}$ the last term can be usually neglected. Then, the switch–on time is a linear function of a_bT with a slope given by $(1-\alpha)/a$ (see Fig. 6).

In order to find conditions of existence of the above situation we substitute τ and $\tau\prime$ by τ_D and evaluate the imposed constrains:

$$I(0) \sim I_0e^{-2a_b(T-\theta(\tau\prime)-\tau\prime)} >> D(\frac{1}{a}+\frac{1}{a_b}) \qquad (47)$$

Using (27) and (46) and the condition $I(0) < I_0$ we obtain

$$AI_0(\frac{1}{a}+\frac{1}{a_b}) > e^{-2a_bT(1-\alpha)} - e^{-2a\alpha T} >> DA(\frac{1}{a}+\frac{1}{a_b})^2 \tag{48}$$

Then, T_{off} must be large enough to have a passage time different from zero but enough small to avoid fluctuations at the end of the period. Note that when one of the conditions is violated, as in the case of the curve with $\alpha = 0.4, a = a_b = 10$ of figure 4 the corresponding situation does not appears. In this case the laser is in average below threshold and for some periods the intensity does not reach the level I_0.

The region of values of a_bT where the two previous approximations do not hold can be estimated from unequality (35) and the second unequality of (48). It can be seen that small changes of the parameter a_bT leads to one unequality or the other. Therefore the range of values of a_bT of the intermediate region between the two approximations is not very large (see Fig. 6).

To conclude we now analyse the stationary statistics of heights . We recall that with the knowledge of $P(\tau)$ the expression of the corresponding density P_H is given by (14) , and we only require the calculation of $H(\tau)$ from the deterministic equation (25).In the on-off modulation case this calculation is exact and given by:

$$H = \frac{I_0 e^{2a(\alpha T-\tau)}}{1+\frac{A}{a}I_0(e^{2a(\alpha T-\tau)}-1)}. \tag{49}$$

Then the probability density is written as:

$$P_H(h) = P_\tau(\tau(h))\frac{1}{2a} \mid \frac{1}{h-\frac{a}{A}} - \frac{1}{h} \mid \tag{50}$$

with

$$\tau(h) = \alpha T - \frac{1}{2a} ln(\frac{h(\frac{AI_0}{a}-1)}{I_0(\frac{Ah}{a}-1)}). \tag{51}$$

In Fig. 7 we show the good agreement between the method and simulation in four differents situations. Even in a critical case with $T = 0.8$ where pulses are in formation this agreement is excelent. A great variety in the behaviour of the heights can be obtained when T decreases, if eq. (35) holds. In this situation the pulses reach the off–stationary state at the end of the period and $P(\tau)$ does not change when changing T. When the period decreases such that $\langle\tau\rangle$ becomes of the order of T_{on} the pulses can not reach the on–stationary state having different heights. We have also analyzed the statistic of the pulse width in the same way finding again a good agreement between the simulation and the present method.

The good results obtained with this method in all cases suggest the possibility of using it as an alternative to simulations in cases where the computing time becomes excessive. As an example we have recently applied the method to a semiconductor laser [16].

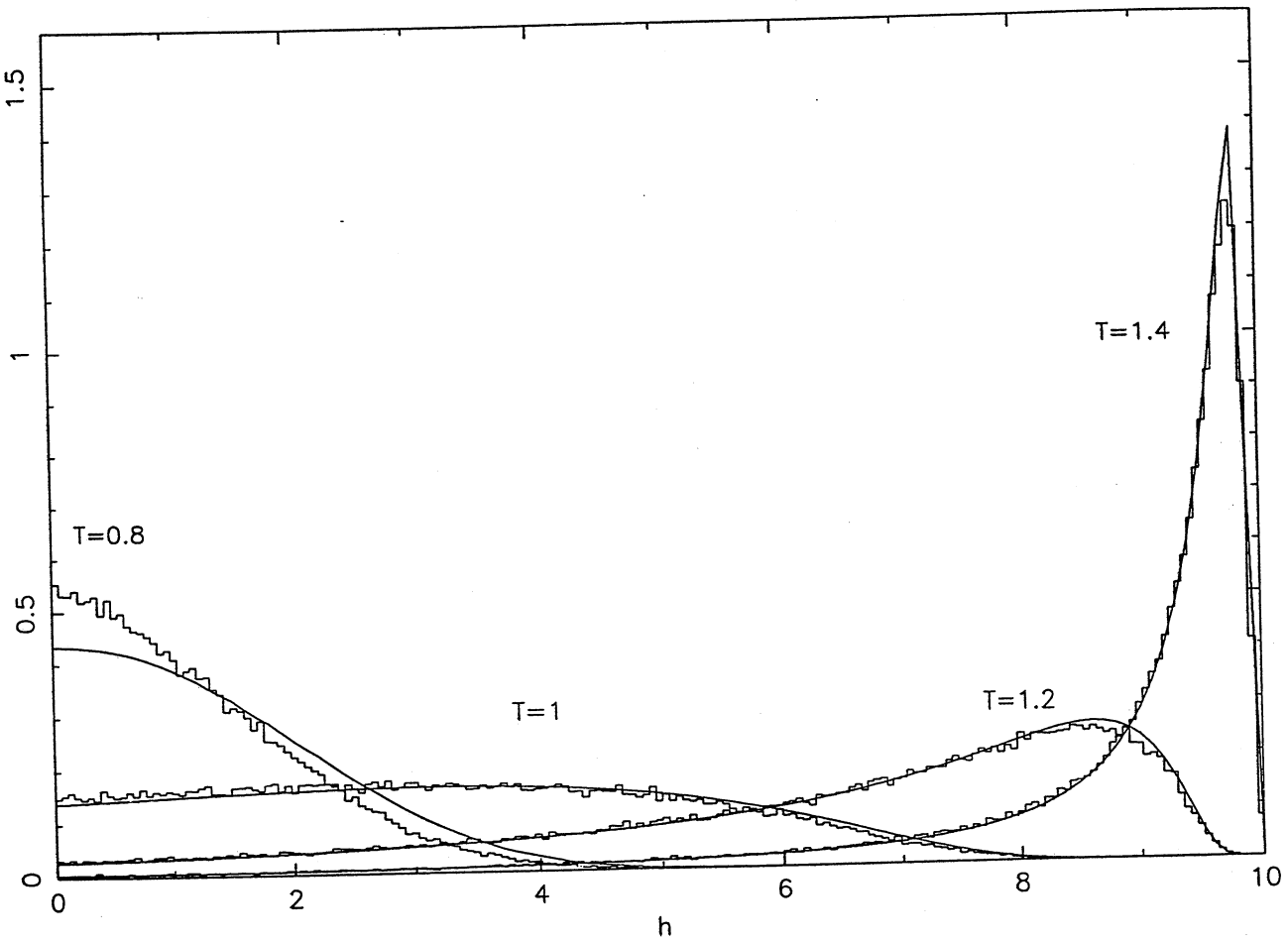

Fig. 7.- Probability density function P_H as a function of the height when changing the period T. The parameters are $a = 10, a_b = 10, \alpha = 0.5, D = 10^{-3}$ and $A = 1$. The solid line corresponds to the eq. (50) and the histogram is the simulation of eq. (15).

REFERENCES

1 .- M. Suzuki, in *Order and Fluctuations in Equlibrium and Nonequlibrium Statistical Mechanics*, edited by G. Nicolis, G. Dewel, and J. Turner (Wiley, New York, 1980).

2.- F. de Pasquale and P. Tombesi, Phys. Lett. **72A**, 7 (1979); F. de Pasquale, P. Tartaglia, and P. Tombesi, Phys. Rev. A **25**, 466 (1982).

3.- a) G. Ahlers, M. C. Cross, P. C. Hohenberg, and S. Safran, J. Fluid Mech. **110**, 297 (1981). b) J. B. Swift, P. C. Hohenberg and G. Ahlers. Phys. Rev. A **43**, 6572 (1991).

4.- G. Broggi, A. Colombo, L. A. Lugiato, and P. Mandel, Phys. Rev. A **33**, 3635 (1986).

5.- M. C. Torrent and M. San Miguel, Phys. Rev. A **35**, 1453 (1987).

6.- A. Valle, L. Pesquera and M. A. Rodríguez, Phys. Rev. A **45**, 5243 (1992).

7.-C. W. Meyer, G. Ahlers, and D. S. Canell, Phys. Rev. Lett. **59**, 1577(1987).

8.- B. McNamara, K. Wiesenfeld, and R. Roy, Phys. Rev. Lett. **60**, 2626 (1988).

9.- O. Svelto, in *Principles of lasers* (Plenum Press, New York, 1982).

10.- K. Petermann, in *Laser diode modulation and noise*, edited by T. Okoshi (Kluwer Academic Publishers, The Netherlands, 1988).

11.- F. de Pasquale, Z. Racz, M. San Miguel, and P. Tartaglia, Phys. Rev. B **30**, 5228 (1984).

12.- M. Suzuki, Phys Lett. A **67**, 339 (1978); Prog. Theor. Phys. (Kyoto) Suppl. **64**, 402 (1978).

13.- P. Jung and P. Hanggi, Europhys. Lett. **8**, 505 (1989); P. Jung, Z. Phys. B **76**, 521 (1989).

14.- M. O. Cáceres, A. Becker, and L. Kramer, Phys. Rev A **43**, 6581 (1991).

15.- *Handbook of Mathematical Functions*, edited by M. Abramowitz and I. Stegun (Dover, New York, 1970).

16.- A. Valle, M. A. Rodríguez and C. Mirasso. Opt. Lett. **17**, 1523 (1992).

Chapter 4

Analytical Calculation of Time Jitter in Single–Mode Semiconductor Lasers Under Fast Periodic Modulation

4.1 Introduction

When a single–mode semiconductor laser is directly modulated by an injection current the time jitter, i.e. the uncertainty in the switch–on time of the laser due to the spontaneous emission noise, plays an important role as a limiting factor in the emission of the optical pulse [1], [2]. For modulation regimes of the order of MHz, in the IM/DD RZ scheme, it is well known that the jitter strongly depends on the bias current, assuming almost negligible values for bias currents far above threshold, due to the fact that the spontaneous emission noise is negligible compared with the stimulated emission [3], [4]. Since two consecutive electrical pulses are well separated (of the order of ns), the number of photons I and the carrier number N have enough time to relax to the steady state given by the bias current. Under these considerations it is clear that, for optical communication systems working at MHz rates, a bias current above threshold would minimize the jitter and consequently the bit error rate (BER) due to this jitter. On the other hand, it has been recently shown, both by numerical simulation [5], [6], and experimentally [7], that, for frequencies of order of GHz, the time jitter is almost independent of the bias current in a periodic–modulation regime. This is due to the fact that neither I nor N has time enough to relax to the steady state, giving rise to an effective initial condition for I and N below threshold, at the beginning of each pulse . This means that the choice of a bias current near (above or below) the threshold value is not very important under a period modulation of the injection current and GHz rates. However, it has been also

shown in ref. [6] that a bias current above threshold produces undesirable pattern effects under pseudorandom word modulation and GHz rates, while a special bias current, slightly below threshold, suppresses pattern effects at all frequencies and gives good on/off ratios.

Almost all available results for the time jitter and the switch–on time, at high frequencies of the injection current, are based on numerical simulation of the rate equations for the laser. Despite the good predictions given by the simulation results, it is very difficult to simulate more than 10^5–10^6 pulses, due to the large computational time.

In this chapter we report a new combined method—numerical and analytical—for calculating the switch–on time and the jitter for single–mode semiconductor lasers under a periodic modulation of the injection current at GHz frequencies.

4.2 The analytical Method

The analysis is based on the noise–driven rate equations for electrical field E and carriers N, inside the cavity, [8]

$$\frac{dE}{dt} = [(1+i\alpha)G - \gamma]\frac{E}{2} + \sqrt{2\beta N}\xi(t) \qquad (1)$$

$$\frac{dN}{dt} = C(t) - \gamma_e N - GI \quad , \qquad (2)$$

where $G = \frac{g(N-N_0)}{\sqrt{1+sI}}$; $g = 5.6\times10^4 s^{-1}$ is the gain rate per carrier; $\gamma = 4\times10^{11}s^{-1}$ is the inverse photon lifetime; $\gamma_e = 5\times10^8 s^{-1}$ is the inverse carrier lifetime; $N_0 = 6.8\times10^7$ is the carrier number at transparency; $s = 1.2\times10^{-6}$ inverse saturation intensity; $\beta = 1.1\times10^4 s^{-1}$ is the spontaneous emission rate and α is the linewidth enhancement factor. As we are only interested in statistical quantities which depend only on the number of photons I, we take $\alpha = 0$ without loss of generality. The injection current

$C(t)$ follows a square–wave modulation of period $T = t_{on} + t_{off}$ with $C(t) = 3.5C_{th}$ during t_{on} ($C_{th} = (\gamma/g + N_0)\gamma_e \approx 3.76 \times 10^{16}\ s^{-1}$ is the threshold current), and C_b, the bias current, during the time t_{off}. The random spontaneous emission term is modeled by a complex Gaussian white noise of zero mean and correlation $< \xi(t)\xi^*(t') >= 2\delta(t - t')$.

The analytical method, recently applied to a gas laser [9], is based on the quasideterministic theory (QDT), originally used for studying the decay from metastable initial conditions [10]. In the spirit of the QDT, we distinguish two different kinds of evolution: one when the electric field E is small and variations are governed by noise (time interval between $-T + Z' + \theta$ and Z in fig. 1) and other one where the noise can be neglected and the evolution is essentially deterministic (time interval between $-T + Z'$ and $-T + Z' + \theta$ in fig. 1). In figure 1 a typical evolution of I and N under periodic modulation regime is shown. I_r is the reference level for I which separates the regions of the two different evolutions, and it is taken as a 10 % of the steady–state value for I with $C(t) = 3.5\,C_{th}$. Z, the switch–on time, and N_Z, the carrier number at time Z, are the relevant variables of the method.

In the region of $I < I_r$ eqs. (1) and (2) can be linearized becoming

$$\frac{dE_i}{dt} = [g(N - N_0) - \gamma]\frac{E_i}{2} + \sqrt{2\beta N}\xi_i(t) \tag{3}$$

$$\frac{dN}{dt} = C(t) - \gamma_e N \tag{4}$$

(where the subindex $i = 1, 2$ stands for the real and imaginary part of E and ξ, respectively), together with the conditions

$$E_1^2(-T + Z' + \theta) + E_2^2(-T + Z' + \theta) = I_r \tag{5}$$

$$N(-T + Z' + \theta) = N_\theta \quad . \tag{6}$$

The solution of eqs. (3) and (4) are given by

$$E_i(t) = h_i(t) \quad \exp\left\{\frac{1}{2}\int_{-(T-Z'-\theta)}^{t} [g(N-N_0)-\gamma] \quad ds\right\} \tag{7}$$

$$N(t) = N_\theta \quad \exp\{-\gamma_e(t+T-Z'-\theta)\} + \int_{-(T-Z'-\theta)}^{t} \exp\{-\gamma_e(t-s)\} \quad C(s) \quad ds \quad , \tag{8}$$

where

$$h_i(t) = E_i(-(T-Z'-\theta)) + \int_{-(T-Z'-\theta)}^{t} \sqrt{2\beta N(t')} \times \quad \exp\left\{-\frac{1}{2}\int_{-(T-Z'-\theta)}^{t'} [g(N-N_0)-\gamma]ds\right\} \quad \xi_i(t') \quad dt' \tag{9}$$

are Gaussian processes of mean $< h_i >= E_i(-(T-Z'-\theta))$ and variance

$$\sigma_{h_i} = \sigma_h = \int_{-(T-Z'-\theta)}^{t} 2\beta N(t') \quad \exp\left\{-\int_{-(T-Z'-\theta)}^{t'} [g(N-N_0)-\gamma]ds\right\} \quad dt' \quad . \tag{10}$$

The intensity I in the linear regime is given by

$$I(t) = E_1^2(t) + E_2^2(t) = \Gamma(t) \quad \exp\left\{\int_{-(T-Z'-\theta)}^{t} [g(N-N_0)-\gamma] \quad ds\right\} \quad , \tag{11}$$

where $\Gamma(t) = h_1^2(t) + h_2^2(t)$. Substituting t by Z and $I(t)$ by I_r in eq. (11), we find a relationship between Z and $\Gamma(Z)$. This is

$$\Gamma(Z) = I_r \quad \exp\left\{-\int_{-(T-Z'-\theta)}^{Z} [g(N-N_0)-\gamma] \quad ds\right\} \quad . \tag{12}$$

From eq. (12) we can calculate the statistical properties of Z through the statistical properties of $\Gamma(Z)$. Let us define $W(Z/Z', N_{Z'})$, the conditional probability of reaching I_r at time Z under the condition that I_r is reached at time Z' in the previous period with carrier number $N_{Z'}$, i.e.

$$W(Z/Z', N_{Z'}) = P_\Gamma(\Gamma(Z))\left|\frac{d\Gamma(Z)}{dZ}\right| \quad . \tag{13}$$

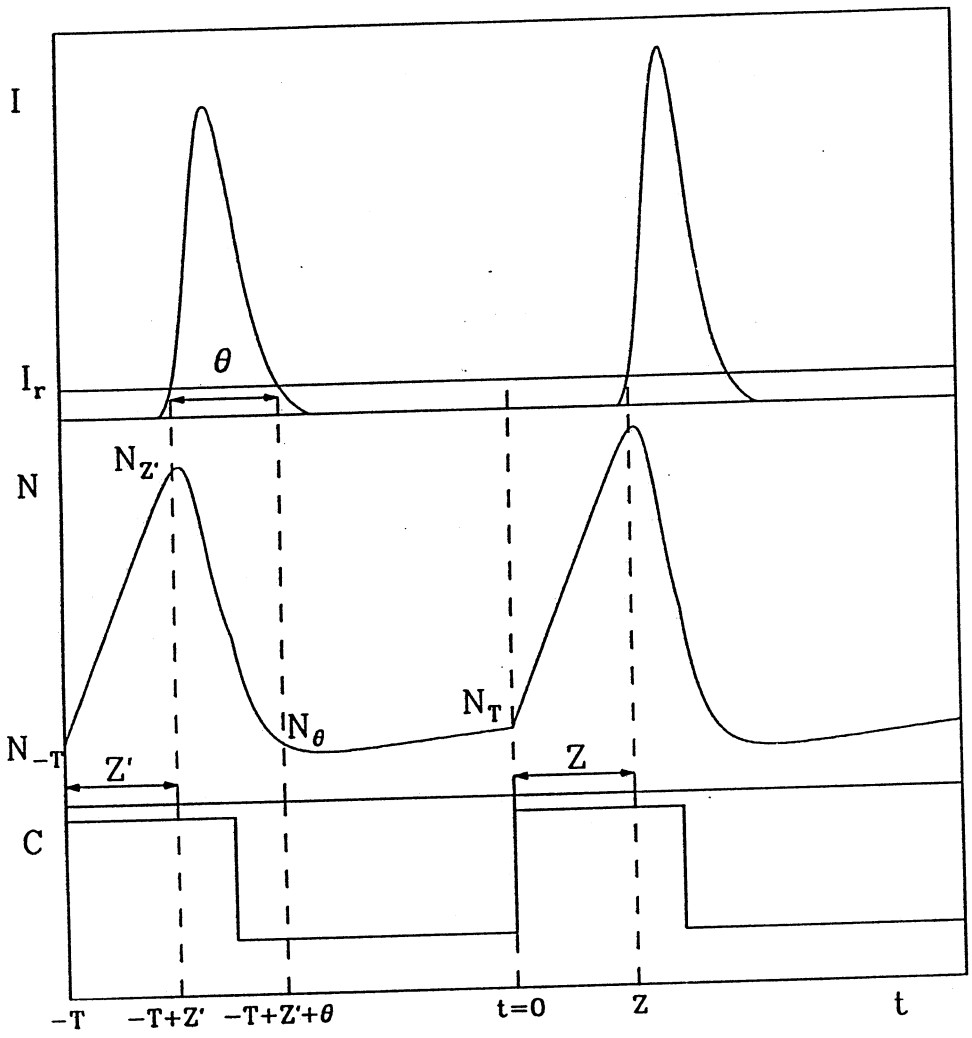

Fig. 1 Qualitative time trace for the number of photons I, the carrier number N and the injection current C as a function of time.

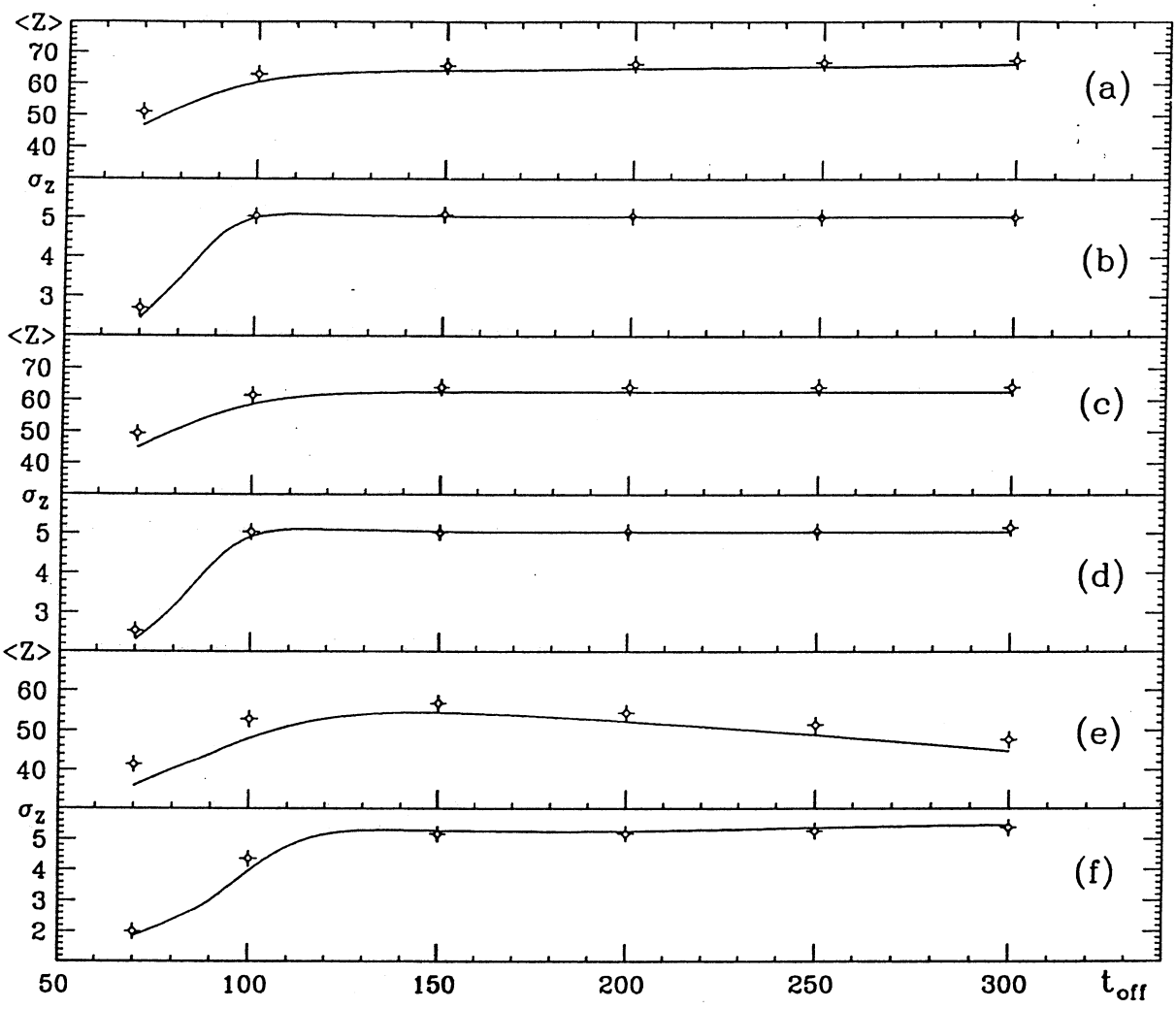

Fig. 2 Mean switch–on time $< Z >$ and time jitter σ_Z as a function of t_{off} for $C_b = 0.95\, C_{th}$ (a) and (b), respectively, $C_b = 0.98\, C_{th}$ (c) and (d), respectively, and $C_b = 1.1\, C_{th}$ (e) and (f), respectively. Solid line correponds to analytical results; stars correspond to numerical integration of eqs. (1) and (2) over 10^4 periods.

Note that $\Gamma(Z)$ also depends on Z' and $N_{Z'}$ through N_θ and θ. The probability density P_Γ can be easily calculated from the statistics of h_1 and h_2, giving

$$P_\Gamma(x) = \frac{1}{2\sigma_h} \exp\left\{-\frac{I_r + x}{2\sigma_h}\right\} \mathcal{I}_0\left(\frac{\sqrt{xI_r}}{\sigma_h}\right) \quad , \tag{14}$$

where $\mathcal{I}_0$ is the Bessel function of order zero.

In order to solve the equation for the whole period, we need to find the time θ during which the system evolves in the deterministic region, and the final number N_θ of the carriers at this time (see fig. 1). This is done by numerically integrating eqs. (1) and (2), neglecting noise effects, together with the boundary conditions $I(-T+Z') = I_r$ and $N(-T+Z') = N_{Z'}$, and tabulating the functions $\theta = \theta(N_{Z'}, Z')$ and $N_\theta = N_\theta(N_{Z'}, Z')$.

The joint probability of the switch–on time Z and carrier number N_Z in a period n, $P_n(Z, N_Z)$, obeys the recursion relation:

$$P_n(Z, N_Z) = \int_0^T dZ' \int_0^\infty dN_{Z'} \delta(N_Z - N(Z)) W(Z/Z', N_{Z'}) P_{n-1}(Z', N_{Z'}) \quad . \tag{15}$$

If a stationary probability $P(Z, N_Z)$ exists, it must satisfy

$$P(Z, N_Z) = \int_0^T dZ' \int_0^\infty dN_{Z'} \delta(N_Z - N(Z)) W(Z/Z', N_{Z'}) P(Z', N_{Z'}) \quad . \tag{16}$$

This equation is the basis of the method. A more general analysis, incorporating a wider range of parameters, will be discussed in a forthcoming paper. Here we consider an approximation valid in the range of parameters given after eq. (2). Since fluctuations of the carrier number at the beginning of the period $N_T, N_{T'}$ seem to be negligible small, we take this random variable as deterministic with a value n_0 estimated as follow. We use the minimum value reached by the carriers after the switch–on of the laser N_m, given in ref. [5], as the value of N at the time t_{on}. We then integrate eq. (2) with $I = 0$ and $C(t) = C_b$ until the time t_{off} in order to obtain

the value n_0 of N at the end of the period. The value of N does estimated is in a good agreement with the one obtained by numerical simulations. Then equation (16) reduces to

$$P(Z) = \int_0^T W(Z/Z', N_{Z'})P(Z')dZ' \tag{17}$$

with $N_{Z'} = (n_0 - \frac{C_{on}}{\gamma_e})\ \exp\{-\gamma_e Z'\} + \frac{C_{on}}{\gamma_e}$. This integral equation for the probability of the switch–on time Z is solved numerically.

4.3 Results of the method

The results of the combined analytical and numerical method, together with the results of the numerical integration of eqs. (1) and (2), are compared in fig. 2, where we have plotted the mean switch–on time and the time jitter for three different bias currents, around the threshold value, as a function of t_{off} ($t_{on} = 90\,ps$ fixed, see ref. [5]). We have included $C_b = 0.98\,C_{th}$ since its value corresponds to the special bias current, slightly below threshold, proposed in ref. [6] for avoiding pattern effects. As can be seen a very good agreement is obtained for all the values of t_{off} and C_b considered. It is to be expected that for $t_{off} < 50\,ps$ the number of photon I remains rather high and the analytical approximation should not be as good as for larger values of t_{off}. Graphs (b), (d) and (f) show that the jitter, at frequencies of 1–5 GHz, is almost independent of the bias current, as was predicted by [5], in contrast to what happens for slow modulation regimes (MHz range) where a strong dependence on the bias current is observed [3]. Also the mean switch–on time $< Z >$ is not very sensitive to the bias currents as can be seen from graphs (a), (c) and (e).

In fig. 3 the probability distribution function for the switch–on time given by (17) is plotted for $C_b = 0.95\,C_{th}$ and $C_b = 1.1\,C_{th}$, together with the probability distribution function obtained by numerical integration of eqs. (1) and (2) over 10^6 period

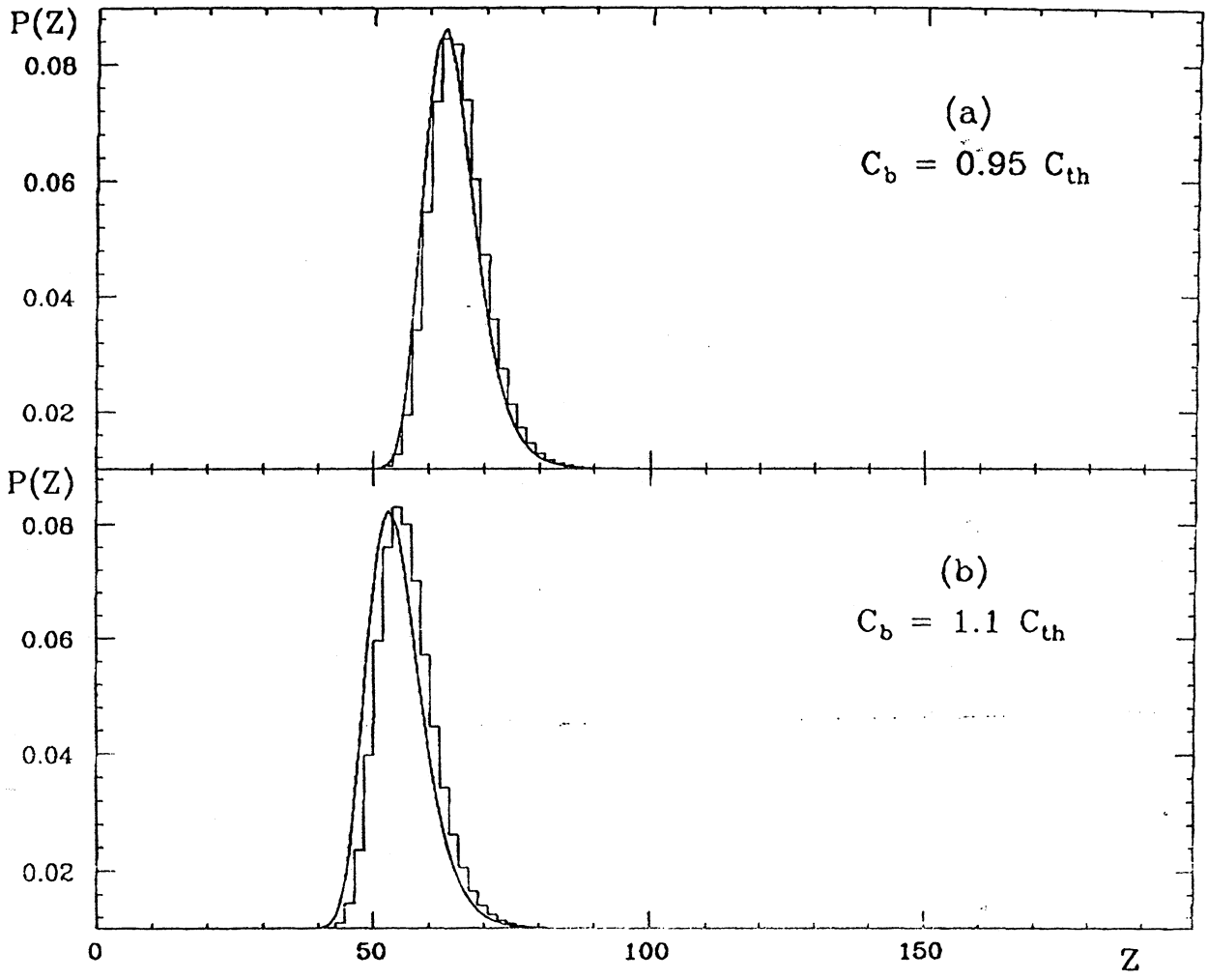

Fig. 3 Normalized probability distribution function $P(Z)$ as a function of Z for $C_b = 0.95\,C_{th}$ (a) and $C_b = 1.1\,C_{th}$ (b). Solid lines correpond to analytical results while the histograms correspond to numerical results.

of modulation. The very good agreement can be seen again, except of a very small shift in the mean value of the switch–on time due to non–linear deterministic effects neglected in the analytical resolution of the eqs. (3) and (4). With the analytical expression for the probability distribution function given by (17) we can estimate the time t_{off} for which the BER is maximum. We consider that we have a BER if any photon of a given period appears, at the output, in the following pulse, i.e. if the switch–on time for a given period is such that $\tilde{Z} \geq T - < w >$, where $< w >$ is the mean width of the optical pulse at I_r. The value $< w >$ can be obtained from the table of the function $\theta = \theta(N_{Z'}, Z')$ mentioned above. In our case, $< w > \sim 60\,ps$. Hence, the value of t_{off} for which the BER is maximum is 80 ps for our parameter values. With this time t_{off} the BER is of the order 10^{-10}.

As a conclusion, we have presented a new simple method for calculating the mean switch–on time and the jitter for a single–mode semiconductor laser under fast periodic modulation of the injection current. The results obtained with this method are in a very good agreement with numerical simulations of the rate equation for the laser. The most important advantage is that the method allows one to obtain accurate results eliminating large computational times due to numerical integrations of the rate equations (1) and (2). This can be done since the stochastic rate equations can be integrated using QDT, in the time interval where the noise effects are dominant.

REFERENCES

[1] See for example P. Spano, A. Mecozzi, A. Sapia and A. D'Ottavi, Springe Proceedings in Physics, vol. 55 "Nonlinear Dynamics and Quantum Phenomena in Optical Systems", Ed. by R. Vilaseca, Springer-Verlag, 259 (1991) and references therein.

[2] G. P. Agrawal, SPIE Proc. vol. 1376, ed. by R. Roy, pp. 224–235, 1990.

[3] P. Spano, A. D'Ottavi, A. Mecozzi and S. Piazzola, Appl. Phys. Lett. vol. 52, pp. 2203–2204 (1988); A. Mecozzi, S. Piazzolla A. D'Ottavi and P. Spano, Phys. Rev. A vol. 38, pp. 3136–3139, 1988; A. Mecozzi, P. Spano, A. D'Ottavi and S. Piazzolla, Appl. Phys. Lett. vol. 55, pp. 769–771, 1989.

[4] A. Weber, W. Ronghan, E. Holger Böttcher, M. Schell and D. Bimberg, J. Quantum Electron. **28**, 441 (1992).

[5] C. R. Mirasso, P. Colet and M. San Miguel, Optics Lett. **26**, 1753 (1991).

[6] C. R. Mirasso, P. Colet and M. San Miguel, "Dependence of timing jitter on bias level for single–mode semiconductor lasers under high speed operation", J. of Quantum Electron., in press.

[7] A.Sapia, P.Spano, C.R.Mirasso, P.Colet and M.San Miguel, CLEO/QELS '92 (California, USA), paper CWG56.

[8] G. P. Agrawal and N. K. Dutta, "Long Wavelength Semiconductor Lasers", Van Nostrand Reinhold Company, New York, 1986.

[9] A. Valle, M. Rodriguez, and L. Pesquera, Phys. Rev. A, (in press).

[10] F. de Pasquale, P. Tartaglia y P. Tombesi., Phys. Rev. A. **25**, 466 (1982).

[11] M. Abramowitz and I. A. Stegun, "Handbook of mathematical functions", Dover Publications, INC, New York, 1965.

Chapter 5

Statistical Properties of Switch–on times of Modulated Gas Lasers

5.1 Introduction

The laser switch–on is an example of relaxation from an unstable state. The description of this process is usually done by using non–linear Langevin type equations in which the fluctuations are modelled by an additive white noise. Transient statistics has been analyzed according to the temporal dependence of the control parameter. Most available theories deal with situations in which the control parameter is instantaneously changed bringing the system from a stable to an unstable state [1, 2]. In other analysis it is assumed that the control parameter is continously swept through the instability point [3–7]. Equations with a periodic change of the control parameter are also studied with the use of different methods [8–11]. These equations model physical systems like modulated convection[12], stochastic resonance[13], Q–switched lasers[14] and gain switched semiconductor lasers[15]. Systems with fluctuations of the control parameter have also been studied. Indeed, the effect of multiplicative and additive noise has been used to explain statistical properties of physical systems like the dye laser[16, 17].

In this paper we study the statistical properties of a modulated single mode Ar^+ laser by means of periodic fluctuating cavity losses (Q-switching). The modulation is performed by using an Acousto Optic Modulator (AOM) that turns on and off the laser. Measurements of the amplitude spectrum of the Radio Frequency (RF) signal that drives the AOM indicate a fluctuating character of the loss factor. This system is an example of modulated system driven by additive and multiplicative noise because of the effect of the spontaneous emission noise and random cavity losses. We present

the results of the switch–on time measurements on this modulated Ar^+ laser. The switch–on time, τ, is defined as the delay time betwen the time in which the AOM is turned off and the time in which the laser intensity reaches a certain threshold. The switch-on time is measured for different laser powers as a function of the time of application of the AOM, t_{off}. The results of the experiment indicates that the mean switch–on time , $< \tau >$, increases in a linear way before reaching a constant value when the time of application of the losses, t_{off}, increases. The variance of the switch–on time, σ_τ, shows a maximum when plotted versus t_{off}.

The switch–on time statistics is also studied by numerical simulation of the equations describing the electric field of the laser. The random character of the loss factor, the noninstantaneous change of the control parameter and saturation effects are included in the simulation. The numerical computations agree well with the experimental measurements. We show that when the laser is below threshold for a short time the statistics of the switch–on time is determined by the loss noise. On the other hand, the statistics of τ is determined by the spontaneous emission noise when the laser is turned off for a long enough time. The maximum of the variance of τ versus t_{off} appears at an intermediate zone between the two previous behaviors, in which both loss and spontaneous emission noise are relevant. In this way a signature of the joint effect of multiplicative and additive noise in a modulated system appears. We develop an analytic approximation to obtain the statistical properties of the switch–on time when t_{off} is small. With the use of this approximation it is shown that $\langle \tau \rangle$ increases linearly with t_{off} and the slope is found to be independent of the noninstantaneous change of the losses, the saturation term and the loss noise. We also obtain the loss noise minimum intensity at which the maximum of σ_τ appears. Finally, this maximum is characterized by the time at which it appears, t_m, and by its value, σ_m.

The paper is organized as follows. In sec. 5.2 we describe the experimental arrangement and measurement techniques used. In sec. 5.3 we describe the modulated gas laser model in terms of stochastic equations for the electric field. In sec. 5.4 we present the experimental results. We also compare the results of our model and the experimental data. Finally, in sec 5.5 we analyze the effect of the fluctuations of the random control parameter on the switch–on time statistics.

5.2 Experimental Arrangement

The experimental set–up is shown in Fig. 1. Similar experimental arrangements have been used by other authors [7]. A commercial Ar^+ laser constituted the object of our research (framed part in Fig. 1). Single mode operation was achieved by means of an intracavity Fabry–Perot etalon of low finesse (FPE)(mirror reflectivity $\approx 40\%$). The spectral characteristics of the laser output were monitored by means of a scanning Fabry-Perot (SFP) and an oscilloscope (SC2). The high reflecting mirror of the laser cavity was removed from its original position and put farther away (≈ 25 cm) in order to introduce into the cavity an acousto–optic light modulator (Newport mod. N35085–3) whose crystal is made of fused quartz ($Si\ O_2$). This was driven by 85 MHz RF generator (RFD) which in turn is modulated by a pulse generator (PG)(HP–8005B). The pulse repetition rate, T, and pulse width could be varied to obtain different experimental situations. The laser output was detected by a fast photodiode (FPD), whose output entered the stop input (Sp. I) of an universal photon counter (TIC)(HP–5308A) working in time interval mode with 10 ns. time resolution. At the same time, the photodiode output and the signal from the pulse generator (PG) were monitored by means of an oscilloscope (SC1). This helped us to fix the experimental parameters (period, T and pulse width t_{off}) of the laser output. The start input (St. I) was triggered by the negative slope of the pulses generated

by the pulse source (PG). The trigger level of the stop input (Sp. I) of the photon counter (TIC) could be varied in order to fix the threshold output intensity, I_{th}, at which we wanted to measure the starting time of the laser action. The measured time intervals were stored and processed in a desk–top computer (D.C.)(HP–300). It is evident that there is a unavoidable delay between both inputs due to the finite value of the sound speed in the SiO_2 crystal ($\approx$ 6 km/s). This delay was estimated experimentally. Its value, 2.6 μs, was measured with high accuracy and was taken as a reference to obtain the true values of τ.

A set of data is taken for several t_{off} as a function of the output laser power. This was varied by changing the plasma current intensity. The pulse repetition rate, T, is kept constant and made large enough ($\approx 50\,\mu s$) to assure that the laser reaches its on–stationary state, I_{st}, during the pulse. The amplitude of the RF signal is also kept fixed and large enough to assure that the laser is always below a certain threshold , I_{th}, when we turn off the RF signal. In this way we always obtain a well defined laser intensity pulse each time we turn on and off the RF signal. We characterize the pulse statistics by the switch–on time, τ, that is the delay between the turn off of the RF signal and the time at which the laser intensity cross the threshold. This threshold is taken as 25 % of the stationary intensity.

5.3 The Model

The modulated single mode on–resonance gas laser is described by the following nonlinear Langevin equation[18]:

$$\frac{dE}{dt} = \frac{gE}{1+\frac{I}{I_s}} - \kappa(t)E + \xi(t)\,, \tag{1}$$

where $E = E_1 + iE_2$ is the slowly varying complex field amplitude, $I = \mid E \mid^2$ is the field intensity, g and κ are the gain and loss factors and I_s is the laser saturation

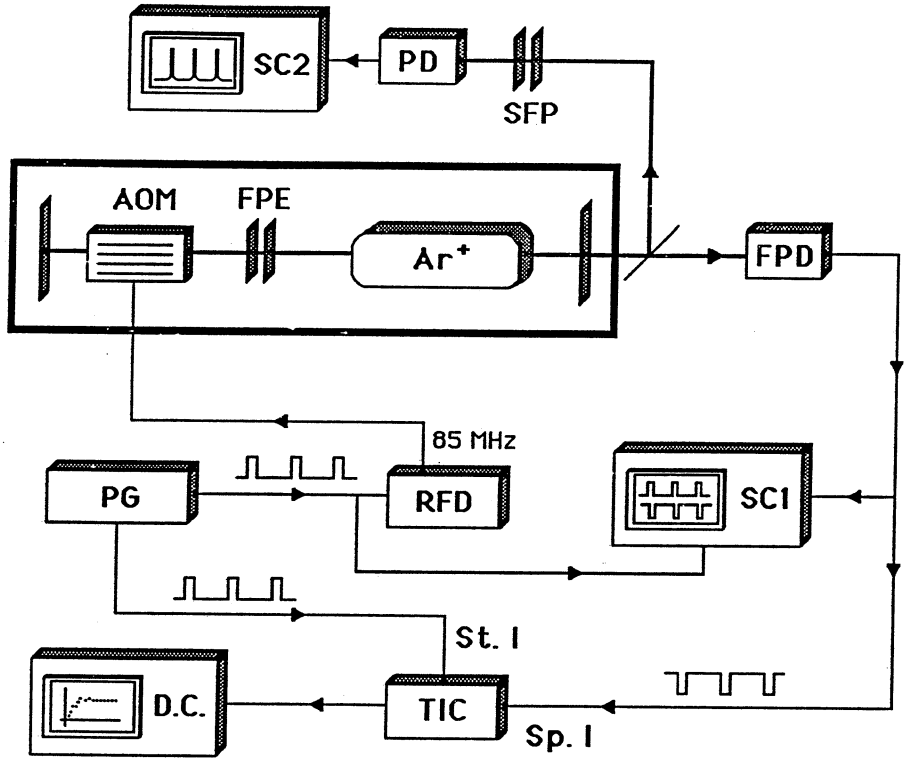

Fig. 1. Experimental arrangement

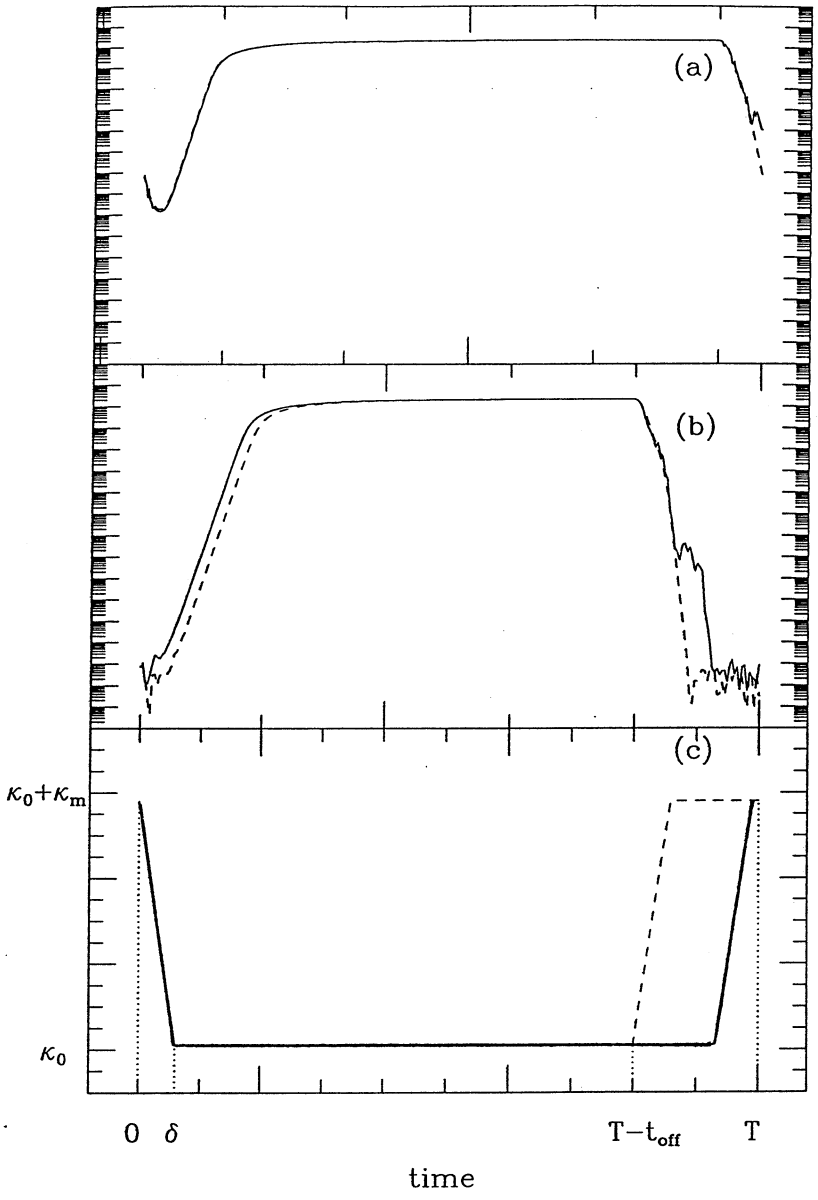

Fig. 2. Qualitative time traces of the laser intensity and loss factor. In Fig. 2 (a) and (b) are plotted the laser intensity during one pulse for t_{off} small and large respectively. The pulses obtained with and without random cavity losses are plotted with solid and dashed lines respectively. The loss factor for t_{off} small and large is plotted in Fig. 2 (c) with solid and dashed lines, respectively.

intensity. The effect of the spontaneous emission on the field is represented by the complex Gaussian white noise, $\xi(t) = \xi_1 + i\xi_2$, of zero mean and correlations

$$\langle \xi_i(t)\xi_j(t')\rangle = D\delta_{ij}\delta(t-t'). \tag{2}$$

The gas laser can also be described near threshold by an expansion of (3.1) to third order in the field. This approximation is often called the cubic model.

The laser is modulated in the experiment by changing periodically the losses in time (Q–switching). These losses are generated by the application of the RF signal to the AOM . The loss factor is then a periodic function of the time, $\kappa(t) = \kappa(t+T)$, that esentially takes two values: κ_0, the losses in the absence of the AOM, and $\kappa_0 + \kappa_m$, where κ_m are the losses due to the AOM. The change from one to another value of the losses takes a time δ. This is the transit time of sound across the waist of the laser beam. This effect is described in our model by means of a linear variation of the loss factor between the two previous values. If the origin of times is chosen just when the intensity of the acoustic wave begins to decrease across the beam, the loss factor is written in the following way:

$$\kappa(t) = \begin{cases} \kappa_0 + \kappa_m - \frac{\kappa_m t}{\delta} & \text{if } 0 < t < \delta \\ \kappa_0 & \text{if } \delta < t < T - t_{off} \\ \kappa_0 + \frac{\kappa_m}{\delta}(t + t_{off} - T) & \text{if } T - t_{off} < t < T + \delta - t_{off} \\ \kappa_0 + \kappa_m & \text{if } T + \delta - t_{off} < t < T \end{cases} \tag{3}$$

where t_{off} is the time of application of the RF signal. In Fig. 2 we plot with dashed lines the evolution of the loss factor, and the intensity of the laser during a pulse for two different t_{off}. When t_{off} is small the effect of the spontaneous emission noise is small and the intensity pulse is esentially deterministic. However, as t_{off} grows, the laser intensity begins to reach the spontaneous emission levels and the switching of the pulse becomes random.

Another outstanding effect is the presence of fluctuations in the amplitude of the RF signal, E_{RF}. Because of this amplitude can be related to the losses due to the AOM [19], this last quantity can be described as an stochastic process. We model this random losses by adding a Gaussian white noise, $\phi(t)$.In this way κ_m becomes $\kappa_m + \phi(t)$, where $\phi(t)$ has zero mean value and correlation given by $\langle\phi(t)\phi(t')\rangle = \epsilon\delta(t-t')$. We have chosen a white character of the noise since a wide spectrum of the RF signal was observed. In Fig. 2 we plot with solid lines two realizations of the stochastic process (3.1) for two different values of t_{off} when using $\kappa(t)$ given by (3.3) with κ_m replaced by $\kappa_m + \phi(t)$. The main effect of the random loss factor is that the intensity becomes fluctuating during the decay of the pulse.

Recently, a new method has been developed to obtain the statistical properties of modulated systems [11]. This method has been applied to a gas laser described with the cubic model[11] and to a semiconductor laser [20]. In both cases a deterministic on–off modulation with an instantaneous change of the control parameter has been considered. A very good agreement is found between this theory and the simulation of the equations describing these systems. With this method the stationary properties of pulses are easily obtained via the solution of an integral equation for the probability density of τ. The results obtained in this way for a modulated gas laser without loss noise [11] show that the mean switch-on time increases linearly with t_{off} with a slope given by $(\kappa_m + \kappa_0 - g)/(g - \kappa_0)$. For large values of t_{off} $\langle\tau\rangle$ saturates going to a constant value. The variance of $\langle\tau\rangle$ is found to increase with t_{off} until a constant value is reached for large values of t_{off}. In the following section the statistical properties of $\langle\tau\rangle$ when the loss noise is included are obtained by using numerical simulation methods. We integrate the stochastic equations for the electric field following the algorithm described in Ref.[21]. with an integration step of 1 ns. In Sect. V we develop an analytic approximation to study the effect of the cavity loss fluctuations

on the statistics of the switch-on time.

5.4 Experimental Results. Comparison of Theory and Experiment

In this section we present three sets of experimental data for the switch-on time. First, second and third sets were taken with the laser operating with a pump power of 15 %, 30 % and 50% above the threshold pump power, respectively. These operation points correspond to a power of 6mW, 12 mW and 24 mW respectively. These data are compared with the results obtaned from numerical simulations of our model (3.3). All the experimental measurements have been fitted by the same values of the parameters $I_s, \delta, \kappa_0, \kappa_m, D$ and ϵ. The losses in the absence of AOM can be splitted in two: κ_e, the losses due to the transmission of the mirror, and κ_i, the internal losses, i.e. $\kappa_0 = \kappa_i + \kappa_e$. κ_e can be obtained from the power transmittance of the mirror (1%), $\kappa_e = 10^6 s^{-1}$. In a first approximation I_s can be estimated by means of known parameters of the Ar^+ laser (laser transition cross section and spontaneous lifetime of the laser transition) [22], giving the value $I_s = 5.2 \times 10^7 N w^2/C^2$. δ is estimated from the speed of the sound across the fused quartz crystal ($\approx 6\, Km/s$) and the beam waist (≈ 1 mm) , obtaining a value for δ smaller than 160 ps. A rough estimation of κ_m can be given through the maximum diffraction efficency of the fused quartz crystal (90%), obtaining a value $1.7 \times 10^8 s^{-1}$. The noise intensity ϵ can also be estimated from the fact that fluctuations of the RF signal that drives the AOM are of the order of 5%. The values of the parameters κ_0, g and D are obtained by comparison of experimental and theoretical results for large values of t_{off}. In this situation the laser has enough time to reach the off-steady state corresponding to the pump parameter given by $-(\kappa_o + \kappa_m - g)$. We have used three experimental relations ($< \tau >$, σ_τ and laser power versus the laser operation point) for ten different values of the laser output power to obtain κ_0, g and D. We note that the comparison of

experimental and theoretical results can be done only when the laser power, W, is estimated in terms of the parameters of our model:

$$W \approx \frac{\kappa_e \epsilon_0 I_s (g - \kappa_0) v}{2\kappa_0}, \tag{4}$$

where ϵ_0 is the permittivity of free space and v the mode volume within the active material ($3.8 \times 10^{-6} m^3$ We have checked that for large values of t_{off}, σ_τ is independent of the loss noise $\phi(t)$. This result is similar to the one found for dye lasers when the threshold value I_{th} is not close to the steady-state intensity [16]. The variance is also found to be independent of δ and κ_m for the estimated values given above. σ_τ is then given by the one corresponding to the case of instantaneous change of the pump parameter [24].

$$\sigma_\tau = \frac{0.64}{(g - \kappa_0)}. \tag{5}$$

Using (4.1) we get $\sigma_\tau = 0.61 mW/(\kappa_0 W)$ and by comparing with the experimental results we obtain $\kappa_0 = 10^6 sec^{-1}$. The values of g for the three experimental data sets are then obtained by using (4.1) and κ_0: minimum power(6 mW), $g = 7.5 \times 10^6 sec^{-1}$; intermediate power (12 mW), $g = 1.4 \times 10^7 sec^{-1}$; maximum power (24 mW) $g = 2.4 \times 10^7 sec^{-1}$. Because of the large value of g a large ratio g/κ_0 is obtained. The ratio

$$\frac{I_{th}}{I_s} = 0.25 \times (g/k_0 - 1)$$

is then greater than one and the saturated gain in eq. (3.1) can not be expanded near the threshold intensity. Therefore, the cubic model can not describe well the laser intensity near the reference value of our experiment. In fact, the cubic model is expected to be valid only near threshold [23, 18, 16]. The value of D obtained from the experimental and theoretical values of $\langle \tau \rangle$ is $D = 5 \times 10^3 N w^2 / C^2$.

The parameters $\kappa_m, \epsilon, \delta$ and the precise value of I_s are obtained by matching the three sets of experimental data for the mean passage time as a function of t_{off} with the simulation results (see Fig. 3). The numerical values we have obtained are $\kappa_m \approx 5.5 \times 10^7 sec^{-1}, \delta = 10^{-7} sec$, $\epsilon = 3 \times 10^6 sec^{-1}$ and $I_s = 5.6 \times 10^7 Nw^2/C^2$. Using these parameter values a good agreement is found for $\langle \tau \rangle$ as a function of t_{off} between the theoretical and experimental results. The discrepancies observed in Fig. 3 can be attributed to the fact that κ_m can vary slightly due to small variations of the relative position of the AOM and the laser beam. We plot in Fig. 4 the variance of the switch–on time as a function of t_{off}. Now, only a qualitative agreement is obtained between the theoretical and experimental results. The agreement is better for the minimum power. In this case both results show a maximum value for σ_τ as a function of t_{off}. However, when the power increases the values of σ_τ are very small of the order of the time resolution of the photon counter. Then the different behavior obtained from theory and experimental data for the intermediate power for small values of t_{off} can be due to this lack of time resolution.

Three different behaviors can be observed in Figs. 3 and 4. The first one occurs when the laser spends a short time below threshold. The mean switch–on time is then a linear function of t_{off} with a slope that decreases when the laser power increases, as it was predicted in Ref. [11]. In this case the intensity at the beginning of the pulse , $I(0)$, has an apreciable value (see Fig. 2–a) and then the spontaneous emission noise has a negligible effect on the evolution. The random character of the decay of the pulse, the statistical distribution of $I(0)$ and therefore the statistics of τ are only determined by the loss noise. The second situation happens when t_{off} is large. The mean value and variance of τ saturate going to the limit of the repetitive Q–switching (no modulation effects). This behaviour was also predicted in Ref. [11]. In this case all the noisy intensity paths decay until the off–steady state (see Fig. 2–b). In this way

the statistical spread of $I(0)$ and τ is mainly due to the spontaneous emission noise. The third situation corresponds to intermediate t_{off}. In this regime the variance of the switch–on time has a maximum when plotted versus t_{off}. This maximum does not appear with the kind of modulation used in Ref. [11], where no loss noise was considered. This is a transition zone between the two previous behaviours in which the joint effect of the loss and spontaneous emission noises determine the statistics of $I(0)$. The statistical properties of the switch–on time in this regime are then due to the combined effect of both noises. We note that the maximum of σ_τ for the minimum power appears for different values of t_{off} according to the theoretical and experimental results. This is due to the fact that the transition zone in $\langle\tau\rangle$ is obtained for different values of t_{off}.

5.5 The Effect of the Random Control Parameter

We now study the effect of the fluctuations of the loss factor on the statistics of the switch–on time. We show in Fig. 5 the variance of the switch–on time obtained from simulations of Eqs. (3.1)-(3.3) with κ_m replaced by $\kappa_m + \phi(t)$ for three different loss noise intensities. It can be seen that changes of the noise strength only leads to changes in the variance of τ when t_{off} is short. The maximum of the fluctuations of the switch–on time only appears when the noise intensity is large enough. We have also checked that the averaged switch–on time changes slightly if ϵ changes when t_{off} is small.

These facts can be explained with the use of an analytic approximation valid when the laser is below threshold for a short time. In this situation the fluctuations due to the spontaneous emission can be neglected. The intensity $I_L = I(-t_{off} + \delta)$ is a random variable whose statistical properties can be obtained by solving numerically the equation (3.1) with $D = 0$ and with the initial condition $I(-t_{off}) = I_{st}$. When

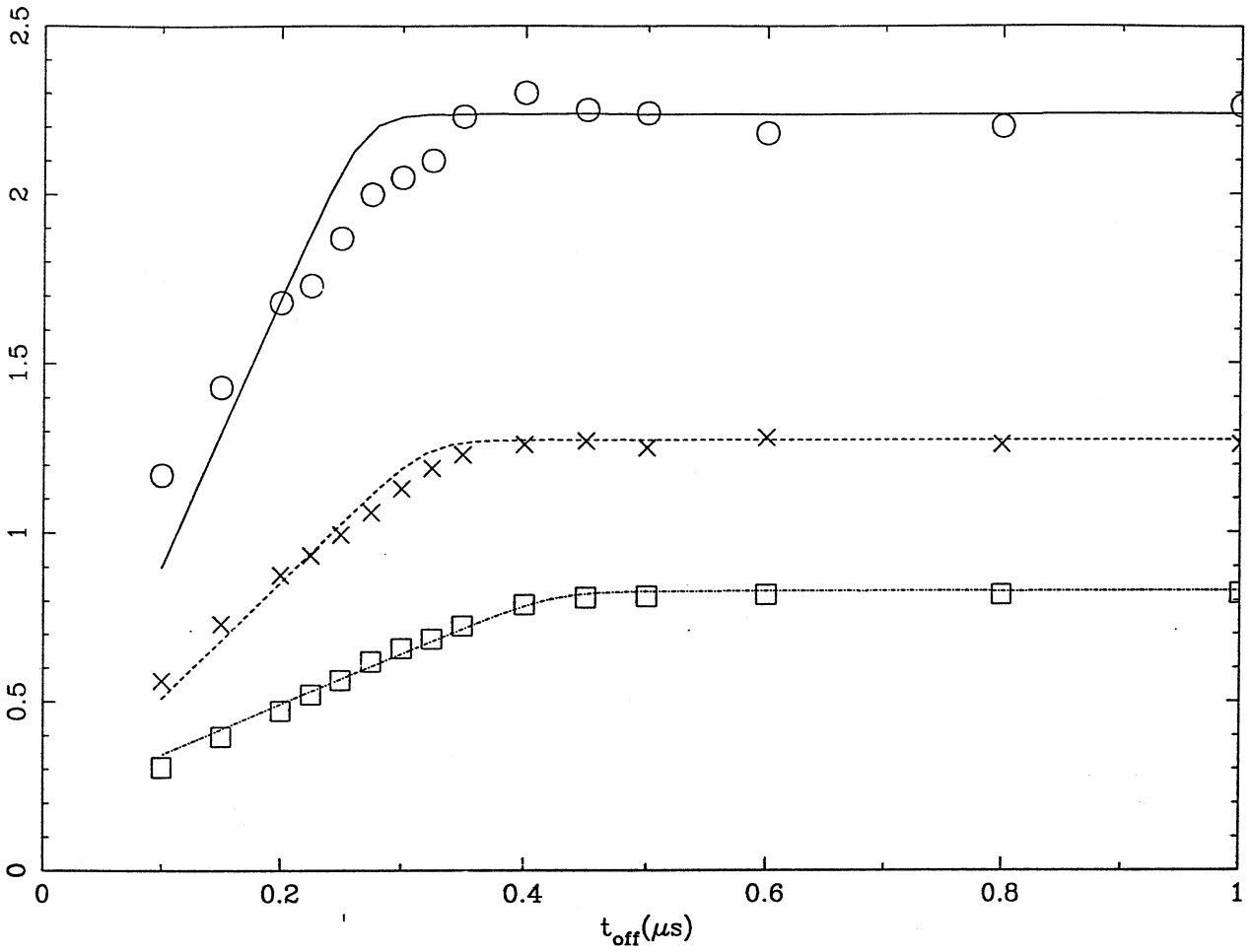

Fig. 3. Mean value of the switch–on time as obtained from simulation (lines) and from the experiment (symbols) for three different laser powers. Circles and solid line correspond to the minimum power, 6 mWatts, ($g = 7.5 \times 10^6 sec^{-1}$). Crosses and dashed line represent the results for the intermediate power, 12 mWatts, ($g = 1.4 \times 10^7 sec^{-1}$). Squares and dot–dashed line correspond to the maximum power, 24 mWatts, ($g = 2.4 \times 10^7 sec^{-1}$).

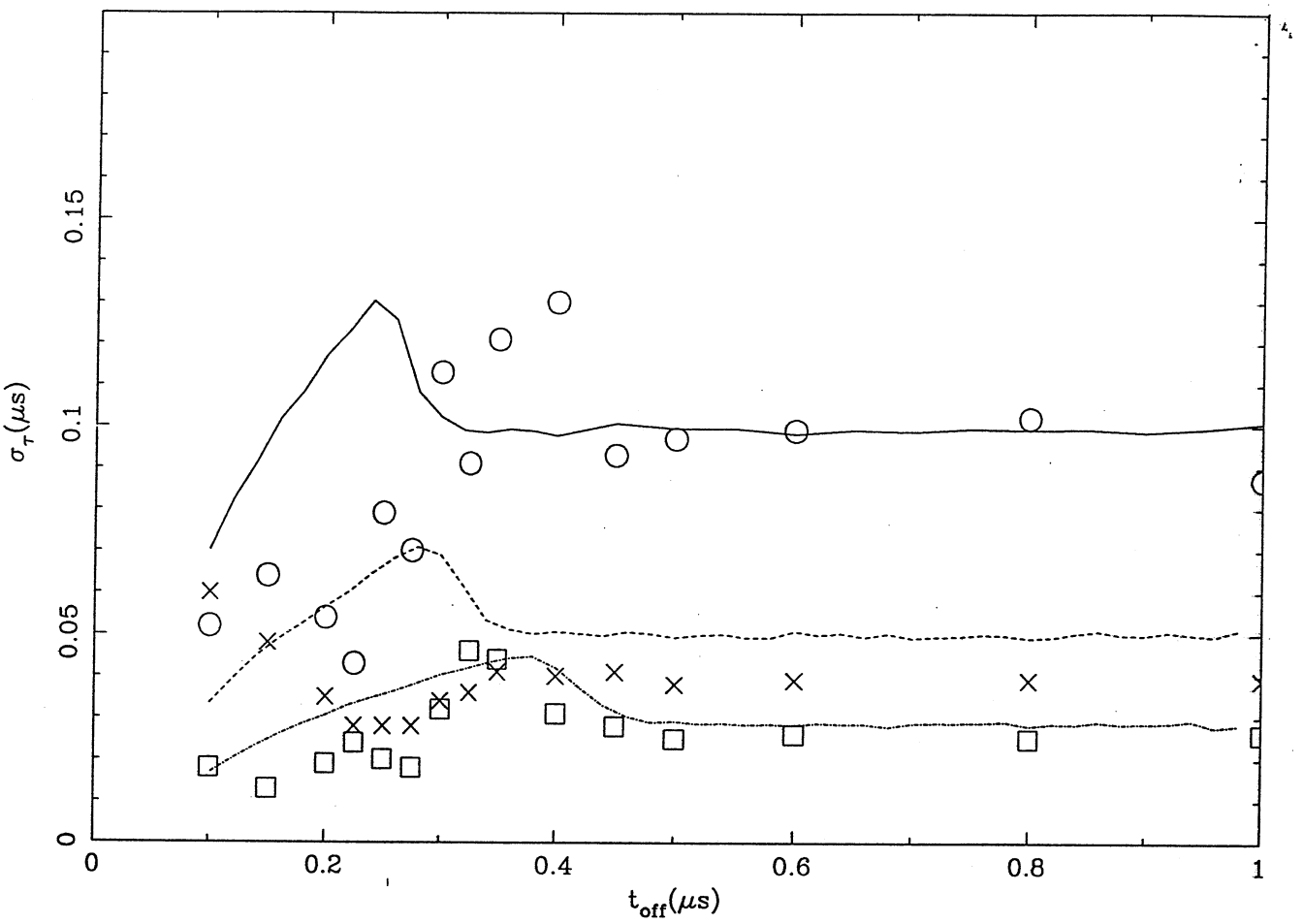

Fig. 4. Variance of the switch–on time as obtained from simulation (lines) and from the experiment (symbols) for three different laser powers. Circles and solid line correspond to the minimum power, 6 mWatts, ($g = 7.5 \times 10^6 sec^{-1}$). Crosses and dashed line represent the results for the intermediate power, 12 mWatts, ($g = 1.4 \times 10^7 sec^{-1}$). Squares and dot–dashed line correspond to the maximum power, 24 mWatts, ($g = 2.4 \times 10^7 sec^{-1}$).

the dynamic evolution can be linearized below the intensity I_L, the solution can be written in the following way:

$$I(t) = I_L \exp 2 \int_{-t_{off}+\delta}^{t} (g - \kappa(s)) ds. \tag{6}$$

We have checked that this is a good approximation for all the sets of parameters used in this work. We then use the former expression to calculate the time, τ_L, at which the laser intensity reaches the mean value of I_L:

$$\tau_L = \frac{(\kappa_m + \kappa_0 - g)}{(g - \kappa_0)}(t_{off} - \delta) + \frac{\kappa_m \delta}{2(g - \kappa_0)} + \frac{1}{2(g - \kappa_0)} \ln \frac{\langle I_L \rangle}{I_L} + \frac{\eta(t)}{(g - \kappa_0)}, \tag{7}$$

where η is given in terms of the Wiener process $W(t)$ by

$$\eta = [W(0) - W(-t_{off} + \delta)] + \frac{1}{\delta} \int_0^{\delta} [W(s) - W(0)]\, ds \tag{8}$$

This last expression for τ_l holds if the laser intensity reaches the value $\langle I_L \rangle$ when the loss factor is constant, i.e. $2(g - \kappa_0) < \kappa_m$. This condition is satisfied for the numerical values of our parameters. The switch–on time is then $\tau = \tau_L + \Delta$, where Δ is the time the laser intensity spends from $\langle I_L \rangle$ to I_{th}. In this way the switch–on time has a mean value given by

$$< \tau >= \frac{(\kappa_m + \kappa_0 - g)}{(g - \kappa_0)}(t_{off} - \delta) + \frac{\kappa_m \delta}{2(g - \kappa_0)} + \frac{1}{2(g - \kappa_0)} \frac{\ln \langle I_L \rangle}{\langle \ln I_L \rangle} + \Delta, \tag{9}$$

and a variance given by

$$\sigma_\tau^2 = \frac{\epsilon(t_{off} - 2\delta/3)}{(g - \kappa_0)^2} + \frac{1}{4(g - \kappa_0)^2} \sigma^2_{\ln I_L}. \tag{10}$$

The mean switch–on time depends in a linear way on t_{off} since δ, Δ and I_L are independent of t_{off}. The slope of this straight line is given by $(\kappa_m + \kappa_0 - g)/(g - \kappa_0)$. This slope agrees with the one obtained with the model of Ref. [11], that is without saturation effects at the reference intensity I_{th} and loss noise ($\epsilon = 0$) and with an instantaneous change of the pump parameter ($\delta = 0$). In this way the existence of

the linear intensity level, I_L, assures that the random nature and finite velocity of the loss factor and the saturation do not affect that slope. The variance of switch–on time as obtained from (5.5) is shown in Fig. 5. A good agreement is obtained when t_{off} is small between this analytic approximation and the simulation of (3.1) for all the loss noise intensities.

This analytic approximation can be used to know when there is a maximum of σ_τ versus t_{off}. This maximum is characterized by the time t_m at which appears and by its value, σ_m. As we noted in Sec. IV the maximum appears at an intermediate region in which the laser intensity at the beginning of the pulse begins to reach the off–stationary state, i.e.:

$$< I(0) > \approx \frac{D}{\kappa_m + \kappa_0 - g}. \tag{11}$$

The use of eq. (5.1) and (5.6) let us estimate the value of t_m:

$$t_m \approx \delta + \frac{1}{2(\kappa_m + \kappa_0 - g)} \ln \frac{\langle I_L \rangle (\kappa_m + \kappa_0 - g)}{D} \tag{12}$$

The maximum appears if the variance of the switch–on time, approximated by (5.5) when $t_{off} \leq t_m$, is greater at t_m than the constant value obtained when t_{off} is large. This variance agrees with the one obtained with the repetitive Q–switching given by Eq. (4.2) as we have checked for the numerical values of our parameters. In this way the maximum appears for any value of δ when

$$\epsilon > \frac{0.41(\kappa_m + \kappa_0 - g)}{\ln \frac{\langle I_L \rangle (\kappa_m + \kappa_0 - g)}{D}}. \tag{13}$$

The value of the maximum is then easily found from Eqs. (5.5) and (5.7). From these expressions we find that t_m increases with the gain factor (laser output power), whereas σ_m is found to decrease with g. This behavior is in agreement with the one observed in the simulations (see Fig. 4).

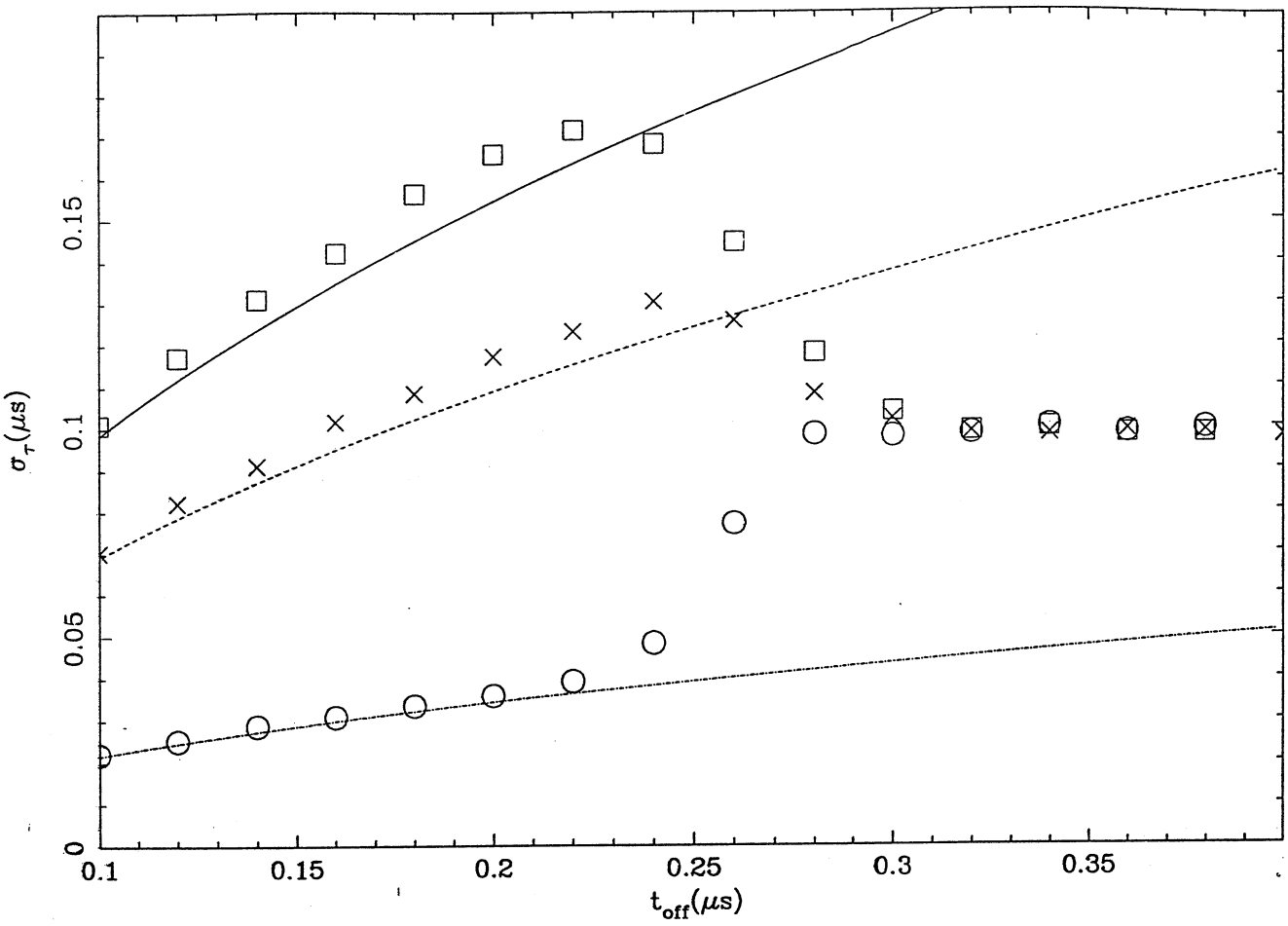

Fig. 5. Variance of the switch–on time as obtained from simulation (symbols) and from Eq. (5.5) (lines) for three different loss noise intensities. The value of the parameters are $\epsilon = 6 \times 10^6 sec^{-1}$ (squares and solid line), $\epsilon = 3 \times 10^6 sec^{-1}$ (crosses and dashed line) and $\epsilon = 3 \times 10^5 sec^{-1}$ (circles and dot–dashed line).

In conclusion we have shown that the mean switch-on time is a linear function of t_{off} for small values of t_{off} with a slope independent of the loss noise. We have also obtained expressions for the time at which the maximum of the variance of τ appears and for this maximum value σ_m.

REFERENCES

[1] M. Suzuki, in *Order and Fluctuations in Equlibrium and Nonequlibrium Statistical Mechanics*, edited by G. Nicolis, G. Dewel, and J. Turner (Wiley, New York, 1980).

[2] F. de Pasquale and P. Tombesi, Phys. Lett. **72A**, 7 (1979); F. de Pasquale, P. Tartaglia, and P. Tombesi, Phys. Rev. A **25**, 466 (1982).

[3] a) G. Ahlers, M. C. Cross, P. C. Hohenberg, and S. Safran, J. Fluid Mech. **110**, 297 (1981). b) J. B. Swift, P. C. Hohenberg and G. Ahlers. Phys. Rev. A **43**, 6572 (1991).

[4] G. Broggi, A. Colombo, L. A. Lugiato, and P. Mandel, Phys. Rev. A **33**, 3635 (1986).

[5] M. C. Torrent and M. San Miguel, Phys. Rev. A **35**, 1453 (1987).

[6] A. Valle, L. Pesquera and M. A. Rodríguez, Phys. Rev. A **45**, 5243 (1992).

[7] W. Scharpf, M. Squicciarini, D. Bromley, C. Green, J. R. Tredicce, and L. M. Narducci, Opt. Comm. **63**, 344 (1987); W. Scharpf, Doctoral Thesis, Drexel University (1988).

[8] F. de Pasquale, Z. Racz, M. San Miguel, and P. Tartaglia, Phys. Rev. B **30**, 5228 (1984).

[9] M. Suzuki, Phys Lett. A **67**, 339 (1978); Prog. Theor. Phys. (Kyoto) Suppl. **64**, 402 (1978).

[10] M. O. Cáceres, A. Becker, and L. Kramer, Phys. Rev A **43**, 6581 (1991).

[11] A. Valle, M. A. Rodríguez and L. Pesquera, Phys. Rev. A, (in press).

[12] W. Meyer, G. Ahlers, and D. S. Canell, Phys. Rev. Lett. **59**, 1577(1987).

[13] B. McNamara, K. Wiesenfeld, and R. Roy, Phys. Rev. Lett. **60**, 2626 (1988).

[14] O. Svelto, in *Principles of lasers* (Plenum Press, New York, 1982).

[15] K. Petermann, in *Laser diode modulation and noise*, edited by T. Okoshi (Kluwer Academic Publishers, The Netherlands, 1988).

[16] a) R. Roy, A. W. Yu, and S. Zhu, Phys. Rev. Lett. **55**, 2794 (1985). b) S. Zhu, A. W. Yu, and R. Roy, Phys. Rev. A **34**, 4333 (1986).

[17] F. de Pasquale, J. M. Sancho, M. San Miguel, and P. Tartaglia, Phys. Rev. Lett. **56**, 2473 (1986).

[18] M. Sargent III, M. O. Scully, and W. E. Lamb, Jr.,*Laser Physics* (Addison–Wesley, Reading, Mass., 1974).

[19] N. Berg, J. Lee, *Acousto–Optic Signal Processing. Theory and Implementation*, (Marcel Dekker, Inc., New York, 1983).

[20] A. Valle, M. A. Rodríguez and C. Mirasso. Opt. Lett. **17**, 1523 (1992).

[21] J. M. Sancho, M. San Miguel, SS. L. Katz, and J. D. Gunton, Phys. Rev. A **26**, 1589 (1982).

[22] B. E. A. Saleh, and M. C. Teich, *Fundamentals of Photonics* (Addison–Wesley, Reading, Mass., 1991).

[23] a) F. T. Arecchi, V. Degiorgio, and B. Querzola, Phys. Rev. Lett. **19**, 1168 (1967). b) F. T. Arecchi and V. Degiorgio, Phys. Rev. A **3**, 1108 (1971).

[24] M. San Miguel in *Laser Noise*, SPIE Proc. Vol. 1376 (SPIE, Bellingham, Washington, 1991).

Chapter 6

Transient statistics for two-mode gas ring lasers

6.1 Introduction

The statistics of laser switch-on has been recently considered in a variety of systems and situations (see Ref. [1] for a recent review). There are in general two different statistical problems to be studied. One is the statistics of the switch-on time at which laser emission is observed. This is described by the method of passage times (PT) in the linear regime of laser amplification. The second problem refers to the large statistical fluctuations of the laser intensity during a later nonlinear regime. For type-A lasers results for PT statistics are well established [2], including the cases with pump noise (dye lasers) [3, 4] and sweeping of the pump parameter [5, 6]. The problem of PT statistics for type-B lasers has been also considered for CO_2 [7] and semiconductor lasers [8, 9]. The intensity fluctuations in the nonlinear regime were considered for type-A lasers earlier [10, 11] than the PT statistics. More recent analysis include the cases with pump noise [4], sweeping [12] and type-B lasers (semiconductor) [13, 14]. A description of the fluctuations in the nonlinear regime is possible by taking a simple average over a distribution of random initial values of the laser field. This is the basic idea of the Quasideterministic Theory (QDT) [15]. Most of the analysis of the laser switch-on problem consider the single-mode case. The transient multimode dynamics has been analyzed only in the linear regime for semiconductor [9, 16] and gas ring lasers [16].

In this paper we study transient statistics during the Q-switching of two-mode on-resonance gas ring lasers including the nonlinear regime. When the pump parameters of both modes, α_1 and α_2, are large with respect to the spontaneous emission noise, we show that the transient regime can be described by the Quasideterministic

Theory (QDT). This case corresponds to situations well above threshold. In the QDT the effect of the noise is replaced by an effective random initial condition, and the evolution in the nonlinear regime is deterministic. In this way explicit expressions for the transient intensity probability densities for both modes are obtained. In the case of non-equivalent modes, intensity fluctuations show a maximum. This is similar to the anomalous fluctuation peak found for a single-mode class A laser.

When the pump parameters are slightly different, the intensity probability density for the secondary mode is shown to have a polinomial tail. This tail appears at times of order $(\alpha_1 - \alpha_2)^{-1}$. This time scale can be much larger than the time scales, α_1^{-1} and α_2^{-1}, corresponding to both modes. The main mode shows a symmetric tail. This tail corresponds to mode competition. In fact the probability density for the total intensity is peaked around its mean value. This phenomenon is similar to the mode partition noise found in semiconductor lasers [17]. The anomalous intensity fluctuations of the two modes are characterized by the time at which its maximum appears and by the value of this maximum. All these results are checked with numerical simulations.

We also consider the case of a very depressed secondary mode. Now the evolution of this mode is dominated by the noise. Then the QDT is not able to describe the transient regime of the secondary mode. We develop a new approximation which includes the spontaneous emission noise and a random pump parameter given by the intensity of the main mode, that is described by the QDT. Numerical simulations show that this approximation describes correctly the transient probability density for both modes and the side mode excitation probability.

6.2 Quasideterministic Theory (QDT)

The two-mode on resonance gas ring laser can be described by the following equations [18]:

$$\dot{E}_1 = \frac{1}{2}[\alpha_1 - \beta(\mid E_1 \mid^2 + \mid E_2 \mid^2)]E_1 + \xi_1$$

$$\dot{E}_2 = \frac{1}{2}[\alpha_2 - \beta(\mid E_1 \mid^2 + \mid E_2 \mid^2)]E_2 + \xi_2 \,, \tag{1}$$

where $E_1(t)$ and $E_2(t)$ are the complex amplitudes of both modes, α_1 and α_2 are the pump parameters and β is a constant. The complex random terms, $\xi_1(t)$ and $\xi_2(t)$, model the spontaneous emission noise. They are taken as Gaussian white noise of zero mean and correlation:

$$\langle \xi_i(t)\xi_j^*(t')\rangle = D\ \delta_{ij}\ \delta(t-t') \quad i,j = 1,2\,. \tag{2.2}$$

We consider that the laser is initially below threshold and that at time $t = 0$ the laser is instantaneously switched on. We can easily obtain from Eq. (2.1) the intensity, $I_i = \mid E_i \mid^2$, when saturation effects are negligible:

$$I_i(t) = \mid h_i(t) \mid^2 e^{\alpha_i t}\,, \tag{2.3}$$

where $h_i(t)$ is a complex Gaussian process playing the role of an effective random initial condition for the deterministic evolution. The variance of this process is

$$\langle \mid h_i(t) \mid^2 \rangle = \frac{D}{\alpha_i}(1 - e^{-\alpha_i t})\,. \tag{2.4}$$

The QDT [15] consists in approximating the actual process (2.1) by a process obtained from the nonlinear deterministic solution of (2.1) changing the initial condition by $\mid h_i(t) \mid^2$:

$$I_i(t) = \frac{\mid h_i(t) \mid^2 e^{\alpha_i t}}{1 + \beta[\mid h_1(t) \mid^2 (e^{\alpha_1 t} - 1)/\alpha_1 + \mid h_2(t) \mid^2 (e^{\alpha_2 t} - 1)/\alpha_2]}\,. \tag{2.5}$$

This approximation is valid whenever two different stages of evolution can be distinguished: an initial linear fluctuating regime and a nonlinear regime where the evolution is essentially deterministic. These different stages appear when the pump

parameters are large with respect to the spontaneous emission noise. For times such that $\exp(-\alpha_i t) \ll 1$ the effective initial condition $\mid h_i(t) \mid^2$ becomes a time independent random variable. As a consequence the evolution will be deterministic with a random initial condition. When the pump parameters are different the steady state obtained from Eq. (2.5) is deterministic. Then the QDT can describe the fluctuations only during the transient.

The joint probability density $P(I_1, I_2; t)$ can be obtained from Eq.(2.5):

$$P(I_1, I_2; t) = \frac{1}{a_1(t) a_2(t) f(I_1, I_2, t)^3} \exp\left[-\left(\frac{I_1}{a_1(t)} + \frac{I_2}{a_2(t)}\right) f(I_1, I_2, t)^{-1}\right], \quad (2.6)$$

where

$$f(I_1, I_2, t) = 1 - \frac{I_1}{c_1(t)} - \frac{I_2}{c_2(t)} \quad (2.7)$$

and

$$a_i(t) = \frac{D}{\alpha_i}(e^{\alpha_i t} - 1) \quad , c_i(t) = \frac{\alpha_i}{\beta(1 - e^{-\alpha_i t})} \, . \quad (2.8)$$

The domain in which $P(I_1, I_2; t)$ is defined is given by $f(I_1, I_2, t) > 0$.

Initially when $\exp(-\alpha_i t) \approx 1$ the evolution is dominated by the spontaneous emission and the modes are not coupled, i.e. $P(I_1, I_2; t) \approx P_1(I_1, t) P_2(I_2, t)$. When $a_i(t) > c_i(t)$ the modes are coupled through the deterministic evolution. This happens for times such that

$$\epsilon_i(t) = \frac{{\alpha_i}^2}{\beta D} \exp[-\alpha_i t] \quad (2.9)$$

is smaller than one. Finally, it is easy to see from Eq. (2.5) that for non-equivalent modes ($\alpha_1 > \alpha_2$) the stationary state is reached in a time scale such that

$$u(t) = \frac{{\alpha_1}^2}{{\alpha_2}^2} \exp[-(\alpha_1 - \alpha_2) t] \quad (2.10)$$

is a small quantity. In the case of equal pump parameters the steady state is reached when the modes become coupled, i. e. $\epsilon_i(t) < 1$.

The transient probability density function of the intensity of both modes can be derived from Eq. (2.6):

$$P_1(I_1,t) = \frac{c_2 a_2 (c_2 a_2^{-1} + I_1[a_1(1-I_1/c_1)]^{-1}+1)}{a_1(c_2(1-I_1/c_1)+a_2 I_1/a_1)^2} \exp\Big[-\frac{I_1}{a_1(1-I_1/c_1)}\Big] \ , \quad I_1 < c_1 \tag{2.11a}$$

$$P_2(I_2,t) = \frac{c_1 a_1 (c_1 a_1^{-1} + I_2[a_2(1-I_2/c_2)]^{-1}+1)}{a_2(c_1(1-I_2/c_2)+a_1 I_2/a_2)^2} \exp\Big[-\frac{I_2}{a_2(1-I_2/c_2)}\Big] \ , \quad I_2 < c_2 \ . \tag{2.11b}$$

Finally, we consider the total intensity $I = I_1 + I_2$. This magnitude is relevant to analyze the coupling of the modes during the transient. From Eq. (2.6) we obtain the probability density function of I ($\alpha_1 > \alpha_2$):

$$P(I,t) = \frac{c_1 c_2 C(I,t)^2}{a_1 a_2 (c_1 - c_2)} \Big\{ \Big(\frac{I}{a_1}(1-I/c_1)^{-1} + \frac{(a_1-a_2)c_1 c_2}{(c_1-c_2)a_1 a_2} + 1 \Big) \exp\Big[-\frac{I}{a_1(1-I/c_1)}\Big] - \Big(\frac{I}{a_2}(1-I/c_2)^{-1} + \frac{(a_1-a_2)c_1 c_2}{(c_1-c_2)a_1 a_2} + 1\Big) \exp\Big[-\frac{I}{a_2(1-I/c_2)}\Big]\Big\} \tag{2.12a}$$

when $I < c_2(t)$ and

$$P(I,t) = \frac{c_1 c_2 C(I,t)^2}{a_1 a_2 (c_1 - c_2)} \Big\{ \Big(\frac{I}{a_1}(1-I/c_1)^{-1} + \frac{(a_1-a_2)c_1 c_2}{(c_1-c_2)a_1 a_2} + 1\Big) \exp\Big[-\frac{I}{a_1(1-I/c_1)}\Big]\Big\} \tag{2.12b}$$

when $c_2(t) < I < c_1(t)$. In these expressions $C(I,t)$ is given by

$$C(I,t) = \Big[\frac{I}{a_1} + \frac{(a_1-a_2)c_1 c_2}{(c_1-c_2)a_1 a_2}(1 - \frac{I}{c_1})\Big]^{-1} \ . \tag{2.13}$$

We have checked with numerical simulations [19] of the equation (2.1) the validity of the QDT. The QDT is found to give a good approximation in the transient regime (see Figs. 1,2) unless a very depressed mode is considered. In this case, $\alpha_1 \gg \alpha_2$, the evolution of the secondary mode is dominated by the noise and a new approximation is required (see Sec. IV). However, the main mode is always well described by the QDT.

6.3 Transient Statistics in the Mode Competition Case

We analyze in this section the transient statistics when the pump parameters for both modes are slightly different, i. e. when the parameter γ defined as

$$\gamma = \frac{\alpha_1}{\alpha_2} - 1 \tag{3.1}$$

is a small quantity. As noted in Sec. II a new time scale $(\alpha_1 - \alpha_2)^{-1}$ appears when $\alpha_1 > \alpha_2$ apart from the usual ones α_1^{-1} and α_2^{-1}. This time scale is related to the competition between both modes and it can be much slower than the first two when $\alpha_1 \approx \alpha_2$. This time $(\alpha_1 - \alpha_2)^{-1}$ is the characteristic time at which the modes approach the stationary state. It is also the typical time for the main mode to be switched on if the side mode has been initially excited.

When the modes are coupled, i.e. $\epsilon_i(t) \ll 1$, the probability densities for both modes (2.11) can be approximated by

$$P_1(x_1,t) = \frac{u(t)}{\left[1 - x_1(1-u(t))\right]^2} \quad , \quad x_1 < 1 \tag{3.2a}$$

$$P_2(x_2,t) = \frac{u^{-1}(t)}{\left[1 + x_2(u^{-1}(t) - 1)\right]^2} \quad , \quad x_2 < 1 \tag{3.2b}$$

except in a small region $x_i \approx 1$ with a negligible contribution to the probability, where the exponential term must be taken into account. In these expressions we use the normalized modal intensities $x_i = \beta I_i/\alpha$. Note that $u(t) < 1$ when $\epsilon_i(t) < 1$. This is due to the fact that $\beta D/\alpha_1^2 \ll 1$, that is the validity condition of the QDT. When $\epsilon_2(t) < 1$ we have $u(t) < (\gamma+1)^2(\beta D/\alpha_2^2)^\gamma$ that is always smaller than one for $\beta D/\alpha_2^2 < \exp(-2)$.

The probability density for the secondary mode has a polinomial tail and the main mode shows a symmetric tail for small values of the intensity (see Fig. 3). These distributions (3.2) are related in a simple way: the probability density of x_1

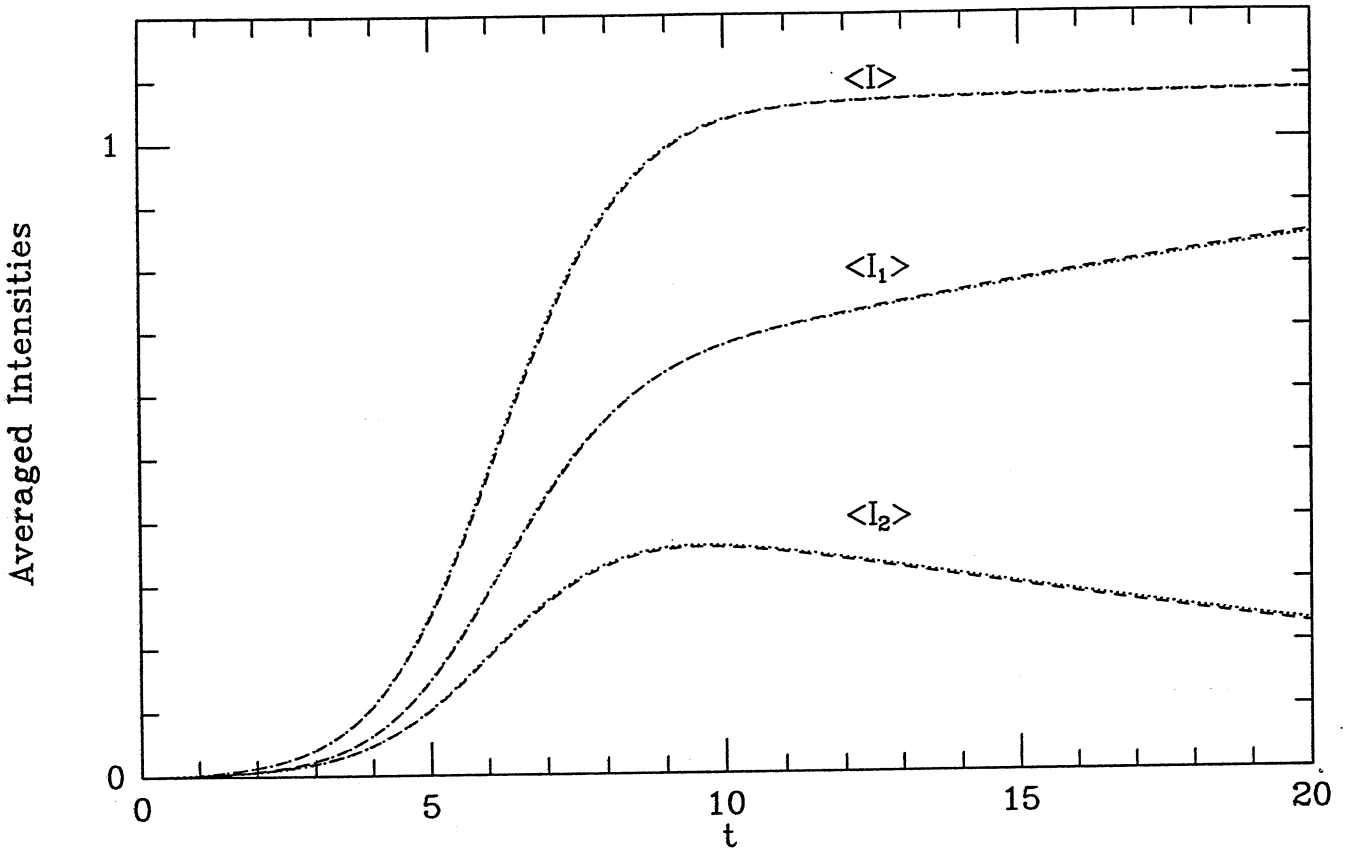

Fig. 1. Mean values of the main mode, $< I_1 >$, depressed mode, $< I_2 >$, and total, $< I >$ intensities. The simulation results are represented by the dotted line and the QDT by the dashed line. The parameters are taken as: $\alpha_1 = 1.1$, $\alpha_2 = 1$, $\beta = 1$ and $D = 10^{-3}$.

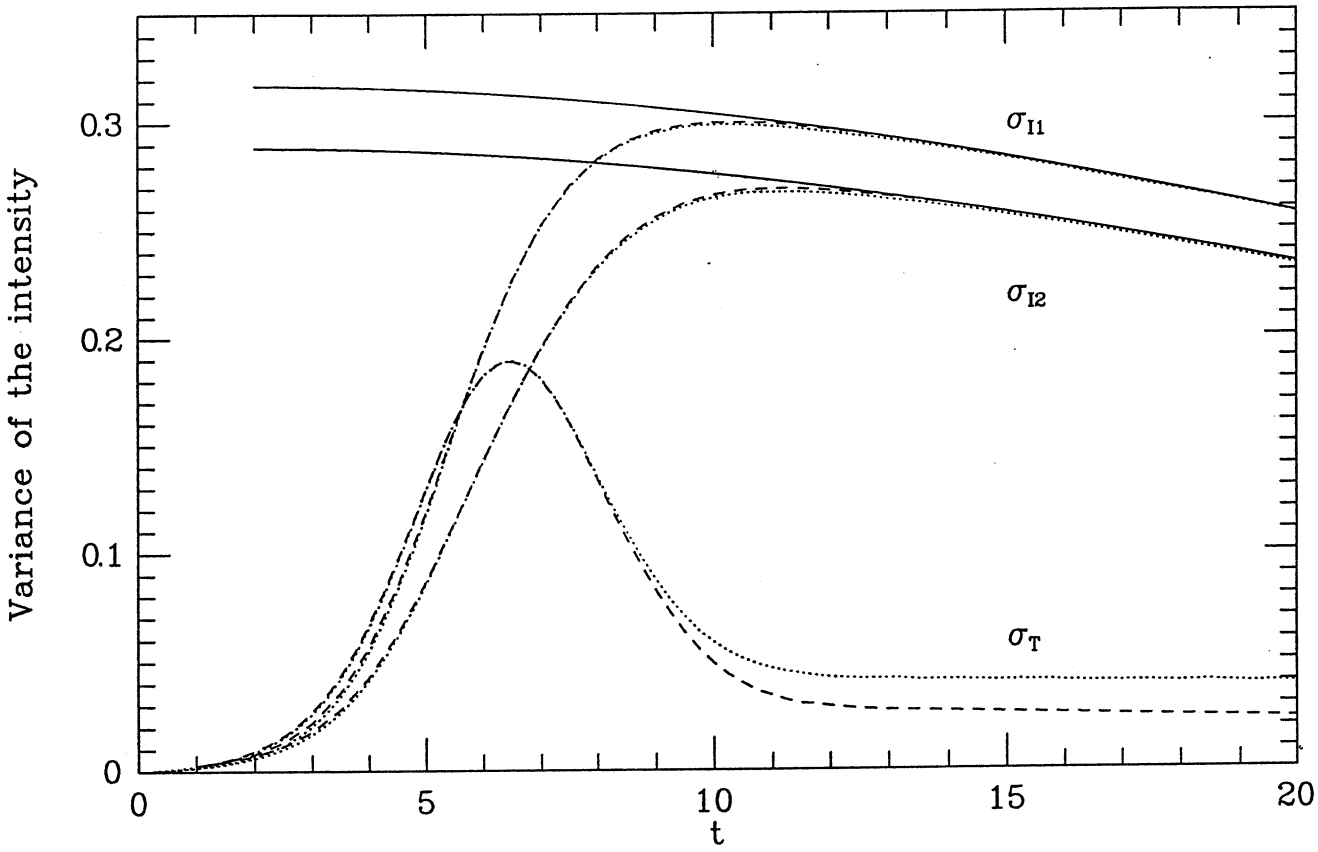

Fig. 2. Variances of the main mode σ_{I_1}, depressed mode σ_{I_2} and total σ_T intensities. We also plot with the solid line the function given by Eq. (3.5). The parameters are the same that in Fig. 1.

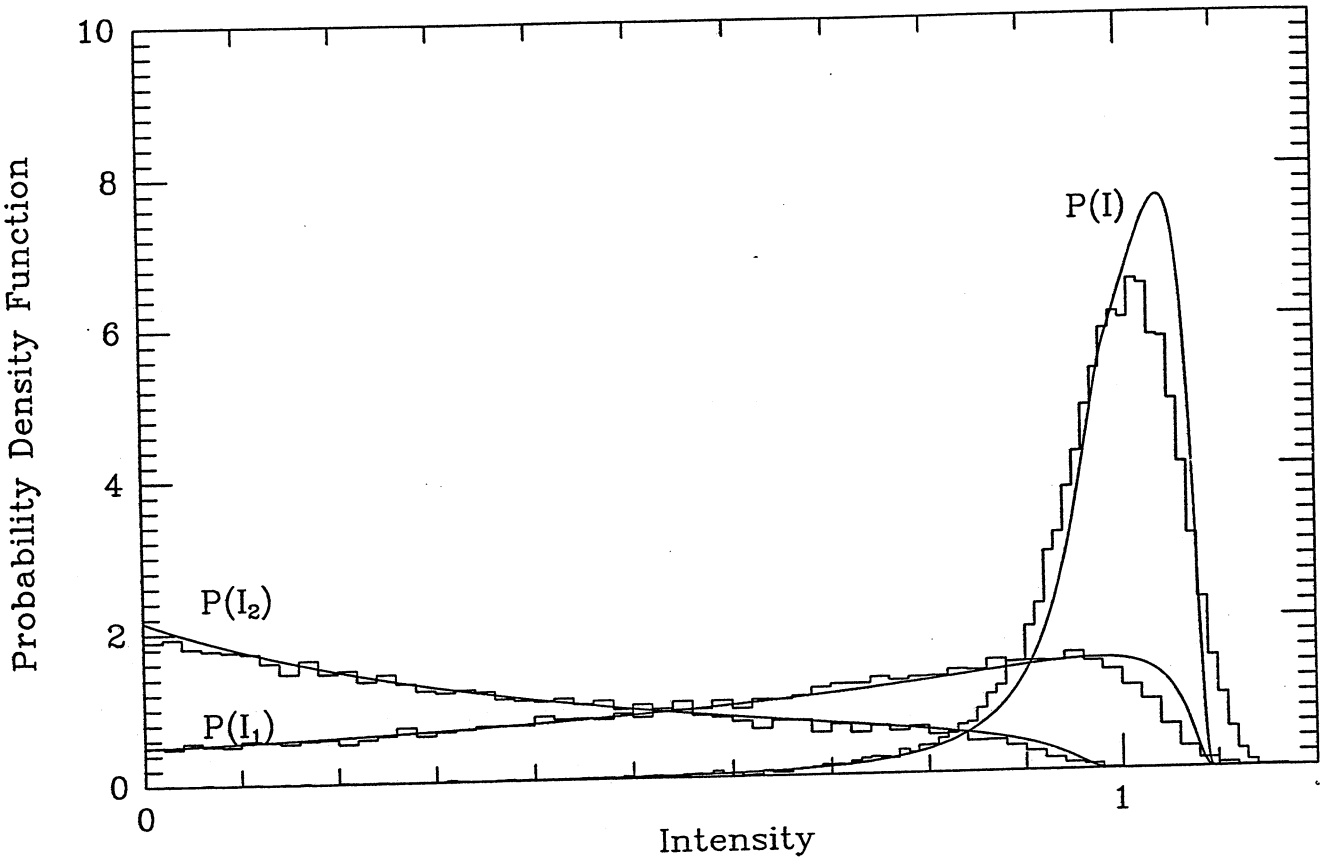

Fig. 3. Probability Density Function of the main mode, depressed mode and total intensities at time $t = 9$. The simulation results are represented by the histogram and the QDT results by the solid curve. The parameters are the same that in Fig. 1.

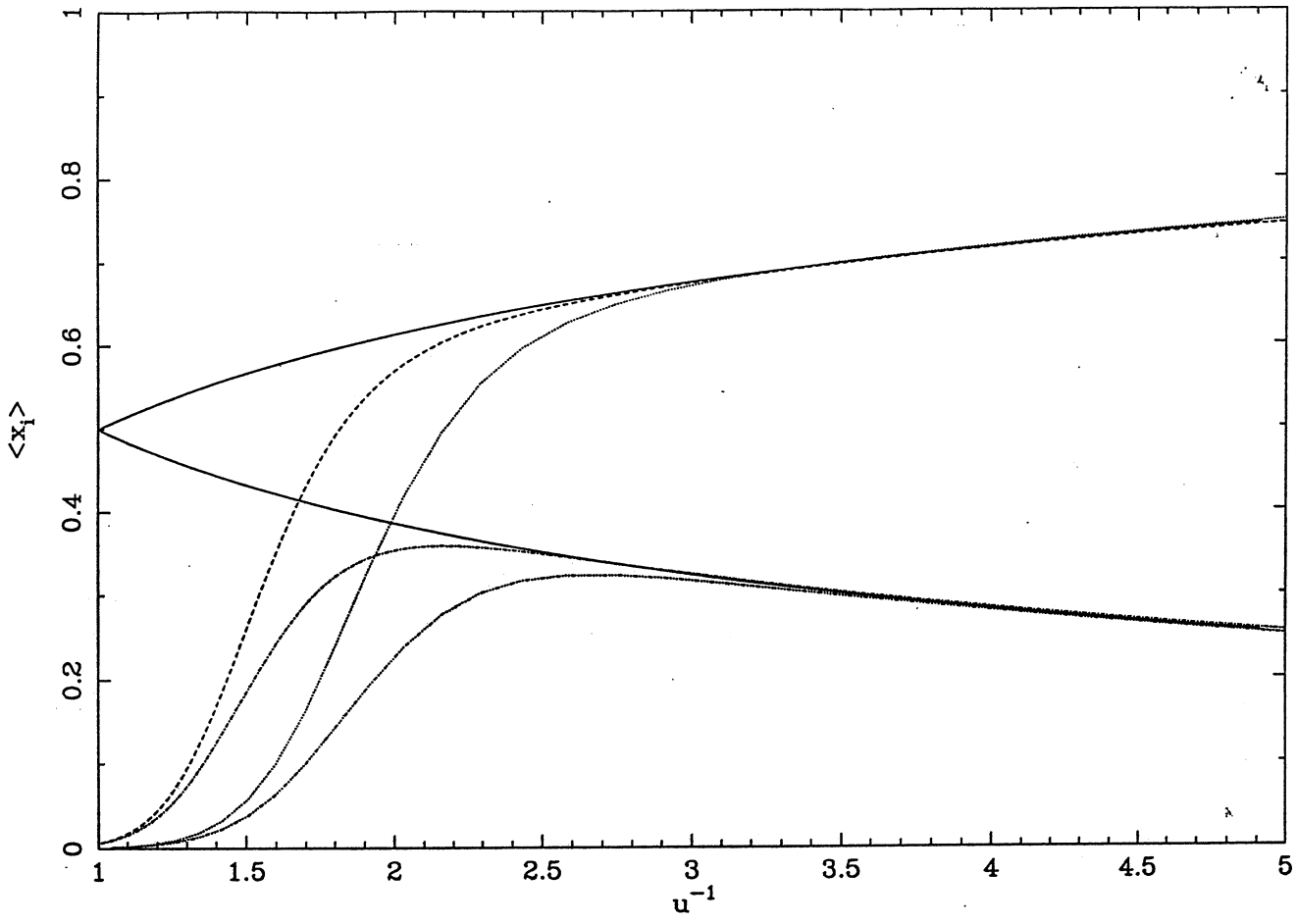

Fig. 4. Mean values obtained from simulation of the main mode and depressed mode normalized intensities as a function of u^{-1}. The mean values of the normalized main mode intensity $\langle x_1 \rangle$ are represented by the dashed line ($\alpha_2 = 1$) and the dotted line ($\alpha_2 = 3$) and the mean values of the normalized depressed mode intensity $\langle x_2 \rangle$ by the dot-dashed line ($\alpha_2 = 1$) and the three dot-dashed line ($\alpha_2 = 3$). We also plot with the solid line the functions given by Eq. (3.3). Other parameters in the figure are $\gamma = 0.1$, $\beta = 1$ and $D = 10^{-3}$.

is given by that of $1 - x_2$. The tails correspond to mode competition. The tail for the main mode corresponds to realizations starting later with respect to the most of the realizations. The meaning of the tail for the secondary mode is that for those realizations for which the main mode starts later there is a large probability that the secondary mode starts. For this reason, the dependence on x_2 of this tail is the same, but symmetric with respect to that of the main mode. In fact, at times such that $\epsilon_i(t) \ll 1$, the probability density for the total intensity is peaked around its mean value like in the mode partition noise phenomenon found in semiconductor lasers [17] (see Fig. 3). Then, the variance of the total intensity σ_T is very small, in contrast with the variances of the two modes that take its maximum values when σ_T decreases. This behavior can be derived from Eq. (2.12) taking into account that for these times the exponential terms are equal to one when $I < (\alpha_2/\beta)$. Then the two terms in Eq. (2.12a) cancel each other and $P(I,t)$ is non negligible only when the total intensity varies between (α_2/β) and (α_1/β).

The expressions for the probabilities densities given by Eqs. (3.2) show that when $\epsilon_i(t) \ll 1$ the temporal dependence of the normalized intensities $x_i(t)$ scales with $u(t)$. The mean intensity values are given by

$$\langle x_1(t)\rangle = 1 - \langle x_2(t)\rangle = \frac{1}{(1-u)} - \frac{u}{(1-u)^2}\ln u^{-1} \,. \tag{3.3}$$

Fig. 4 shows the dynamical scaling given by $u(t)$.

We have also studied the scaling of the moments of the intensity of the secondary mode. We find from Eq. (3.2b) that for $n > 1$ and times such that $u(t) < 1$:

$$\langle x_2^n\rangle \approx \frac{u(t)}{n-1} \,. \tag{3.4}$$

This result shows the non-Gaussian character of the transient statistics.

We now study the transient fluctuations of the intensity using the QDT. When the modes are non equivalent ($\alpha_1 > \alpha_2$) the intensity fluctuations of both modes show a maximum (see Fig. 2). This is similar to the anomalous fluctuation peak found

for a single mode class A laser [10]. As concerns the total intensity, $I = I_1 + I_2$, its variance also shows a maximum. We will characterize anomalous fluctuations of the two modes normalized intensities by the time at which the maximum appears, $t_{m,i}$, and by the value of this maximum $\sigma_{m,i}$. When $\epsilon_i(t) = [{\alpha_i}^2/(\beta D)] \exp[-\alpha_i t] \ll 1$ these fluctuations can be derived from Eq. (3.2):

$$ {\sigma_i}^2(t) = \frac{u(t)}{(1-u(t))^2} - \frac{u(t)^2}{(1-u(t))^4} (\ln u(t))^2 \, . \tag{3.5} $$

Then for these times the fluctuations of the normalized intensities coincide and they show a temporal dependence given by a dynamical scaling parameter $u(t)$ (see Fig. 5). This generalizes the dynamical scaling found in the single mode case [20].

The variance given by Eq. (3.5) is a decreasing function of t in its validity region given by $\epsilon_i(t) < 1$ and then $u(t) < 1$. Then it can not be used to obtain the time at which the maximum of the fluctuations appears $t_{m,i}$. The maximum appears when the modes become coupled, i. e. $\epsilon_i(t) \lesssim 1$ and the mode competition is strong. This corresponds to a time regime such that the mean intensity for the side mode takes its maximum value (see Figs. 1,2,4 and 5). For times such that side mode intensity is depressed by the main mode, i. e. $\epsilon_i(t) \ll 1$, fluctuations decrease with time. When the pump parameters are similar, i. e. γ small, the competition between modes lasts for a long time and the variance changes very slowly (see Figs. 2 and 5). Then the variance obtained from Eq. (3.5) at $u = u(t_{m,i})$, that is valid when $\epsilon_i(t) \ll 1$, is a good approximation for $\sigma_{m,i}$ (see Figs. 2 and 5). However, since $\sigma_i(t)$ decreases for times $t < t_{m,i}$ in an appreciable way only when $\epsilon_i(t) \gtrsim 1$, Eq. (3.5) can not describe this behavior.

To obtain $t_{m,i}$ we use Eqs. (2.11) instead of Eqs. (3.2). The main difference between both expressions lies in the exponential term. When γ is small the moments for the mode intensities at $t_{m,i}$ can be obtained from Eqs. (3.2). Using this approximation the following equations for $t_{m,i}$ can be derived

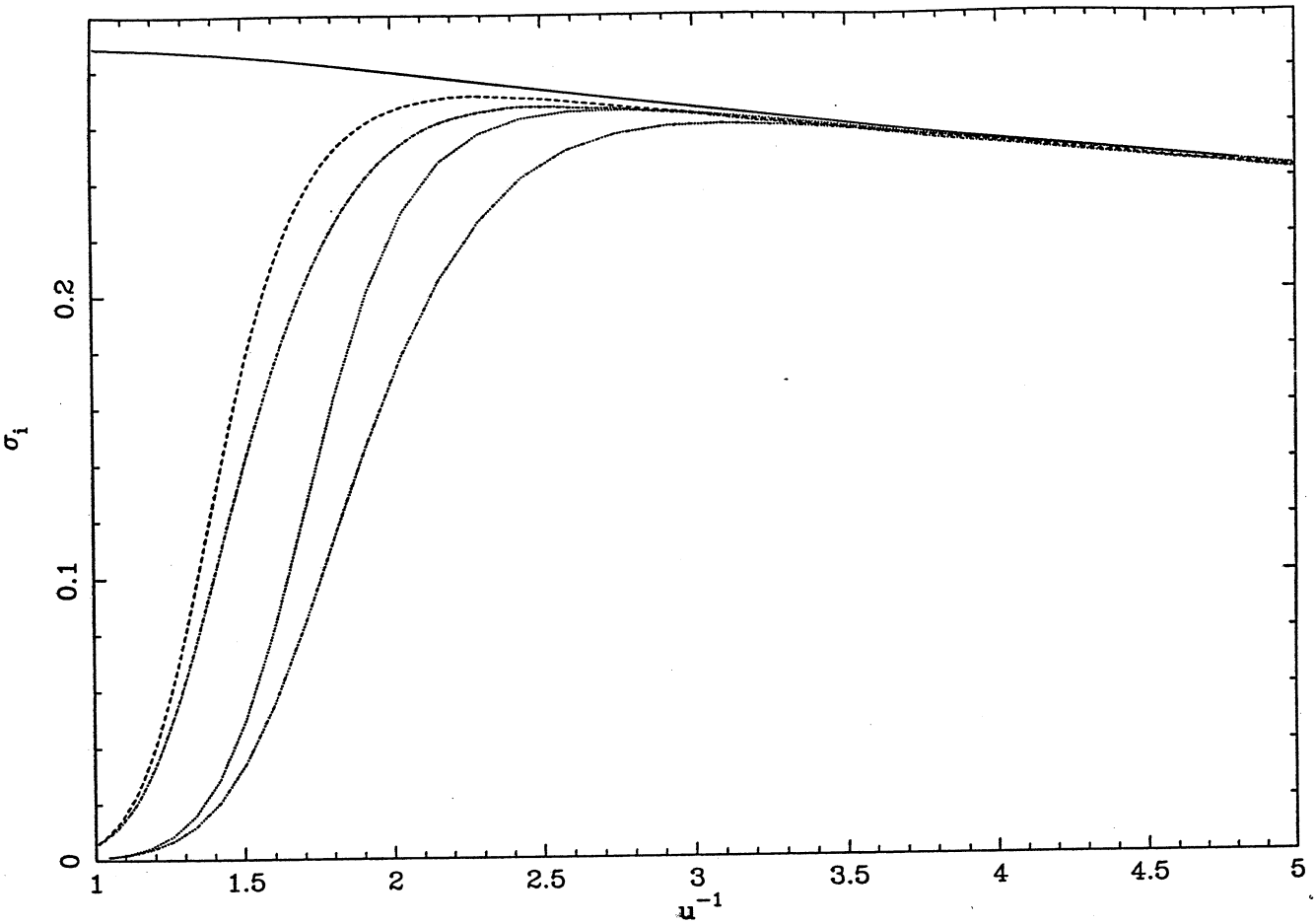

Fig. 5. Variances obtained from simulation of the main mode and depressed mode normalized intensities. The variance of the main mode intensity σ_1 is represented by the dashed line ($\alpha_2 = 1$) and the dotted line ($\alpha_2 = 3$) and the variance of the depressed mode σ_2 by the dot-dashed line ($\alpha_2 = 1$) and the three dot-dashed line ($\alpha_2 = 3$). We also plot with the solid line the function given by Eq. (3.5). The other parameters in the figure are the same that in Fig. 4.

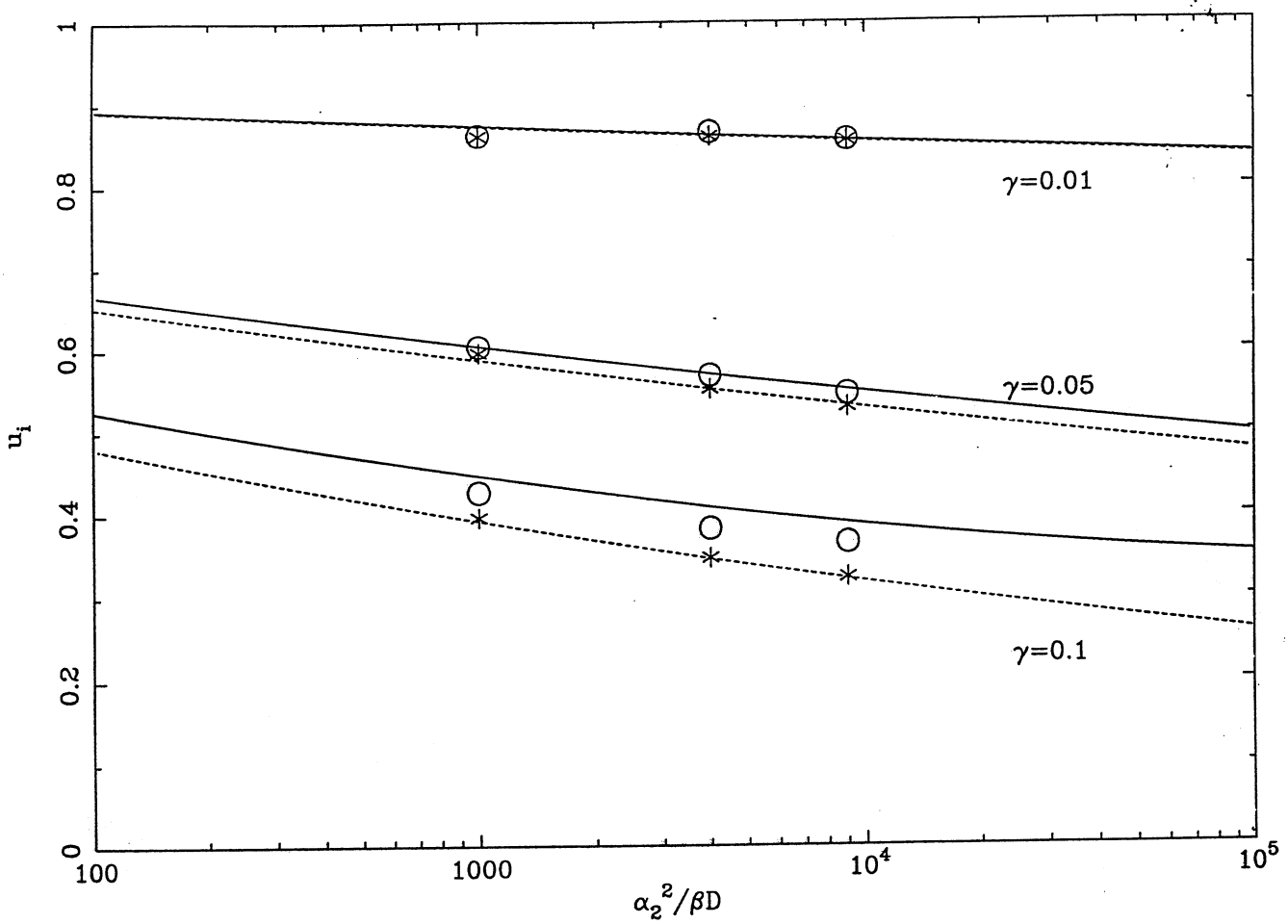

Fig. 6. u_1 and u_2 as functions of γ and $\alpha_2^2/(\beta D)$. The results given by Eqs. (3.6a) and (3.6b) are represented by the solid and dashed lines respectively. The simulation results for u_1 are plotted with circles and for u_2 with stars. The parameters used in these simulations are $\alpha_2 = 1, 2, 3$, $\beta = 1$ and $D = 10^{-3}$.

$$g(u_1) = \left(\frac{{\alpha_2}^2}{\beta D}\right)\frac{{u_1}^{1/\gamma}}{(1+\gamma)^{2/\gamma\gamma}}\left[\frac{-1}{(1-u_1)} - \frac{2u_1}{(1-u_1)^3}\ln u_1^{-1} + \frac{2u_1}{(1-u_1)^4}(\ln u_1^{-1})^2 - \frac{\gamma}{u_1}\left[\frac{(1+u_1)}{(1-u_1)} - \frac{2u_1}{(1-u_1)^2}\ln u_1^{-1}\right]\right] \tag{3.6a}$$

$$g(u_2) = \left(\frac{{\alpha_2}^2}{\beta D}\right)\frac{{u_2}^{1/\gamma}}{(1+\gamma)^{2/\gamma\gamma}}\left[\frac{1}{(1-u_2)} - \frac{2u_2}{(1-u_2)^3}\ln u_2^{-1} + \frac{2{u_2}^2}{(1-u_2)^4}(\ln u_2^{-1})^2 - \gamma\left[\frac{(1+u_2)}{(1-u_2)} - \frac{2u_2}{(1-u_2)^2}\ln u_2^{-1}\right]\right], \tag{3.6b}$$

where

$$g(u) = \frac{(1+u)}{(1-u)^3} + \frac{2u}{(1-u)^4}\ln u^{-1} - \frac{2u(1+u)}{(1-u)^5}(\ln u^{-1})^2 \tag{3.7}$$

and $u_i = (\alpha_1/\alpha_2)^2 \exp[-(\alpha_1 - \alpha_2)t_{m,i}]$. In Fig. 6 it is shown that Eqs. (3.6) give correctly the time at which the maximum of the fluctuations appears and that the approximation works better when γ decreases.

It is not possible to get an analytic solution for u_i from Eq. (3.6). However, when γ decreases u_i approaches 1 (see Fig. 6) and an approximation can be obtained. In this case it is found that u_i changes very slowly with $({\alpha_2}^2/\beta D)$in the following way: $(1 - u_i) \approx \gamma \ln({\alpha_2}^2/\beta D)$. Then u_i depends mainly on γ when the pump parameters are similar.

Finally we consider the case of equivalent modes, $\alpha_1 = \alpha_2 = \alpha$. Since the modes compete forever the variance increases until the steady state is reached. Now the QDT describes the fluctuations in the stationary state (see Eq. (2.5)), that is given from Eq. (2.11) by an uniform probability between 0 and (α/β). This result is in agreement with the exact result [21] well above threshold.

6.4 Transient Statistics in the very depressed mode case.

When the secondary mode is very depressed, $\alpha_2 \ll \alpha_1$, the evolution of I_2 is mainly due to the spontaneous emission noise. Then the evolution is not deterministic and

the QDT does not describe correctly the secondary mode. Since the effect of a very depressed secondary mode is negligible, the evolution of the main mode is given by the QDT for the single mode laser:

$$I_1^{SM}(t) = \frac{\mid h_1(\infty) \mid^2 e^{\alpha_1 t}}{1 + (\beta/\alpha_1) \mid h_1(\infty) \mid^2 e^{\alpha_1 t}}\,, \tag{3}$$

where we consider times such that $\mid h_1(t) \mid^2 \approx \mid h_1(\infty) \mid^2$, that is $e^{-\alpha_1 t} << 1$ (see Eq. (2.4)).

For the secondary mode we develop a new approximation by using a random pump parameter given by the intensity of the main mode and by including the spontaneous emission noise. Using this approximation the evolution equation for the secondary mode is

$$\dot{E}_2 = \frac{1}{2}(\alpha_2 - \beta I_1^{SM})E_2 + \xi_2\,. \tag{4}$$

The probability density of I_2 can be obtained from the conditional probability density $P(I_2 \mid I_1; t)$ by integrating over I_1 the function $P(I_1, I_2; t)$ defined by

$$P(I_1, I_2; t) = P(I_2 \mid I_1; t) P_1^{SM}(I_1, t)\,. \tag{5}$$

In this expression $P(I_2 \mid I_1; t)$ is an exponential distribution with mean value

$$\langle I_2 \mid I_1; t \rangle = \frac{D}{\alpha_2}(e^{\alpha_2 t} - 1)(1 - \frac{\beta I_1}{\alpha_1}) + \frac{D}{\alpha_1}\frac{\beta I_1}{\alpha_1} \approx Dt(1 - \frac{\beta I_1}{\alpha_1}) + \frac{D}{\alpha_1}\frac{\beta I_1}{\alpha_1}\,, \tag{6}$$

and $P_1^{SM}(I_1, t)$ can be obtained from (4.1):

$$P_1^{SM}(I_1, t) = \frac{\alpha_1 e^{-\alpha_1 t}}{D(1 - \beta I_1/\alpha_1)^2} \exp -\Big[\frac{\alpha_1 e^{-\alpha_1 t} I_1}{D(1 - \beta I_1/\alpha_1)}\Big]. \tag{7}$$

For short times such that $\epsilon_1(t) \gg 1$ the main mode intensity is small and the side mode intensity increases due to the spontaneous emission noise. Then the probability density of I_2 is an exponential distribution with mean value Dt. For intermediate times such that $\alpha_1 t \epsilon_1 \gg 1$ the mean value (4.4) can be approximated by the first term and the following approximation holds

$$P(I_2) = \frac{e^{-I_2/(Dt)}}{Dt}\Big[\frac{1}{(1+I_2/(Dt\epsilon_1))} + \frac{1}{\epsilon_1(1+I_2/(Dt\epsilon_1))^2}\Big] . \tag{8}$$

In this time regime $\langle [I_2/(Dt)]^n \rangle$ is a function only of ϵ_1. Finally, when the steady state is attained, i.e. when $\epsilon_1(t) \ll 1$, the probability density of I_2 is again an exponential distribution with mean value D/α_1.

The moments of the intensity of the depressed mode can be easily obtained from Eqs. (4.4)-(4.5). The mean value is given by

$$\langle I_2(t) \rangle = \frac{D}{\alpha_1}(1 - \epsilon_1 e^{\epsilon_1} E_1(\epsilon_1)) + Dt\epsilon_1 e^{\epsilon_1} E_1(\epsilon_1) , \tag{9}$$

where E_1 is the exponential-integral function [22]. The fluctuations are given by

$$\sigma_2^2(t) = 2\Big[\frac{D}{\alpha_1}(1-\alpha_1 t)\frac{\beta\sigma_1(t)}{\alpha_1}\Big]^2 + \langle I_2(t) \rangle^2 , \tag{10}$$

where σ_1 is the variance of the main mode:

$$\sigma_1(t)^2 = (\alpha_1/\beta)^2\Big[\epsilon_1 - \epsilon_1^2 e^{\epsilon_1} E_1(\epsilon_1)(e^{\epsilon_1} E_1(\epsilon_1) + 1)\Big] . \tag{11}$$

Fig. 7 shows that the mean value and the variance of the depressed mode are well described by the approximation. We observe that initially $\langle I_2 \rangle = \sigma_2 = Dt$ in agreement with the discussion above. When I_2 starts to be depressed by the main mode we have $\langle I_2 \rangle \approx \sigma_2 \approx Dt(1 - \langle \beta I_1/\alpha_1 \rangle)$. This corresponds to small values of $\langle I_1 \rangle$ and σ_1 (see Eqs. (4.4) and (4.7)-(4.9)). This time regime, that includes the times at which the maximums of $\langle I_2 \rangle$ and σ_2 appear, can be described by (4.6). When the main mode increases the two terms in Eq. (4.4) are important and $\sigma_2 > \langle I_2 \rangle$. Finally in the steady state we have $\langle I_2 \rangle = \sigma_2 = D/\alpha_1$.

Finally, we calculate the probability, $\Phi(I_1)dI_1$, that when the intensity is for the first time $I_1 + I_2 = I_T$ the main mode intensity is between I_1 and $I_1 + dI_1$. This probability gives direct information about the side-mode excitation probability and it has been obtained by neglecting the nonlinear terms for the semiconductor and gas lasers [16] when the side mode is not very depressed. The calculation of this probability is

equivalent to find, in the multidimensional phase space of the system, the direction of departure from the initial laser unstable point. The probability density, $\Phi(I_1)$, can be written as a function of the probability current (J_1, J_2), associated to the Fokker-Planck equation equivalent to the Langevin equations of our approximation, in the following way

$$\Phi(I_1) = \int_0^\infty (J_1 + J_2)(I_1, I_T - I_1)dt \,, \tag{12}$$

where

$$J_1(I_1, I_2, t) = (\alpha_1 - \beta I_1) I_1 P(I_1, I_2, t) \tag{13}$$

$$J_2(I_1, I_2, t) = (\alpha_2 - \beta I_1) I_2 P - D(I_2 \frac{\partial P}{\partial I_2} + P)(I_1, I_2, t) \,. \tag{14}$$

To obtain Φ one should impose absorbing boundary conditions. However, a good approximation can be obtained by using natural boundary conditions. This corresponds to the fact that for large enough values of α_1 the boundary $I_1 + I_2 = I_T$ is only crossed one time. In this way we obtain that the function $P(I_1, I_2, t)$ appearing in the expression of the probability current coincides with (4.3). We compare in Fig. 8 $\Phi(I_1)$ calculated from (4.10) and by using the linear theory [16] with the simulation results. It is not posible to obtain an analytical expresion for the integral appearing in (4.10). This integral is evaluated numerically by using (4.11), (4.12) and the joint probability density given by (4.3). It is clear that the approximation (4.10) gives very good results and that the linear theory is unable to describe correctly $\Phi(I_1)$.

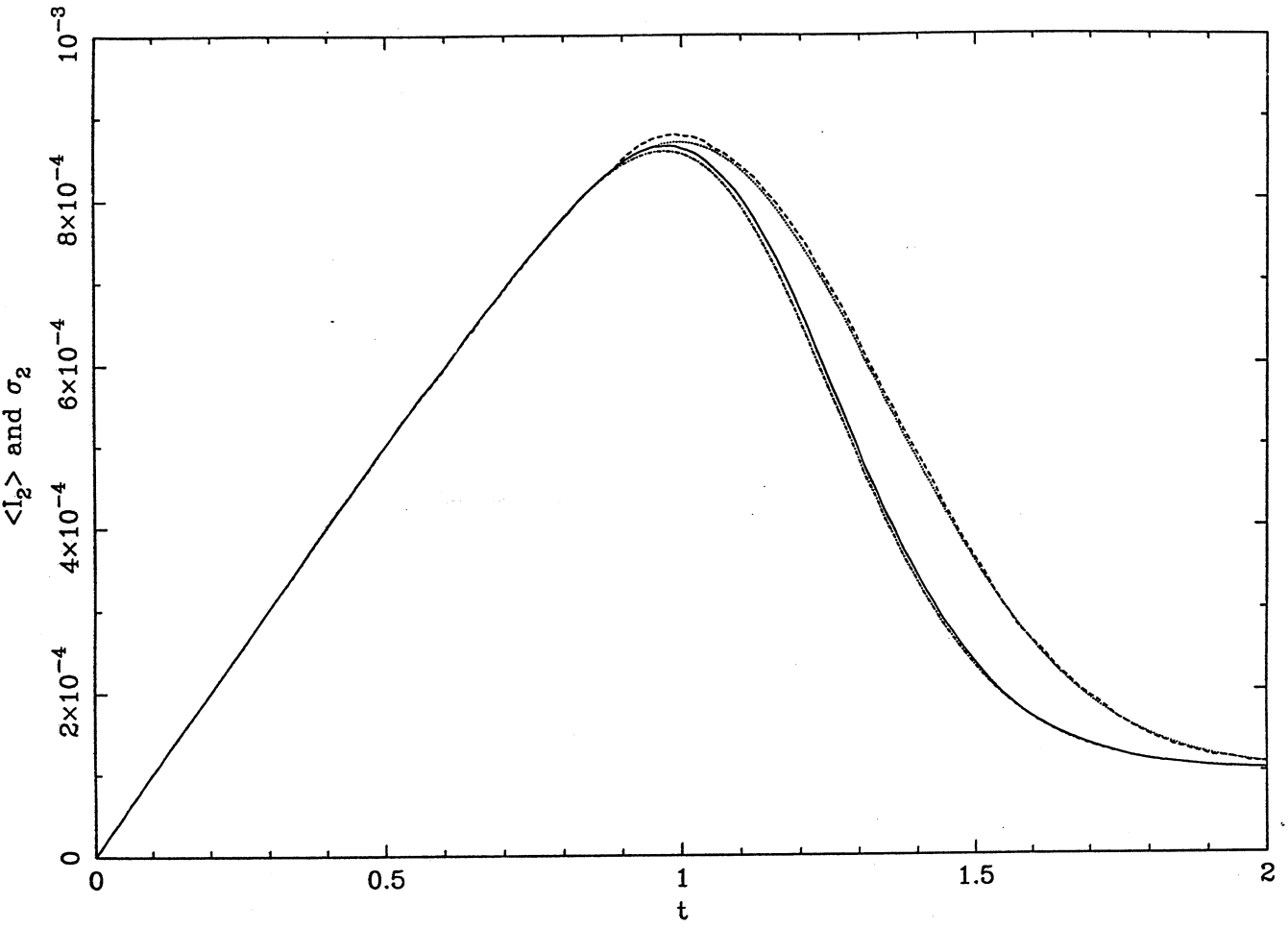

Fig. 7. Mean value and variance of the intensity of a very depressed mode. Simulation results for the mean value and the variance are represented with the solid and dashed line respectively. We also plot the mean value (dot-dashed line) and variance (dotted line) given by the approximation. The parameters in this figure are $\alpha_1 = 10$, $\alpha_2 = 0.01$, $\beta = 1$ and $D = 10^{-3}$.

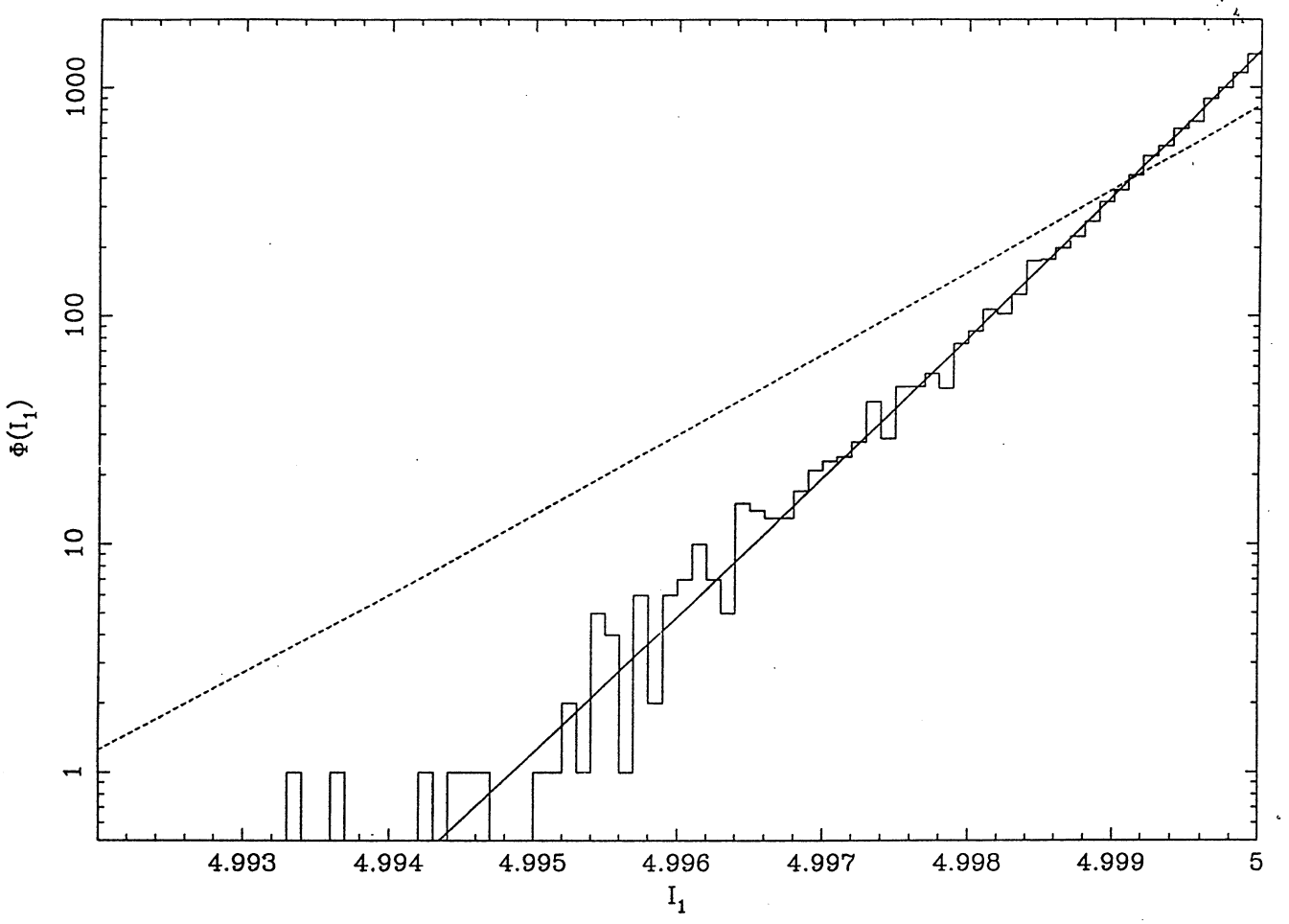

Fig. 8. $\Phi(I_1)$ obtained from simulation (histogram), linear theory (dashed line) and from (4.10) (solid line). The threshold intensity, I_T, has been fixed to one half the stationary intensity of the main mode. The parameters are taken as: $\alpha_1 = 10.$ $\alpha_2 = 0.1$, $\beta = 1$, and $D = 10^{-3}$.

REFERENCES

[1] M. San Miguel, in Laser Noise, edited by R. Roy (SPIE, Boston, 1990), 272.

[2] M. R. Youngh and S. Singh, Phys. Rev. A **35**,1453 (1987); J. Opt. Soc. Am. B **5**, 1011 (1988).

[3] R. Roy, A. W. Yu, and S. Zhu, Phys. Rev. Lett. **55**, 2794 (1985); Phys. Rev. A **34**, 4333 (1986).

[4] F. De Pasquale, J. M. Sancho, M. San Miguel, and P. Tartaglia, Phys. Rev. Lett. **56**, 2473 (1986).

[5] G. Broggi, A. Colombo, L. A. Lugiato, and P. Mandel, Phys. Rev. A **33**, 3635 (1986).

[6] M. C. Torrent and M. San Miguel, Phys. Rev. A **35**, 1453 (1987).

[7] F. T. Arecchi, R. Meucci, and J. A. Roversi, Europhys. Lett. **8**, 225 (1989); F. T. Arecchi, W. Gadomsky, R. Meucci, and J. A. Roversi, Phys. Rev. A **39**, 4004 (1989); M. Ciofini, R. Meucci, and F. T. Arecchi, Phys. Rev. A **42**, 482 (1990).

[8] A. Mecozzi, S. Piazzolla, A. D'Ottavi, and P. Spano, Phys. Rev. A **38**, 3136 (1988); Appl. Phys. Lett. **55**, 769 (1989).

[9] P. Spano, A. D'Ottavi, A. Mecozzi, B. Daino, and S. Piazzolla, IEEE J. Quantum Electron. **25**, 1440 (1989).

[10] F. T. Arecchi, V. de Giorgio, and B. Querzola, Phys. Rev. Lett. **19**, 1168 (1967); F. T. Arecchi and V. de Giorgio, Phys. Rev. A **3**, 1108 (1971).

[11] D. Meltzer and L. Mandel, Phys. Rev. Lett. **25**, 1151 (1970).

[12] A. Valle, L. Pesquera, and M. A. Rodriguez, Phys. Rev. A **45**, 5243 (1992).

[13] S. Balle, P. Colet and M. San Miguel, Phys. Rev. A **43**, 498 (1991).

[14] P. Spano, A. Mecozzi, and A. Sapia, Phys. Rev. Lett. **64**, 3003 (1990); A. Mecozzi, P. Spano and A. Sapia, Opt. Lett. **15**, 1067 (1990).

[15] F. de Pasquale, P. Tartaglia, and P. Tombesi, Physica **99A**, 581 (1979); Phys. Rev. A **25**, 466 (1982).

[16] A. Mecozzi, A. Sapia, P. Spano, and G. P. Agrawal, IEEE J. Quantum Electron. **27**, 332 (1991).

[17] M. M. Choy, P. L. Lui, and S. Sasaki, Appl. Phys. Lett. **52**, 1762 (1988).

[18] S. Singh, Physics Reports **108**, 217 (1984).

[19] The numerical simulations have been performed following the algorithm described in J. M. Sancho, M. San Miguel, S. L. Katz and J. D. Gunton, Phys. Rev. A **26**, 1589 (1982). Typical averages were taken over 5×10^4 realizations using a step of integration of 2×10^{-4}.

[20] M. Suzuki, Adv. Chem. Phys. **46**, 195 (1981).

[21] M. M. Tehrani and L. Mandel, Phys. Rev. A **17**, 677 (1978).

[22] *Handbook of Mathematical Functions*, edited by M. Abramowitz and I. Stegun (Dover, New York, 1970).

Chapter 7

Transient multimode statistics in nearly single-mode semiconductor lasers

7.1 Introduction

Mode–partition noise in optical fiber communication systems is still causing an error rate floor even with distributed-feedback (DFB) lasers sources [1], [2] having a side-mode suppression ratio (SMSR) larger than 30 dB in stationary conditions. The excitation of a side mode during the transient operation has been initially studied using the rate equation approach without considering fluctuations. However, spontaneous-emission noise must be taken into account to have a correct description of this problem [3]-[11]. Even though the laser usually starts to oscillate in the main mode, i.e., the mode having the minimum cavity loss, spontaneous-emission noise can trigger the laser to oscillate on a side mode as well. For nearly single-mode DFB lasers only one side mode can have an appreciable probability to be excited during the transient. The analysis can then be limited to two modes.

In this chapter we study analytically and numerically the transient dynamics of the density of photons in the main I_m and side I_s modes for nearly single-mode semiconductor lasers when the injected current is suddenly switched from a value C_b below to a value C above the threshold current. The dynamics of the laser is modelled using noise driven rate equations for the density of minority carriers n and for the photon densities I_m and I_s. The relative net gain difference $\alpha_r = (\alpha_s - \alpha_m)/\alpha_m$ and the laser operating point, given by C, are taken as parameters. Here α_m (α_s) corresponds to the loss of the main (side) mode.

We characterize the statistics of the rare turn-on events in which the depressed mode carries significant output power using two different but related magnitudes: i)side-mode excitation probability during the switch on and ii) the mean output power associated with each mode during a time interval that includes the relaxation oscillations. When the laser is biased below threshold the first characterization corresponds to a linear regime such that the carrier depletion can be neglected. In the second characterization nonlinearities due to gain depletion play a crucial role.

In Section 7.2 we analyze the statistics of the power partition between the two modes during the laser switch on. Analytic expressions were previously obtained with the use of a linear approximation neglecting the coupling between the main and side modes [7]. However, this approximation is not accurate when the side mode is highly suppressed, α_r large and/or C small. A new theory is developed taking into account the gain saturation for the side mode due to the main mode. A better agreement than using the linear theory is found between this theory and numerical simulations. Using this approximation the probability that the side mode has a photon density larger than the main mode during the switch-on of the laser is obtained. We calculate the SMSR required to have this probability lower than 10^{-9} for different values of the injection current.

Section 7.3 contains the results of our second characterization of the statistics of rare events and its relation with the first characterization. A theory is developed to obtain the mean output power of the depressed mode as a function of the output power of the main mode at the turn-on time. This approach is similar to the one carried out recently for the periodic intensity modulation regime [11]. Our main result is to show that both characterizations are directly connected. We find a simple relation for the rare events between the mean output power of the depressed mode and the output power of the main

mode at the turn-on time. Given this relation the probability for a significant contribution of the side mode to the mean total output power is obtained as a simple transformation of the output power statistics at the turn-on time. Our results show that this quantitative measure of errors due to rare events decreases with the relative net gain difference and operating close to threshold. The SMSR required for this probability to be lower than 10^{-9} is obtained.

7.2 Side-mode excitation probability: Theory and simulations

The dynamics of a nearly single-mode DFB laser can be modelled using the well-known noise driven rate equations for the density of minority carriers n and for the density of photons in the cavity modes I_i, $i = m$ (main mode), s (side mode) [12], [13]:

$$\frac{dn}{dt} = C - \frac{n}{\tau_{sp}} - \frac{c}{\eta n_g} g(I_m + I_s) \tag{1}$$

$$\frac{dI_i}{dt} = \frac{c}{n_g}(g - \alpha_i)I_i + \frac{\gamma}{\tau_{sp}} Dn + \sqrt{\frac{2\gamma}{\tau_{sp}} D I_i n}\, F_i(t) \tag{2}$$

with

$$g = \frac{\eta n_g A(Dn - n_0)}{c(1 + \frac{I_m + I_s}{\chi})}. \tag{3}$$

The meaning of the symbols and typical values [7] of the different parameters involved in these equations are listed in Table I. The total output power of the laser is proportional to $I = I_s + I_m$ with a proportionality factor of the order of $4 \times 10^{-15}\ mW\ cm^3$. The parameter D gives the fraction of the minority carriers interacting with each mode [14]. We have assumed that $D_m = D_s = D$, a valid assumption when the frequency difference between the two modes is much less than the spontaneous-emission linewidth. The random spontaneous-emission process is modeled by uncorrelated Gaussian white noise terms $F_i(t)$

of zero mean and correlation functions:$\langle F_i(t)F_j(t')\rangle = \delta_{ij}\delta(t-t')$. We neglect the effect of the radiative and non-radiative carrier generation and recombination noise in the rate equation for $n(t)$ since it is negligible in comparison with the fluctuations induced by $F_i(t)$ during the transient, as they are amplified by the stimulated-emission process. The stochastic differential equations (1) and (2) are defined in the Ito sense [15].

According to eqs. (1)-(3), the laser threshold is given by:

$$C_{th} = \frac{2}{\tau_{sp}}\left(\frac{\alpha_m c}{A\eta n_g} + n_0\right)$$

and the value of the carrier density at threshold is $n_{th} = \tau_{sp}C_{th}$. We will consider the transient evolution after the injected current is suddenly switched at time $t = 0$ from a bias value C_b below C_{th} to a value C above threshold. Throughout our study we fix a bias current sufficiently below threshold so that the results are independent of C_b. The initial conditions are sampled from the steady state associated to this value of C_b. The relative importance of the side mode depends on various parameters C_b, C, A, χ, and $\Delta g \equiv \alpha_s - \alpha_m$. For larger bias value the effect of the side mode is reduced, but it is not always convenient to have a very large C_b because of the reduction of the on/off ratio [5].

The saturation parameter χ is not very important for this matter [7] and A only affects [7] in the combination $A(C - C_{th})$. We will study the statistics of TMP taking as parameters the operating point given by C and the relative net gain difference α_r. We report results for $C = 1.2\,C_{th}$, $C = 1.5\,C_{th}$ and α_r between 7.9% and 49.7%. The largest value of the α_r is too large for presently available DFB lasers but it will be used to predict possible improvements in situations of large SMSR. Typical experimental values of the SMSR are 42 dB [16], [17] for $\lambda/4-$shifted DFB lasers and 38 dB for not shifted DFB lasers [18]. These values correspond to $\alpha_r = 18$ % and $\alpha_r = 7$ %, respectively.

Our numerical simulations integrate the equations for the electric field corresponding to equations (1)–(2) with an integration step of 0.5 ps. We integrate the equations until 2 ns. and 1 ns. for currents $C = 1.2C_{th}$ and $C = 1.5C_{th}$ respectively. Typically our statistics are obtained from $5 \times 10^5 - 2.5 \times 10^6$ different turn-on events. The largest number of events is needed for the largest values of α_r and the smallest of C. These are the values for which the probability of a rare event becomes smaller.

Some examples of turn-on events obtained from our simulations are shown in Fig. 1 where two events in which the side mode carries significant output power are compared with a typical turn-on event. The turn on time is defined as the time $\bar{t}$ in which total photon density $I_m + I_s$ reaches a prescribed value I_T defined here as $I_T = \frac{I_{st}}{2}$, being I_{st} the stationary value of the total photon density in the on state. It is clear that rare events are associated with large turn-on times. For a large turn-on time, the side mode turns-on before the main mode and the later the main mode turn-on the larger is the optical pulse associated with the side mode. At steady state the side mode is depressed and the total photon density is carried by the main mode. We will characterize the statistics of these rare events by two probability densities: $\phi(I_m/I_T)$ is the probability density that the main mode has a fraction I_m/I_T of the total photon density at the turn-on time $\bar{t}$, and $P_T(W_s/W_T)$ that is the probability density that the mean photon density W_s of the side mode is a fraction of the total mean photon density W_T during a time T. The mean photon densities are defined as

$$W_{s,m} = \frac{1}{T}\int_0^T I_{s,m}(t)dt \tag{4}$$

and $W_T = W_s + W_m$.

It is seen in Fig. 1b, 1c that a large value of W_s in a given event is tipically associated

with a small value of $I_m(\bar{t})$. The probability $P_T(W_s/W_T)$ depends crucially on the value of T. A precise relation between $\phi(I_m/I_T)$ and $P_T(W_s/W_T)$ will be established in the following Section for values of T which include the whole optical pulse.

In this Section we study the statistics of the power partition between the two modes during the switching of the laser in terms of the probability density function (PDF) $\Phi(I_m)$ of the main-mode photon density I_m at the turn-on time. An analytic expression for $\Phi(I_m)$ was obtained [7] with the use of a linear approximation neglecting the last term in (1) and the gain-saturation factor in (3). This approximation is valid below threshold and during the first stage of the exponential growth of the photon density. Since we take $I_T = I_{st}/2$, I_{st} being the stationary value of the total photon density in the *on* state, it is reasonable to assume that the carrier depletion due to stimulated emission can be neglected. The linear theory has been used to obtain $Pr(I_s > I_m)$, i.e., the probability that the side mode has a photon density larger than that of the main mode when the total photon density is $I_{st}/2$:

$$\delta_1 = Pr(I_s > I_m) = \int_0^{I_T/2} \Phi(I_m)\, dI_m \ . \tag{5}$$

Since each time that $I_s > I_m$ an error occurs, this magnitude is analogous to an error rate in optical communication systems. In fact, δ_1 gives an upper bound for the error rate because the main mode can recover during the evolution to the steady state and average power of the main-mode over a large enough time interval can be larger than that of the side mode. We will see in the following Section that for low modulation rates this is always the case [10]. The results for $Pr(I_s > I_m)$ show [7] that the side-mode excitation probability decreases with the relative net gain difference α_r and it increases with $A(C - C_{th})$. This dependence upon $A(C - C_{th})$ can be explained by noting that the side-mode gain at the laser switching time increases with this parameter [7].

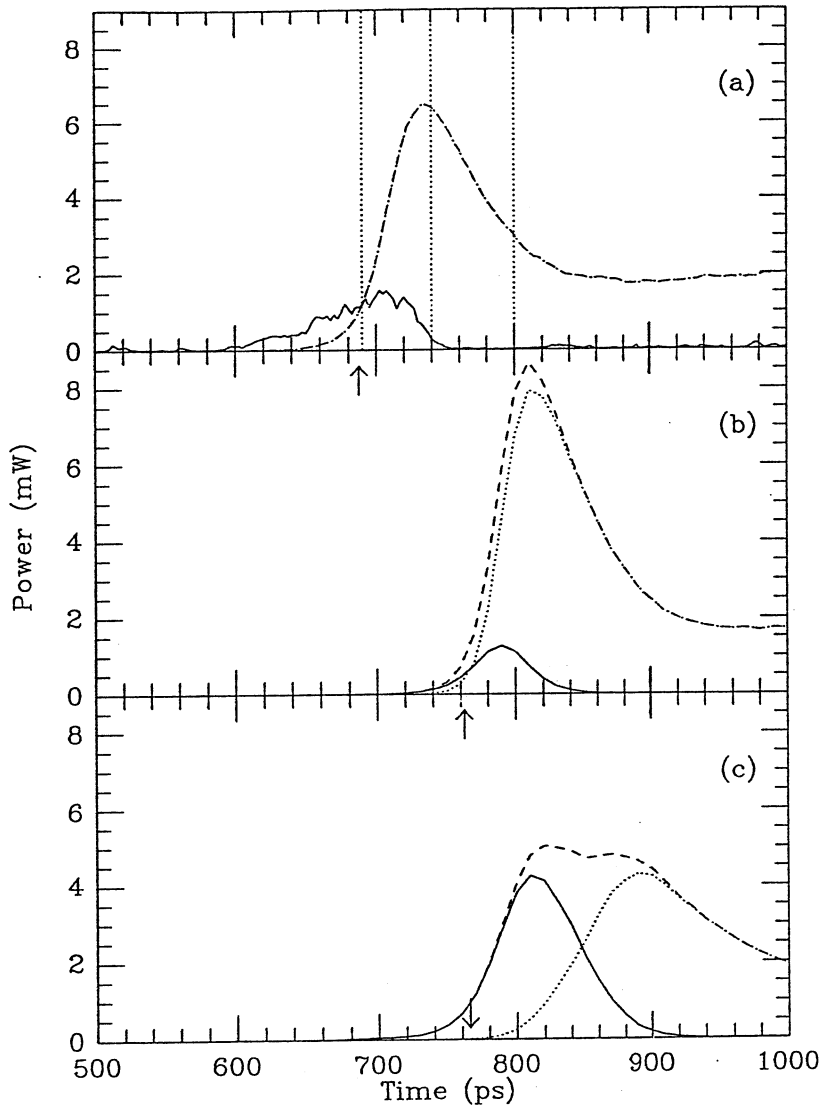

Fig. 1 Time traces showing the evolution of the power in three different turn–on events. We plot the power of the main mode (dotted line), the side mode (solid line) and the total power (dashed line). In Figure (a) we have plotted a normal turn–on event in which the power of the depressed mode has been increased in a factor of 100. Figures (b) and (c) contain two rare turn–on events. The turn–on times , $\bar{t}$, are indicated with arrows. The parameters corresponding to this figure are $\alpha_r = 14.9\%$ and $C = 1.5\, C_{th}$.

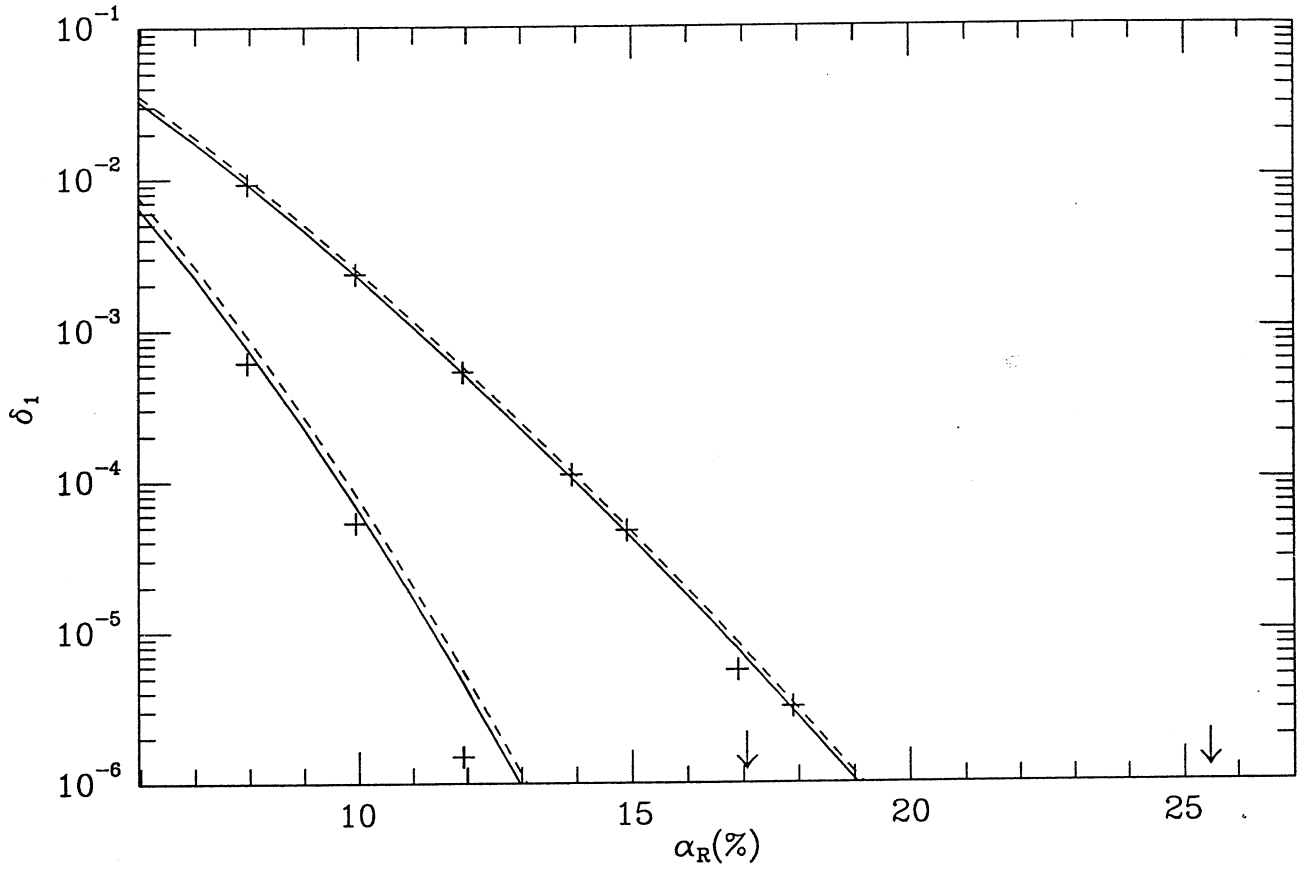

Fig. 2 δ_1 vs. the relative net gain difference, α_r, for two different injection currents: $C = 1.5\,C_{th}$ (upper figure) and $C = 1.2\,C_{th}$ (lower figure). Crosses, dashed line and solid line represent respectively the results of the simulation, linear theory and the approximate theory. The values of δ_1 in which $\delta_1 = 10^{-9}$ are indicated with arrows.

The bit error rate (BER) required in optical communication systems (usually smaller than 10^{-9}) leads to large values for the gain difference between the modes [6]. It turns out that the linear approximation is not accurate when the side mode is highly suppressed (α_r large and/or C close to C_{th}). In Fig. 2 we compare the results obtained for δ_1 from the linear theory [7] and the numerical simulations of eqs. (1)-(3) for several values of α_r and C. We note that no previous comparison between theory and simulation for δ_1 had been reported. It is clear that δ_1 decreases with the relative net gain difference and operating close to threshold. Probabilities as low as $10^{-5} - 10^{-6}$ can be obtained in our simulation. The number of turn-on events involved in the simulations is shown in table II. We consider a situation of repetitive gain-switching with an injection current that is suddenly (zero rise-time) switched from a value C_b below to a value C above the threshold current. The repetition frequency (400 MHz) is such that the laser reaches the steady state in the *on* and *off* states. We always consider a bias current $C_b = 0.85C_{th}$ sufficiently below threshold ($C_b/C_{th} < 0.95$) such that the results are independent of the value of C_b [9]. The results show that the linear theory overestimates the side-mode excitation probability. In this theory the modes are decoupled and the depletion of the side mode due to the main mode is not considered. However, for large SMSR and in a typical turn-on event, the photon density associated to the main mode I_m grows while I_s remain small. The growth of I_m contributes significantly to prevent the growth of I_s through saturation of the gain of the side mode.

In this chapter we improve the calculation of Ref. [7] by taking into account the gain saturation for the side mode due to the main mode. In this approximation the dynamics is described by the linear theory but with a gain saturation factor for the side mode in eq.

(3) that is approximated by $1 - I_m/\chi$:

$$\frac{dn}{dt} = C - \frac{n}{\tau_{sp}} \tag{6}$$

$$\frac{dI_i}{dt} = rn + G_i I_i + \sqrt{2rnI_i}\, F_i(t) \tag{7}$$

with

$$G_m = a(n - n_{th}),\ G_s = a(n - n_{th}) - \Delta g \frac{c}{n_g} - a(n - 2n_0)\frac{I_m}{\chi} \tag{8}$$

$$n_{th} = \tau_{sp} C_{th},\ \Delta g = (\alpha_s - \alpha_m),\ r = \frac{\gamma}{2\tau_{sp}},\ a = \frac{\eta A}{2}. \tag{9}$$

For large values of Δg the probability of a turn-on event in which I_s develops significantly is very low so that good accuracy is needed. We expect that the term proportional to I_m in G_s is important for a good description of the normal turn-on events and as a consequence it improves the determination of the probability of the different turn-on events.

The main mode is then described as in the linear theory, but the side mode is coupled to the main one. Replacing the solution of (6)

$$n(s) = C\tau_{sp}\left[1 - \exp(-\frac{s}{\tau_{sp}})\right] + C_b \tau_{sp} \exp(-\frac{s}{\tau_{sp}}) \tag{10}$$

in (7), $I_m(t)$ can be approximated [19] as the solution of the linear eq. (7) without spontaneous emission ($r = 0$) and with a random initial condition $I_m(t_{th})$ at the time t_{th} at which n crosses its threshold value n_{th}:

$$I_m(t) = I_m(t_{th}) \exp\left\{a\tau_{sp}(C - C_{th})\left[(t - t_{th}) - \tau_{sp}\left(1 - \exp\frac{-(t - t_{th})}{\tau_{sp}}\right)\right]\right\}. \tag{11}$$

The effective initial random condition $I_m(t_{th})$ is an exponentially distributed random variable with mean value

$$\langle I_m(t_{th})\rangle = \frac{\gamma}{4}\sqrt{\frac{\pi}{v}}\left\{C\left[1 + fer(\sqrt{v}t_{th})\right] +\right.$$

$$(C - C_{th}) \exp(\frac{1}{4v\tau_{sp}^2}) \left[fer(\frac{1}{2\sqrt{v}\tau_{sp}} - \sqrt{v}t_{th}) - 1 \right] \Big\}, \tag{12}$$

where $v = \frac{a}{2}(C - C_{th})$ and $fer(x)$ is the error function.

Using (11) in (7) it is easy to obtain the statistical properties of $I_s(t)$ conditioned to a value I_m of the main mode power at time t. The joint probability density $P(I_m, I_s, t)$ takes then the form

$$P(I_m, I_s, t) = \frac{e^{-I_m/<I_m(t)>}}{< I_m(t) >} \frac{e^{-I_s/<I_s(t)|I_m>}}{< I_s(t)|I_m >}, \tag{13}$$

where $\langle I_s(t) \mid I_m \rangle$ is the mean value of $I_s(t)$ conditioned to a value of I_m at time t:

$$\langle I_s(t) \mid I_m \rangle = \langle I_s(t_{th}) \rangle \exp\Big[\int_{t_{th}}^{t} ds\, G_s(s, I_m) \Big] + r \int_{t_{th}}^{t} ds\, n(s) \exp\Big[\int_{s}^{t} ds'\, G_s(s', I_m) \Big]. \tag{14}$$

In this expression $\langle I_s(t_{th}) \rangle$ can be obtained using the linear theory [7] since at times before $t = t_{th}$ the gain saturation factor is negligible, and $G_s(s, I_m)$ is given by

$$G_s(s, I_m) = a(n(s) - n_{th}) - \Delta g \frac{c}{n_g} - a(n(s) - 2n_0) \frac{I_m}{\chi} \times$$

$$\times \exp \left\{ a\tau_{sp}(C - C_{th}) \left[(s - t) + \tau_{sp} \left(\exp \frac{-(s - t_{th})}{\tau_{sp}} - \exp \frac{-(t - t_{th})}{\tau_{sp}} \right) \right] \right\}. \tag{15}$$

The PDF $\Phi(I_m)$ can be obtained in a similar way than for the linear theory by using the probability current [7], [14] associated with (6), (7), and the joint probability density (13),

$$\Phi(I_m) = \int_{t_{th}}^{\infty} dt \left\{ a(n(t) - n_{th}) I_T - [a(n(t) - 2n_0) \frac{I_m}{\chi} + \Delta g \frac{c}{n_g}](I_T - I_m) + \right.$$

$$\left. \frac{rn(t)(I_T - I_m)}{\langle I_s(t) \mid I_m \rangle} \right\} P(I_m, I_T - I_m, t). \tag{16}$$

This result reproduces the one of Ref. [7] in the formal limit $\chi \to \infty$.

Our result (16) for $\phi(I_m/I_T) = \Phi(I_m)I_T$ is compared in Fig. 3 with the linear approximation ($\chi \to \infty$) and with direct numerical simulations of eqs (1)-(3). As a general conclusion we see that (16) provides a good description of the simulation and that the correction due to gain saturation of the side mode becomes more important the smaller is the injection current and the larger is the SMSR, that is in the situations in which the probability of a rare event is smaller. The inclusion of gain saturation lowers the probability ϕ except for values of I_m very close to I_T. Due to the normalization of ϕ the two curves in Fig. 3 for the two approximations cross at a value very close to I_T. For very rare events such that I_m is nearly zero at the laser switch on both theories coincide. Since I_m is very small in this case the effect of the gain saturation due to the main mode is negligible. For rare events ($I_m < I_s$, i.e., $I_m/I_T < 0.5$, but I_m not zero) $\phi(I_m/I_T)$ is always smaller in our theory than in the linear one due to the gain saturation factor. Then, the results obtained for δ_1 are closer to the numerical simulation results than the ones derived from the linear theory (see Fig. 2). However, as in the linear theory, our theory still overestimates the side-mode excitation probability when the injection current C is small and the side mode is highly suppressed. In this case the carrier depletion must be taken into account to obtain a better description of the switching process. When C increases the overshoot of the carrier density is larger and our theory gives better estimates for δ_1. A precise comparison of the results of simulation, the linear theory and our result (16) is given in Table II. The improvement upon linear theory by the consideration of gain saturation can be as large as 25% and it is more important the smaller is C.

The statistics for small (I_m/I_T) is very poor for the extreme value of the relative net gain difference considered (49.7%) for which no rare events have been recorded. However, the overall good agrement with the simulation gives confidence in the use of (16)

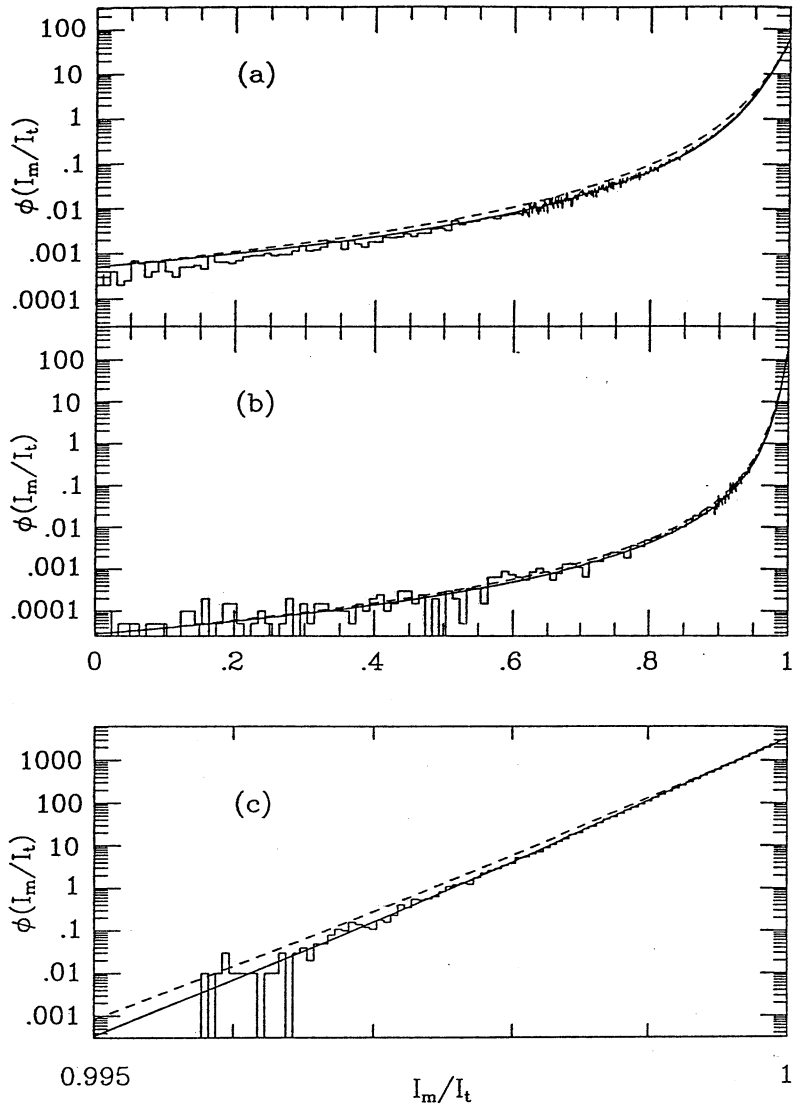

Figure 3 Probability density function, $\phi(\frac{I_m}{I_T})$, calculated from simulation (histogram), linear theory (dashed line) and the aproximate theory (solid line). Figure (a) corresponds to $C = 1.2\,C_{th}$ and $\alpha_r = 7.9\%$; Figure (b) to $C = 1.5\,C_{th}$ and $\alpha_r = 14.9\%$ and Figure (c) to $C = 1.5\,C_{th}$ and $\alpha_r = 49.7\%$. The number of turn–on events in the three figures is 2×10^6.

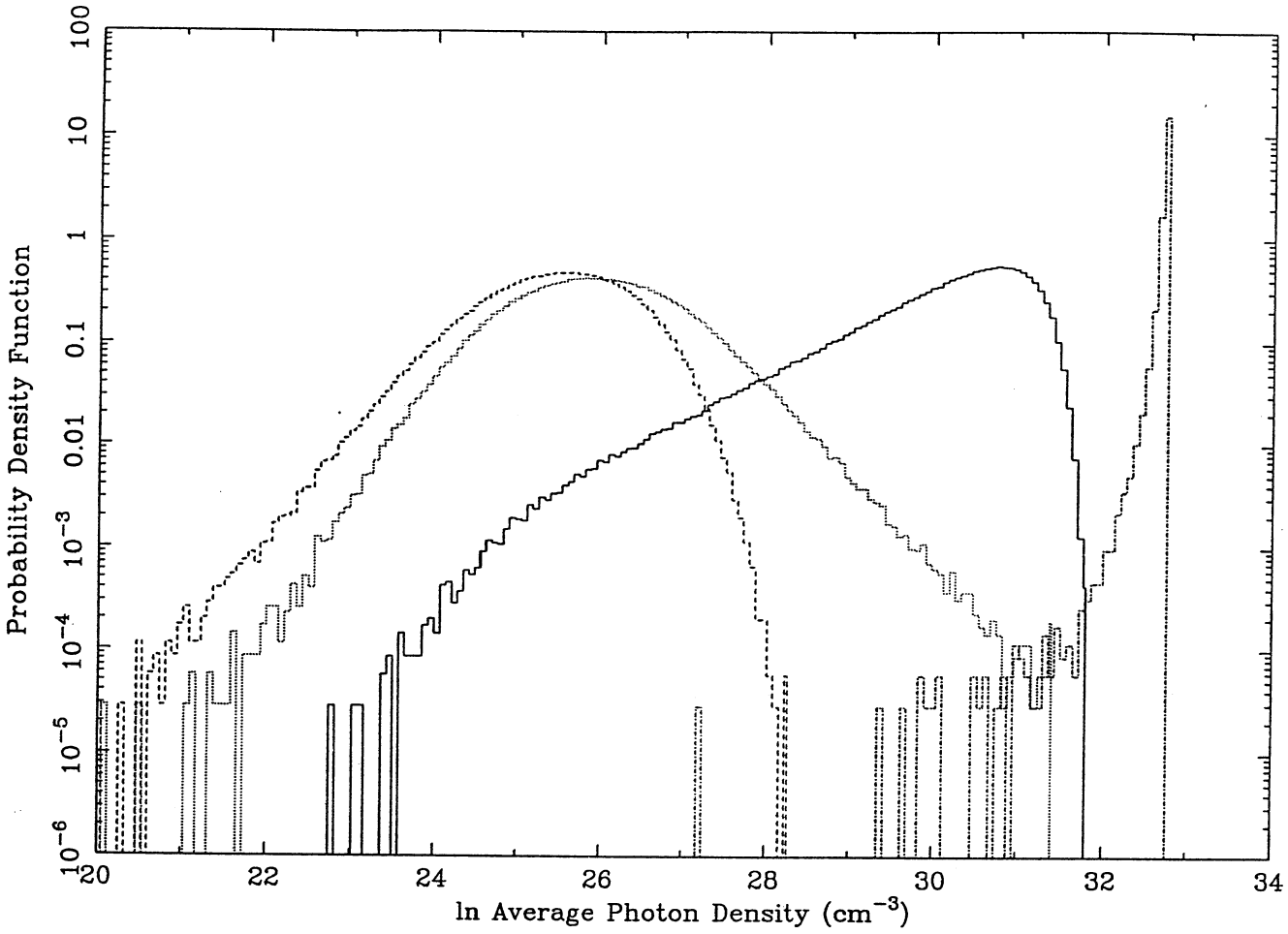

Fig. 4 PDF of the average photon density of the main mode and side mode for two different integration intervals T. The parameters are taken as: $\alpha_r = 14.9\%$ and $C = 1.5\,C_{th}$. The solid line (main mode) and the dashed line (side mode) correspond to an average performed until the time 0.69 ns. The dash-dotted line (main mode) and the dotted line (side mode) correspond to an average performed until the time 0.8 ns.

to determine events with very low probability. Our theoretical results predicts that to have a probability lower than 10^{-9} the SMSR has to be larger than 31.7 dB, 37.4 dB for $C = 1.2,\ 1.5\,C_{th}$ respectively. These values correspond to relative net gain differences given by $\alpha_r = 17\%$ and $\alpha_r = 25.5\%$, respectively. Given the simulation results it is expected that these values of SMSR are a safe upper bound since consistently our theoretical result yields a slightly larger value than the simulation.

7.3 Statistics for the average photon densities

Mode-partition effects have been analyzed in the previous Section using the probability δ_1 that the main mode is smaller than the side mode at the turn-on time. However, as we have noticed in Sect. 2, the main mode can recover during the pulse interval and the average of the photon density carried by the main-mode over the duration of the pulse can be larger than that of the side mode. Then, to have a complete description of power partition during the transient, we must follow the evolution until the steady state is reached. In the following we focus on the characterization of pulses by the mean photon densities (4). We first analyze the statistics for the average of the main and side mode photon densities for different values of T. In this way it is possible to determine whether the mode evolution in time is essentially deterministic or dominated by spontaneous-emission noise. Second, we study in detail the photon densities averaged during the whole pulse emission for the rare events such that at the turn-on time I_m is smaller than I_s.

Since we are interested in photon densities emitted above a noise level, $I_{s,m}(t)$ in (4) have to be understood as being above a threshold value that we take $I_0 = 8 \times 10^{-4} mW$. Whenever $I_{s,m}(t) < I_0$ it has to be replaced by $I_{s,m}(t) = 0$ in (4). When the side mode is

not highly suppressed (α_r small and/or C large) the PDF for the average photon densities during a time interval T change with T. Results for $P_T(W_s)$ and $P_T(W_T)$, the probability densities of the mean side and total power respectively, obtained from numerical simulation for an intermediate relative net-gain difference 14.9% and two different integration times, 0.69 ns and 0.8 ns, are shown in Fig.4. The PDF for the side mode has a tail that extends to larger values when T increases. In this case the evolution is not dominated by spontaneous-emission noise and most of the side mode pulses are not noisy and carry significant output power. When T is large enough to include all the relaxation oscillations, the PDF does not change anymore. As concerns the main mode, the PDF for the average photon density over T becomes a sharp distribution peaked around its maximum value when T increases. An important point to notice in Fig. 4 is that there exist some events where the average photon density of the secondary mode is larger than the one of the main mode, even when we consider times large enough to include the relaxation oscillations for most of the realizations. These events are associated with a delay in the switching of the main mode, which reaches its maximum later than most of the realizations. For large values of α_r(49.7 %) we have checked that the PDF for the side mode remains unchanged when T increases. In this case the side mode evolution is mainly due the spontaneous-emission noise.

We next consider the statistics for the average photon densities of the main mode, W_m, and side mode, W_s, over a time interval large enough to include all the relaxation oscillations for all the events. In this case the average total photon density $W_T = W_m + W_s$ is found to be a constant for all the realizations (see Fig. 5). This result indicates that the depletion of the carrier number is profited by the two modes in a different partition in each turn-on event but keeping W_T constant. We have checked this result (also obtained by Marcuse [10]) for different values of α_r and C. We also find that W_m is always larger

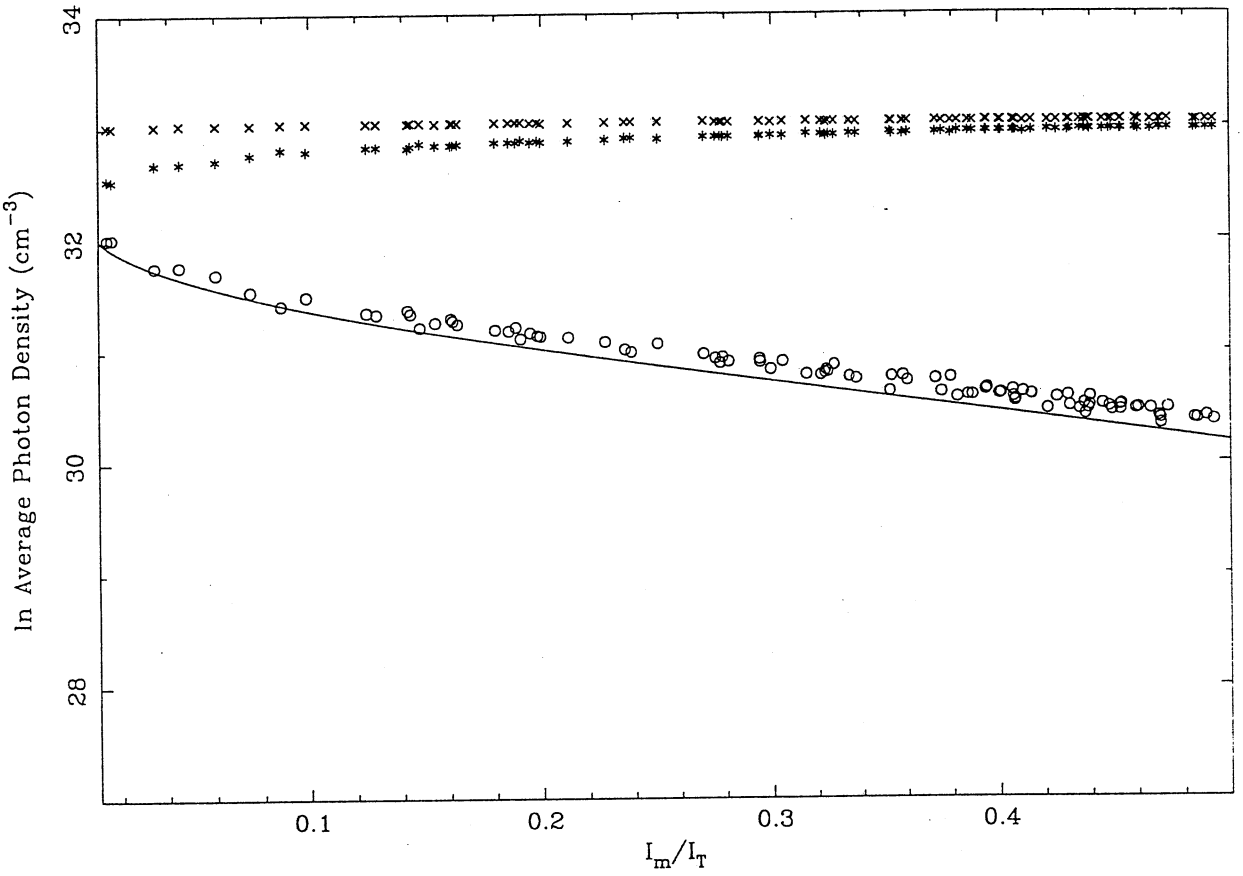

Fig. 5 Natural logarithm of the average photon density vs. I_m/I_T for $\alpha_r = 14.9\%$ and $C = 1.5\,C_{th}$. The average is performed until the time 1 ns. The total, main and side mode average photon densities are represented by crosses, stars and circles, respectively. Each symbol represents a realization of equations (1)-(4). We also plot the results of our analytical approximation for the side mode average photon density.

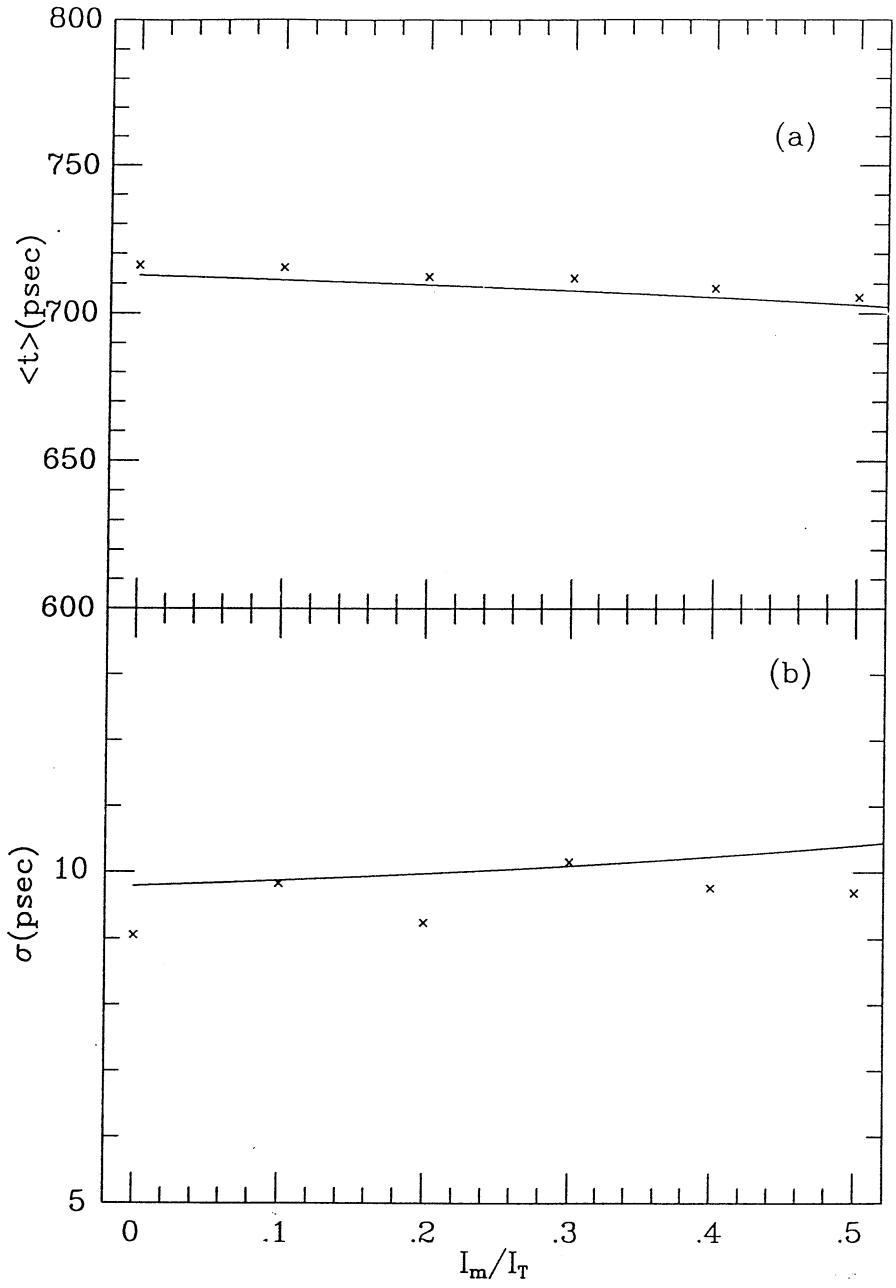

Fig. 6 Mean value (a) and variance (b) of the turn–on time, conditionated by crossing the threshold with a value I_m of the main mode power. The parameters are the same that in Fig. 1.

than W_s even for rare events such that I_m is smaller than I_s at the switch-on time. Since the side-mode suppression ratio in the steady state is very large, the main mode always recovers during the evolution to the steady state [10]. This result might be changed if the laser is modulated at high rates [6]. Finally, a linear relation is seen in Fig. 5 for rare events ($I_m < I_s$) between the logarithm of W_s and the main mode photon density at the turn-on time I_m. These relation does not hold only for very rare events when I_m/I_s is close to zero.

From now on we fix a value of $T = 1$ nsec for which W_T is constant. An alternative measure to (5) of errors associated with rare events is given by the probability that the mean power associated with the side mode is larger than a given fraction of the mean total power.

$$\delta_2 = \int_a^1 P_T(\frac{W_s}{W_T}) d(\frac{W_s}{dW_T}), \tag{17}$$

where $P_T(W_s/W_T)$ as defined in Section 2 is given by $P_T(W_s/W_T) = P_T(W_s)W_T$. The lower limit of integration is fixed to 1/10. For this value of a the two magnitudes δ_1, δ_2 that measure the errors due to rare events are of the same order.

The probability of the average side mode photon density and then the error δ_2 can be obtained from the statistics of the power partition at the turn-on time $\phi(I_m/I_T)$ using the following method. For a rare event the side mode develops a pulse (see Fig. 1). Then the evolution of the main and side modes after the turn-on time is deterministic. This evolution can be obtained by integrating numerically the eqs. (1)-(3) without noise. The initial time for this integration is given by the turn-on time $\bar{t}(I_m)$ at which the main mode power is I_m and the side mode is $I_s = I_T - I_m$. Since the carrier depletion can be neglected during the regime of amplification until the turn-on time, the initial condition

for the carrier density is given by its value at $\bar{t}(I_m)$ obtained from eq. (10). The turn-on time probability density $P(\bar{t} \mid I_m)$ can be obtained by neglecting also the gain saturation ($\chi = \infty$) in eq. (3). Using the probability current associated to eqs. (1), (2) with $\chi = \infty$ and eq. (3) the following expression is obtained [7]

$$P(\bar{t} \mid I_m) = \frac{1}{\Phi(I_m)} \frac{1}{m_1(t)m_2(t)} \left[\frac{\dot{m}_1(t)}{m_1(t)} I_m + \frac{\dot{m}_2(t)}{m_2(t)}(I_T - I_m)\right] \exp\left[-\frac{I_m}{m_1(t)} - \frac{I_T - I_m}{m_2(t)}\right], \tag{18}$$

where the dots stand for time derivatives and $m_i(t)$ ($i = 1,2$) are the mean values of the main and side mode intensities, respectively. These mean values can be obtained from the linear eqs. (1)-(3) with $\chi = \infty$ and from eq. (10) (see Ref. [7]). The mean turn-on time $\langle \bar{t} \mid I_m \rangle$ and its jitter can be calculated by using eq. (18). The theoretical results agree with the simulation results (see Fig. 6). However, due to the fact that carrier depletion is neglected, the mean turn-on time obtained from (18) is smaller than the simulation result.

Since the jitter of $\bar{t}(I_m)$ is very small (see Fig. 6), a relation between (I_m/I_T) and (W_s/W_T) can be found by integrating numerically the deterministic version of eqs. (1)-(3) with the initial conditions I_m and $I_s = I_T - I_m$ for the main and side modes respectively at a time $t = \langle \bar{t} \mid I_m \rangle$. The results of this method shown in Fig. 5 reproduces well the relation found from the simulation including the deviation from the linear relation when $(I_m/I_T) \to 0$. However, our theoretical result yields slightly smaller values for W_s/W_T than the simulation. This result is due to the smaller value of the turn-on time given by the theory (see Fig. 6). Then the main mode has more time to recover during the evolution to the steady state and the mean side mode power is smaller.

Theoretical and simulation results for δ_2 for different values of relative net gain difference and different values of the injection current are given in Fig. 7. We find that like δ_1

the error given by δ_2 decreases with α_r and operating close to threshold. The agreement between theory and simulation is better the larger is the injection current. Again this is due to the fact that the analytical result for $\phi(I_m/I_T)$ is more accurate when the injection current increases. Our theory predicts that to have an error δ_2 smaller than 10^{-9} the SMSR has to be larger than $37.15dB$ for $C = 1.5\,C_{th}$. This value is close to the one found by using the first characterization of rare events in terms of δ_1.

Finally, we show that the relation $W_s(I_m/I_T)$ obtained integrating numerically the deterministic rate equations can be derived in an analytic way. Our numerical simulations indicate that the following linear relation holds in the region of interest

$$\ln \frac{W_s}{W_T} = \alpha \frac{I_m}{I_T} + \beta, \qquad \frac{I_m}{I_T} < 0.5 \tag{19}$$

Since $\alpha < 0$ the side-mode mean photon density is a decreasing function of the value of I_m at the switching. Evidence of this relation is given in Fig. 5. Deviations from this linear relation are observed only when I_m/I_T is very close to zero. The number of turn-on events considered has to be large enough to have enough data points to establish (19). The number of rare events recorded can be read from the table II. In any case we have between 4610 events and 3 events for the worst case considered of $\alpha_r = 11.9\%$ and $C = 1.2\,C_{th}$. Table III contain the values of α and β obtained from our simulations. We find that for $C = 1.5C_{th}$ α is constant and the slope is given by the linear relation $\beta = -0.0733\alpha_r - 1665$ with a regression coefficient 0.997.

The origin of the relation (19) for rare events and the constant value of the slope α can be understood in the following way. When $I_m < I_s$ at the laser switch on time (rare events) the side mode evolution is not dominated by spontaneous emission noise. Using

the deterministic evolution (eq. (2) with $\gamma = 0$) the following relation can be derived

$$\frac{I_m(t)}{I_s(t)} = \frac{I_m(t_{on})}{I_s(t_{on})} \exp[\Delta G(t - t_{on})], \tag{20}$$

where t_{on} is the turn-on time and $\Delta G = c\Delta\alpha/n_g$. Then the average side-mode photon density (4) is given by

$$W_s = \frac{1}{T}\int_{t_{on}}^{T} \frac{I(t)}{1 + u\exp[\Delta G(t - t_{on})]}\, dt \tag{21}$$

where $u = I_m(t_{on})/I_s(t_{on})$, I is the total photon density and we have neglected the contribution to W_s due to times $t < t_{on}$. Since the average total photon density is independent of u, we can assume that $I(t)$ is nearly independent of u. For rare events such that $(I_T/I_m)\exp[-\Delta G(T - t_{on})] \ll 1$ (that is I_m/I_T not very close to zero) we obtain from (21) the relation $\ln(W_s/W_T) = \ln[-\ln(I_m/I_T)] + b$ where b is a constant. When I_m/I_T varies from 0.1 to 0.5 this relation can be well approximated by a linear relation and a good approximation for α can be obtained by calculating the slope of $\ln(-\ln[I_m/I_T])$ at an intermediate point such as $I_m/I_T = 0.3$. This explains the constant value obtained from the simulations for the slope α. From the previous derivation it is clear that the following relation also holds: $(W_s/W_T) = -[I/(W_T T\Delta G)]\ln(I_m/I_T)$. Since no linear approximation is required to derive this relation, its validity region includes values of I_m/I_T closer to zero than those corresponding to the relation (19). However, the slope of this linear relation changes with ΔG. Evidence of this relation is given in Fig. 8 for different relative net gain differences and injection currents.

The importance of the relation (19) is that the two proposed characterizations of the statistics of rare events, based on the probabilities $P_T(W_s/W_T)$ and $\phi(I_m/I_T)$, are related in a simple way for the range of their variables associated with rare events. To give evidence

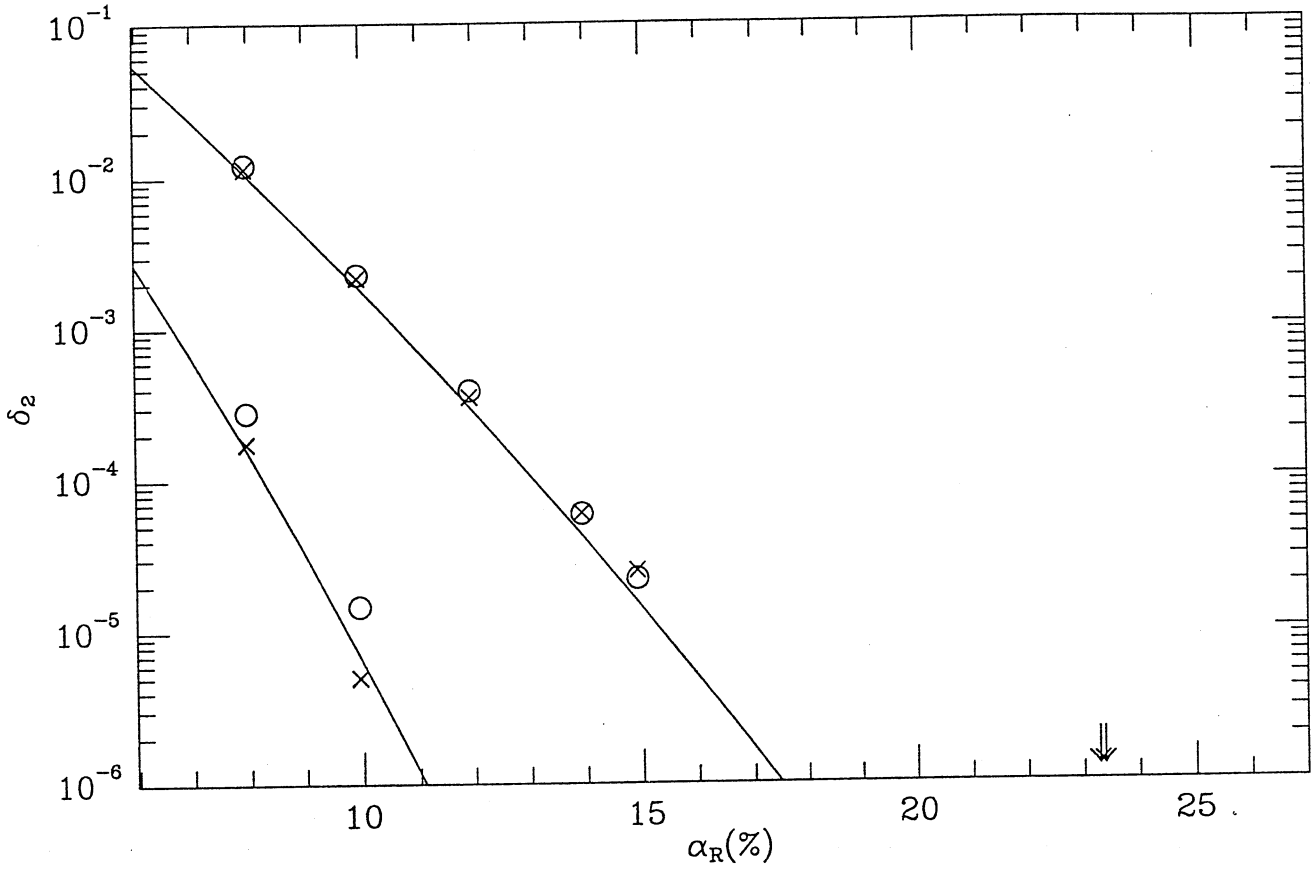

Figure 7 δ_2 vs. α_r for two different injection currents: $C = 1.5\,C_{th}$ (upper figure) and $C = 1.2\,C_{th}$ (lower figure). Crosses, circles and solid line represent respectively the results of the simulation, the fit, and the approximate theory. We indicate with arrows the values of α_r such that $\delta_2 = 10^{-9}$ for $C = 1.5C_{th}$. The left arrow corresponds to the approximate theory and the right arrow to the fit of the simulation results.

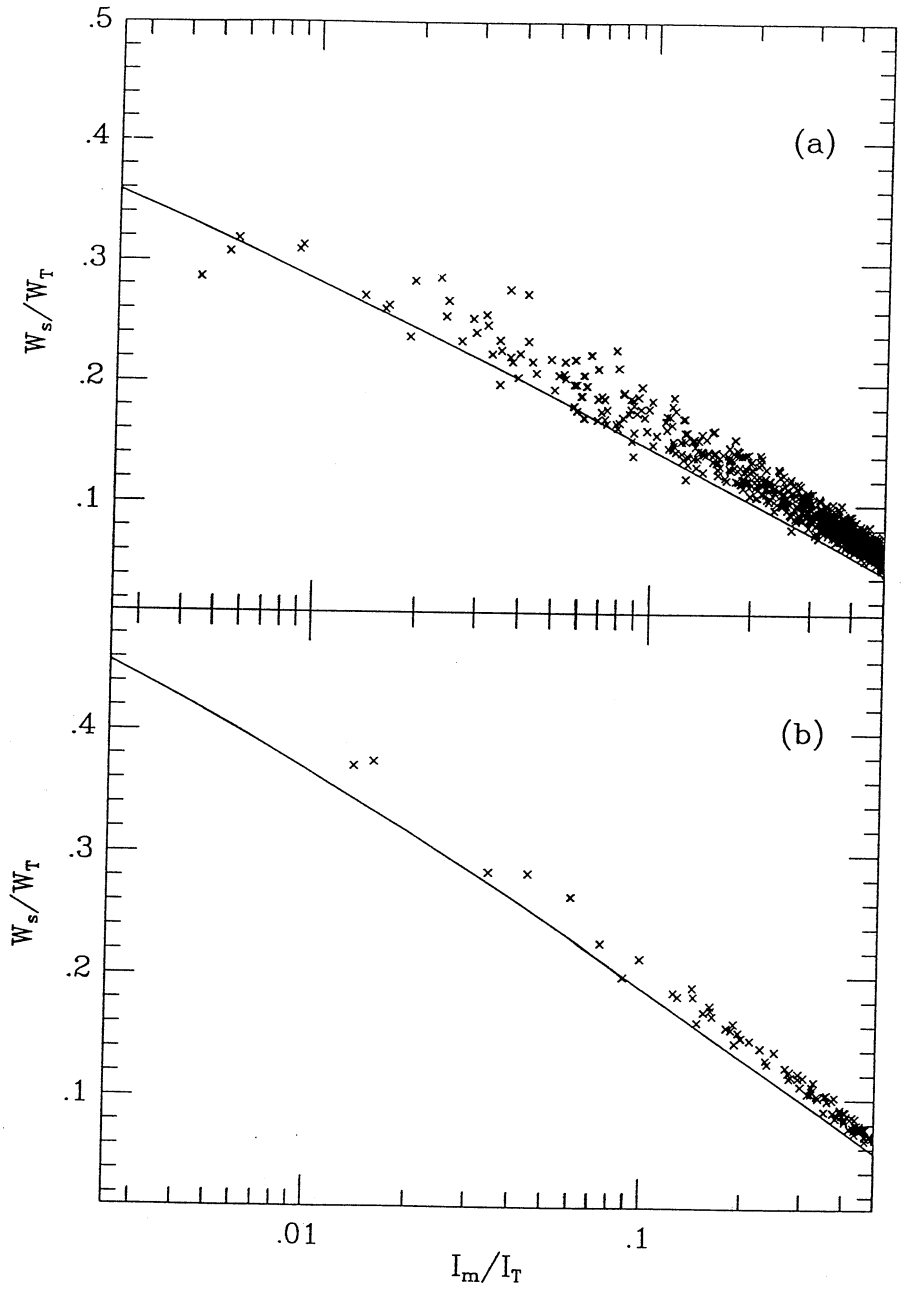

Fig. 8 $\frac{W_s}{W_T}$ **vs. the fraction of power of the main mode at the turn–on time,** $\frac{I_m}{I_T}$**. Each symbol represents the result of one turn–on event. In Fig. (a) the parameters are** $C = 1.2C_{th}$ **and** $\alpha_R = 7.9\%$ **with an average time of 2 ns. In Fig. (b) the average time is 1 ns,** $C = 1.5C_{th}$ **and** $\alpha_R = 14.9\%$**.**

Each symbol represents a realization of equations (1)-(4). We also plot the results of our analytical approximation for the side mode average photon density.

of this fact we compare in Fig. 7 the values of δ_2 obtained from (19) and direct numerical simulation to obtain $P_T(W_s/W_T)$, with the values obtained determining $P_T(W_s/W_T)$ from our analytical result for $\phi(I_m/I_T)$ (see eq. (16)) through (19):

$$P_T(\frac{W_s}{W_T}) = \frac{W_T}{\alpha W_s}\phi\Big(\frac{\ln \frac{W_s}{W_T} - \beta}{\alpha}\Big). \tag{23}$$

The agreement between the two values is better the larger is the injection current. This is related to the fact that the analytical result for ϕ provides a better description of the simulation when the injection current increases. Using the relation (23), the analytical result for ϕ and the linear relation for β obtained from numerical simulations, it is found that the required value of α_R (and then of the SMSR) to have δ_2 smaller than 10^{-9} is very close to the one found above by integrating numerically the deterministic rate equations (see Fig. 7).

7.4 Conclusions

We have studied in this paper analytically and numerically the transient statistics of the density of photons in the main and side modes for nearly single-mode semiconductor lasers biased below threshold. The dynamics of the laser is modelled using noise driven rate equations. Mode-partition noise effects are analyzed in two different but related ways. We first consider the output power at the turn-on time. We improve the calculation of Ref. [7] based on the linear approximation by including the effect of gain saturation of the depressed mode due to the growth of the main mode. Using numerical simulations it is shown that going beyond the linear aproximation is necessary when the side mode is highly supressed. A quantitative measure of errors associated with rare events is given by the probability δ_1 that the side mode has a larger photon density than the main mode

at the turn-on time. The SMSR required to have δ_1 smaller than 10^{-9} is calculated for different operational points of the laser.

Our second characterization is in terms of the mean output power during the duration of the optical pulse. The first characterization involves heavily the role of spontaneous emission noise triggering the turn-on of the laser in a regime of linear amplification, while the second characterization involves the whole nonlinear dynamics of optical pulse emission. The mean total photon density is found to be constant for different turn-on events when the time average is taken over $T = 1$ nsec, which includes the whole duration of the pulse. We calculate analytically and numerically the probability that the side mode carries a fraction of the total mean output power. Our main result is to show that both characterizations are directly connected. For the rare events a linear relation between the logarithm of the mean output power of the side mode and the output power of the main mode at the turn-on time is found. Given this relation the probability δ_2 for a contribution of the second mode larger than 10 % of the mean total output power is obtained as a simple transformation of the output power statistics at the turn-on time. Finally, the SMSR required to have δ_2 smaller than 10^{-9} is calculated.

REFERENCES

[1] M. M. Choy, P. L. Liu, and S. Sasaki, "Origin of modulation- induced mode partition and Gb /s system performance of highly single mode 1.5μm distributed feedback lasers", Appl. Phys. Lett., vol. 52, pp. 1762–1764, 1988.

[2] S. Sasaki, M. M. Choy, and N. K. Cheung, "Effects of dynamic spectral behavior and mode-partitioning of 1550 nm distributed feedback lasers on Gbit/s transmission signals", Electron. Lett. vol. 24, pp. 26–28, 1988.

[3] P. L. Liu and M. M. Choy, "Modelling rare turn-on events of injection lasers", IEEE J. Quantum Electron., vol. 25, pp. 1767–1770, 1989.

[4] P. L. Liu and M. M. Choy, "Effect of bias on transient mode partition-An analysis based on photon statistics", IEEE J. Quantum Electron., vol. 25, pp. 854–857, 1989.

[5] S. E. Miller, "On the injection laser contribution to mode partition noise in fiber telecommunication systems", IEEE J. Quantum Electron., vol. 25, pp. 1771–1781, 1989.

[6] S. E. Miller, "On the prediction of the mode partitioning floor in injection lasers with multiple side modes at 2 and 10 Gb/s", IEEE J. Quantum Electron., vol. 26, pp. 242–249, 1990.

[7] A. Mecozzi, A. Sapia, P. Spano, and G. P. Agrawal, "Transient multimode dynamics in nearly single-mode lasers", IEEE J. Quantum Electron., vol. 27, pp. 332–343, 1991.

[8] J. C. Cartledge, "On the probability of side mode fluctuations in pulse modulated nearly single-mode semiconductor lasers", IEEE J. Quantum Electron., vol. 26, pp. 2046–2051, 1990.

[9] P. Spano, A. Mecozzi, A. Sapia and A. D'Ottavi, "Noise and transient dynamics in

semiconductor lasers", in *Nonlinear Dynamics and Quantum Phenomena in Optical Systems*, ed. by R. Vilaseca and R. Corbalán. Berlin: Springer Verlag, 1992.

[10] D. Marcuse, "Computer simulation of laser photon fluctuations: DFB laser", IEEE J. Quantum Electron., vol. 21, pp. 161-167, 1985.

[11] T. B. Anderson and B. Clarke, IEEE J. Quantum. Electron **QE29**, 3 (1993).

[12] S. E. Miller and D. Marcuse, "On fluctuations and transients in injection lasers", IEEE J. Quantum Electron., vol. 20, pp. 1032-1044, 1984.

[13] G. P. Agrawal and N. K. Dutta, "Long wavelength semiconductor lasers", New York: Van Nostrand Reinhold, 1986.

[14] D. Marcuse, "Computer model of an injection laser amplifier", IEEE J. Quantum Electron., vol. 19, pp. 63-73, 1983.

[15] C. W. Gardiner, "Handbook of stochastic methods". Berlin: Springer-Verlag, 1983.

[16] K. Uomi, H. Nakano and N. Chinone, "Ultrahigh-speed 155 μm $\lambda/4$–shifted DFB PIQ-BH lasers with bandwidth of 17 GHz", Electron. Lett., vol. 25, pp. 668-669, 1989.

[17] K. Uomi, S. Sasaki, T. Tsuchiya, M. Okai and N. Chinone, "Spectral linewidth reduction by low spatial hole burning in 1.5 μm multi-quantum-well $\lambda/4$-shifted DFB lasers", Electron. Lett., vol. 26, pp. 52-53, 1990.

[18] L. D. Westbrook, I. D. Henning, A. W. Nelson and P. J. Fiddyment, "Spectral properties of strongly coupled 1.5μm DFB laser diodes", IEEE J. Quantum Electron., vol. 21, pp. 512-518, 1985.

[19] S. Balle, P. Colet and M. San Miguel, "Statistics of transient response of a single-mode semiconductor laser gain switching", Phys. Rev. A, vol. 43, pp. 498–506, 1991; S. Balle, N.B. Abraham, P. Colet and M. San Miguel, "Parametric dependence

of stochastic frequency variations in the gain-switching of a single-mode laser diode", IEEE J. Quantum Electron., vol. 29, pp. 33-41, 1993.

TABLE I

PARAMETER	VALUE	MEANING
η	0.5	mode confinement factor
D	0.5	line shape factor
τ_{sp}	2 ns	spontaneous lifetime
n_g	4	group index
γ	2.2×10^{-5}	fraction of spontaneous emission coupled into the mode
A	$5.62 \times 10^{-6} cm^3 s^{-1}$	differential gain
n_0	$6.8 \times 10^{17} cm^{-3}$	carrier density at transparency
α_m	$50.3 cm^{-1}$	loss of the main mode
c	$3 \times 10^{10} cms^{-1}$	speed of the light in vacuum
χ	$20\, I_{st}$	saturation photon density

Meanings and values of the parameters in Eqs. (1)-(3).

TABLE II

$\alpha_R\%$	SIMULATION	THEORY	LINEAR THEORY	TURN–ON EVENTS
7.9	6.17×10^{-4}	7.68×10^{-4}	9.18×10^{-4}	2×10^{6}
9.9	5.30×10^{-5}	6.90×10^{-5}	8.28×10^{-5}	2×10^{6}
11.9	1.5×10^{-6}	4.66×10^{-6}	5.61×10^{-6}	2×10^{6}
7.9	9.22×10^{-3}	9.30×10^{-3}	1.02×10^{-2}	5×10^{5}
9.9	2.34×10^{-3}	2.33×10^{-3}	2.56×10^{-3}	5×10^{5}
11.9	5.26×10^{-4}	5.22×10^{-4}	5.74×10^{-4}	5×10^{5}
13.9	1.10×10^{-4}	1.05×10^{-4}	1.16×10^{-4}	5×10^{5}
14.9	4.70×10^{-5}	4.51×10^{-5}	4.98×10^{-5}	2×10^{6}
16.9	5.60×10^{-6}	7.69×10^{-6}	8.53×10^{-6}	2.5×10^{6}
17.9	3.20×10^{-6}	3.04×10^{-6}	3.39×10^{-6}	2.5×10^{6}

$P(I_s > I_m)$ versus relative net gain difference. The first set of values correspond to $C = 1.2C_{th}$ and the second one to $C = 1.5C_{th}$. We also indicate the number of turn–on events in each simulation.

TABLE III

$\alpha_R\%$	α	β
7.9	-2.70	-1.51
9.9	-2.58	-1.72
7.9	-2.92	-0.73
9.9	-2.93	-0.90
11.9	-2.91	-1.06
13.9	-2.93	-1.19
14.9	-2.98	-1.24

Values of the parameters α and β for different relative net gain differences. The first set of values correspond to $C = 1.2C_{th}$ and the second one to $C = 1.5C_{th}$.

Chapter 8

Pseudorandom Word Modulation of Nearly Single-Mode Semiconductor Lasers

8.1 Introduction

Mode partition noise (MPN) can severely affect the performance of optical communication systems, even when using DFB lasers, yielding a large Bit Error Rate (BER) [1]-[9]. This occurs because different modes are dispersed in the optical fibre. An important magnitude to characterize BER due to MPN is the Side Mode Suppression Ratio (SMSR). Even though SMSR larger than 30 dB has been measured at stationary conditions in DFB lasers, spontaneous emission noise can trigger the laser to oscillate in a side mode under intensity modulation conditions [8], [9].

Monte Carlo simulations of the Langevin rate equations has been recently done [1], [4]-[7] in order to understand the effect of MPN on the BER. Despite of the progress on computer simulations, we are far from the possibility of simulating 10^{11}-10^{12} bits in order to predict BER's smaller than 10^{-9} as required for optical communication systems. This fact makes necessary to develop analytical approximations to understand how the various laser parameters influence on the BER. Some analytical studies on transients in nearly single-mode lasers have been reported in refs. [2], [3], [6]. More recently, two analytical and similar approaches have been carried out for repetitive gain-switching [1] and intensity modulation [7] of nearly single-mode lasers. The main difference between both approaches is that the one of ref. [7] considers two different methods: one for high probably events and the other for rare events. This is so because the time the laser is in the "on" state (t_{on}) used in ref. [7] is large enough for the pulse to develop relaxation oscillations. If we take $t_{on} \sim 90\,ps$, very close to the

pulse emission time, the pulse has not time enough to develope relaxation oscillations and consequently it is not necessary to distinguish between the two different regimes.

In this chapter we calculate, following the analytical approach developed in ref. [1], upper and lower bounds of the SMSR required for a BER = 10^{-9} under pseudorandom word modulation of the injection current, BER_{PR}, in the Intensity Modulation / Direct Detection Return to Zero scheme. The results are tested by an extensive numerical simulation of the noise-driven rate equations over 2×10^6 pseudorandom input bits. We count an error when the averaged side mode power W_s during a bit "1" pulse is larger than the one of the main mode W_m. The bounds of the BER are obtained by using periodic modulation of the injection current BER_P (...1111...) and repetitive gain-switching BER_{GS} (...0001...). The main idea is that errors are associated with large turn-on times [1]-[7]. For $t_{on} = 90ps$ and modulation frequencies up to 6 GHz the turn-on time depends mainly on the initial condition for the carriers $n(0)$. When the laser is biased above threshold $n(0)$ is smaller for the periodic regime than the for the repetitive gain-switching regime, leading the former to a larger turn-on time. Therefore BER_P (BER_{GS}) is an upper (lower) bound of the BER_{PR}. The contrary happens for a bias current below threshold.

An important feature that appears from the simulations is the presence of multimodal distribution functions of the turn-on time and the mean output power, when the laser is pseudorandomly modulated with a bias current above threshold. This multimodal distributions yield non-desirable pattern effects at the output. These pattern effects can be represented as superposition of different periodic sequences of input bits [10]. On the other hand, a bias current slightly below threshold avoids pattern-effects at the output. This means that this special bias current makes the response of the laser to a bit "1" independent of the previous input bits. We find that by biasing slightly below threshold the BER is independent on the modulation

frequency and it is the same in the periodic, gain-switching and pseudorandom word modulation regimes. This behaviour is very similar to the one observed for single-mode semiconductor lasers [10]-[12].

The chapter is organized as follows. In section 8.2 we describe the rate equations and the theoretical model. In section 8.3 we present the results of the calculations and its comparison with numerical simulations.

8.2 Rate Equations and Theoretical Model

The dynamics of a nearly single-mode DFB laser can be modeled by the noise driven rate equations for the density of minority carriers n and for the density of photons in the cavity modes I_i, $i = m$ (main mode), s (side mode) [13]:

$$\frac{dn}{dt} = C(t) - \frac{n}{\tau_{sp}} - \frac{c}{\eta n_g} \sum_{i=s,m} g I_i \tag{1}$$

$$\frac{dI_i}{dt} = \frac{c}{n_g}(g - \alpha_i) I_i + \frac{\gamma}{\tau_{sp}} Dn + \sqrt{\frac{2\gamma}{\tau_{sp}} D I_i n}\, F_i(t) \quad i = s, m \tag{2}$$

with

$$g = \frac{\eta n_g A(Dn - n_0)}{c(1 + s(I_S + I_m))}. \tag{3}$$

The meaning of the symbols and typical values of the different parameters involved in these equations are listed in Table I. The total output power of the laser is proportional to $I_T = I_s + I_m$ with a proportionality factor of the order of $4 \times 10^{-15}\, mW\, cm^3$. The random spontaneous-emission process is modeled by uncorrelated Gaussian white noise terms $F_i(t)$ of zero mean and correlation $\langle F_i(t) F_j(t') \rangle = \delta_{ij} \delta(t - t')$. We neglect the effect of the radiative and non-radiative carrier generation and recombination

noise in the rate equation for $n(t)$ since it is negligible in comparison with the fluctuations induced by $F_i(t)$ during the transient, as they are amplified by the stimulated-emission process. The stochastic differential equations (1) and (2) are defined in the Ito sense [14].

According to eq. (1) and (2), the laser threshold is given by:

$$C_{th} = \frac{2}{\tau_{sp}} \left(\frac{\alpha_m c}{A \eta n_g} + n_0 \right) \tag{4}$$

and the value of the carrier density at threshold is $n_{th} = \tau_{sp} C_{th}$.

We will study the statistics of transient MPN taking as parameters the bias current C_b, the modulation frequency and the relative net gain difference $\alpha_R = (\alpha_s - \alpha_m)/\alpha_m$. The laser operating point is fixed by taking $C_{on} = 3.5\, C_{th}$.

As we noted above bounds for the BER_{PR} can be obtained by using the periodic modulation (...1111...) and repetitive gain-switching (...0001...) sequences. We then consider three different operating regimes according with the time dependence of the injection current $C(t)$:

Gain switching (GS): At time $t = 0$ the injection current is changed from a value $C = C_b$ to a value above threshold C_{on} during a time t_{on}. For $t > t_{on}$, $C = C_b$ and the laser relaxes to steady-state conditions.

Periodic modulation (P): The injection current follows a square-wave modulation of period $T = t_{on} + t_{off}$ taking values C_{on} during t_{on} and C_b during t_{off} in each period. The gain-switching regime is recovered for very large t_{off}.

Pseudorandom word modulation (PR): The injection current is composed of a stochastic sequence of 0 and 1 bits. A bit 1 has an injected current of C_{on} during t_{on} and C_b during t_{off}. On the other hand, a bit 0 has an injected current C_b during the full period T.

We fix $t_{on} = 90\, ps$ such that the injection current changes from C_{on} to C_b at a time

intermediate between the pulse emission time and the time at which n goes through its minimum value. In this way a good on-off ratio is obtained and no relaxation oscillations appear [10].

The typical time trace obtained from (1) and (2) in the gain-switching and periodic modulation regimes can be described as follows [10]. For fast modulation frequencies up to 6 GHz and larger than 2 GHz t_{off} is large enough for the output power to be very small at the beginning of a period of modulation in the periodic modulation regime. Then the turn-on time depends mainly on the initial condition for the carriers $n(0)$. The role of the intensity at the beginning of the pulse ,$I_m(0)$, is negligible in this case. For larger t_{off} the effect of $I_m(0)$ is to reduce the turn–on time. For bias current above threshold under fast periodic modulation $n(0)$ is below its threshold value. Then the initial value $n(0)$ is smaller for the periodic regime than for the gain-switching regime (see Fig. 1), leading the former to a larger turn-on time. The contrary happens for a bias current below threshold (see Fig. 1). Rare events in which the side mode carries significant ouput power are associated with large turn-on times [1], [7]. For a large turn-on time the side mode turns on before the main mode and the later the main mode turns on the larger is the optical pulse associated with the side mode. Therefore we get the relation $\mathrm{BER_{GS}} < \mathrm{BER_{PR}} < \mathrm{BER_P}$ for a bias above threshold and $\mathrm{BER_P} < \mathrm{BER_{PR}} < \mathrm{BER_{GS}}$ for a bias below threshold.

The BER of the periodic and gain-switching sequences can be calculated by considering two different regimes of evolution. In the first regime of amplification until the turn-on time $\bar{t}$ the photon density is small. Then the carrier density depletion and gain saturation due to the growth of the output power can be neglected. The turn-on time $\bar{t}$ can be defined as the time at which the total photon density reaches the threshold value $I_T = I_{st}/2$, being I_{st} the stationary value of the *on* state. In the second regime for times $t > \bar{t}$ the evolution can be approximated as deterministic for

rare events such that the side mode carries a significant fraction of the total power. The first regime can be characterized by the probability density $\phi(I_m)$ that the main mode has a total photon density I_m at the laser turn-on. In order to calculate the probability distribution function $\phi(I_m)$ we follow ref. [6]. We obtain

$$\phi(I_m) = \int_0^T \frac{1}{m_1 m_2}\left[\frac{\dot{m}_1}{m_1} I_m + \frac{\dot{m}_2}{m_2}(I_T - I_m)\right] \exp\left(-\frac{I_m}{m_1} - \frac{I_T - I_m}{m_2}\right) dt, \qquad (5)$$

where the dots stand for time derivatives and $m_i(t)$ $(i = 1,2)$ are the mean values of the main and side mode intensities, respectively, whose expressions are given in the appendix A of ref. [6]. The initial conditions for the modes are chosen as follows. The value of the main mode photon density at the beginning of the pulse is taken as an exponential distribution with a mean value $< I_m(0) >$. The initial value of $n(0)$ has very small fluctuations. Then we use the mean value $< n(0) >$. $< I_m(0) >$ and $< n(0) >$ are obtained by numerical integration of the rate equations for a few number of bits. The value of the side mode photon density at the beginning of the pulse is taken as zero.

The turn-on time at which the main mode takes a value I_m and the side mode takes a value $I_s = I_T - I_m$ has a very small jitter. Then it is given by

$$< \bar{t} \mid I_m >= \frac{1}{\phi(I_m)} \int_0^T t \frac{1}{m_1 m_2}\left[\frac{\dot{m}_1}{m_1} I_m + \frac{\dot{m}_2}{m_2}(I_T - I_m)\right] \exp\left[-\frac{I_m}{m_1} - \frac{I_T - I_m}{m_2}\right] dt. \qquad (6)$$

After the turn-on time, and until the end of the period, a non-linear regime holds. For rare turn-on events the spontaneous emission noise has a neglegible effect, making the evolution purely deterministic. The relationships $W_m(I_m)$, $W_s(I_m)$ are then obtained by a simple numerical integration of the rate equations without noise. The initial conditions at $t =< \bar{t} \mid I_m >$ for integrating the deterministic rate equations are the values of the main mode I_m and side mode $I_s = I_T - I_m$ photon densities,

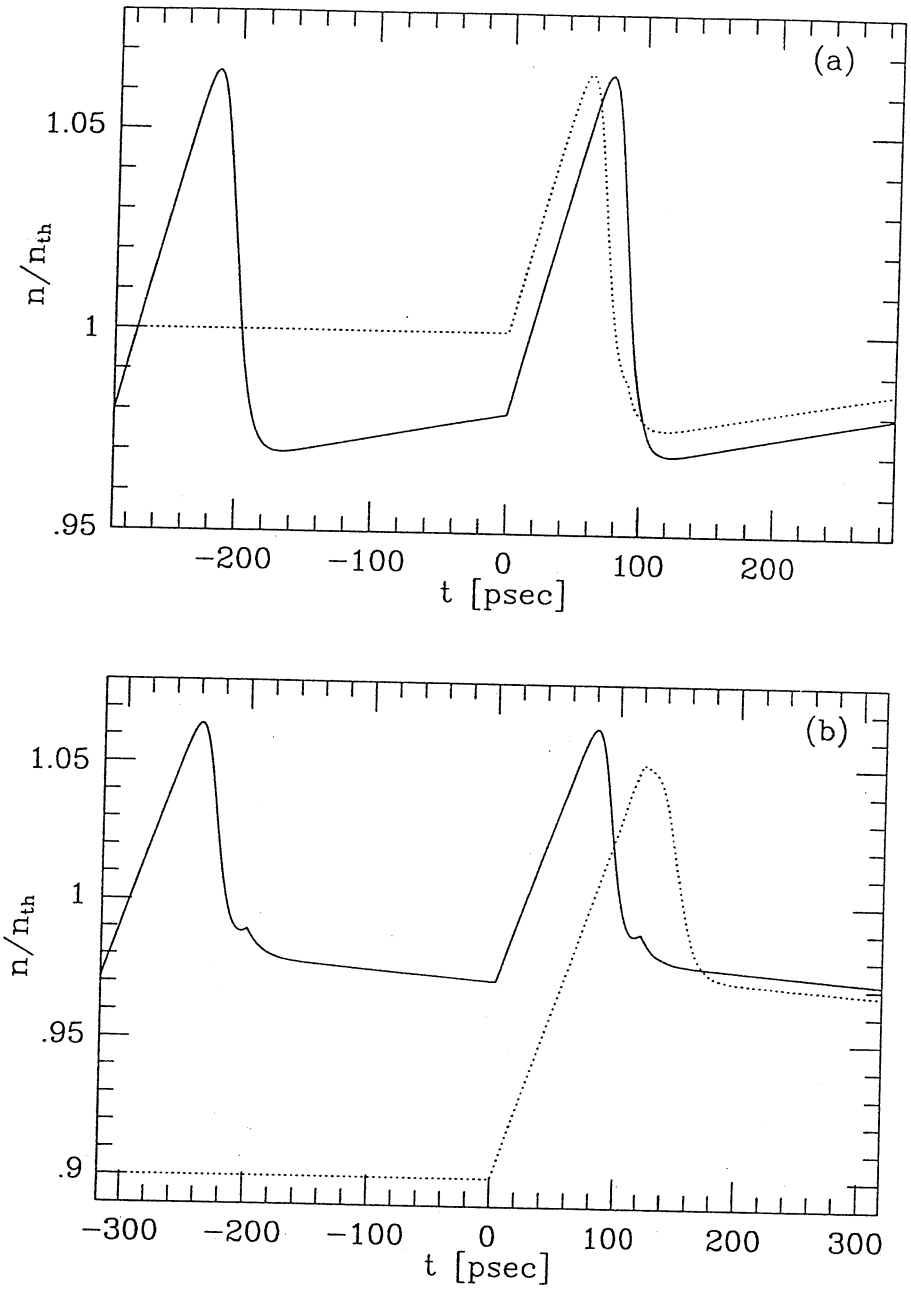

Fig. 1 Time evolution of the carrier density under two different operating regimes: periodic (solid line) and gain switching (dashed line). Carrier density corresponding to $C_b = 1.1C_{th}$ and $C_b = 0.9C_{th}$ are plotted in part (a) and (b) respectively.

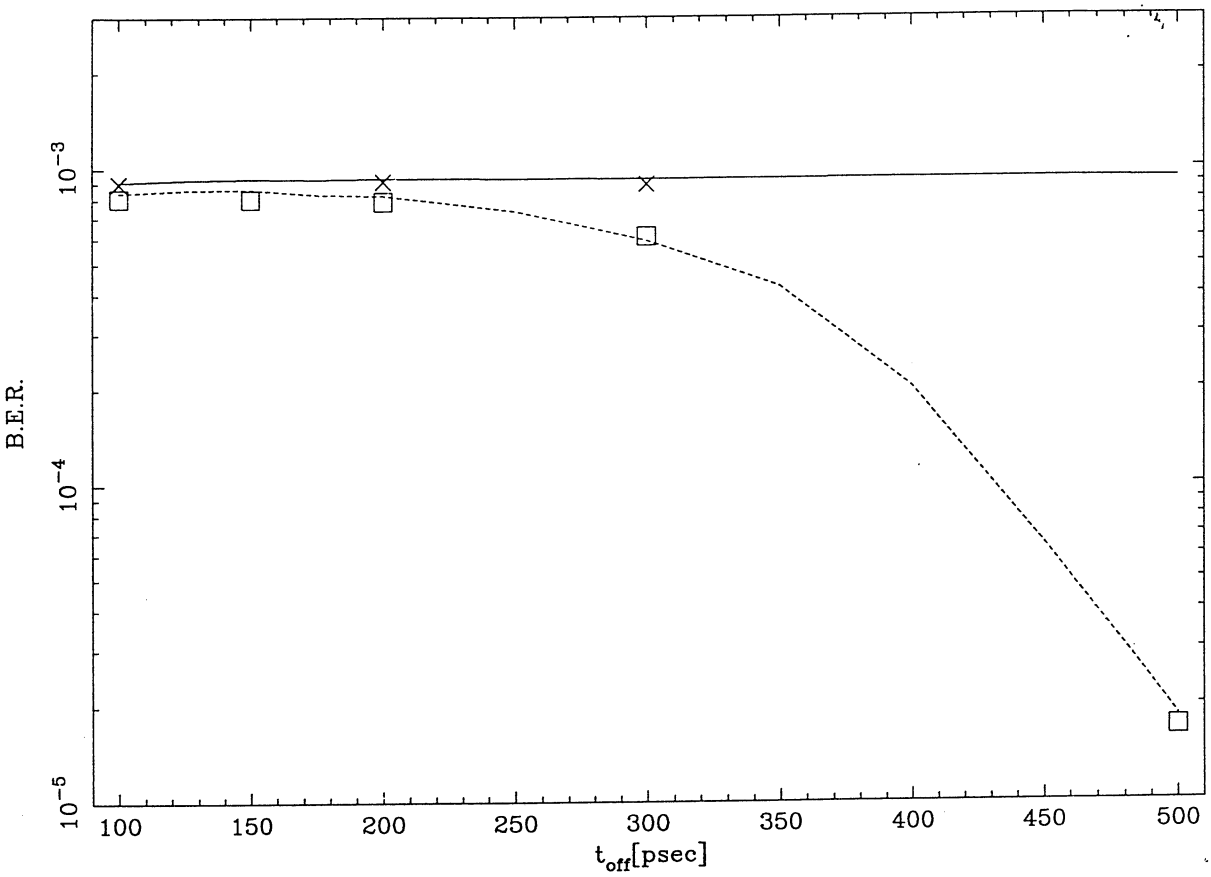

Fig. 2 BER_P as a function of t_{off} for $\Delta\alpha = 12.5cm^{-1}$. Squares and crosses, obtained by numerical simulations, correspond to $C_b = 1.1C_{th}$ and $C_b = 0.98C_{th}$ respectively. We also plot the analytical results for BER_P with solid line ($C_b = 0.98C_{th}$) and dashed line ($C_b = 1.1C_{th}$).

and the carrier density $n(< \bar{t} \mid I_m >)$ obtained by neglecting carrier depletion from $< n(0) >$. The probability that the mean power of the main mode is smaller than the mean power of the side mode can be obtained from

$$P(W_m < W_s) = \int_0^{\bar{I}_m} \phi(I_m) dI_m, \tag{7}$$

where $\bar{I}_m$ is such that $W_m(\bar{I}_m) = W_s(\bar{I}_m)$. Then the BER_P and BER_{GS} can be obtained from the knowledge of the probability density function of I_m, $\phi(I_m)$. We have checked the theoretical results with numerical simulations (see Fig. 2).

8.3 Results

As we mentioned above, we consider three regimes of modulation: periodic, gain-switching and pseudorandom. We count an error when the mean output power of the side mode, W_s, is larger than the mean output power of the main mode, W_m. We plot in Fig. 3 the BER_{PR} vs. the frequency of modulation for a bias current above threshold, $C_b = 1.1\, C_{th} = 6.6$ mA , and a bias current slightly below threshold, $C_b = 0.98\, C_{th} = 5.88$ mA, for $\Delta\alpha = 12.5 cm^{-1}$ obtained by numerical integration of the stochastic rate equations (1)-(2) with an integration step of 0.1 ps. Our statistics are obtained from 2×10^6 pseudorandom input bits. Two important features appear. The BER for a bias current above threshold is always smaller than the one for the bias current below threshold and it is found to increase with the modulation frequency. The shorter is t_{off} the smaller is the value of $n(0)$ (see Fig. 1). This corresponds to an smaller effective value for the bias current and then the BER increases. However, the BER for $C_b = 0.98\, C_{th} = 5.88$ mA does not change with the frequency of modulation. This behavior is due to the fact that the response of the system for this special value of C_b is almost independent of previous bits (no pattern effects) [10]-[12]. We discuss this problem in detail later. The other feature is that the BER is more

insensitive to the bias current when the frequency increases and both BER's tend to each other as the frequency increases. In Fig. 4 the case of a bias current below threshold ($C_b = 0.9\,C_{th} = 5.4$ mA) is presented. Now the $\mathrm{BER_{PR}}$ decreases with the modulation frequency. This is due to the fact that $n(0)$ increases when t_{off} decreases (see Fig. 1) and then the effective bias current increases.

As we have discussed above we expect that the following relation $\mathrm{BER_P} < \mathrm{BER_{PR}} < \mathrm{BER_{GS}}$ holds for bias current below threshold and that the contrary happens, i.e., $\mathrm{BER_{GS}} < \mathrm{BER_{PR}} < \mathrm{BER_P}$ for a bias current above threshold. This two assumptions can be now checked. The BER is calculated numerically for the pseudorandom sequence, and analytically for the periodic and gain-switching sequences. The relationship $\mathrm{BER_P} < \mathrm{BER_{PR}} < \mathrm{BER_{GS}}$ is shown to hold for a bias below threshold in Fig. 4. For a bias current above threshold ($C_b = 6.6$ mA) the relationship $\mathrm{BER_{GS}} < \mathrm{BER_{PR}} < \mathrm{BER_P}$ is shown in Fig. 3.

We also plot in Fig. 3 the $\mathrm{BER_P}$ and $\mathrm{BER_{GS}}$ for the special value $C_b = 0.98\,C_{th}$. Very close values are obtained for the three regimes, periodic gain-switching and pseudorandom. The response of the laser to an input "1" bit, randomly chosen, is independent of previous bits. This special value of C_b is associated with the minimum value n_m reached by n during the relaxation from C_{on}. After a "1" bit the system evolves with $n = n_m$ constant independently of t_{off}. If the following input bit is a "0" the system remains with $n = n_m$ during the full period, giving the same initial conditions for the following input pulse, as if the input was a "1" (see Fig. 5). The pulse statistics are then independent of t_{off} and the probability distribution functions of the turn-on time (see Fig. 6) and average main mode photon density W_m are then single peaked (see Fig. 7). However, for bias above threshold these distributions are not single peaked (see Figs. 8 and 9). This behavior is due to the memory of the system, i.e. the response of the laser to an input bit depends on previous bits (pattern

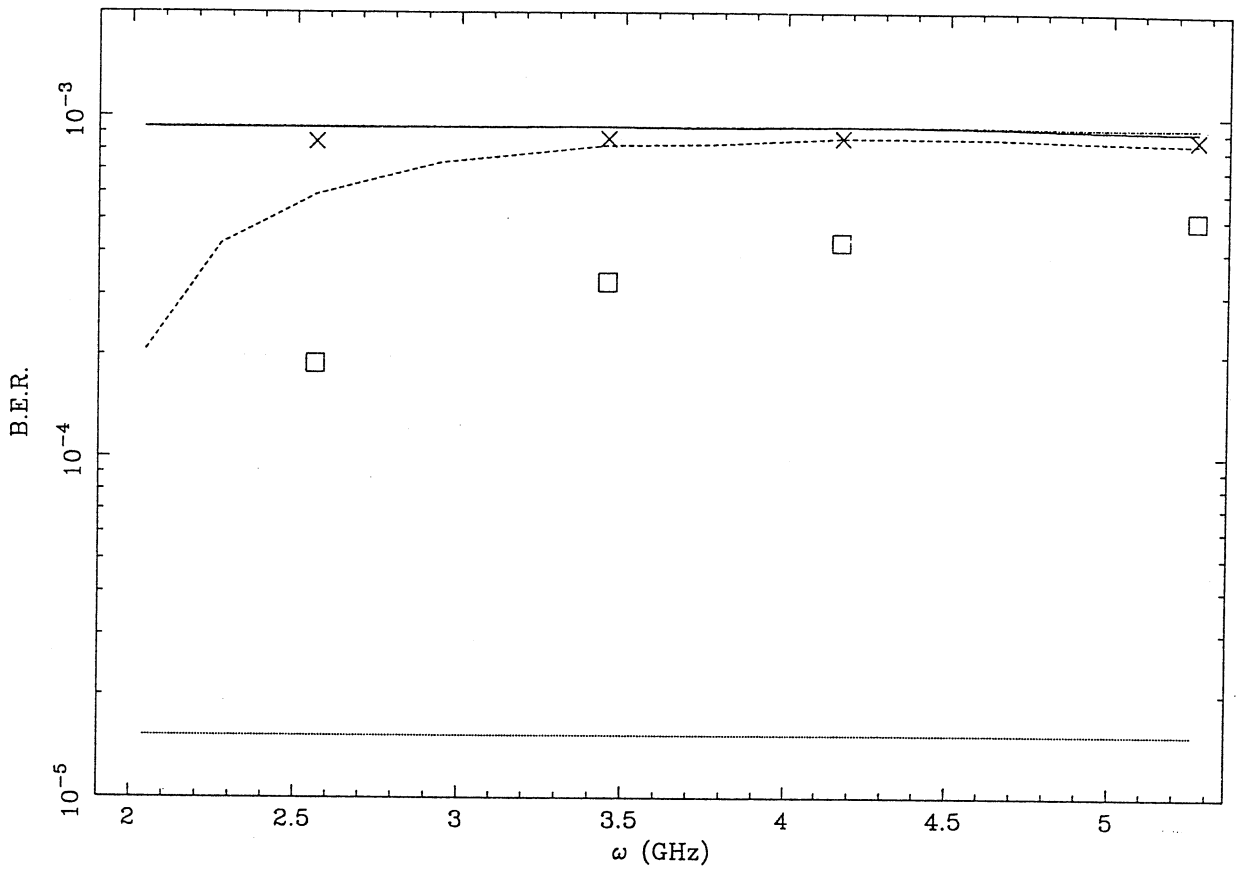

Fig. 3 BER as a function of the modulation frequency for $\Delta\alpha = 12.5cm^{-1}$. Squares and crosses, obtained by numerical simulations, correspond to $C_b = 1.1C_{th}$ and $C_b = 0.98C_{th}$, respectively. BER_P and BER_{GS}, obtained analytically, are plotted with dashed and dotted lines, respectively, for $C_b = 1.1C_{th}$ and with dot–dashed and solid line for $C_b = 0.98C_{th}$

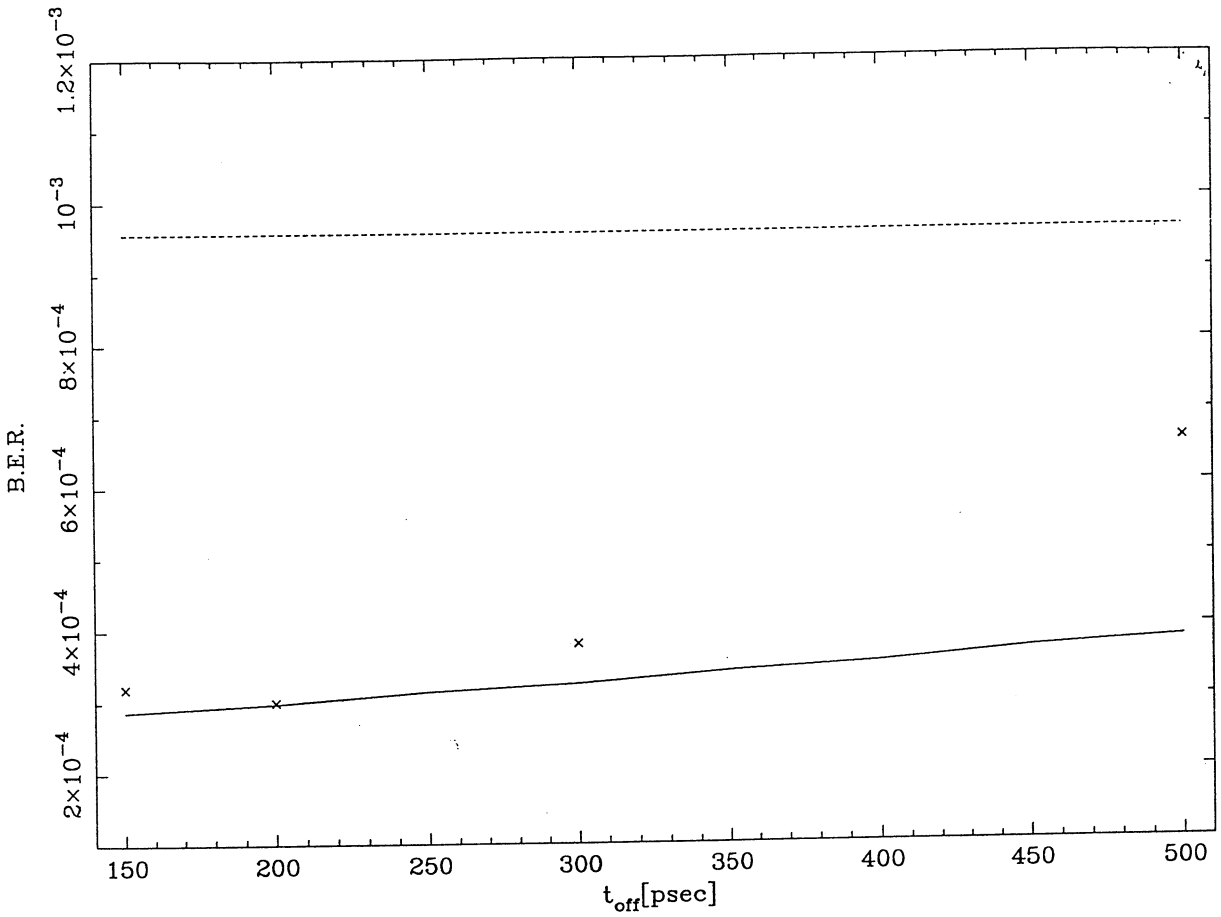

Fig. 4 BER as a function of t_{off} for a bias current of $0.9C_{th}$ and $\Delta\alpha = 12.5cm^{-1}$. BER_{PR}, obtained from simulation, is plotted with crosses while BER_{P} and BER_{GS},obtained analytically, are plotted with solid and dashed lines respectively.

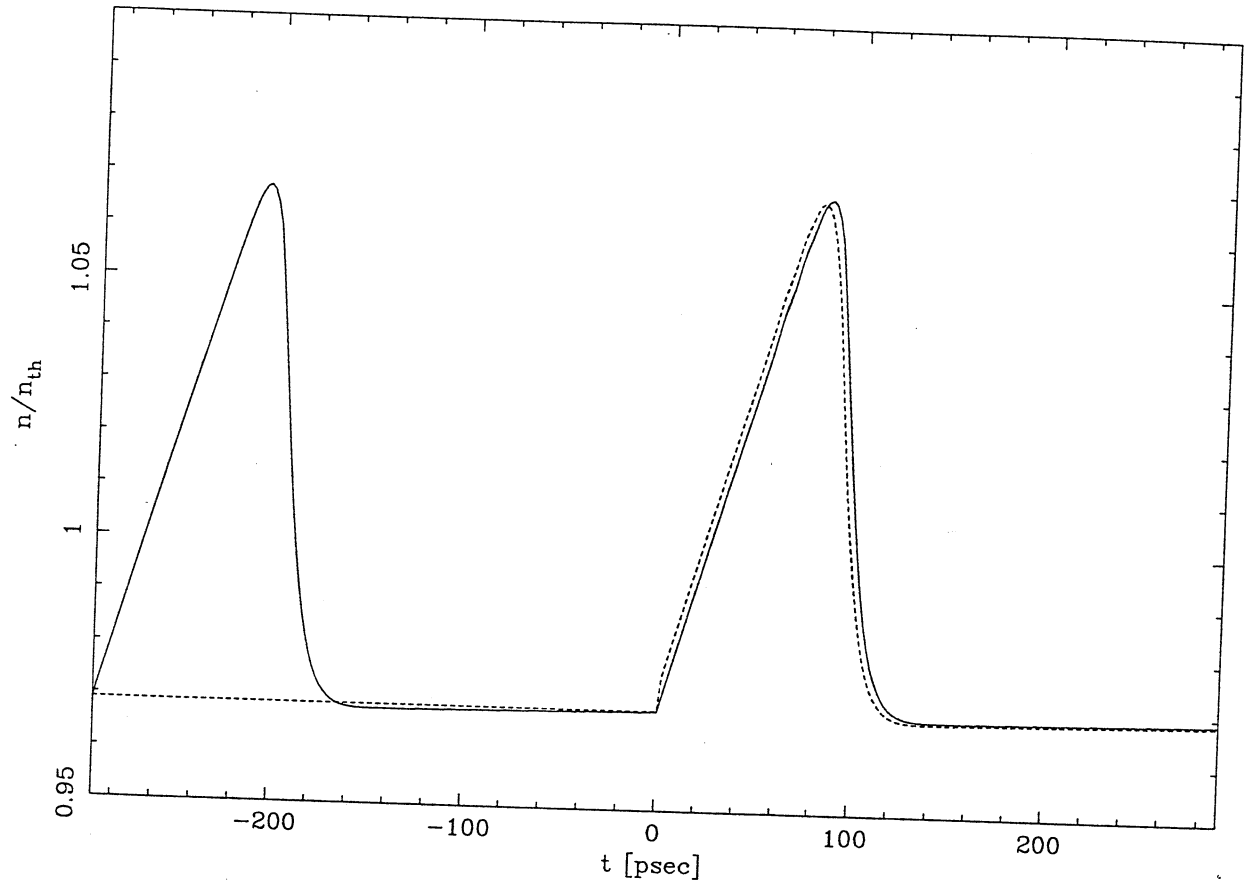

Fig. 5 Time evolution of the carrier density under two different operating regimes: periodic (solid line) and gain switching (dashed line) when $C_b = 0.98C_{th}$

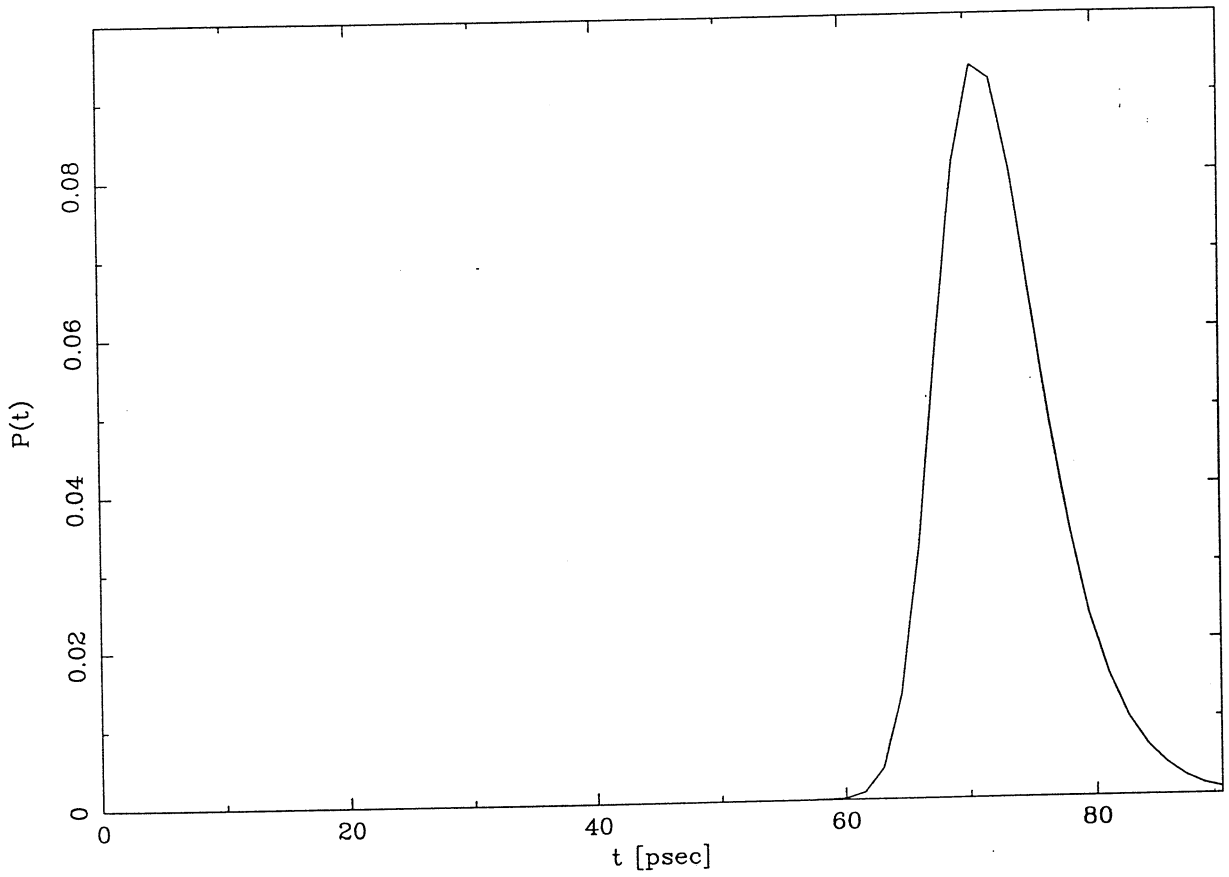

Fig. 6 Probability density function of the turn–on time for $C_b = 0.98C_{th}$, $t_{off} = 150$psec ($\omega = 4.2GHz$) and $\Delta\alpha = 12.5cm^{-1}$.

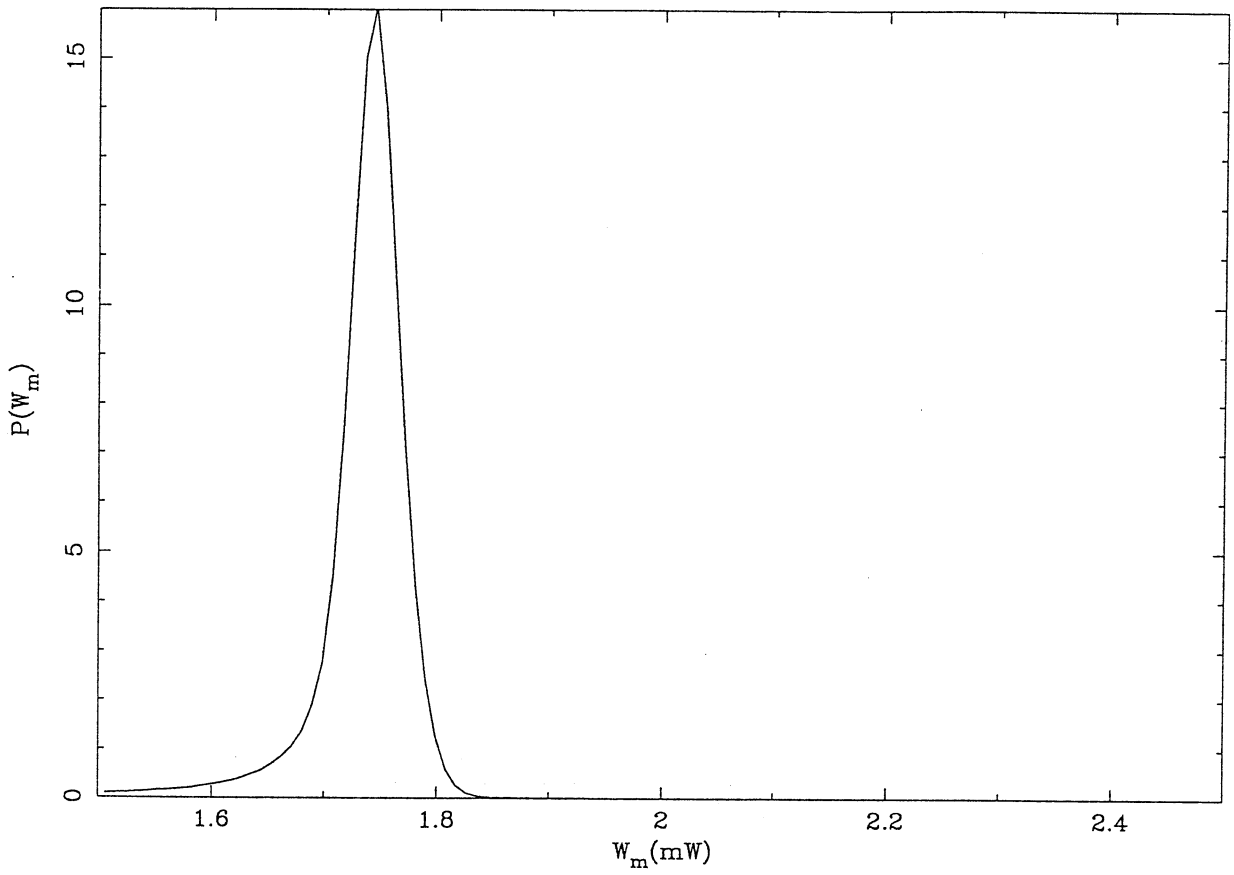

Fig. 7 Probability density function of the mean power of the main mode for $C_b = 0.98C_{th}$, $t_{off} = 150$psec and $\Delta\alpha = 12.5cm^{-1}$.

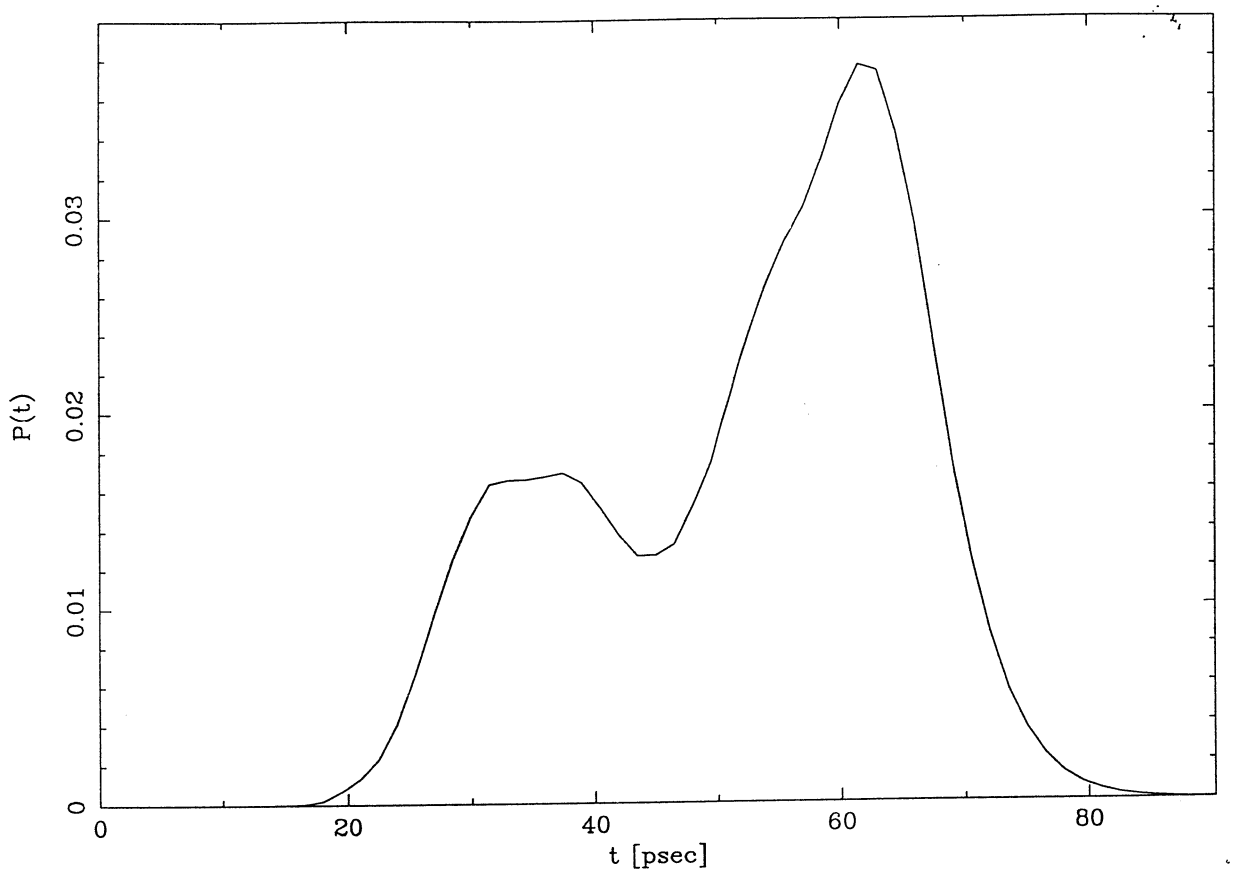

Fig. 8 Probability density function of the turn–on time for $C_b = 1.1C_{th}$, $t_{off} = 150$psec and $\Delta\alpha = 12.5cm^{-1}$.

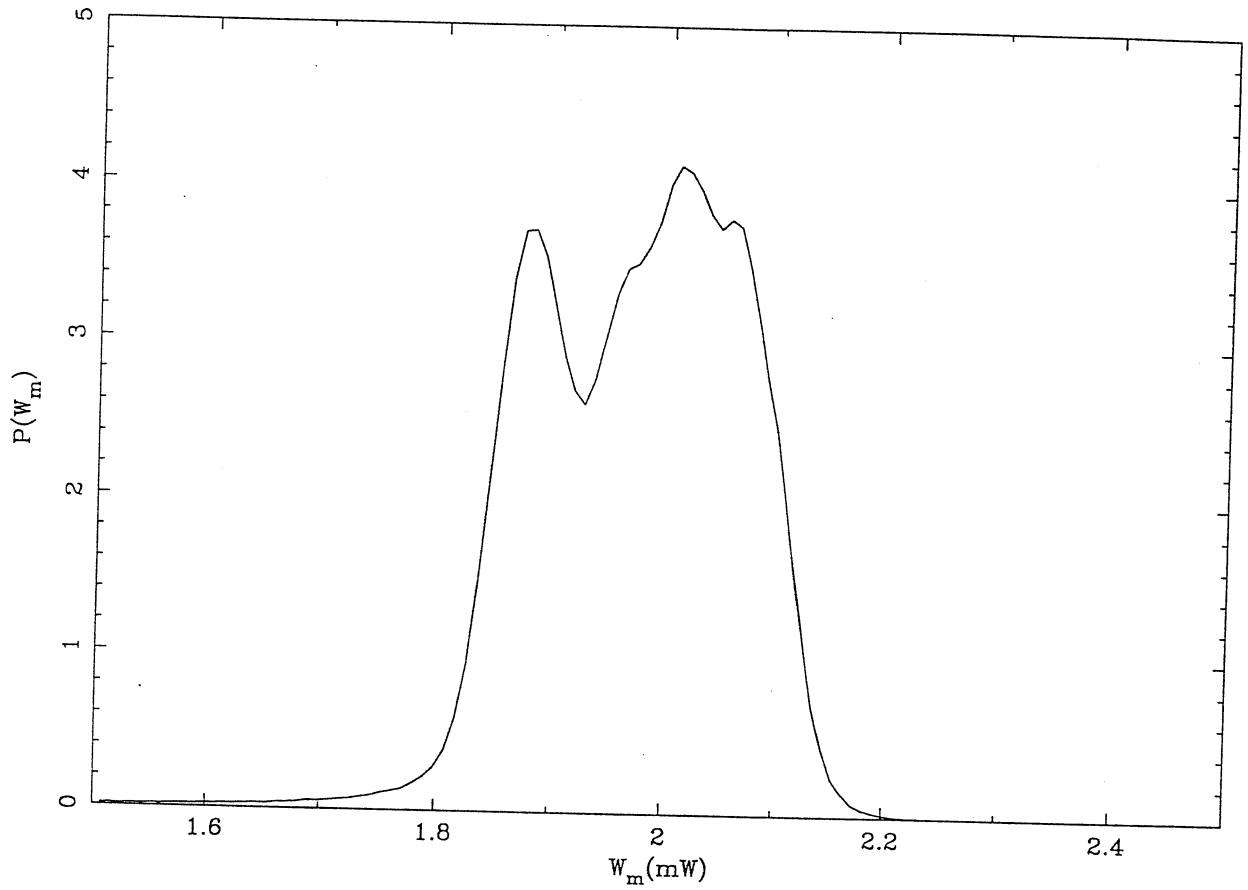

Fig. 9 Probability density function of the mean power of the main mode for $C_b = 1.1C_{th}$, $t_{off} = 150$psec and $\Delta\alpha = 12.5cm^{-1}$

effects) [10].

As the final point, we calculate upper and lower bounds for the SMSR required for a BER_{PR} smaller than 10^{-9}. For $C_b = 6.6$ mA we found a loss difference between the side and main modes of $25.5\,cm^{-1} < \Delta\alpha < 28.6\,cm^{-1}$ for $\omega = 4.2$ GHz, and $25.5\,cm^{-1} < \Delta\alpha < 25.8\,cm^{-1}$ for $\omega = 1.7$ GHz. For $C_b = 5.88$ mA we obtain $\Delta\alpha \approx 28.5\,cm^{-1}$ independent of the modulation frequency.

[1] A. Valle, P. Colet, L. Pesquera and M. San Miguel, "Transient Multimode Statistics in Nearly Single- Mode Semiconductor Lasers", IEE Proceedings Part J, Optoelectronics, to be published. A. Valle, P. Colet, L. Pesquera and M. San Miguel (unpublished).

[2] P. L. Liu and M. M. Choy, "Modeling Rare Turn-on Events of Injection Lasers", IEEE J. Quantum Electron. **QE25**, pp. 1767-1770, 1989.

[3] P. L. Liu and M. M. Choy, "Effect of Bias on Transient Mode Partition: An Analysis Based on Photon Statistics", IEEE J. Quantum Electron. **QE25**, pp. 854-857, 1989.

[4] S. E. Miller, "On the Injection Laser Contribution to Mode Partition Noise in Fiber Telecommunication Systems", IEEE J. Quantum Electron. vol **QE25**, pp. 1771-1780, 1989; S. E. Miller, "On the Prediction of Mode-Partitioning Floor in Injection Lasers with Multiple Side Modes at 2 and 10 Gb/s", IEEE J. Quantum Electron. vol **QE26**, pp. 242-249, 1990.

[5] J. C. Cartledge, "On the Probability Characterization of Side Mode Fluctuations in Pulse-Modulated Nearly Single.-Mode Semiconductor Lasers, IEEE J. Quantum Electron. vol **QE26**, pp. 2046-2051, 1990.

[6] A. Mecozzi, A. Sapia, P. Spano, and G. Agrawal, "Transient Multimode Dynamics in Nearly Single-Mode Lasers", IEEE J. Quantum Electron. vol **QE27**, pp. 332-343, 1991.

[7] T. B. Anderson and B. R. Clarke, "Modelling Mode Partition Noise in Nearly

Single-Mode Intensity Modulated Lasers", IEEE J. Quantum Electron. vol **QE29**, pp. 3-13, 1993.

[8] M. M. Choy, P. L. Liu, and S. Sasaki, "Origin of modulation-induced mode partition and Gb/s system performance of highly single mode 1.5μm distributed feedback lasers", Appl. Phys. Lett. vol. 52, pp. 1762-1764, 1988.

[9] S. Sasaki, M. M. Choy, and N. K. Cheung, "Effects of dynamical spectral behavior and mode-partitioning of 1550 nm distributed feedback lasers on Gbit/s transmission signals", Electron. Lett. vol. 24, pp. 26-28, 1988.

[10] C. R. Mirasso, P. Colet and M. San Miguel, "Dependence of Timing Jitter on Bias Level for Single-Mode Semiconductor Lasers under High Speed Operation", IEEE J. Quantum Electron. vol **QE29**, pp. 23-32, 1993.

[11] C. R. Mirasso, P. Colet and M. San Miguel, "Pseudorandom Word Modulation of Single-Mode Semiconductor Lasers at GHz rates", IEE Proceedings Part J, Optoelectronics, **Vol. 140**, pp. 26-29, 1993.

[12] P. Colet, C. R. Mirasso and M. San Miguel, "Memory Diagram of Single-Mode Semiconductor Lasers", IEEE J. Quantum Electron., to be published; C. R. Mirasso, A. Valle and L. Pesquera , "A Simple Method for Estimating the Memory Diagram in Single-Mode Semiconductor Lasers", unpublished.

[13] G. P. Agrawal and N. K. Dutta, "*Long wavelength semiconductor lasers*", New York: Van Nostrand Reinhold, 1986.

[14] C. W. Gardiner, "*Handbook of stochastic methods.* Berlin: Springer-Verlag, 1983.

TABLE I

PARAMETER	VALUE	MEANING
η	0.5	mode confinement factor
D	0.5	line shape factor
τ_{sp}	2 ns	spontaneous lifetime
n_g	4	group index
γ	1.76×10^{-4}	fraction of spontaneous emission coupled into the mode
A	$2.24 \times 10^{-5} cm^3 s^{-1}$	differential gain
n_0	$3.4 \times 10^{17} cm^{-3}$	carrier density at transparency
α_m	$53.3 cm^{-1}$	loss of the main mode
c	$3 \times 10^{10} cm s^{-1}$	speed of the light in vacuum
s	$6 \times 10^{-17} cm^3$	saturation parameter
C_{th}	$3.76 \times 10^{26} cm^{-3}$	threshold current
V	$10^{-10} cm^{-3}$	volume of the active region

Conclusiones

En este trabajo se ha abordado el estudio de la estadística de transitorios en sistemas ópticos no lineales dedicando una especial atención al encendido del laser. Este estudio se ha llevado a cabo principalmente mediante la aplicación de la Teoría Cuasideterminista. La idea básica de esta teoría es la separación de la evolución de la intensidad del sistema óptico no lineal en dos regímenes. El primer régimen, de amplificación lineal y dominio del ruido de emisión espontánea, determina las características estadísticas de todo el transitorio. El cálculo de la estadística en este régimen se puede realizar de forma analítica. En el segundo régimen, de evolución no lineal, el ruido ya no influye en la evolución pudiendose describir ésta de forma numérica y en algunos casos analítica. De esta forma la estadística en este régimen se encuentra como una simple transformación de la estadística en el primer régimen sin necesidad de recurrir a la simulación de las ecuaciones diferenciales estocásticas que describen la evolución. Este esquema no funciona en la relajación de un estado marginal en dispositivos ópticos biestables pues no es posible determinar de forma analítica las propiedades estadísticas de la intensidad en la región dominada por las fluctuaciones debido al carácter no lineal del problema.

Dos problemas principales han podido ser abordados mediante el uso de la anterior aproximacion. El primero se refiere a la influencia de la dependencia temporal de un parámetro de control externo sobre la estadística de la intensidad del laser en el transitorio. El segundo se refiere al estudio de la competencia entre los diversos modos que pueden aparecer en el encendido de un laser. Ambos problemas han sido tratados en laseres de gas y semiconductor. En estos sistemas hemos descrito la estadística del laser durante el transitorio bien a través de la dependencia temporal de los momentos de la intensidad o a

través de la estadística de tiempos de paso por un cierto umbral.

Resumimos ahora los resultados obtenidos (un resumen mas amplio puede encontrarse en la sección 0.2):

*En el problema de la relajación de un estado marginal en óptica biestable hemos conseguido relacionar las fluctuaciones anómalas de la intensidad con la estadística de tiempos de paso por un cierto umbral.

*En el problema de un láser de gas encendido mediante una disminución lineal de las pérdidas en el tiempo hemos obtenido relaciones de escala de los tiempos de retraso con la velocidad de disminución de las pérdidas. También hemos encontrado leyes de escala dinámicas de los momentos de la intensidad

*Hemos desarrollado también un método para el cálculo de la estadística en sistemas estocásticos modulados. La estadística de los pulsos formados la caracterizamos mediante la estadística del tiempo de paso de la intensidad por un cierto umbral. Este método lo hemos aplicado con éxito a laseres de gas y de semiconductor modulados. En el primer caso hemos observado la existencia de dos tipos de comportamiento: uno en que el ruido de emisión espontánea determina la estadística del pulso (tiempos de apagado largos) y otra de comportamiento determinista (tiempos de apagado cortos). En el caso del laser de semiconductor modulado hemos calculado la densidad de probabilidad de tiempos de paso en función de la frecuencia de modulación.

*Predicciones anteriores para los tiempos de encendido de un laser de gas han sido verificadas en un experimento en el que un laser de Ar^+ es modulado mediante un modulador acusto óptico. La aparición de un máximo de la varianza del tiempo de encendido (que no aparece con el modelo anterior) es interpretada mediante un modelo en el que fluctuaciones en el parámetro de control (motivadas por la aleatoriedad de la amplitud de la señal de

radiofrecuencia que es aplicada al modulador) son tenidas en cuenta.

*En el problema de un laser de gas bimodal de anillo hemos descrito la evolución dinámica de la estadística de la intensidad de ambos modos para el caso de competencia fuerte (parámetros de bombeo de los dos modos similares) y de competencia débil (el parámetro de bombeo de uno de los modos es mucho mayor que el del otro). Aparece una escala de tiempo nueva ligada a la competencia entre modos que puede ser mucho mayor que las asociadas a cada modo por separado, a medida que los parámetros de bombeo son más parecidos.

*Hemos analizado también el problema de un laser de semiconductor cuasimonomodo. Hemos estudiado en detalle los sucesos en que el modo con mayores pérdidas (modo lateral) tiene más potencia que el principal durante el transitorio. La probabilidad de estos sucesos (que dan lugar a errores en sistemas de comunicaciones ópticos) ha sido caracterizada de dos formas: mediante la probabilidad de modo lateral tenga mayor potencia que el modo principal en el instante de encendido y mediante la probabilidad de que la potencia del modo lateral integrada en el tiempo sea mayor que la correspondiente del modo principal. Ambas probabilidades han sido calculadas. Este mismo problema ha sido analizado en el caso de una modulación pseudoaleatoria rápida (2 a 6 GHz) de la corriente de inyección. Hemos calculado cotas superiores e inferiores a la supresión del modo lateral (SMSR) necesaria para obtener BER de 10^{-9}. También hemos observado efectos de pattern en la salida del laser para una corriente de bias por encima del umbral debido a la secuencia pseudoaleatoria de bits en la entrada.

La ventaja de las aproximaciones analíticas usadas a lo largo de este trabajo se hace patente cuando se requiere predecir BER en sistemas de comunicaciones ópticas menores que 10^{-9} pues la capacidad de cálculo de los ordenadores actuales está lejos de permitir

calcular probabilidades tan bajas mediante simulación numérica.

Publicaciones relacionadas con esta tesis

"Relaxation from a marginal state in optical bistability. Anomalous fluctuations and first–passage time statistics", A. Valle, L. Pesquera, M.A. Rodríguez; Optics Communications **79** 156–164 (1990).

"Transient statistics for a good cavity laser with swept losses", A. Valle, L. Pesquera, M. A. Rodríguez. Phys. Rev. **A**, 5243–5250 , (1992).

"Analytical calculation of time jitter in single–mode semiconductor laser under fast periodic modulation" , A. Valle, C. Mirasso, M. A. Rodríguez. Optics Letters, **17**, 1523–1526, (1992).

"Statistical properties of pulses. Application to modulated gas lasers". A. Valle, M. A. Rodríguez and L. Pesquera, Phys. Rev **A**. (en imprenta).

"Transient statistics for two mode gas ring lasers". A. Valle, A. Mecozzi, L. Pesquera, M. A. Rodríguez and P. Spano, Phys. Rev. **A**. (en imprenta).

"Transient multimode statistics in nearly–single mode semiconductor lasers". A. Valle, P. Colet, L. Pesquera and M. San Miguel, IEE Proc. **J**. (en imprenta).

"Anomalous fluctuations in a good–cavity laser with swept losses", A. Valle, L. Pesquera, M.A. Rodríguez. "Nonlinear dynamics quantum phenomena in optical systems", Eds. R. Vilaseca, R. Corbalán, Ed. Springer Verlag, Berlin, 318–322 (1991).

Otras publicaciones

" Diffusion in a disordered line", A. Valle, L. Pesquera, M.A. Rodríguez; "Large–Scale molecular systems: Quantum and Stochastic aspects. Beyond the simple molecular picture", NATO–ASI series, eds. W. Gans, A. Blumen, A. Amann. Ed. Plenum, New York, 425–430 (1991).

"Diffusion in a continuous medium with space correlated disorder", A. Valle, M.A. Rodríguez, L. Pesquera; Phys. Rev. **A 43** 948–952 (1991).

"Diffusion in a random multiplying medium. Exact bounds and simulations", A. Valle, M.A. Rodríguez, L. Pesquera; Phys. Rev. **A 43** 2070–2073 (1991)